BULGARIAN CHEMICAL COMMUNICATIONS

2022 Volume 54 / Special Issue C

Selected papers presented on the Conference on Cutting Edge Research in Materials and Sustainable Chemical Technologies (CRMSCT-2022) – Department of Chemical Engineering and Department of Chemistry, Decennial year celebrations, Manipal University Jaipur, Jaipur, India

Journal of the Chemical Institutes
of the Bulgarian Academy of Sciences
and of the Union of Chemists in Bulgari

Bulgarian Chemical Communications, Volume 54, Special Issue C (pp. 05-10) 2022 DOI: 10.34049/bcc.54.C.0005

A review: conductive polymer-based aluminium current collector for Li-ion batteries

M. Goyal[1], S. N. Agarwal[2], K. Singh[3], A. Shrivastava[4], N. Bhatnagar[1*]

[1]*Department of Chemistry, Manipal University Jaipur, India*
[2]*Department of Electrical Engineering, Manipal University Jaipur, India*
[3]*Department of Electronics and Communication Engineering, Manipal University Jaipur India*
[4]*Skill Faculty of Engineering and Technology, Shri Vishwakarma Skill University, Gurugram, Haryana, India*

Received: March 14, 2022; Revised: July 22, 2022

Conductive polymers are favourable materials in lithium-ion batteries because of their high electrical conductivity and coulombic efficiency and their ability to be cycled hundreds or thousands of times with only slight degradation. This review paper presents an overview of the lithium ion batteries (LIB) fabricated by using various types of conductive polymers (CP) based on aluminum as a current collector (CC). More attention is paid to aluminum which can be used as a cathode current collector. The conductive polymer can minimize the interface resistance between the current collector and the active material to increase the performance of lithium batteries. Furthermore, it can help to lower the battery's internal resistance during usage. The most used conductive polymers are polyaniline (PANI), poly(ethylene glycol) (PEG), poly-dopamine (PDA), polyacetylene (PA), polypyrrole (PPy), polythiophene (PTH), PEDOT: PSS (poly(3,4-ethylenedioxythiophene)) and poly (styrene sulfonate), because of their ability to store and conduct lithium ions. The reason to use the conductive polymer binders is their high energy density, porous nature, high electrical conductivity and many other. This review article discusses the basic structure of the Li ion battery followed by analysis of various types of conductive polymers which can be used in lithium ion battery, and highlight the influence of aluminum as a cathode current collector.

Keywords: Conductive, Lithium; Aluminum; Resistance; Electrical; Sulfonate

INTRODUCTION

Lithium ion battery has high density, voltage stability, longevity, environmental security and low self-discharge rate [1, 2], which makes this battery more efficient and useful for electrical items such as phones, vehicles, portable devices, power tools, hybrid electric vehicles, etc. [3] The lithium ion batteries changed the area of energy storage and its production because of their dynamic properties. Flexible lithium ion battery is in progress which demands the high energy capacity in the development of the applications of soft mobiles [4]. Furthermore, in the periodic table, lithium is ranked on third number, implying that it contains the shortest radius of any single-charged ion, permitting lithium-based batteries to have an excellent power density and gravimetric capacity [5]. Li-ion batteries are known to be the common energy storage cells for powering handy electronic devices, and their use in automotive, defence, and aerospace applications is increasing. Despite their widespread use and commercial domination, LIBs have undergone extensive research and development in order to improve their features [6]. Electrochemical cell is defined as a device which converts chemical energy (C.E.) into electrical energy (E.E.). It is a redox process like in Daniel cell. In electrochemistry, the substance which conducts electricity, causes the dissociation of ions, which generates the positive and negative terminals, i.e. cathode and anode of an electric circuit. In electrochemistry the anode behaves as a negative terminal while the cathode behaves as a positive terminal. Further, they are distributed into acids, bases and salts as they give ions while dissolving into aqueous or non-aqueous solvents. These solutions are known to conduct the electricity. When electrolytes are put between two electrodes and voltage is provided, the electrolytes conduct electricity through charge carriers or ions transfer. The selection of electrodes depends on the basis of process not on the charge and polarity. As a consequence, chemical reactions occur at the cathode, which contain e^- from the anode, and produce electrons for the cathode to take. Hence, in an electrolyte, negative charge occurs at cathode and positive charge occurs at anode [7]. The ions in an electrolyte cell are non-spontaneous which transfer electrical energy into chemical energy.

To replace graphite anode with Li metal produces higher energy density of Li-ion batteries and these batteries are called lithium metal batteries. Lithium metal batteries consist of four parts: anode material, cathode material, electrolyte, and separator [8].

* To whom all correspondence should be sent:
E-mail: niturbhatnagar@gmail.com

HIGH CONDUCTIVITY	HIGH THERMAL AND CHEMICAL STABILITY	LIGHTWEIGHT AND FLEXIBLE	INEXPENSIVE AND FEASIBLE
• To collect and transfer electrons, electrical conductivity is required, which can increase the rate performance of lithium ion batteries.	• Current collector is stable and unaffected by active materials and electrolytes.	• Current collector should be strong and flexible enough to suit the demands of production. Since lightweight current collectors enhance the mass and volumetric specific capacity of lithium metal batteries has increased.	• Current collector should be inexpensive and simple to obtain so that it may be utilized in other applications.

Figure 1. Various properties of current collector used in lithium ion battery

The cathode current collector (CC) is largely utilized in battery creation, and it is mainly cycled into aluminium foil paper with a thickness of 10-20 μm [9, 10], whereas copper is employed as an anode current collector with a thickness of 5-8 μm [11].

Aluminum can be used as the best current collector (CC) due to its cheap cost, conductivity and availability [12, 13] In Figure 1, the properties of the current collector are explained. For the better performance and stability of the Li-ion battery, aluminum can be used as a carbon coating [14].

Conductive polymer is used in cathode material especially. Conductive polymers have also been explored for a variety of uses, including active electrode materials in LIB [15]. The reason to use conductive polymer is its electrochemically active stable nature, high electronic conductivity and the great porosity for electrolyte. For the battery performance, internal resistance is proportional to the depth of charge and discharge. It means that in battery discharge there is increment in internal resistance which further reduces the electrolyte concentration.

The review aims at examining and summarizing some of the research work on conductive polymer-based aluminum current collectors for lithium ion battery.

Basic structure of Li ion battery

Lithium ion battery is a secondary rechargeable battery. The cathode and anode of lithium ion batteries are separated by a polymer membrane and are all wetted by the electrolyte [16]. In a lithium ion battery, two electrodes with two distinct electron affinities can be used, with electrons flowing from one electrode to another outside the battery and the electrolyte ions closing the circuit within the battery [7]. In this case, the electrode reaction converts the chemical energy into electrical energy. During the charging phase, lithium ions are put into the anode after being extracted from the cathode, and the opposite reaction happens during the discharging process. Hence, lithium ions move from cathode to anode as shown in Figure 2 [16]. The redox reactions occurred simultaneously with the advancement or retreating of the electrode surfaces in a conventional galvanic battery system.

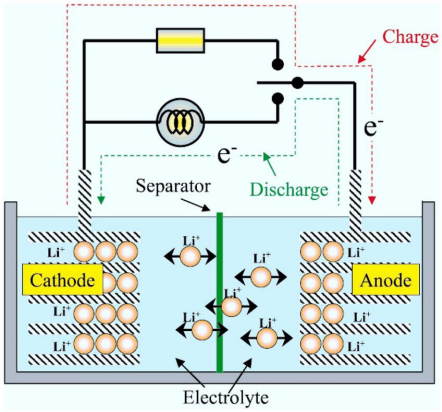

Figure 2. Mechanism of Li ion battery [17]

The first lithium ion battery was discovered by Yoshino using $LiCoO_2$ cathode and the discharged carbon anode as shown in equation below [18]:

$$C + xe^- + xLi^+ = LixC \text{ (anode)} \quad (1)$$

$$LiCoO_2 - xe^- - xLi^+ = Li - xCoO_2 \text{ (cathode)} \quad (2)$$

Heterogeneous redox reactions in lithium ion batteries are invariably followed by volume expansion and solid-state mass diffusion [19]. One of the challenges that new materials try to overcome is voluminal variation. The most important materials that define the electrochemical parameters of a lithium ion battery are the anode, cathode, and electrolyte. Despite this, graphite has a specific capacity about is 372 $mAhg^{-1}$ due to which every 6-C atoms combine with one lithium ion to form LiC_6 [20]. Figure 3 represents the properties of the Li ion battery [33]. The following factors influence Li storage capacity [21]:

- the sufficient space for admitting lithium

ions;

- the electrode material's ability to shift valence states.

Those key elements outlined above serve as motivation and guidance for learning about new and improved composite materials in order to address the growing need for energy storage.

The current collectors in lithium metal batteries should have high conductivity, high chemical and thermal stability, lightweight, flexibility, cheap cost and easy access. Figure 3 describes the advantages, limitations and applications in lithium metal batteries [22-24].

Li-ion batteries contain electrolyte salts such as lithium perchlorate ($LiClO_4$), lithium hexafluoro arsenate ($LiAsF_6$), lithium tetrafluoroborate ($LiBF_4$), lithium hexafluorophosphate ($LiPF_6$), lithium trifluoromethanesulfonate ($Li(CF_3SO_3)$), lithium oxalyldifluoroborate ($Li[BF_2(CO_2)_2]$, etc. Brief discussion on some salts is given in Table 1. These salts should meet some criteria, as follows [7]:

1. Ionic conductivity is high in a variety of non-aqueous solvent systems.
2. Electrolyte solutions should be inert to anions.
3. Anion should be safe to use.
4. It should be able to prevent anodic breakdown of an aluminum current collector.

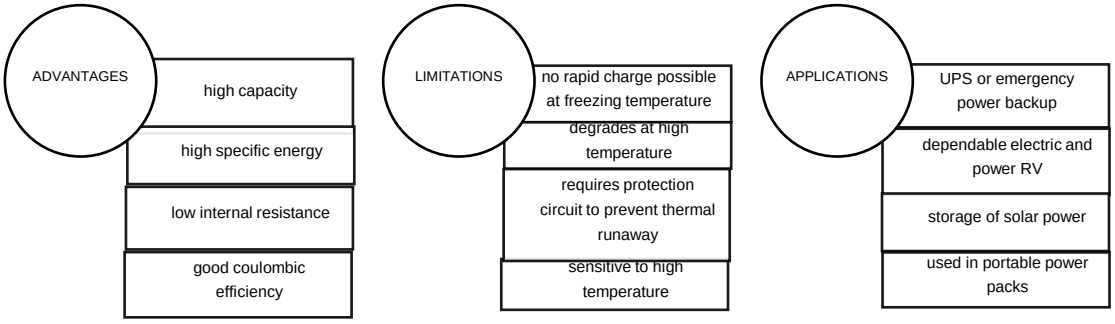

Figure 3. Advantages, limitations and applications of Li ion battery [33]

Table 1. Summary of some lithium salts

S. No.	Salt	Characteristics	Equations
1.	Lithium perchlorate [25,26] ($LiClO_4$)	• Strong acid • High solubility • High anodic stability • Good ionic conductivity in non-aqueous solvents	1. $LiClO_4 + ne^- + 2nLi^+ \leftrightarrows Li_2O + LiClO_3, LiClO_2 + LiCl$
2.	Lithium tetrafluoroborate [27] ($LiBF_4$)	• Smaller anionic size • High ionic conductivity • Moisture problem	1. $Li^+ + BF_4^- \leftrightarrow LiF\downarrow + BF_3\uparrow$ 2. $BF_3 + H_2O \rightarrow BOF\uparrow + 2\,HF$
3.	Lithium hexafluoroarsenate [25,28] ($LiAsF_6$)	• Higher ionic conductivity • Passivates the aluminum current collector on both sides of the electrode surface, which creates the solid electrolyte interface.	1. $LiAsF_6 + H_2O \rightarrow HF + AsF_5 + LiOH$ 2. $LiAsF_6 + 2e^- + 2Li^+ \rightarrow AsF_3 + 3LiF$ 3. $AsF_3 + 2ne^- + 2nLi^+ \rightarrow Li_nAsF_{3-n} + nLi^+$
4.	Lithium trifluoromethane sulfonate ($Li(CF_3SO_3)$) [29]	• High dissociation constant • Low dielectric media • In non-aqueous solvents, ionic conductivity is poor	1. $2\,Li(CF_3SO_3) + 2e^- + 2\,Li^+ \rightarrow 2Li_2SO_3\downarrow + C_2F_6\uparrow$ 2. $C_2F_6 + 2e^- + 2Li^+ \rightarrow CF_3CF_2Li + LiF\downarrow$ 3. $Li_2SO_3 + 6e^- + 6Li^+ \rightarrow Li_2S\downarrow + 3\,Li_2O\downarrow$
5.	Lithium bis(trifluoromethane sulfonyl)imide [30,31] ($Li[N(CF_3SO_2)_2]$	• Thermally stable • High conducting • Low dielectric constant • Higher dissociation	1. $Li[N(CF_3SO_2)_2] + 4e^- + 4Li^+ \rightarrow Li_3N\downarrow + 2\,Li(CF_3SO_2)\downarrow$ 2. $2\,Li(CF_3SO_2) + ne^- + n\,Li^+ \rightarrow Li_2S_2O_4\downarrow + C_2F_xLi_y + LiF\downarrow$ 3. $Li_2S_2O_4 + 6e^- + 6\,Li^+ \rightarrow 2\,Li_2S\downarrow + 4Li_2O\downarrow$
6.	Lithium tris(perfluoroethyl) trifluorophosphate [32] ($Li[PF_3(CF_3CF_2)_3$)	• Lower reactivity • Lower viscosity	1. $(CF_3CF_2)3PF_2 + LiF + 5\,H_2O \rightarrow Li[(CF_3CF_2)3PF_3].5\,H_2O$

Table 2. Cathode materials and conducting polymer binders: capacity adjusted by electrode weight [40]

Electrode	Speed of charging conventional Li-ion battery	Normalized discharge capacity ($mAhg^{-1}$)	Cycles	Parameter variation of Li-ion battery after addition of conductive polymer
LFP/PEDOT:PSS/SBR-CTS/C [41] (90:3:4:3 wt%)	0.2	140	100	Increased electron density and best cyclicity
LFP/PEDOT:PSS [15] (92:8 wt%)	0.2 1	110 97	100	No redox activity and better cyclic stability
LCO/PVDF/C (95:3:2 wt%) (*in situ* polymerized PANI/LiV_3O_8)/PVDF/C (85:10:5 wt%) [42]	0.2 0.1 1	133 204 195 157 160	 30 55	Cyclicity increase and better rate capability
LFP/SA-PProDOT [43] (80:20 wt%)	0.1 1	136 96	400	Better binding capability and electronic conductivity
Hydrogel-derived Cu-PPy/C-LFP [44] (~15:85 wt%)	1	128	1000	Better cyclic performance

Table 3. Anode materials and conducting polymer binders: capacity adjusted by electrode weight [40]

Electrode	Speed of charging conventional Li-ion battery	Normalized discharge capacity ($mAhg^{-1}$)	Cycles	Parameter variation of Li-ion battery after addition of conductive polymer
Si/PEDOT:PSS/CMC/C [45] (70:10:10:10 wt%)	~0.06 (0.2 Ag^{-1}) ~2.8 (10 Ag^{-1})	2700 609	100	Better cyclicity and rate performance
LTO/PEDOT:PSS/CMC/C [46] (90:2:2:6 wt%)	0.2 1	141 138	1000	Better cyclic stability
Hydrogel-derived Si/P-PPy/CNT [47] (~70 wt% Si:~0.2 wt% CNT)	0.78	1120	1000	Enhancement in performance
Si/FA/PEDOT:PSS [48] (80-20 wt%)	0.28	1542	100	Better electrochemical stability
Si/PF-COONa [49] (66.6:33.4 wt%)	0.1	2180 1852	100	Better electronic conductivity

Table 4. Some used current collectors

Material	Current collector		Properties
	Cathode	Anode	
Aluminum (Al)	Used in a variety of cathode materials	At low potential it reacts with Li	• High electrical conductivity • Low cost
Copper (Cu)	Oxidized at high potential	Used in a variety of anode materials.	• Lightweight • High electrical conductivity • Low cost
Nickel (Ni)	Cathode material made of $LiFePO_4$	Used for NiO and Si/ C anode material	• In acidic and alkaline solutions, it is stable.
Stainless steel	Cathode material made of $LiMnO_4$	Used for MnO_2 and Fe_3O_4 anode material	• The corrosion resistance of the surface oxide layer is excellent.

Conductive polymers for lithium ion batteries

Many groups have observed in recent years that thin coatings of conducting polymers such as polyaniline (PANI), polypyrrole (PPy), and polythiophene (PT) on the surface of active particles can significantly boost the capacity and rate capability of cathodes. PEDOT (poly(3,4-ethylenedioxy thiophene)) has been utilized to coat $LiFePO_4$ and $LiCoO_2$ particles and increase their performance [34-39]. PEDOT:PSS is a binder and conductive additive for Li ion battery and by adding the conductive polymer it behaves as current collector which decreases contact resistance. The following tables (Tables 2 and 3) summarize the normalized capacities of electrodes having poly(3,4-ethylenedioxythiophene) polystyrene sulfonate (PEDOT: PSS) binders and other conductive polymers also.

Aluminum-based current collector for Li-ion battery

The basic step to use the current collector is performance, safety or stability in lithium ion battery, so aluminium foil is an important cathode current collector. Al foil has high conductivity, light weight, low price, and easy processing. However, it is easy to reacts with Li at low voltage, so it is often used in various cathode materials [50-52]. Current collector thickness of Al foil has decreases from 16 μm to 10 or 12 μm, but some manufactures even utilize 8 μm Al foil. Also, to increase the conductivity, cathode CC employs carbon coated Al foil [53, 54]. In Li-free cathode current collector, aluminium foil and carbon coated aluminium foil are the most used cathode materials. As a result, the most often utilized cathode current collectors are titanium, nickel, stainless steel, and carbon [55-58]. Nickel is quickly dissolved when exposed to high voltage, which limits its use. Like aluminum, titanium can form oxide coating on the surface. Stainless steel is a metal alloy composed mostly of iron, chromium, nickel, and manganese. Because of the passivation coating like chromium oxide (Cr_2O_3) on the surface, it has a strong corrosion resistance. Carbon materials have low density which can lower down the specific gravity of CC. Flexible battery systems with good flexibility are a suitable choice [8].

The restricted contact surface with active materials, along with interface resistance, are some drawbacks of using aluminum foil as a current collector. Surface treatment is the method which is commonly used for improving and enhancing the aluminum foil current collector (CC) [59-62]. In Table 4, a brief description of some used current collectors with their properties is given [8].

CONCLUSION

In this paper we have highlighted the recent developments in the design and manufacturing of conductive polymer-based aluminum current collectors (CC) for Li-ion batteries. As a result, current collectors with high strength, lightweight, high flexibility, and ultrathin profiles will continue to be developed in the future [63]. Major focus on the increment of energy density should be increased, C-rate should be increased. If C-rate increases, then the chances of battery charging and discharging should be increased. Cycling rate also increases which leads to an increase of discharge rate. Further, research should be taken on various properties that should be optimized.

Acknowledgement: *The authors gratefully acknowledge the facility provided by the Manipal University Jaipur.*

Conflict of Interest: *There is no conflict of interest.*

REFERENCES

1. C. Liu, F. Li, L. P. Ma, H. M. Cheng, *Adv. Mater*., **22**, 28 (2010).
2. Y. Luo, L. Guo, M. Xiao, S. Wang, S. Ren, D. Han, Y. Meng, *J. Mater. Chem. A*, **8**, 4629 (2020).
3. U. S. Kim, C. B. Shina, C. S. Kim, *J. Power Sources*, **189**, 841 (2009).
4. J. Y. Choi, D. J. Lee, Y. M. Lee, Y. G. Lee, K. M. Kim, J. K. Park, K. Y. Cho, *Adv. Funct. Mater*., **23**, 2108 (2013).
5. H. Vikstrom, S. Davidsson, M. Hook, *Appl. Energy*, **110**, 252 (2013).
6. L. Lu, X. Han, J. Li, J. Hua, M. Ouyang, *J. Power Sources*, **226**, 272 (2013).
7. V. Aravindan, J. Gnanaraj, S. Madhavi, H. K. Liu, *Chem. Eur. J*., **17**, 14326 (2011).
8. Y. Liu, D. Gao, H. Xiang, X. Feng, Y. Yu, *Energy Fuel*, **35**, 12921 (2021).
9. M. Wang, M. Tang, S. Chen, H. Ci, K. Wang, L. Shi, L. Lin, H. Ren, J. Shan, P. Gao, Z. Liu, H. Peng, *Adv. Mater*., **29**, 1703882 (2017).
10. S. Yi, B. Wang, Z. Chen, R. Wang, D. Wang, *RSC Adv*., **8**, 18597 (2018).
11. H. Chu, H. Tuan, *J. Power Sources*, **346**, 40 (2017).
12. C. Iwakura, Y. Fukumoto, H. Inoue, S. Ohashi, S. Kobayashi, H. Tada, M. Abe, *J. Power Sources*, **68**, 301 (1997).
13. A. H. Whitehead, M. Schreiber, *J. Electrochem. Society*, **152**, A2105 (2005).
14. H. C. Wu, H. C. Wu, E. Lee, N. L. Wu, *Electrochem. Comm*., **12**, 488 (2010).
15. P. R. Das, L. Komsiyska, O. Osters, G. Wittstock, *J. Electrochem. Society*, 162, A674 (2015).
16. X. Meng, *IOP Conf. Ser.: Earth and Environ. Sci., IOP Publishing*, **300**, 042039 (2019).
17. Y. Nishi, *The Chemical Record*, **1**, 406 (2001).

18. C. Liu, Z. G. Neale, G. Cao, *Mater. Tod*., **19**, 109 (2016).
19. M. N. Obrovac, V. L. Chevrier, *Chem. Rev.*, **114**, 11444 (2014).
20. S. J. Dillon, K. Sun, *Curr. Opinion in Solid State and Mater. Sci.*, **16**, 153 (2012).
21. M. S. Islam, C. A. Fisher, *Chem. Soc. Rev*., **43**, 185 (2009).
22. P. Zhu, D. Gastol, J. Marshall, R. Sommerville, V. Goodship, E. Kendrick, *J. Power Sources*, **485**, 229321 (2021).
23. L. Liu, H. Zhao, Y. Lei, *Small Methods*, **3**, 1800341 (2019).
24. L. Kong, H. Peng, J. Huang, Q. Zhang, *Nano Res*., **10**, 4027 (2017).
25. O. Y. Chusid, E. E. Ely, D. Aurbach, M. Babai, Y. Carmeli, *J. Power Sources*, **43**, 47 (1993).
26. N. S. Choi, Y. M. Lee, J. H. Park, J. K. Park, *J. Power Sources*, **119**, 610 (2003).
27. S. Hossain, Handbook of Batteries, 2nd edn., 1995.
28. D. Guyomard, J. M. Tarascon, *Solid State Ion*ics, **69**, 222 (1994).
29. D. Aurbach, A. Zaban, Y. Ein-Eli, I. Weissman, O. Chusid, B. Markovsky, M. Levi, E. Levi, A. Schechter, E. Granot, *J. Power Sources*, **68**, 91 (1997).
30. D. Aurbach, O. Chusid, I. Weissman, P. Dan, *Electrochim. Acta***, 41**, 747 (1996).
31. D. Aurbach, *Nonaqueous Electrochem*., 289 (1999).
32. J. S. Gnanaraj, E. Zinigrad, M. D. Levi, D. Aurbach, M. A. Schmidt, *J. Power Sources*, **119**, 799 (2003).
33. M. Oswal, J. Paul, R. Zhao, University of Southern California, 2419 (2010).
34. D. Lepage, C. Michot, G. Liang, M. Gauthier, S. B. Schougaard, *Angew. Chem*., **123**, 7016 (2011).
35. L. J. Her, L. J. Hong, C. C. Chang, *J. Power Sources*, **157**, 457 (2006).
36. C. Arbizzani, M. Mastragostino, M. Rossi, *Electrochem. Comm*., **4**, 545 (2002).
37. A. V. Murugan, *Electrochim. Acta*, **50**, 4627 (2005).
38. X. Liu, H. Li, M. Ishida, H. Zhou, *J. Power Sources*, **243**, 374 (2013).
39. D. L. Ma, Z. Y. Cao, H. G. Wang, X. L. Huang, L. M. Wang, X. B. Zhang, *Energy Environ. Sci*., **5**, 8538 (2012).
40. V. A. Nguyen, C. Kuss, *J. Electrochem. Society*, **167**, 065501 (2020).
41. H. Zhong, A. He, J. Lu, M. Sun, J. He, L. Zhang, *J. Power Sources*, **336**, 107 (2016).
42. H. Guo, L. Liu, Q. Wei, H. Shu, X. Yang, Z. Yang, M. Zhou, J. Tan, Z. Yan, X. Wang, *Electrochim. Acta*, **94**, 113 (2013).
43. M. Ling, J. Qiu, S. Li, C. Yan, M. J. Kiefel, G. Liu, S. Zhang, *Nano Letters*, **15**, 4440 (2015).
44. Y. Shi, X. Zhou, J. Zhang, A. M. Bruck, A. C. Bond, A. C. Marschilok, K. J. Takeuchi, E, S. Takeuchi, G. Yu, *Nano Letters*, **17**, 1906 (2017).
45. D. Shao, H. Zhong, L. Zhang, *Chem. ElectroChem*., **1**, 1679 (2014).
46. S. N. Eliseeva, E. V. Shkreba, M. A. Kamenskii, E. G. Tolstopjatova, R. Holze, V. V. Kondratiev, *Solid State Ionics*, **333**, 18 (2019).
47. B. Liu, P. Soares, C. Checkles, Y. Zhao, G. Yu, *Nano Letters*, **13**, 3414 (2013).
48. T. M. Higgins, S. H. Park, P. J. King, C. Zhang, N. McEvoy, N. C. Berner, D. Daly, A. Shmeliov U. Khan, G. Duesberg, V. Nicolosi, J. N. Coleman, *ACS Nano*., **10**, 3702 (2016).
49. D. Liu, Y. Zhao, R. Tan, L. L. Tian, Y. Liu, H. Chen, F. Pan, *Nano Energy*, **36**, 206 (2017).
50. G. Zhang, K. Lin, X. Qin, L. Zhang, T. Li, F. Lv, Y. Xia, W. Han, F. Kang, B. Li, *ACS Appl. Mater. Interfaces*, **12**, 37034 (2020).
51. S. Myung, Y. Hitoshi, Y. Sun, *J. Mater. Chem*., **21**, 9891 (2011).
52. T. Ma, G. Xu, Y. Li, L. Wang, X. He, J. Zheng, J. Liu, M. Engelhard, P. Zapol, L. Curtiss, J. Jorne, K. Amine, Z. Chen, *J. Phys. Chem. Lett*., **8**, 1072 (2017).
53. L. Luo, P. Zhao, H. Yang, B. Liu, J. G. Zhang, Y. Cui, G. Yu, S. Zhang, C. M. Wang, *Nano Letters*, **15**, 7016 (2015).
54. Y. Y. Zhang, S. J. Zhang, J. T. Li, K. Wang, Y. C. Zhang, Q. Liu, R. S. Xie, Y. R. Pei, L. Huang, S. G. Sun, *Electrochim. Acta*, **298**, 496 (2019).
55. S. Jin, S. Xin, L. Wang, Z. Du, L. Cao, J. Chen, X. Kong, M. Gong, J. Lu, Y. Zhu, H. Ji, *Adv. Mater*., **28**, 9094 (2016).
56. D. Shin, Y. Song, D. Nam, J. H. Moon, S. W. Lee, J. Cho, *J. Mater. Chem. A*, **9**, 2334 (2021).
57. H. Xu, H. Jin, Z. Qi, Y. Guo, J. Wang, Y. Zhu, H. Ji, *Nanotech*., **31**, 205710 (2020).
58. S. Jin, Y. Jiang, H. Ji, Y. Yu, *Adv. Mater*., **30**, 1802014 (2018).
59. C. Jeong, S. Lee, J. Kim, K. Y. Cho, S. Yoon, *J. Power Sources*, **398**, 193 (2018).
60. C. Portet, P. L. Taberna, P. Simon, C. Laberty-Robert, *Electrochim. Acta*, **49**, 905 (2004).
61. J. Li, C. Rulison, J. Kiggans, C. Daniel, D. L. Wood, *J. Electrochem. Soc*., **159**, A1152 (2012).
62. C. Busson, M. Blin, P. Guichard, P. Soudan, O. Crosnier, D. Guyomard, B. Lestriez, *J. Power Sources*, **406**, 7 (2018).
63. L. Liu, H. Zhao, Y. Lei, *Small Methods*, **3**, 1970023 (2019).

Bulgarian Chemical Communications, Volume 54, Special Issue C (pp. 11-18) 2022 DOI: 10.34049/bcc.54.C.0011

Green synthesis of metallic nanoparticles and its potential to enhance production of agricultural crops: A review

Kh. Parveen, L. Ledwani*

Manipal University Jaipur, India

Accepted: July 06, 2022

Nanoscience and nanotechnology have gained much attention in recent years in the agricultural field. The small size (1-100 nm) and large surface area of nanomaterials unlocks their applications in several potential functions. The chemical and physical nature of metallic nanoparticles is different as compared to non-metallic nanoparticles. Green synthesis of metallic nanoparticles is less costly and not harmful to the environment. Therefore, applications of these metal-based nanoparticles are very effective and quite safe in the development of agricultural crops. Sustainable agriculture is the need of the hour. Review also shows the impact of nanomaterials on seed germination, crop growth and quality improvement. Agricultural crops diseases are one of the major factors that can limit crop productivity and have a serious impact on the economic output of a farm. This paper provides a compilation of technologies involved in the green synthesis of metallic nanoparticles and an overview of the application of nanotechnology in agriculture with a special focus on plant protection products and nano-pesticides.

Keywords: Nanotechnology, Green synthesis, Metallic nanoparticles, Agricultural field

INTRODUCTION

Many practical applications of metallic nanoparticles (particles sized less than 100 nm) are studied due to their number of special properties [1-4]. Different processes are widely used to synthesize metallic nanoparticles (NPs). Metallic nanoparticles involved zinc (Zn), cooper (Cu), silver (Ag), gold (Au) and their oxides, etc. However, the production of these metallic nanoparticles through chemical and physical methods is usually very costly, labor-intensive and they are very dangerous to the ecosystem [5. 6]. Thus, there is the need for an alternative method, which is cost-effective and at the same time environment-friendly and less toxic, that is known as green nanotechnology. In the past years, many biological systems like plants, fungi, bacteria, algae, human cells, etc. are used for the synthesis of metal nanoparticles. These biological systems contain proteins and metabolites that can be reduced to inorganic metal ions and form metal nanoparticles. This formation of metallic NPs through metal ions involves a capping process.

Agriculture is an important field of economics development where new techniques are often applied to enhance crops' productivity and quality. Application of nanoparticles in agriculture area called nano-agriculture i.e., advanced technology is often applied to increase the yield [7]. Synthesized NPs through various biological sources can be used in agriculture [8]. The use of metallic nanoparticles (NPs) in the sector of agriculture was found to be very effective in controlling biotic and abiotic stresses, decreasing the use of agrochemicals like pesticides and fungicides, and supervising the use of insecticides in a good and non-polluting manner. Farmers use many agrochemicals such as insecticides, herbicides, fungicides, either by spaying or by broadcasting at different time intervals. A large quantity of fertilizers is lost-because of various factors, namely, leaching, decomposition, photolysis, hydrolysis and microbial reduction, etc. Therefore, there is a need for non-toxic agrochemicals that can stay for long time on agricultural land. The major techniques of nanoparticle applications on crops include traditional approaches such as direct exposure to seeds and through culture media or by soil, spraying the NPs on the surface of plants, hydroculture (culture in water) and many more. New approaches for introducing NPs include cell isolation, protoplast incubation, biolistics etc. The support of nanotechnology in phytopharmaceutical products has increased exponentially, which may assure increased crop yield.

Rouhani *et al.* have carried out an *in-vivo* study for understanding the metallic NPs and chemical suspensions efficiency on cotton plants, affected by aphid that can be taken as a reference [9]. The results showed that NPs solution slows down the speed of action in the plant in comparison to the chemical solution but on the other hand, NPs solution was better in increasing the insertion in the plant [10].

* To whom all correspondence should be sent:
E-mail: lalitaledwani@gmail.com; lalita.ledwani@jaipur.manipal.edu

NPs can insert into the crop by various pathways, and the uptake rate of NPs depends on the size, shape, concentration, and charge present on the surface of nanoparticles [11]. NPs present on shoot surfaces of crops initiate the interaction with aerial parts. The use of NPs was found to have a positive impact on crop parameters of growth like germination, length, development, etc. Application of NPs like carbon-based, metal- and metal oxide-based shows effects on crop development (number of seminal rooting, elongation of root, length of shoot, seeds quantity, and quality of the flowers), leading to enhanced crop biomass and productivity [12-14].

The application of NPs into the soil can proceed directly to the soil or indirectly by nano fertilizers and pesticides [15, 16]. Study and monitoring of activity of microbes and diversity shows the effects of NPs on the soil. The activity of microorganisms fully depends on the NPs features and properties (category, amount, size, and functional groups present in the NPs).

The present compilation article gives a brief glimpse of a present global scenario on the effective utilization of bioinspired metallic nanoparticles and their research in the agricultural field. There are the following important elements for obtaining productive results: i) ability of nanofabricating novel materials, and its mechanism; ii) understanding the plant and soil interaction with nanoparticles; iii) micronutrient's deficiency improvement, and their availability increases; iv) environment safety and environmental obedience. Nanotechnology can sustainably reduce production costs in agriculture. Nano-farming has become a truly revolutionary area for the future of sustainable agriculture.

Raw materials for food industries are dependent upon the important and stable sector that is 'Agriculture'. Growth of the world population increases with the limitations of natural non-renewable resources (productive land, water, soil). That's why necessities claim for agricultural development to be economically strong, viable, eco-friendly and efficient. The improvement in the field of agriculture is mandatory for removing poverty and hunger. Therefore, new, sustainable and cost-effective techniques should be adopted for better agricultural production [17]. Sustainable growth of agriculture totally depends upon the new and innovative technologies just like nanotechnology. In order to ensure sustainable development of agriculture some important points are listed below [18-20]:

1. Specialized institutes with trained expertise can be established to assess the biosafety of NPs on the field and also reduce farming problems. With the passage of time, people become more trained for practical applications in agriculture.
2. For monitoring and evaluation of NPs based system, strict and clear guidelines should be followed in the context of food safety.
3. Evaluation of NPs-mediated toxicity on the environment and organisms should be properly documented for the researchers and for the farmers.
4. More research and collaboration should be carried out for better development of portable, easy-to-use nano-sensor and NPs-based applications.
5. Controlled and naturally produced NPs through plant root endophytes and *mycorrhizae* fungi must be studied for a better understanding of the interaction of NPs with plants.

The reason behind applying nanoparticles in the field of agriculture is to reduce chemicals amount, minimize nutrient loss due to fertilizers and increase production with good quality. Nanotechnology has the ability to advance NPs techniques for controlling crop pests and diseases with improved nutrient absorbing capacity. The significant interests of using nanotechnology in the agricultural field include fertilizers with NPs suspension and pesticides with NPs for obtaining less harmful products and to increase nutrient level without impurities in soil, water and protection against crop diseases. Nitrogen loss from leaching, emission and microbial degradation can be recovered due to NPs techniques. Nanotechnology may act as a detector for observing soil quality in the agricultural fields and hence to maintain the health of agricultural crops. Nano farming techniques do not contaminate water and soil while improving the productivity of crops.

NATURE OF METALLIC NANOPARTICLES

Nanoparticles have properties (physical and chemical) through which they can be applied in agricultural industries. Though it's very difficult to understand the nature of nano-scale particles but their properties are different and unique as compared to the bulk materials [21, 22]. For the application in agriculture, NPs production, characterization and mechanism must be well understood.

Physical properties

Physical properties of NPs include many features as shown in Fig. 1 but size, shape, surface area and size distribution are few important factors that can control the uptake of nanoparticles like lead, copper, zinc, cadmium, etc. [23-25]. Cell wall permeability and size of the stomata can affect the transportation of the nanoparticles.

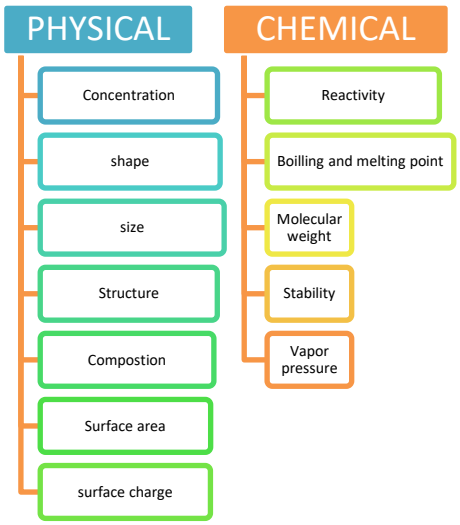

Figure 1. Physical and chemical nature of nanoparticles

Size and shape. The size and shape of nanoparticles are identified as important properties. It was postulated that nanoparticles size below 20-30 nm are thermodynamically unstable and are full of energy at the surface [26]. As the size of nanoparticles decreases, the surface area of the molecules present in the material increases in an exponential trend. The studies showed the different effects of nanoparticles size ranging from 50-200 nm on the growth of the *Arabidopsis* plant [27]. Different shapes of synthesized metallic NPs like square, tube, spherical, etc., are gaining lot of attention. The optical features of NPs also depend on the shape and size of the NPs.

Surface and size distribution of nanoparticles. Scanning electron microscope (SEM) and Brunauer–Emmett–Teller (BET) are the techniques that detect surface structure and area of synthesized NPs. The large surface area of NPs has faster effects as compared to the bulk materials. Dynamic light scattering (DLS) used to calculate the size distribution of NPs, and zeta potential can be used to evaluate the charge present on the surface of the synthesized NPs. Charge present on NPs affects the interaction of NPs with the plant cell membrane [28]. Cellular uptakes by plants are usually dependent on the surface hydrophobicity, size and charge of the solution. NPs with positive charge are taken up faster by plant cells as compared to neutral or negatively charged NPs. The diffusion of NPs in a liquid solution mainly depends on the surface charge of these NPs.

Chemical properties

Properties like structure, composition, phase identity, surface chemistry and reactivity are the chemical properties of metallic nanoparticles. Chemical features also include the surface chemistry and photocatalytic properties of nanomaterials in which elemental composition is studied by zeta potential [29, 30]. Property of NPs is understood by the kind of electronic motion occurring in the particles. There are many varieties of NPs that are contributing different chemical properties [31]. Metallic NPs have flexible properties which can be modified by their own, when they are interacting with other materials.

During synthesis, nanoparticles can control over their size and shape. They can also change their morphology, encapsulation freedom and optical properties while it is limited to selected NPs only. While synthesizing the metal oxide nanoparticles, they show these unique chemical properties because of their size and high density of corner surface. Size of the NPs also affects many features of any matter. Morphology feature includes shape, area and size which all are related to the electronic nature of metal oxide NPs [32]. Nanotechnology can have huge impact in agriculture production. Optimizing of process parameters can help in formulating nanoparticle-based fertilizers [33].

SOURCES AND GREEN SYNTHESIS OF METALLIC NANOPARTICLES

As compared with chemical (toxic) synthesis of NPs, the green method is innovative, simple (easy), economic and re-usable and gives stable products. Green nanomaterials can be synthesized mainly by plants and microorganism sources, Fig. 2. The green synthesis of NPs through plants parts is easier to be realized in large scale in comparison to the synthesis by microorganisms.

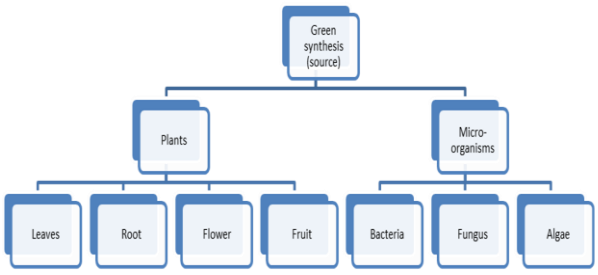

Figure 2. Different sources of synthesis of nanoparticles through a green method.

Eco-friendly and non-toxic route of bioinspired nanomaterials is advantageous in agriculture field [33]. Improvement in germination, growth and productivity along with the improvement of quality of crops has been reported with the use of green nanomaterials [34, 35, 38]. Consequently, the

applications of metal-based nanoparticles are very effective and safe for the development of agricultural cultures.

METHODS OF USING NANOPARTICLES ON AGRICULTURAL CROPS

Nanoparticles exposure on crops has gained attention in recent years. Numerous studies were done on the effect of metallic nanoparticles on different varieties of agricultural crops. The method by which NPs are introduced on the crops gives profitable effect on the interaction of NPs and plants. NPs availability, collection, storage and movement (translocation) by plants also get affected. Though the nanoparticles-plant interactions seem lucrative, the ultimate availability, translocation, accumulation, and subsequent effects of nanoparticles depend primarily on the mode of their administration in addition to the element's availability, uptake and storage capacity of plants. Consequential human exposure of NPs represents an important pathway that considers carrying and assimilation of nanoparticles in plants. Therefore, the techniques that were used for good and efficient NPs–plant interaction need more attention and consideration in consequential process [39]. The major methods of using nanoparticles on agriculture crops include traditional methods such as direct seed and seedling exposure, spaying, hydroculture, etc., while modern techniques include isolated cells, protoplast incubation and biolistics. Some techniques are discussed below.

Seed exposure

Germination of the seed is basically described as the inhibition of water and nutrient which leads to sprouting of radicle and plumule by puncturing the coat of seeds [40]. Protection of the seed from biotic and abiotic factors can be done by the selective permeability of the seed cover. The nature of the seed coat is selectively permeable for definite size, shape and charge of outsider particles that were trying to reach at the sensitive parts of the seed. There have been reports conducted to understand the effects of NPs on the sprouting of seeds (germination), and uptake of the NPs [41, 42]. Primary methods of NPs introduction in seeds are either soaking the seeds in NPs solution for some days or direct germinating seeds in nanoparticle-spiked media or soil.

Application of 5 kinds of NPs (carbon nanotube (MWCNT), Al, alumina, Zn, and ZnO_2) on different seeds, *viz*., rape (*Brassica napus)*, radish (*Raphanus sativus*),), lettuce (*Lactuca sativa*), ryegrass (*Lolium perenne*), maize (*Zea mays*), and cucumber (*Cucumis sativus*) were recorded by an incubation process in which seeds were soaked in NP solution, and then transferred in different petri plates with distilled water and put in an incubator [43-46]. Seeds with NPs solution give bettwe results as compared to the normal soaking. It has been reported that the process of soaking is good and less time consuming [47].

Spraying

Recently, many studies are involved in NPs-plant exposure *via* roots, either directly or during the stage of germination. Although the knowledge of responding after contacting plant foliar part and leaves with atmospheric NPs is limited, so more research is required in this field. The significant responses of crop leaf are unavoidable because of collecting of atmospheric particles or by applications of purpose-built NPs [39].

The spraying process of nanoparticles that was used in large-scale field is same as that used by farmers for controlling pests. The NPs spays are safe for the crops and can resist against the pest for a long time. Plant protection technologies are more successful when applied by foliar spraying of NPs in comparison to traditional soil-root treatment. To further advance this technology, it is also necessary to look at significant elements that inhibit the uptake of NPs by foliage, such as wax deposits on leaf surfaces, environmental conditions (such as light, temperature, and humidity), and the physical and chemical characteristics of NPs.

Biolistics

Direct introduction of DNA or RNA into plant cells defines the biolistic transformation technique. In this method, artificial/modified DNA or RNA was constructed by coating onto metallic NPs like gold. Coated DNA or RNA was released through gun with high pressure helium gas that directly inserts in the host cell wall. Torney *et al*. have reported a coated DNA from Type-II MSNs (mesoporous silica nanoparticles system) for endocytosis experiments in which 1 mg of filtered plasmid DNA was incubated with 10 mg of MSN with 50 ml of water for 2 h. The MSNs were washed with W5 media for isolating protoplasts [48]. Y-segmented petri dishes were used in the germination of plants. After bombardment with nanoparticles the plants were evaluated for 48 hrs. This method is also very modern and innovative, but it cannot be used for a large number of crops [48].

NANOPARTICLES' EFFECT ON SEED GERMINATION, CROP GROWTH AND QUALITY IMPROVEMENT

Due to special physiochemical properties of nanomaterials, they provide many opportunities in the agricultural sector. The interconnection of NPs with plants shows several physiological, morphological, and genotoxic changes, and their interpretation is important for the productive use of nanotechnology in agriculture. Metallic nanoparticles can be inserted in plants through various ways. NPs can be produced by itself or by metal ions oxidized by metal oxide in soil solution and followed by the reduction in plant system and transferred as ions [49]. Different biotic and abiotic stresses influenced the growth of plants.

Physicochemical properties of NPs like shape, size, charge, composition, surface modification and reactivity give subsequent effect on NPs-plant interaction [50, 51]. Along with other factors, concentration of NPs is also giving effect on NP-plant relation and the effect is varying from plant to plant.

Seed germination

Germination of the seed is the premier stage of a phytology. Interaction between plant system and NPs mainly occurs through seeds as they are the first point of interaction. Seed germination and growth can be estimated by the appearance of radical and plumule in seed. The effect of NPs on the seed growth can be estimated by the seed germination as the 1st stage of primary database. It was reported by Siddiqui et al that when low concentration of silica NPs (SiO_2 NPs) was introduced on tomato seeds, improved germination was occurred [52]. It was also reported that when the SiO_2 were mixed with growth medium and absorb by maize seeds with adequate pH turn the rate of germination increases and give positive effects on better nutrient availability [52, 53]. Seed germination and growth of roots of zucchini seeds were cultured in hydroponic medium augmented with ZnO NPs which showed no adverse effects [54] whereas in the case of rye grass (*Lolium perenne*) and maize (*Zea mays*), the seed sprouting was improved by Zn NPs with 35 nm in size and by ZnO_2 with 15–25 nm, respectively [55]. Zheng *et al.* (2007), Hong *et al.* (2005), Yang *et al.* (2007) and Gao *et al.* (2008) showed positive effects of TiO_2 NPs on plants [56-59]. TiO_2 NPs have been recorded to improve the germination and enhance the radicle and plumule growth of canola (*Brassica napus*) seedlings [60]. When TiO_2 NPs were inserted in the spinach seeds improved germination was observed with enhanced vigor [56].

Growth of crops

After germination of seeds, enhancement in plant length (shoot and root) describes the growth of plant. Growth of crops is also characterized by its shoot and root length, number of laterals and leaves and size of leaves with total biomass. When NPs interact with the plant roots, they either promote the growth of the roots and other parts of the plants after translocated to higher tissues or block the channels of penetration of the nutrient supply through the root. A few reports are available on the movement of NPs in plant tissues, therefore the mechanism behind the movement is also not clearly understood. Overall, the effects observed are related to the interaction of NP with roots, facilitating or preventing nutrient supply and transport to higher tissues [61].

When SiO_2 NPs were introduced into Changbai larch (*Larix olgensis*) seedlings, the rate of growth was increased, involving shoot height, root collar diameter, length, number of root laterals and it also gave effect on the chlorophyll synthesis [62]. In another research, rice plants were treated with bare quantum dots (QDs) and silica-coated QDs and found that silica-coated QDs significantly promoted root growth [63].

Au NPs showed good results in increasing the number of leaves and area, shoot height and the amount of chlorophyll of the treated plant [64, 65]. In the previous studies it was witnessed that Ag NPs can improve the growth of mustard, bean (*Phaseolus vulgaris*), and maize and the area of their leaves also increases [66, 67]. Copper NPs (Cu NPs) were mixed with agar media for testing of seeds of mung bean and wheat [68]. During the experiment it was observed that mung bean shows higher sensitivity to Cu NPs as compared to the wheat plant, noticeable inhibition in the growth of seedlings being observed [68].

Quality improvement

The physical and chemical changes taking place in the plant spread light on the efficiency and metabolic process that were actively happening in the plant system which includes growth, reproduction and development. These parameters are much affected by biotic and abiotic factors of environment along with NPs. Application of metallic and metal oxide NPs gives positive result in growth parameters which ultimately lead to high productivity and quality.

When Ag NPs were applied in the soil of wheat crops, an improvement in growth and yield was reported [69].

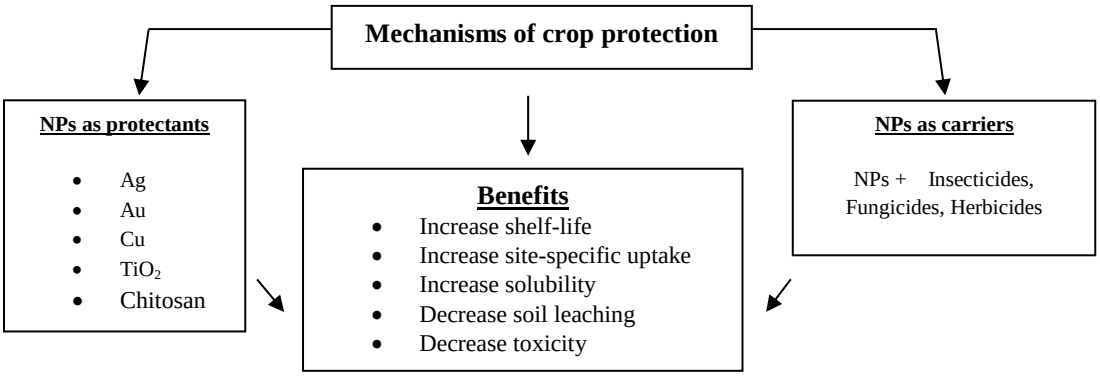

Figure 3. Crop protection by nanoparticles

Comparing with normal growth of wheat crops exposed to 25 to 50 ppm Ag NPs give better results in height and dry weight. Similar effects were shown in Indian mustard (*Brassica juncea*) where improvement in root and shoot length was reported and chlorophyll contents were also good [67].

NANOMATERIALS IN CONTROLLING CROPS PATHOGENS

Every 20% to 40% crops are destroyed due to pest and pathogens [70]. Nanotechnology offers advantages over toxic pesticides which could have positive impacts on environment. The use of NPs to protect crops can occur *via* two different mechanisms: a) NPs themselves providing crop protection b) NPs as carriers for existing pesticides, Fig. 3.

Nanoparticles as pesticides

Metallic nanoparticles can be applied on crops for the management of harmful pests and weeds and NPs can be used for preparing nano pesticides, nano fungicides and nano herbicides [70].

Insecticides. Insects are common creatures which are found all over the ecosystems. They almost depend on all the varieties of agricultural crops. Important crops like wheat, maize, rice, barley, etc. are facing lots of problems due to insects which spread diseases [71]. Nanotechnology offers a wide number of metallic NPs which can be synthesized by green methods and can be used as insecticides in controlling insects [72].

Stadler *et al.* reported that alumina NPs activity on two varieties of stored grains, namely *Rhyzopertha dominicoorzae* and *Sitophilus oryzae*, results show that NPs action is based on physical phenomenon instead of biochemical phenomenon in which insects become dead due to dehydration [73]. Silica NPs of 0.5 mg/cm killed the larvae of *Spodoptera litura* [74]. Researchers reported that a 5-25 mg/l concentration of Ag NPs killed adult *Hematophagous* flies, *Hippobosca maculate*, cattle ticks, and *Rhipicephalus* (Boophilus*) microplus* [75].

Fungicides. Fungi are the reason of damaging many crops by spreading fungal diseases [76]. It is evaluated that 85% crops diseases are due to fungus. To combat fungi, farmers have been using many chemical fungicides. This can lead to damage of the human body system. NPs that were made by green methods are less harmful when used as fungicides. Recently, *in vitro* assay conducted by many researchers showed strong inhibitory effects of biosynthesized Ag NPs against various fungal diseases [77-79]. Eco-friendly solutions of nanoparticles and fungicides enable smaller amounts of the nano-fungicides to be applied in given time period. In that way the modified NPs helps to protect the environment.

Herbicides. Herbicides that were made up of NPs can take the place of herbicides which were made of chemicals and are very much hazardous if the consumption becomes high. Nanoparticles-based herbicides improve the solubility and decrease the toxic effect when compared with chemical herbicides. The synthesis of herbicides made with particular NPs targeted at the point of root where the weeds are born. Nano-herbicides enter the root of the weeds and inhibit the cycle of glycolysis of the weed. This inhibition action generates deficiency of nutrients in the targeted weed and thus the weed become dead.

CONCLUSION

Nanoscience and nanotechnology have attracted a great deal of attention in recent years in the field of agriculture. The green synthesis route of metallic nanoparticles is more cost-effective, environmentally friendly and sustainable for agricultural development. The diseases of agricultural crops are one of the main factors that can restrict the productivity of crops and have a serious impact on the economic production of an agricultural enterprise. This article presents a compilation of technologies involved in the green synthesis of

metallic nanoparticles, including an overview of the application of nanotechnology in agriculture with particular emphasis on phytopharmaceutical and nano-pesticide products. Green nanomaterials have potential to substitute a conventional agricultural practice as they can enhance the crop productivity in a targeted way without the release of any harmful chemicals with maintenance of soil fertility. Although there is a huge potential of green nanomaterials in crop productivity and disease resistance, systematic and detailed study needs to be carried out to understand exact mechanism pathways along with its long-term effect in future.

REFERENCES

1. M. C. Roco, *Curr. Opin. Biotechnol*., **14**, 337 (2003).
2. L. Zhang, F. X. Gu, J. M. Chan, A. Z. Wang, R. S. Langer, O. C. Farokhzad, *Clin Pharmacol Ther.*, **83**, 761 (2008).
3. M. C. Daniel, D. Astruc, *Chemical Reviews*, **104**, 293 (2004).
4. T. S. Wong, U. Schwaneberg, *Curr. Opin. Biotechnol*., **14**, 590 (2003).
5. K. B. Narayanan, N. Sakthivel, *Adv. Colloid Interface Sci*., **156**, 1 (2010).
6. P. P. Gan, S. H. Ng, Y. Huang, S. F. Li, *Bioresour. Technol*., 113, 132-5 (2012).
7. J. S. Duhuan, R. Kumar, N. Kumar, P. Kaur, K. Nehra, S. Duhan, Nanotechnology: The new perspective in precision agriculture Biotechnology Reports, 2017, p. 11.
8. P. Kaur, R. Thakur, J. S. Duhan, A. *Chaudhary, Journal of Chemical Technology and Biotechnology*, **10**, 1002 (2018).
9. Rouhani, S. Mohammad, K. S. Mohammad, *Journal of Agricultural Research*, **10** (1), 590 (2012).
10. A. L. Boehm, I. Martinon, R. Zerrouk, E. Rump, H. Fessi, *J. Microencapsul*., **20**, 433 (2003).
11. J. C. Tarafdar, Y. Xiang, W.-N. Wang, Q. Dong, P. Biswas, *Appl. Biol. Res*., **14**, 138 (2012).
12. C. M. Rico, S. Majumdar, M. Duarte-Gardea, J. R. Peralta-Videa, J. L. Gardea-Torresdey, *J. Agric. Food Chem*., **59**, 3485 (2011).
13. H. Feizi, P. R. Moghaddam, N. Shahtahmassebi, A. Fotovat, *Biol. Trace Elem. Res*., **146**, 101 (2012).
14. N. Bala, A. Dey, S. Das, R. Basu, P. Nandy, *Iran. J. Plant Physiol.* **4**(3), 1061 (2014).
15. P. Gajjar, B. Pettee, D. Britt, W. Huang, W. Johnson, A. Anderson, *J. Biol. Eng*., **3**, 9 (2009).
16. M. V. Khodakovskaya, B. Kim, J. N. Kim, M. Alimohammadi, E. Dervishi, T. Mustafa, C. E. Cernigla, *Small.*, **9**, 115 (2013).
17. C. Yunlong, B. Smit, *Agric. Ecosyst. Environ.*, **49**, 299 (1994).
18. G. Pandey, *Environmental Technology & Innovation*, **11**, 299 (2018).
19. A. Acharya, P. K. Pal, *Nano Impact*, **19**, 100232 (2020).
20. R. Prasad, A. Bhattacharyya, Q. D. Nguyen. *Frontiers in Microbiology*, **8**, 1014 (2017).
21. D. L. Slomberg, M. H. Schoenfisch, *Environ. Sci. Technol*., **46**, 10247 (2012).
22. S. Honary, F. Zahir, *Trop. J. Pharmaceut. Res*., **12**, 255 (2013).
23. A. Cadden, *J. Food Sci*., **52**, 1595 (1987).
24. C. Rao, K. Biswas, *Annu. Rev. Analyt. Chem.*, **2**, 435 (2009).
25. G. Schmid, Wiley-VCH, Weinheim, Germany, 2011.
26. P. Ayyub, V. Palkar, S. Chattopadhyay, M. Multani, *Phys Rev B.*, **51**, 6135 (1995).
27. D. Nath, P. Banerjee, B. Das, *J. Nanomedicine Biother. Discov*., **4**, 1 (2014).
28. K. M. Manjaiah, R. Mukhopadhyay, R. Paul, S. C. Datta, P. Kumararaja, B. Sarkar, in: M. Mariano, S. Binoy, L. Alessio, (eds.), Modified Clay and Zeolite Nanocomposite Materials, Elsevier, Amsterdam, The Netherlands, 2019, p. 309.
29. M. V. Khodakovskaya, A. S. Biris, *U.S. Patent Application*, 13, 509,487 (2010).
30. A. Joshi, S. Kaur, K. Dharamvir, H. Nayyar, G. Verma, *J. Sci. Food Agric.*, **98**, 3148 (2018).
31. C. Lu, C. Zhang, J. Wen, G. Wu, M. X. Tao, *Soybean Sci.*, **21**, 168 (2002).
32. H. A. Kordon, *J. Biol. Educ*., **26**, 247 (1992).
33. K. Parveen, N. Kumar, L. Ledwani, *Chemistry Select*., **17**, e202200415 (2022).
34. K. Ibrahim, S. Khalid, K. Idrees, *Arabian Journal of Chemistry*, **12**, 908 (2019).
35. K. Parveen, N. Kumar, L. Ledwani, *ChemistrySelect*, **7**, e202200415 (2022).
36. M. Khodakovskaya, E. Dervishi, M. Mahmood, Y. Xu, Z. Li, F. Watanabe, A. S. Biris, *ACS Nano*., **3**, 3221 (2009).
37. A. Shelar, A.V. Singh, R.S. Maharjan, P. Laux, A. Luch, D. Gemmati, V. Tisato, S.P. Singh, M.F. Santilli, A. Shelar, M. Chaskar, R. Patil, *Cells*, **10**, 2428 (2021).
38. A. Maity, *Proc. Natl. Acad. Sci. India Sect. B Biol. Sci*., **88**, 595 (2018).
39. C. Kole, D. Kumar, Sakthi, M. V. Khodakovskaya, Plant Nanotechnology: Principles and Practices, 1st edn., 2016.
40. H. A. Kordan, *J. Biol. Educ*., **26**, 247 (1992).
41. W. Mahakham, P. Theerakulpisut, S. Maensiri, S. Phumying, A.K. Sarmah, *Sci. Total Environ*., **573**, 1089 (2016).
42. J. Banerjee, C. Kole, in: C. Kole, D. Kumar, M. Khodakovskaya, (eds.), Plant Nanotechnology. Springer; Cham, Switzerland: 2016. p. 1.
43. M. H. Lahiani, E. Dervishi, J. Chen, Z. Nima, A. Gaume, A. S. Biris, M. V. A. C. S. Khodakovskaya, *Appl Mater. Interfaces*, **5**, 7965 (2013).
44. A. Srivastava, D. Rao, *Eur. Chem. Bull.*, **3**, 502 (2014).
45. M. V. Khodakovskaya, A. S. Biris, *U.S. Patent Application.* 13, 509,487, 2010.
46. A. Joshi, S. Kaur, K. Dharamvir, H. Nayyar, G. J. Verma, *Sci. Food Agric.*, **98**, 3148 (2018).
47. D. Lin, B. Xing, *Environ. Pollut.*, **150**, 243 (2007).

48. , F. Torney, B. G. Trewyn, V. S. Y. Lin, K. Wang, *Nat. Nanotechnol*., **2**, 295 (2007).
49. C. M. Rico, S. Majumdar, M. Duarte- Gardea, J. R. Peralta-Videa, J. L. Gardea-Torresdey, *J. Agric. Food Chem*., **59**, 3485 (2011).
50. X. Ma, J. Geiser-Lee, Y. Deng, A. Kolmakov, *Sci. Total Environ*., **408**, 3053 (2010).
51. M. V. Khodakovskaya, K. de Silva, A. S. Biris, E. Dervishi, H. Villagarcia, *ACS Nano*., **6**, 2128 (2012).
52. M. H. Siddiqui, M. H. Al-Whaibi, M. Faisal, A. A. Al Sahli, *Environ. Toxicol. Chem*., **33**, 2429 (2014).
53. R. Suriyaprabha, G. Karunakaran, R. Yuvakkumar, V. Rajendran, N. Kannan, *Curr. Nanosci*., **8**, 902 (2012).
54. D. Stampoulis, S. K. Sinha, J. C. White, *Environ. Sci. Technol*., **43**, 9473 (2009).
55. D. Lin, B. Xing, *Environ. Pollution*, **150**, 243 (2007).
56. L. Zheng, M. Su, C. Liu, L. Chen, H. Huang, X. Wu, X. Liu, F. Yang, F. Gao, F. Hong, *Biol. Trace Elem. Res.*, **119**, 68 (2007).
57. F. Hong, P. Yang, F. Q. Gao, C. Liu, L. Zheng, *Chem. Res. Chin. Univ*., **21**, 196 (2005a).
58. F. Yang, C. Liu, F. Gao, M. Su, X. Wu, L. Zheng, F. Hong, P. Yang, *Biol. Trace Elem. Res*., **119**, 77 (2007).
59. F. Gao, C. Liu, C. Qu, L. Zheng, F. Yang, M. Su, F. Hong, *Biometals*, **21**, 211 (2008).
60. H. Mahmoodzadeh, M. Nabavi, H. Kashefi, *J. Ornam. Hortic. Plants*, **3**, 25 (2013).
61. B. Nowack, R. Schulin, B. H. Robinson, *Environ. Sci. Technol*., **40**, 5225 (2006).
62. L. Bao-shan, D. Shao-qi, L. Chun-hui, F. Li-jun, Q. Shu-chun, Y. Min, *J. Forest Res*., **15**, 138 (2004).
63. A. Wang, Y. Zheng, F. Peng, *J. Spectrosc.*, 169245 (2014).
64. S. Arora, P. Sharma, S. Kumar, R. Nayan, P. K. Khanna, M. G. H. Zaidi, *Plant Growth Regul*., **66**, 303 (2012).
65. K. Gopinath, S. Gowri, V. Karthika, A. Arumugam, *J. Nanostruct. Chem*., **4**, 1 (2014).
66. H. M. H. Salama, *Int. Res. J. Biotechnol*., **3**, 190 (2012).
67. P. Sharma, D. Bhatt, M. G. Zaidi, P. P. Saradhi, P. K. Khanna, S. Arora, *Appl. Biochem. Biotechnol*., **167**, 2225 (2012).
68. W. M. Lee, Y. J. An, H. Yoon, H. S. Kweon, *Environ. Toxicol. Chem*., **27**, 1915 (2008).
69. A. Razzaq, R. Ammara, H. M. Jhanzab, T. Mahmood, A. Hafeez, S. A. Hussain, *J. Nanosci. Technol*., **2**, 55 (2016).
70. R. K. Mujeebur, F. R. Tanveer, *Plant Pathology Journal*, **13**, 214 (2014).
71. E. C. Oerke, *J. Agric. Sci.*, **144**, 31 (2006).
72. M. Ramezani, F. Ramezani, M. Gerami, in: D. Panpatte, Y. Jhala (eds.) Nanotechnology for Agriculture: Crop Production & Protection. Springer, Singapore. 2019.
73. T. Stadler, M. Buteler, D. K. Weaver, *Pest Manag. Sci*., **66**, 577 (2010).
74. N. Debnath, S. Mitra, S. Das, A. Goswami, *Powder Technol*., **221**, 252 (2012).
75. T. Santhoshkumar, A. A. Rahuman, A. Bagavan, S. Marimuthu, C. Jayaseelan, A. V. Kirthi, C. Kamaraj, G. Rajakumar, A. A. Zahir, G. Elango, K. Velayutham, M. Iyappan, C. Siva, L. Karthik, R. K. V. Bhaskara, *Exp. Parasitol*., **132**, 156 (2012).
76. T. Giraud, P. Gladieux, S. Gavrilets, *Trends Ecol. Evol*., **7**, 387 (2010).
77. C. Krishnaraj, R. Ramachandran, K. Mohan, P. T. Kalaichelvan, *Spectrochim. Acta A, Mol. Biomol. Spectrosc.*, **93**, 95 (2012).
78. V. Gopinath, P. Velusamy, *Spectrochim Acta A, Mol. Biomol. Spectrosc*., **106**, 170 (2013).
79. K. J. Lee, S. H. Park, M. Govarthanan, P. Hwang, Y. S. Seo, M. Cho, W. H. Lee, J. Y. Lee, S. K. Kannan, *Mater. Lett*., **105**, 128 (2013).

Bulgarian Chemical Communications, Volume 54, Special Issue C (pp. 19-26) 2022 DOI: 10.34049/bcc.54.C.0019

Scope of biopolymers in food industry: A review

J. Rawat, L. Ledwani*

Faculty of Science, Manipal University Jaipur, India

Accepted: July 06, 2022

Plastics have significantly advanced the ever-demanding food industry since the last century. However, it has also induced ecological problems like threat to fragile ecosystems like coral reefs and aquatic life, pollution of air and land, as well as harm to animals through direct digestion due to its non-biodegradable nature. Owing to their extensive desirable properties, polymers as plastics are a fundamental part of the contemporary world. Biodegradable polymers have potential to contribute majorly to reduce the environmental impact of plastic production and processing especially in the food packaging industry. They can be a favourable option as packaging material due to their properties like availability, stability, flexibility, cost effectiveness, etc. It has been reported that certain edible films made of biopolymers such as cellulose, chitosan, pectin can not only be used for packaging of eatables but also improve their texture, flavour, and shelf life. The present review aims to highlight the approaches to replace plastic by biopolymers in food packaging industry and accentuate the research done in this field. This article emphasizes on the types of biopolymers, their sources, properties, assets, drawbacks along with trends of biodegradable packaging that may possibly be followed in the coming times.

Keywords: Biopolymers, Biodegradable packaging, Properties of biopolymers, Edible films, Food preservation

INTRODUCTION

Customer demands for assortments of food consistently, and inclination for comfort have empowered uncommon development of new advancements in packaging to guarantee accessibility of quality food. The essential capacity of foodstuff packaging is to isolate edibles from the general climate, limiting exposure to decay factors including the impacts of microbes, air, atmospheric conditions, and humidity to avoid nutrition loss therefore extending the service life. Thus, it plays a huge role in food safety [1]. Packaging safeguards the food product throughout its life cycle. All conventional methods like wrapping in paper, storing edibles in plastic, glass, and metal containers, have encountered difficulties in edible food packaging. Plastics like polyethylene and PETE are harmful to the environment. Most plastics used for food packaging can be used only once and end up in the ocean or landfill after use. They are acquired through petroleum and are called petroleum-based products. The burning of plastic has resulted in increased emissions of greenhouse gases with carbon dioxide being the most prominent [2].

Petrochemical industries manufacture most of the plastic material from non-renewable sources like synthetic plastics (around 95-99%). Synthetic plastic has a high resistance to physical, chemical, and biological disintegration, resulting in waste accumulation. Waste causes serious environmental and health issues. It builds up on the streets and highways, clogging the drain and causing it to overflow. Plastic waste is discarded in copious quantities into oceans and rivers, endangering marine life. Incineration releases harmful gases into the atmosphere, bringing down the air quality, increasing the risk of climate change, and posing various ailments. Moreover, some types of plastics are non-recyclable making them more vulnerable to single usage. The increasing challenge in discarding of wastes, as well as the negative consequences on the human health and environment caused by the non-degradability of many synthetic polymers, has sparked global alarm [3]. In many industrial applications, biodegradable polymers have evolved as a viable alternative to non-biodegradable plastics.

Biopolymers are not comparable to synthetic plastic in their physical and chemical properties. Hence, they need to be assessed carefully for modifications by blending with other materials. Biopolymers are naturally available. Some sources of biopolymers are shown in Figure 1. Derivatives of biopolymers may be synthesized for obtaining materials with more desirable properties (Table 1).

This article focuses on the types of biopolymers, their properties, and future biodegradable packaging trends. The purpose of this review is to emphasize the importance of using alternatives to plastic in the food packaging industry, as well as the research that has been conducted in this area.

* To whom all correspondence should be sent:
E-mail: lalitaledwani@gmail.com; lalita.ledwani@jaipur.manipal.edu

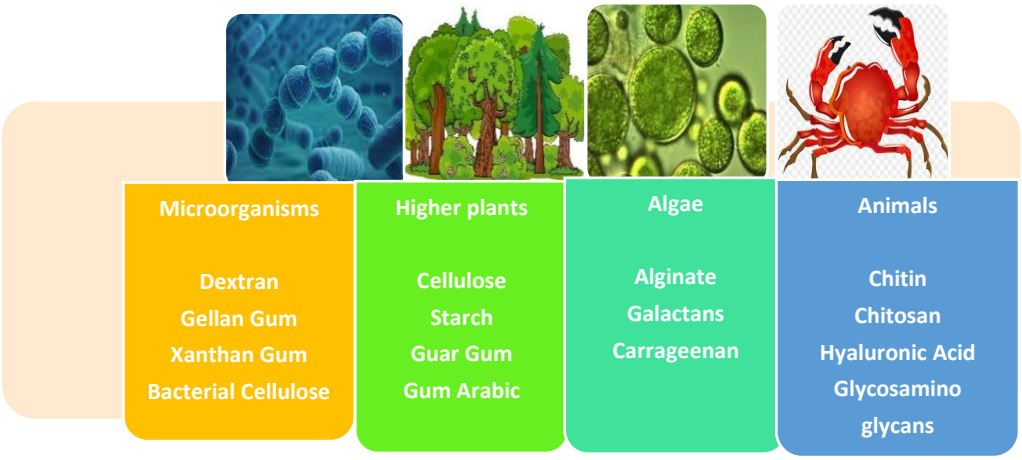

Figure 1. Sources of biopolymers ailments [4].

Table 1. Sources and derivatives of some biopolymers.

Biopolymer	Sources	Derivatives	Ref.
Cellulose	Wood Cotton Bran Plants Bacteria	Cellulose acetate Cellulose sulfate Cellulose nitrate Carboxylmethyl cellulose Ethyl cellulose Methyl cellulose Nanocellulose	[3]
Chitosan	Chitin (exoskeleton of marine invertebrates)	Alpha chitosan Beta chitosan	[1] [5]
Pectin	Citrus peels Apple pomace Sunflower head Sugar beet waste Mango waste	High methoxyl pectin Low methoxyl pectin	[6]
Proteins	Milk Milk products Animal origin Animal origin Corn Soybean	Whey Casein Collagen Gelatin Zein protein Soy protein	[2]
Polyhydroxyalkanoates (PHA)	Extracted from bacteria *via* fermentation of sugar or lipids	Poly(3-hydroxyalkanoate) PHA Poly(3-hydroxyvalerate) PHV Poly(3-hydroxyhexanoate) PHHex Poly(3-hydroxyoctanoate) PHO Poly(3-hydroxydecanoate) PHD	[7] [8]
Polylactic acid (PLA)	Fermented plant starch from corn, cassava, sugarcane	Poly-L-lactic acid (PLLA) Poly-D-lactic acid (PDLA) Poly-DL-lactic acid (PDLLA)	[9]
Alginate	Cell wall of Brown algae (*Phaeophyceae*)	Sodium alginate ($NaC_6H_7O_6$) Potassium alginate ($KC_6H_7O_6$) Calcium alginate ($CaC_6H_7O_6$)	[10] [11]
Thermoplastic starches (TPS)	Starches from plant materials heated with water and then mixed with plasticizers	Thermoplastic cassava starch Thermoplastic corn starch Thermoplastic sugar-palm starch	[12]

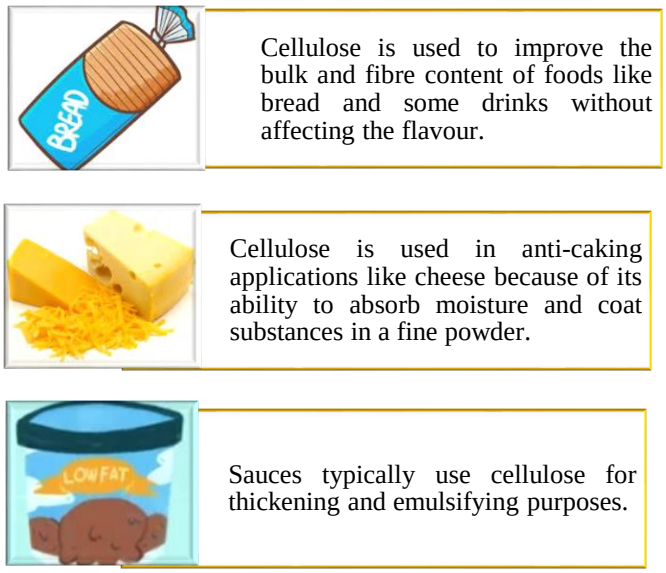

Figure 2. Uses of cellulose in food [19].

Types of biopolymers

Cellulose

Cellulose is a naturally occurring biodegradable polymer that is widely used as it contributes to the reduction of synthetic packaging and wastes. It is low in weight and helps to reduce packaging material weight. Cellulose and its derivatives can be found in a variety of natural settings. They are both bioavailable and cost effective due to the availability of sources. Wood is a key source of cellulose. Cellulose can be obtained from pulp of wood and utilised in a variety of applications. Cotton, which is commonly used for threads and garments, is another rich source; cotton blooms are composed of cellulose. Cellulose and its derivatives have high biocompatibility, material properties, heat capacity, moisture absorption, permeability, antimicrobial properties, crystallinity, hygroscopicity, and organoleptic attributes like smell, taste, colour. Despite cellulose's limited antioxidant and antibacterial capabilities, the addition of natural plant extracts fulfils this need. Antimicrobial properties of cellulose are limited. Therefore, derivatives of cellulose are preferable as they have enhanced antimicrobial properties like nanocellulose, methyl cellulose, CNC [13]. Cellulose and its derivatives are mechanically robust owing to its crystallinity [14].

It was reported that gallic acid-loaded nanofibers prevented oxidation of walnuts during storage [15]. Moreover, during the storage period, mangoes packed using CNC films were devoid of mango-associated postharvest deterioration [16]. Cellulose containing herbal extracts increased the storage period of button mushrooms with green tea extract incorporated bacterial cellulose being the most effective in preserving the colour of mushrooms [17]. It was observed that carboxymethyl cellulose increased the shelf life of white soft cheese and was effective against bacterial count, molds and yeast [18]. Cellulose is also used as a food additive for a variety of reasons as shown in Figure 2.

Chitosan

Chitosan is a N-deacetyl derivative of the polysaccharide chitin. This polymer has piqued the interest of researchers due to its potential as a natural antioxidant and its antimicrobial properties. Chitosan engages with pathogenic and decomposing bacteria's cell membrane, triggering structural and functional changes, as well as influencing cell wall permeability. Chitosan's unique properties make it ideal for film production, and chitosan-based films have a lot of potential as active packaging materials attributed to its antibacterial properties, non-toxicity, and reduced oxygen permeability. Chitosan-based films exhibit poor mechanical properties and lack of water resistance. Here arises the need to blend chitosan with other materials to improve its physical properties [20]. The tensile strength of chitosan films made using acetic acid is greater than that made with citric, lactic, or malic acids, and it rises over time. Plasticizers such as glycerol or sorbitol could be used to increase the coatings' elastic properties. Combining cellulose and its derivatives to chitosan films improves elasticity, structural rigidity, and optical clarity while retaining antibacterial property [21, 22].

It was reported that papaya fruit was longer preserved when stored with chitosan solutions at room temperature [23] and they also offered antioxidant mechanisms inhibiting guava ripening during storage at room temperature, prolonging the

fruit's qualitative characteristics after harvest [24]. It was observed that phytochemical profiles of plum fruit were preserved with chitosan coatings [25]. Furthermore, the shelf life of carrots wrapped in composite films was up to nine days [26]. The chitosan layer altered tomato quality criteria by slowing down the ripening process [27].

Pectin

In many plants, pectin is a complex heteropolysaccharide that acts as a key multifunctional component of the cell wall [28]. Pectin is a robust molecule that can be employed in a variety of food applications, including stiffening and gelation agents, colloidal stabilisers, texturizers, and emulsifying agents. These major uses include packaging, coatings on fresh and cut fruits and vegetables, and microencapsulation agents. Pectin is water-soluble and insoluble in organic solvents. Pectin has been successfully produced as a natural organic biopolymer that may be derived from agricultural-waste products, aiding waste management. The final application of pectin composites is quite versatile yet very appealing in many domains associated with food packaging, especially when active formulations are sought, due to the variety in pectin structure. To better regulate the pectin-based products, more research on pectin composites and improvement of polymeric techniques would be required [6].

Antimicrobial substances are added to pectin edible films to obtain antimicrobial active packaging to prevent growth of microbial colonies and extend product shelf life [29].

It was reported that soybean oil can be kept from oxidizing for thirty days due to its bioactive pectin films [30]. The incorporation of halloysite nanotubes to modern food packaging materials provides significant benefits. Halloysite nanotubes containing peppermint [31], salicylic acid [32], and rosemary [33] essential oils have been shown to have an effect in pectin films. A greater compatibility of halloysite nanotubes enhances the mechanical, thermal, and moisture barrier qualities of pectin films. The antibacterial activity of these films can be upgraded with the increase in release rate of active constituents.

Proteins

A polymer made up of amino acids is referred to as a protein. The amino acids create peptide bonds between chains, indicating that they have polymerized into proteins [2]. Protein-based films are hydrophilic, which means they have relatively lower water barriers and lose their stability when exposed to elevated humidity. They serve as an excellent barrier against hydrophobic chemicals like oil and fragrance. Antimicrobial and antioxidant substances are also found in protein-based films [34]. The antimicrobial activity depends upon the variety of proteins, as well as additive compounds used in the edible coatings. For instance, lysosome can be used as an antimicrobial in pea protein or starch-based films and can be stored up to 15 days before use [35].

Milk protein films are ductile and transparent in nature with disinfectant properties. They also include strong antimicrobial and antioxidant compounds that serve to boost food quality. Whey and casein protein are two types of protein found in milk. Casein protein accounts for most of the milk protein. After casein precipitation, whey protein can be produced. After dissolving the casein protein in water, an alkali solution containing agents are added. When these substances bind with amino acids, calcium caseinate and sodium caseinate are produced. These ions improve the barrier properties and mechanical robustness of the film by increasing protein cross-linking. Whey protein films have better oxygen gas barrier properties than caseinate films. Animal muscles and tissues contain collagen protein. Gelatine is created when collagen is broken down with the assistance of water. Dry gelatine is flavourless and translucent. To make the film-forming solution, it is dissolved in hot water. Casting is used to create the film, which is then dried in the oven. Corn is also used to make zein protein. It is hydrophobic and can produce insoluble coatings in water. It can be utilised as an edible packaging material to preserve the standard and shelf life of food goods due to its inherent antibacterial and antioxidant capabilities. Soybeans are unique and the primary source of soy protein. Boiling soymilk initiates dehydration resulting in the formation of a soy protein film. This is followed by an air-drying procedure. When compared to lipid and polysaccharide-based films, soy protein films have a higher gas barrier [36]. It was reported that zein-based films containing monolaurin or eugenol had shown increase in elasticity and hydrophobicity [37]. It was observed that milk-based edible films showed difference in mechanical, optical, antioxidant and hydrodynamic properties depending upon the type of milk protein with casein being the most favourable [38]. It was observed that gelatine and gelatine mixed with papaya-based films showed bendability and lower moisture permeability [39].

Polyhydroxy alkanoate (PHA)

PHAs are made by a variety of bacteria that use agricultural waste as a carbon source. PHAs are employed in a variety of applications, including

packaging, medicinal, and agricultural, due to their biodegradability and biocompatibility. The PHAs' inherent good gas barrier qualities make them appealing as a single-use packaging alternative to traditional plastics in order to reduce plastic pollution in the environment [16].

It has been discovered that a majority of short chain length-PHA copolymers with a minor fraction of medium chain length-PHA generate features similar to standard petroleum-based plastics such as polypropylene when generating PHAs with similarthermal and mechanical properties [40]. The advantages of PHA are that it is non-carcinogenic, non-toxic, and biodegradable. PHAs have good barrier properties against oxygen, carbon dioxide, and moisture, making them a better choice as food packaging materials [41, 42]. Its high production cost and short polymer chains that let through oxygen are the downsides which need to be focused on in future studies [43].

PHA lacks antimicrobial properties, thus there is a need to incorporate it with additives. Poly(3-hydroxybutyrate) or PHB is one of the most common forms of PHA. It has been reported that metal nanoparticles were used to create antibacterial PHB films [44].

It was observed that the PHAs including organic or inorganic fillers demonstrated useful water vapor barrier qualities, as well as improved crystallization behavior, thermal stability, mechanical properties, and lower production costs [45].

It was reported that drinking straws made from PHA were biodegradable and non-toxic, but the production cost was high [46].

Polylactic acid (PLA)

PLA is an acid-derived aliphatic linear poly(α-ester) or α-hydroxyalkanoic polyester. PLA is made from lactide that has been ionic-polymerized. Lactide is a cyclic chemical formed when two molecules of lactic acid are dehydrated and then condensed. As lactic acid is a chiral molecule possessing d-type and l-type isomers, it can be divided into three types of polylactic acid: poly-l-lactic acid (PLLA), poly-d-lactic acid (PDLA), and poly-d, l-lactic acid (PDLLA). In terms of optical activity, polylactic acid can be crystallized into three forms attributed to its two components (L and D enantiomers) [47, 48].

PLA has a low melt viscosity that is required for mould shaping. Yet there are some disadvantages. PLA, for example, has a low crystallisation rate during long moulding cycles and has poor gas characteristics. Furthermore, as compared to other synthetic polymers, PLA has low mechanical strength, as well as thermal resistance. PLA has been mixed with other polymers to circumvent these restrictions. PLA's glass transition temperature of 50–80 °C is relatively low to most polyesters, significantly limiting the applicability of this amorphous material in its pure state. PLA has low mechanical strength, as well as thermal resistance [44].

Plasticizers and fillers have also been introduced into PLA. In addition to the preparation of PLA nanocomposites, these technologies have proven successful in making PLA more commercially viable [9]. The films made from PLA are biodegradable, have good oxygen barrier properties, and have lower migration levels than those made from food contact materials [49].

Antimicrobial additives like nisin and ethylene oxide are needed to be introduced in PLA due to its lack of such properties [50]. Antibacterial food packaging made from PLA/PBS blends (90:10) was found to reduce both microorganisms (*S. aureus* and *E. coli*) and provide an effective barrier layer against water vapour transmission [51, 52].

Some applications of polylactic acid in food industry are shown in Figure 3.

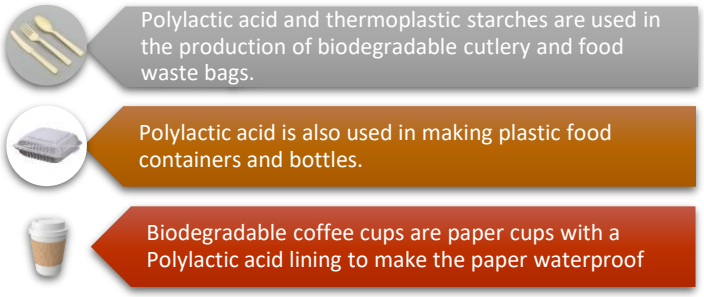

Figure 3. Applications of polylactic acid in food industry [53].

Table 2. Possible applications of biopolymer food packaging

Biopolymer	Food item	Form of packaging	Function of the biopolymer	Ref.
Cellulose	Cheese	Film	Enhanced shelf life of cheese	[61]
	Chicken breast fillets	Film	Enhanced shelf life of meat due to decrease in microbial count	[62]
Chitosan	Bread	Film	Enhanced shelf life against aerobic bacteria and molds (up to 5 days and 7 days respectively)	[63]
PLA	Vegetable	Film and bag	Higher shelf life and antimicrobial activity was observed in composite bag as compared to the film	[64]
Zein	Pork sausages	Active film	Green tea extract was infused into chitosan film and utilized to package pork sausages that were preserved at 4^0C.	[65]
Gelatin	Melon	Container	Freshly cut melon stored in PLA container for 10 days was preserved well and no change in pH, stiffness was observed at 10ºC	[66]
Starch	Salad	Film	Antimicrobial properties observed during preservation of salad	[67]
Thermoplastic starch	Broccoli	Film	No change in broccoli was evident after 6 days of preservation at 5ºC	[68]
	Sea bass	Film	Antimicrobial and antioxidation properties were observed in sea bass stored in gelatin film at 4ºC for 12 days	
	Chicken breast fillets	Film	Antimicrobial activity observed in the food item. 1% SANAFOR incorporated tapioca starch film was used	[69]
	Sunflower oil	Active film	Films produced from cassava starch were used to encase wine grape pomace. Antioxidant activity was greater in the microencapsulated film with gum arabic.	[70]
	Pasta	Active film	TPS and PBAT were used to make active packaging films. The film inhibited the growth of germs, extending the pasta's storage period.	[71] [72]

Starch

Starch is a polysaccharide composed of 1,4 linkages between glucose monomers. The linear polymer amylose is the most basic type of starch, while amylopectin is the branched form. According to the FTIR test, the sago starch based biodegradable plastic was degradable after 14 days, with the primary chemical inside the sago starch-based biodegradable plastic disappearing. The sago starch-based biodegradable plastic was also shown to have strong acid resistance but low alkalis resistance [54]. Antimicrobial qualities must be imposed on starch because it does not have them naturally. For instance, cationic starch was also utilised in combination with starch and sodium alginate to create antibacterial polyelectrolyte films [40]. Mechanical integrity, thermal stability, and humidity absorption are some of the constraints of native starches. These drawbacks lead to starches being combined with other materials to improve their properties [55]. In addition to lowering production costs, blended starches improve barrier properties, dimensional stability, minimise hydrophilicity, and increase biodegradability. Various low molecular mass plasticizers, including glycerol, glucose, sorbitol, urea, and ethylene glycol, are blended with starches to enhance their properties [56]. By adding plasticizers, thermoplastic starch (TPS) is formed [57], which is characterized by the spontaneous breakdown of starch's semi-crystalline structure and the formation of hydrogen bonds between plasticizers and starch molecules [58]. TPS can be made in a variety of qualities depending on the plasticizer added to the starch. Plasticizers weaken the intermolecular chain connections, resulting in greater flexibility, extensibility, and fluidity. TPS is also an extremely hydrophilic compound. TPS and PLA combined provide significant benefits in terms of cost, property, and biodegradability [59].

It was reported that 1% SANAFOR incorporated

polybutylene succinate/tapioca starch film for packaging of chicken breast fillet was the most successful in keeping the food item fresh and devoid of microbial activity [60].

Various experiments have been carried to use biopolymers for food packaging. Some of the possible applications are shown in Table 2.

CONCLUSION

Biodegradable polymers have an immense potential in turning the plastic industry upside down as they can reduce the negative impact on the environment. Biodegradable polymers such as cellulose, chitosan and starch are abundant in nature and can be used effectively for packaging of many food materials. Some of the biodegradable polymers such as polylactic acid (PLA) may be expensive to develop at the moment but future studies may help to synthesize them in more economical ways. Properties of biopolymers have been discussed to help understand the various aspects that can be advantageous or if disadvantageous may be modified to suit the needs. Cellulose, due to its abundance in nature and preferable properties, is the most widely assessed biopolymer. Some experiments have been mentioned in the form of examples to clarify how we might synthesize biopolymers for food packaging. Biodegradable polymers cannot replace plastic in the majority of the cases due to higher demand and lower availability. Researchers from all over the world are currently researching in this direction. Use of biodegradable polymers in food packaging including other industries has indeed started. Future studies need to focus on affordability and accessibility of some of the biodegradable polymers such as PHA and PLA as they can help in overall environmental sustainability.

REFERENCES

1. S. Kumar, A. Mukherjee, J. Dutta, *Trends in Food Science & Technology*, **97**, 196 (2020)
2. L. Kumar, D. Ramakanth, K. Akhila, K. K. Gaikwad, *Environmental Chemistry Letters*, **20**, 875 (2022)
3. S. Shaikh, M. Yaqoob, P. Aggarwal, *Current Research in Food Science*, **4**, 503 (2021)
4. J. K. Patra, G. Das, L. F. Fraceto, E. V. Ramos Campos, M. D .P. Rodriguez-Torres, L. S. Acosta-Torres, L. A. Diaz-Torres,R. Grillo, M. K. Swamy, Shivesh Sharma, S. Habtemariam, H. S. Shin, *Journal of Nanobiotechnology*, **16**, 71 (2018).
5. V. L. Kabanov, L.V. Novinyuk, *Food Systems*, **3**(1) (2020).
6. C. Mellinas, M. Ramos, A. Jiménez, M. C. Garrigós, *Materials* **13**(3), 673 (2020).
7. P. Basnett, S. Ravi, I. Roy, *Science and Principles of Biodegradable and Bioresorbable Medical Polymers, Materials and Properties*, 257 (2017).
8. S. Vigneswari, M. Shahrul M. Noor, T. Suet M. Amelia, K. Balakrishnan, A. Adnan, K. Bhubalan, A.-A. Abdullah Amirul, S. Ramakrishna, *Life*, **11**(8), 807 (2021).
9. A. Z. Naser, I. Deiab, F. Defersha, S. Yang, *Polymers*, **13**(23), 4271 (2021).
10. S. Kopacic, A. Walzl, A. Zankel, E. Leitner W. Bauer, *Coatings*, **8**(7), 235 (2018).
11. M. Poletto, Composites from Renewable and Sustainable Materials, IntechOpen, DOI10.5772/62936, (2016).
12. P. Srivastava, R. Malviya, *Indian Journal of Natural Products and Resources*, **2**(1), 10 (2011).
13. D. Beaton, P. Phillip, R. R. Goulet, *Frontiers in Microbiology*, **10**, 204 (2019).
14. Y. Liu, A. Saeed, D. E. Sameen, Y. Wang, R. Lu, J. Dai, L. Suqing, W. Qin, *Trends in Food Science & Technology*, **112**, 532 (2021).
15. A. Aydogdu, G. Sumnu, S. Sahin, *Material Carbohydrate Polymers*, **208**, 241 (2019).
16. D. Dey, V. Dharini, S. P. Selvam, E. R. Sadiku, M. M. Kumar, J. Jayaramudu, U. N. Gupta Upendra, *Materials Today: Proceedings*, **38**(2), 860 (2021).
17. S. Moradian, H. Almasi, S. J. Moini, *Journal of Food Processing and Preservation*, **42**, Article e13537 (2018).
18. A. M. Youssef, S. M. El-Sayed, H. S. El-Sayed, H. H. Salama A. Dufresne, *Carbohydrate Polymers*, **151**, 9 (2016).
19. https://www.thespruceeats.com/what-is-cellulose-1328464.
20. G. L. Robertson, University of Queensland, Brisbane, Australia, Elsevier, 2014.
21. G. Kerch, V. Korkhov, *European Food Research and Technology*, **232**, 17 (2011).
22. S. Kumar, F. Ye, S. Dobretsov, J. Dutta, *Applied Sciences*, **9**(12), 2409 (2019).
23. G. L. Dotto, M. L. G. Vieira L. A. A. Pinto, *Lebensmittel Wissenschaft und Technology/ Food Science and Technology*, **64**(1), 126 (2015).
24. W. Batista Silva, C. Silva, G. M. Santana, D. B. Salvador, A. R. Medeiros, D. B. Belghith, I., M. D. Silva, N. H. M. Cordeiro, M. Polete, G. Misobutsi, *Food Chemistry*, **242**, 232 (2018).
25. X. Lu Chang, Y. Q. Li, Z. Lin, J. Qiu, C. Peng, S. Brennan, C. X. Guo, *Foods*, **8**(8), 338(2019).
26. K. S. Sarojini, M. P. Indumathi, G.R. Rajarajeswari, *International Journal of Biological Macromolecules*, **124**, 163 (2019).
27. P. Kaewklin, U. Siripatrawan, A. Suwanagul, Y.S. Lee, *International Journal of Biological Macromolecules*, **112**, 523 (2018).
28. A. Noreen, Z.-H. Nazli, J. Akram, I. Rasul, A. Mansha, N. Yaqoob, R. Iqbal, S. Tabasum, M. Zuber, K.M. Zia, *Int. J. Biol. Macromol.*, **101**, 254 (2017).
29. E. P. J. Pérez, W. Du, A. Xian, R. de Jesús Bustillos, S. N. de Fátima Ferreira, H. McHugh, *Tara Food Hydrocolloids*, **35**, 287 (2014).
30. P. Rodsamran, R. Sothornvit, *Food Hydrocoll*., **97**, 105 (2019.

31. G. Biddeci, G. Cavallaro, D. Blasi, F.; G. Lazzara, M. Massaro, S. Milioto, F. Parisi, S. Riela, G. Spinelli, *Polymer*, **152**, 548 (2016).
32. M. Makaremi, P. Pasbakhsh, G. Cavallaro, G. Lazzara, Y. K. Aw, S. M. Lee, S. Milioto, *ACS Appl. Mater. Interfaces*, **9**, 17476 (2017).
33. G. Gorrasi, *Carbohydrate Polymer*, **127**, 47 (2015).
34. P. S. Saklani, S. Nath, K. Das, S, S. M. Singh, *International Journal of Current Microbiology and Applied Science*, **8**(07), 28852895 (2019).
35. F. María José; S. G. Laura; C. Amparo, *LWT - Food Science and Technology*, **55**(1), 22 (2014).
36. B. Hassan, S. A. S. Chatha, A. I. Hussain, N. Akhtar, *International Journal Biological Macromolecules*, **109**, 1095 (2018).
37. J. Sedlarivoka, M. Janalikova, P. Peer, L. Pavlatkova, A. Minarik, P. Pleva, *International Journal of Molecular Sciences*, **23**(1), 384 (2022).
38. G. E. F. Flores, I. A. Aguayo, B. Marcos, B. A. Camargo-Olivas, R. Sánchez-Vega, M. C. Soto-Caballero, N. A. Salas-Salazar, M. A. Flores-Córdova, M. J. Rodríguez-Roque, *Coatings*, **12**(2), 196 (2022).
39. J. Ashfaq, I. A. Channa, A. A. Shaikh, A. D. Chandio, A. A. Shah, B. Bughio, A. Birmahani, S. Alshehri, M. M. Ghoneim, *Materials*, **15**(3), 1046 (2022).
40. H. Ahari, S. P. Soufiani, *Frontiers in Microbiology*, **12**, 657233 (2021).
41. M. Koller, *Applied Food Biotechnology*, **1**(1), 3 (2014).
42. J. Vandewijngaarden, M. Murariu, P. Dubois, R. Carleer, J. Yperman, P. Adriaensens, S. Schreurs, N. Lepot, R. Peeters, M. Buntinx, *Journal of Polymer Environment*, **22**, 501 (2014).
43. S. Mohapatra, K. Vishwakarma, N. C. Joshi, S. Maity, R. Kumar, M. Ramchander, S. Pattnaik D. P. Samantaray *Environmental and Agricultural Microbiology: Applications for Sustainability*, **5**, 83 (2021).
44. A. Z. Naser, I. Deiab, F. Defersha, S. Yang, *Polymers*, **13**(23), 4271 (2021).
45. J. Vandewijngaarden, R. Wauters, M. Murariu, *Journal of Polymer and Environment*, **24**, 104 (2016).
46. A. Barrett, Danimer, Scientific UrthPact Launch New Compostable Straw. (2019). Available online: https://bioplasticsnews.com/2019/10/30/danimer-scientific-and-urthpact-launch-new-compostable-straw/.
47. K. G. Jagiela, K. Sulak, Z. Draczyński, S. Podzimek, S. Galecki, S. Jagodzińska, D. Barkowski, *Polymers*, **13**(21), 3651 (2021).
48. G. L. Menghui Zhao, F. Xu, B. Yang, X. Li, X. Meng, L. Teng, F. Sun, Y. Li, *Molecules*, **25**(21), 5023 (2020).
49. P. J. Jandas, S. Mohanty, S. K. Nayak, *Industrial Eng. Chem. Res*., **52**, 17714 (2013).
50. A. M. Bonilla, C. Echeverria, A. Sonseca, M. P. Arrieta, M. F.-Gracia, *Polymeric Materials: Surfaces, Interfaces and Bioapplications*, **12**(4), 641 (2019).
51. N. Hongsriphan, S. Sanga, *J. Plastic Film Sheeting*, **34**, 160 (2018).
52. J. Y. Boey, L. Mohamed, Y. S. Khok, G. S. Tay, S. Baidurah, *Polymers*, **13**(10), 1544 (2021).
53. https://www.compoundchem.com/2019/06/26/biodegradable-plastics/
54. Z. A. M. Zawawi, N. H. F. Akam, D. Dose, A. Syauwye, R. A. Ahma, Z. Yusof, *Journal of Mechanical Engineering Department Politeknik Kuching Sarawak*, **1**(1) (2017).
55. A. Campos, K. B. R. Teodoro, E. M. Teixeira, A. C. Corrêa, J. M. Marconcini, D. F. Wood, L. H. Mattoso, *Polymer Engineering and Science*, **53**(4), 800 (2013).
56. P. Bhanu, G. Vinod, P. Deepak, A. Singha, *Carbohydrate Polymers*, **109**, 171(2014).
57. F. Soares, Y. Fabio, M. Carmen, P. Alfredo, *Polymer Testing*, 33 (2014).
58. A. Bendaoud, C. Yvan, *Carbohydrate Polymers*, **97**(2), 665 (2013).
59. K. Encalada, E. Aldás, M. Belén, V. Proaño, *Valle Revista Ciencia e Ingeniería*, **39**(3), 245 (2018).
60. N. L. Yusof, N.-A. Abdul Mutalib, U. K. Nazatul, A. H. Nadrah, N. A. H. Fouad, M. Jawaid, A. Ali, L. K. Kian, M. Sain, *Foods*, **10**(10), 2379 (2021).
61. M. Al-Moghazy, M. Mahmoud A. A. Nada, *International Journal of Biological Macromolecules*, **160**, 264 (2020).
62. M. A. N. Ala, Y. J. L. Shahbazi, *LWT Food Science and Technology*, **111**, 602 (2019).
63. Eco-friendly food packaging material created by NUS researchers doubles shelf-life of food products, National University of Singapore, 2016.
64. Plastic Materials. Free online database for plastic industry. https://omnexus.specialchem.com (2020).
65. U. Siripatrawan, S. Noipha, *Food Hydrocolloids*, **27** (1), 102 (2012).
66. H. Zhou, S. Kawamura, S. Koseki, T. Kimura, *Environmental Control in Biology*, **54** (2), 93 (2016).
67. M. Llana-Ruiz-Cabello, A. Pichardo, S., Banos, C. Núnez, J. M. Bermúdez, E. Guillamon, S. Aucejo Cameán, *LWT-Food Science and Technology*, **64** (2), 1354. (2015).
68. A. M. Rakotonirainy, Q. Wang, G. W. Padua, *J. Food Sci.*, **66** (8), 1108 (2001).
69. M. Ahmad, S. Benjakul, P. Sumpavapol, N. P. Nirmal, *Int. J. Food Microbiol*., **155** (3), 171 (2012).
70. N. L. Yusof, N. A. A. Mutalib, U. K. Nazatul, A. H. Nadrah, A. Nurain, H. Fouad, M. Jawaid, A. Ali, L. K. Kian, M. Sain, *MDPI Foods*, **10**(10), 2379 (2021).
71. L. Stoll, T. M. H. Costa, A. Jablonski, S. H. Flores, A. de Oliveira Rios, *Food Bioprocess. Technol*., **9** (1), 172 (2016),
72. T. P. de Camargo Andrade-Molina, M. A. Shirai, M. V. E. Grossmann, F. Yamashita, *LWT-Food Science and Technology*, **54** (1), 25 (2013)

Bulgarian Chemical Communications, Volume 54, Special Issue C (pp. 27-34) 2022 DOI: 10.34049/bcc.54.C.0027

Biopolymeric membranes and their role in CO_2 separation: A review

R. Basrur, L. Ledwani*

Faculty of Science, Manipal University, Jaipur, India

Accepted: July 06, 2022

A new avenue in combatting carbon dioxide emissions is "Membrane Engineering Technology". Membranes are used to separate mixtures by allowing some substances to pass through and not others. Thus, selective permeability is a big factor in the manufacturing of membranes. There are several chemicals used to make the varied layers that are utilized to obtain the exact permeability required. The purpose of this review paper is to discuss the need and usage of such polymeric membranes, with specific attention to the usage of biopolymers in membranes. The focus is primarily on membranes designed to allow the passage of CO_2 while the other components of air do not pass through. Polymeric membranes are used for the separation of CO_2 produced during various chemical reactions before it is released into the air. The separation of carbon dioxide with the help of membranes made up of biopolymers will be a new approach to green chemistry. The biopolymers utilize animal or plant-based polymers like cellulose, starch and polylactic acid which is beneficial to the environment in more ways than one. The world relies heavily on the combustion of fossil fuels for its energy needs. The increasing amount of carbon dioxide emitted by industries is concerning because of its contribution to climate change. The increased usage of membranes would therefore aid in containing the emissions and reusing the CO_2 for more beneficial purposes.

Keywords: CO_2 separation, Biopolymer membranes, Membrane separation, Biopolymer

INTRODUCTION

Over the last century, the rise in carbon dioxide in the atmosphere has increased drastically. The relationship between CO_2 emissions and global warming was a point of critical debate among many scholars [1]. Carbon dioxide is responsible for over 60% of the greenhouse effect, causing a rise in global temperatures [2].

It is predicted that by the year 2100 the temperature of oceans will increase by 3-4°C [3]. Therefore, researchers have been looking at methods to reduce the rate at which the global temperature rises. In lieu of this, biopolymeric membranes are being developed and used to reduce the emissions of carbon dioxide in combustion and other manufacturing reactions. This paper will focus on the process of the membrane-employed separation as well as review some of the bio-polymeric membranes that are being utilised. It will also enumerate the advantages and disadvantages of the process.

The greenhouse effect has multiple causes. The Intergovernmental Panel on climate change (IPCC) has reported that agriculture accounted for about 23% of net global greenhouse gas emissions produced by the human population during the period 2007-2016 represents, which in turn consisted of CO_2 (13%), CH_4 (44%), and N_2O (43%). It is reported that approximately 21%–37% greenhouse gas emission was by 2050 [4,5]. The main role to CO_2 emission because of the global energy consumption by fossil fuels is connected to the electricity grid 44.4%, followed by transportation 24%, industry 19.4% and residential 7% and can be seen in Fig. 1 [6]. Bio-membrane technology is used in the industrial sector addressing 19.4% of CO_2 emissions.

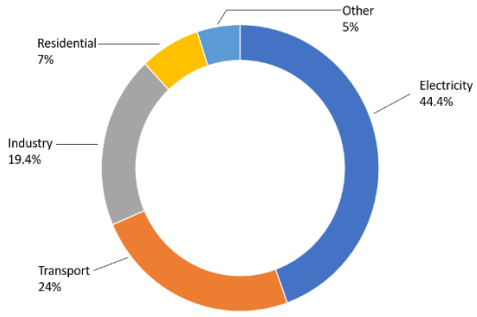

Fig. 1. CO_2 emissions by each sector

Of all the greenhouse gases, carbon dioxide is the biggest threat. Carbon dioxide absorbs the infra-red radiation (i.e., heat) reflected from the earth by virtue of its carbon- oxygen bonds vibrating more strongly; and so, the heat is trapped within the Earth's atmosphere. Carbon dioxide is a stable molecule and removing it from the atmosphere by reaction is not viable. Methane traps heat more effectively than carbon dioxide by its carbon-hydrogen bond vibrations but its concentration in the atmosphere has not increased as significantly as that of carbon dioxide and its shorter lifetime in the atmosphere is less important of a crisis.

* To whom all correspondence should be sent:
E-mail: lalitaledwani@gmail.com; lalita.ledwani@jaipur.manipal.edu

To abate this crisis, many researchers have proposed various technological solutions for lowering the CO_2 emissions. Some include decreasing the global energy usage, substituting carbon fuels with other sources, and CO_2 capture by membrane engineering technology. This separation technology is believed as a possible avenue because of the numerous advantages compared to other conventional techniques like adsorption and cryogenic distillation. The advantages such as higher separation efficiency, higher stability, low operating cost and investment, low energy requirement, and ease of operation have created a new focus on this technology.

The separation of gases through a polymeric membrane is a pressure-based process. A mixture of gases is fed into a diffusion mechanism where a specific gas is allowed to pass through the membrane. For an effective separation of CO_2 there are two requirements: high CO_2 permeability and CO_2 selectivity with respect to the other gases present in the mixture [7].

The introduction of various membranes in the same industrial cycle can lead to other important advantages in terms of product quality, installation compactness, environmental impact and energy consumption [8].

The selectivity of the membrane is important. Such as the selectivity between CO_2 and CH_4 or CO_2 and N_2, the stability of the materials used to manufacture the membranes can have their own impact on the separation process.

The membranes used for these procedures are inorganic and organic. The inorganic membranes are most commonly used in combustion processes due to their high thermal resistance. Unfortunately, compared to organic membranes, inorganic membranes show the disadvantage of increased production costs [8].

The usage of biopolymers for these membranes further reduces the carbon footprint as the polymers will not be synthetic (i.e., made from fossil fuels), they will also be biodegradable. Cellulose [9] and thermoplastic starch are produced in plants and can be utilised in the manufacture of the membranes. Chitosan is a polymer that can be found in the shell of crustaceans. Polylactic acid (PLA), polyhydroxyalkanoates (PHA), and polyvinyl alcohol (PVA) are synthetically manufactured but are biodegradable, which reduce its carbon footprint, and non-toxic and are better suited for the manufacture of the membranes because of the modification that can be made to their properties.

There are different time periods during which separation can occur. This is integral to the efficiency of the process. CO_2 can be separated at pre-combustion, post-combustion and oxy-combustion. In the pre-combustion, the efficiency of CO_2 capture is close to 90-95%. The fuel is converted into hydrogen and carbon monoxide, which is then transformed to CO_2 by a water-gas shift reaction and is separated from hydrogen. In post-combustion capture, CO_2 is ventilated to liquid state. This facilitates the separation of CO_2 from the gas escape while the gas mixture is in contact with a liquid solvent. This solvent is usually an aqueous amine that absorbs about 85% of the CO_2 The oxy-combustion shows 100% of CO_2 capture but it requires a lot of energy input for combustion in oxygen with recycling of exhaust gases (CO_2 and H_2O) and purification of the CO_2 flow [10].

POLYMERIC MEMBRANES AND THE SEPARATION PROCESS

As iterated above, the process and its efficacy are reliant on 3 factors: the stage of combustion, the selectivity and the physical structure of the membrane itself. This section of the paper will explain and provide insight on the impact of these factors and its respective influence on the selection of the membrane being used in the actual process.

Combustion

In the range of methods employed for CO_2 capture, membranes are used in post-combustion capture, pre-combustion capture and oxy-combustion. Pre-combustion separation is when fossil fuels are converted into a synthesis gas which mainly consists of hydrogen and carbon monoxide. CO can undergo additional conversion with steam to form more hydrogen and CO_2 through the water-gas shift reaction. The CO_2 and hydrogen can be separated with the help of membranes. CO_2 is separated using physical adsorption through the membrane and is sent to the compression unit. The most optimal separation process takes place as a function of partial pressure of CO_2 in the gas to be separated. In pre-combustion, the separation of the carbon dioxide depends on the pressure of the process selected for natural gas. The rise in pressure is not a free operation and must assure the increase in capture due to the high pressure and additional energy needed to achieve it [11].

Oxy-fuel combustion or oxy-combustion is a process of combustion where nitrogen is separated from the air that is used for combustion. This is so that combustion takes place in oxygen and recycled flue gas. Flue gas consists mostly of carbon dioxide and water vapour. Most industrial plants are designed to involve flue gas recirculation to the

combustion to control the temperature of the flame. The modifications that are needed in the powerplants to apply oxy-fuel combustion is larger than that of post-combustion. This is due to the fact that the combustion process is modified by the recycling of flue gas in place of the nitrogen present in the oxidiser [12].

Post- combustion separation is when the carbon dioxide is separated after the combustion process has taken place. The gases produced by combustion are allowed to interact with the membrane and the CO_2 is separated.

Selectivity and permeability

A membrane is a selective barrier that allows only specific species to pass through it. In this instance the polymeric membranes are designed to separate CO_2 from a feed mixture of gases. It is effective as they have high efficiency and low operation costs compared to orthodox separation methods as mentioned earlier.

The most critical criteria for a membrane are permeability and selectivity. For membranes to be effective there has to be a trade-off between selectivity and permeability. The permeability will reduce with an increase in selectivity. However, this can be overcome by adopting a selective CO_2 carrier and a selective metal-organic framework (MOFs) because the porosity and selectivity properties can be manoeuvred in MOFs using a combination of metallic ions and organic linkers during the manufacture [13].

Metal-organic frameworks (MOFs) are solid crystalline porous materials that have been broadly studied in the last few decades due to their unique yet useful properties that they tend to display, like gas adsorption and separation, which are significant in this topic, while they also show properties of magnetism, conductivity, catalysis, and water harvesting [14].

The comprehension of the interaction between gases and adsorbent properties of the MOFs are very important in the implementation of materials in the separation process. One such MOF is derived from L-histidine amino acid and has a formula of Cu(II) 2(S,S)-hismox·5H2O, it has a structure of a hemilabile chiral 3D MOF with a qtz-e-type topology. It exhibits a constant reversible breathing behaviour due to the hemi ability of the carboxylate groups from the L-histidine. The breathing motion is used to create an efficient separation of gases of significance, CO_2/NO_2 and CO_2/CH_4. The MOF is stacked in columns and dispersed in a matrix membrane [14].

The membrane-based separation selectivity is based on the membranes itself. The shapes of the polymers used to make the thin layers of the membranes allow the passage of gases. The rate of separation differs based on the size of the gas molecules and the diffusion coefficients in the membrane material [15].

Physical structure

Structures of polymeric membranes are very irregular and random. The membrane morphology depends on the material fabricated and its production processes [16]. The matrix of a membrane is the space or free volume available between the polymer chains which is where the molecules will interact in their process to move to the other side of the membrane.

The movement that occurs across a polymeric membrane is different. The gas through a dense membrane is described with the help of a solution-diffusion (SD) model. This mechanism has 3 key steps; 1-the desired gas molecules dissolve into the polymer matrix and move about the chains. 2- the molecules are moved down the concentration gradient to the other side. 3- the dissolved gases are desorbed out of the other side of the membrane. The S-D system takes place because of the thermodynamic differences between the two sides of the membrane. The permeability properties are defined by the matrix properties of the polymeric membranes. This can be seen in Fig 2. These encompass the density, rubbery or glassy texture of the membrane, and the amount of free volume present. Another factor in the gas permeability is the physical interaction between the gas molecules and the polymer chains in the membrane. Permeability is calculated by multiplying the solubility coefficient and the diffusion coefficient P=S×D [7].

The solubility differs with the chemical similarity of the gas molecules and the polymer chains of the membrane. Whereas the diffusivity varies on the free volume and the size of the gases in the polymer membrane matrix [7].

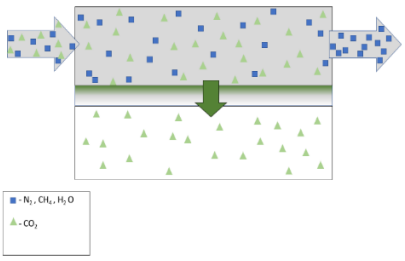

Fig. 2. Separation mechanism.

BIOPOLYMERS USED AND MANUFACTURE OF THE MEMBRANES

The world of biopolymers is vast and never-

ending. It is the perfect alternative to synthetic polymers, even in membrane preparation. They can be sourced from animals, plants, bacterial fermentation or even synthetically produced. At the moment, several biopolymeric membranes are being used in different separations. Chitosan, starch, polyvinyl alcohol, polylactic acid, and polyisoprene can be used in the separation of CO_2 from a concoction of gases with the help of SD model as the main principle, which is the separation that is obtained by a difference in solubility and the capacity for diffusion across the dense membrane of chemical products in a mixture [15-17]. This paper will review four of them and shine light on their properties and influence in the process of the membrane separation.

Chitosan

Natural form. Chitosan is a polymer that has a large portion of its residues in deacetylated form. It can be found in nature in a pure state but is usually found in a combined manner with polysaccharides, proteins, and the possibility of minerals. Chitosan is obtained by the deacetylation of chitin. It is a copolymer of glucosamine and N-acetyl-glucosamine, a deacetylated monomer and acetylated monomer respectively. They are linked through a β-4 glycosidic bond. It is usually manufactured by deacetylation of a-chitin by 40-50% aqueous alkali solution at a temperature of 100-160°C for a number of hours. The achieved degree of chitosan can reach to about 0.95. The alkaline treatment can be done again to attain complete deacetylation. Chitin (Fig. 3) and chitosan are produced from waste by-products of the crustacean products in the food industry [18].

Processing of Chitosan. The processing of chitosan involves the crushing of crustacean shells. The proteins are then separated and washed with NaOH. Followed by a washing with HCl to ensure mineralisation does not take place. Washing and dewatering is the next step, after which decolouration takes place, at this step chitin is obtained. Deacetylation with NaOH, washing and dewatering give us the final product of chitosan (Fig. 4) [18].

Properties. Chitosan (Fig. 5) is a linear amino polysaccharide with a high nitrogen content, in a rigid D-glucosamine structure. This causes the following properties: high hydrophilicity due to the crystallinity. Chitosan is a weak base due to the deprotonated amino group acting as a powerful nucleophile. The structure enables the formation of hydrogen bonds intermolecularly, which in turn expresses a high viscosity in the polymer. The reactive functional groups present cause cross-linking and chemical activation of the polymer chain. Chitosan is soluble only in dilute acidic solutions. It also has the capacity to form salts with organic and inorganic acids. It is a cationic biopolymer with high charge density. It has entrapment and adsorption properties which benefits its application in filtration and separation. As it is a biopolymer it is biodegradable [19]. Owing to the hydrophilicity and chemical resistance chitosan is used in dense membranes for pervaporation and gas separation [17]. A chitosan membrane alone is too rigid a polymer due to its glass transition temperature being around 130°C, but when the membrane is swollen in water the Tg (glass transition temperature) decreases, and the membrane is turned from a glassy condition to a rubbery one. This helps to increase the gas permeability; the gas permeation tests were carried out at room temperature where the CO_2 permeability was around 163 and the CO_2/N_2 separation ratio at 42 which is ideal [19].

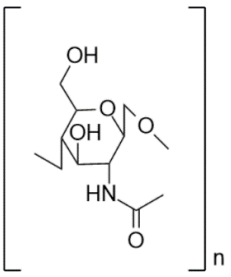

Fig. 3. Structure of chitin

Starch

Natural Form and Structure. Starch is a natural polymer which holds numerous unique properties and drawbacks. Starch-based polymers have the potential for applications in environmental fields due to the biodegradable and naturally occurring properties. Therefore, it receives extra attention and more in-depth research. Starch is predominantly made up of two homopolymers of D-glucose: amylose, typically a linear D(1,4) glucan and branched amylopectin, having a similar structure as amylose but with many 1,6 linked branch points. There are multiple hydroxyl groups, two secondary hydroxyl groups at C_2 and C_3 of each glucose residue, in addition to a primary hydroxyl group at C_6 when it is not linked (Fig. 6) [20, 21].

Properties. Starch membranes by themselves are too brittle so glycerol and sorbitol are used as plasticisers, which reduces the intermolecular interactions between the chains and improves the bad mechanical properties of starch [18].

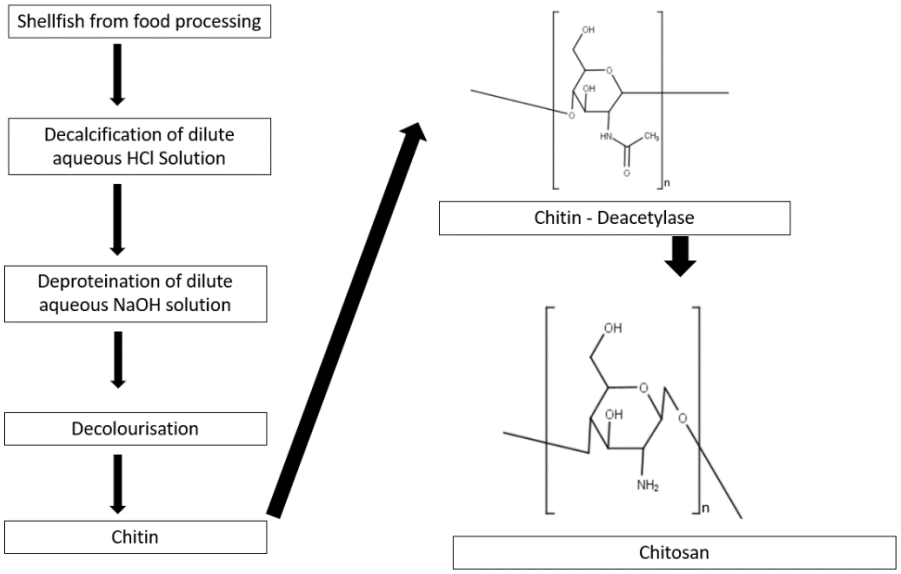

Fig. 4. Processes that give chitin and chitosan.

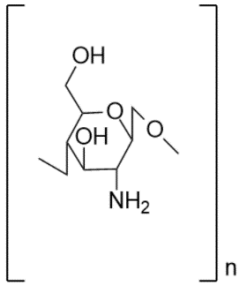

Fig. 5. Structure of chitosan.

A small amount of starch can be used without the loss of its plasticity properties. Starch is then transformed into a thermoplastic polymer by the application of forces and heat with the plasticisers [21].

A starch and chitosan polymer-based membrane has an antibacterial property. This was tested with *E. coli*; the growth of the bacteria was entirely inhabited on the membrane surface. This demonstrates the possible application of starch-chitosan membranes in the medical and food industry.

The addition of carboxymethyl cellulose and nano clay to starch improves the water resistance which is helpful as starch is hydrophilic. Thin films of thermoplastic starch and poly(butylene trans-1,4-cyclohexanedicarboxylate) blends were manufactured and the gas permeability for CO_2 and O_2 were tested under wet and dry conditions. There were no considerable differences registered between the different tests conducted (dry and wet) with a permeability in terms of gas transmission rate of ~20 cm^3 cm m^{-2} d^{-1} bar^{-1} for CO_2 and ~6 cm^3 cm m^{-2} d^{-1} bar^{-1} for O_2 [6].

Dialdehyde starch and chitosan have a good biocompatibility which is why they were selected to build self-healing films. The dynamic Schiff base linkage between the monomers gives the film/membrane a self-healing property. In the separation process the carbon dioxide reacts with the amino acids and water in the membrane to form a bicarbonate ion. The ion is then transferred through the membrane and converted back to carbon dioxide. In the experiment conducted the water content of the membrane was an important factor in the case of the carbon dioxide separation [22].

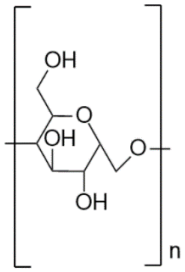

Fig. 6. Structure of starch [19]

Polylactic acid (PLA)

Properties. It has the properties of high-water resistance, solubility in various non-polar organic solvents, high melting point (between the range of 170-180°C) and a Tg of 50 to 65°C, depending on the degree of crystallinity of the structure [6]

The thermal resistance and mechanical properties can cause issues during the production of PLA products. By compounding PLA and blending it with other polymers, it improves the properties so that it can be utilised for in many sectors of the market.

Processing of PLA. Lactic acid is the single and only polymer in PLA (Fig. 7). 2-hydroxy propionic acid is produced through the processes of fermentation or chemical synthesis. The L+ and D-stereoisomers are optically active and can be

produced by the fermentation of carbohydrates carried out by bacteria. The bacterial fermentation is carried out in homofermentation and heterofermentation. The industrial production of lactic acid is usually carried out by the fermentation over synthesis because the latter process is dependent on the by-product of another reaction which tends to reduce the yield of lactic acid. The homofermentative method is favored because the reaction pathway results in a greater yield of lactic acid and lower levels of waste by-products. Pure lactic acid is used to produce PLA. PLA is produced by three techniques: direct condensation polymerisation, direct polycondensation in an azeotropic solution, and polymerisation through the formation of lactide formation. Direct condensation is centred around the esterification of the lactic acid monomers by the aid of solvents while the by-product, water, is separated using progressive vacuum and high temperatures. Gaining high molecular weight polyesters with ideal properties through this method is not easy. The production of high molecular weight PLA can be attained by direct polycondensation in azeotropic solutions and catalysts. PLA separation from the solvent is aided by the azeotropic solution by forming molecular sieves, it also decreases the pressure needed for distillation. The molecular weight of the polylactic acid obtained is 6.6×10^4 [23].

PLA pellets were dissolved in 1,4-dioxane to form solutions by stirring at 40°C. this is followed by the degassing of the solutions under a vacuum at 0.1MPa to remove air bubbles. The solutions are then cast onto glass plates and are then placed in a coagulating container. A metal tube is used to connect the container to a steam generator to supply hot water droplets continuously. The drops fall onto the surface of the membranes to induce phase inversion. The glass plates are kept inside for 2 hours to form porous membranes by coagulation, next the glass plates are removed and positioned in distilled water to remove traces of the dioxane. Later the membranes are dried in an oven for 72 hours at a temperature of 30°C ± 2. This step is taken to dry up any leftover water [24]. The permeability of the membrane does not depend on the dilution of the solution used to prepare the membranes, while the resistance of the membrane increases as the concentration of the PLA used is more [25].

Poly-hydroxybutyrate (PHB) compounded with an oligomer of lactic acid (OLA). OLA is a green plasticizer used to enhance the ductility of the membrane which increases the suitability for gas separation. Membranes of PLA formed using phase inversion were used in the separation of CO_2. The CO_2 permeability was around 70 Barrer. Overcoming the upper bound for CO_2/CH_4 selectivity at 285. This brought special interest for the purpose of biogas separation. The selectivity of H_2/CO_2 was also tested and found to be 26.5. until recently PLA was predominantly used in the medical field but with new studies and new methods of manufacture, PLA with higher molecular weights is made for multiple uses, one of which being gas separation [6, 26].

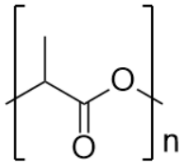

Fig. 7. Structure of PLA

Poly (vinyl alcohol)

Although poly (vinyl alcohol) (PVA) is a synthetic polymer, it is biodegradable. It is not a biopolymer, but it is still an important polymer in the membrane industry and therefore this paper includes a brief review of it.

PVA is obtained by the polymerisation of a single monomer - vinyl alcohol (Fig. 8). It is known for the properties it possesses such as transparency, toughness, barrier properties, non-toxicity, and biodegradability [27]. The solubility of PVA creates some problems when membranes made from it are used in separating processes. To overcome this, it is compounded with several chemicals to increase its hydrophobia. Glycerol, ethylene, glycol, citrate, urea, formamide, and ethanolamine are all added to decrease the solubility and crystallinity, which in turn will improve the performance of the membranes. PVA membranes can be used in pervaporation, for the separation of different organic mixtures, or for the dehydration of organic solvents for instance acetic-acid, alcohol, and ethyl-acetate.

A membrane made from PVA selective layer and a PSF porous support was synthesized. A light enzyme, Zn-cyclen, was added to the composite of the membrane to improve the CO_2 permeability. The results obtained displayed a CO_2/N_2 separation factor equal to 107 with 255.5 GPU as its CO_2 permeation, this is much higher than that of a pure PVA membrane. These membranes were then fortified with carbon nanotubes (CNT). This helped in reaching an ideal CO_2/N_2 selectivity and an optimal CO_2 permeation. This is due to the capability of the CNTs to stimulate swelling in the membrane [28].

A membrane made from PVA, and polyvinyl amine (PVAm) was created on a polysulfone

support. The CO_2/N_2 separation factor was found to be up to 174 and the permeance of CO_2 to be up to $0.58 m^3$. The experiment conducted found that the CO_2 was transported by binding to the fixed amino groups in the PVAm while the PVA added mechanical strength to the membrane. The entwined polymer chains created a supporting network, where the mechanical properties of the PVA goes hand-in-hand with the transportation factor of the PVAm resulting in high selectivity and permeance. Stability is also seen as a major problem that is solved by the blend of PVA and PVAm, which is stable at 2 atm and 35°C [29, 30].

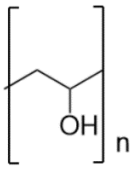

Fig. 8. Structure of PVA

CONCLUSION

The need for carbon-based energy resources is not reducing which sequentially causes a large amount of carbon dioxide to be released into the atmosphere. The increase in carbon dioxide is escalating the rise in planetary temperatures and climate change. To help address this, the study of membranes has progressed bounds in the last few years. The membranes are used to separate out the carbon dioxide and store it in tanks so that it does not get into the atmosphere.

This review has concentrated on the usage of biopolymers to manufacture these membranes. Biopolymers are readily available and biodegradable. They have good physical, and chemical properties to be used as effective and efficient membranes. If biopolymers are able to replace synthetic polymers, it allows for eco-friendlier operations. By the usage of biopolymers, the cost of production and installment of the membranes decrease drastically. This makes it easier for power plants and manufacturing plants to set it up.

While biopolymeric membranes are effective there are shortcomings which should be fixed in the future. The lifetime of biopolymer membranes needs to extend. The durability and strength tend to reduce with usage over time. The process of manufacture is not easy to build in bulk, if these processes can be refined and distributed, it will assist in the establishment of these membranes as a permanent and common fixture in the plethora of industries that use carbon-based fuels.

In this review, the discussion of various biopolymers that are used in the manufacture of membranes utilised for the separation of CO_2 from feed gases. The need for the usage of biopolymers is progressively increasing and new polymers and materials with new properties are being discovered and created. However, with what is available to us now, bio-polymers seem to hold a large share of the hope that we can have towards reducing our carbon footprint and mitigating the dire consequences of former practices on the planet and our survival.

REFERENCES

1. Y. Cai, C, Y. Sam, T. Chang, *Journal of Cleaner Production*, (2018), doi:10.1016/j.jclepro. 2018.02.035.
2. Sh. P. Raghuvanshi, A. Chandra, A. Kumar, *Energy Conversion and Management* **47,** 427 (2006), doi:10.1016/j.enconman.2005.05.007
3. S. Alfonso, M. Gesto, B. Sadoul, Temperature Increase and Its Effects on Fish Stress Physiology in The Context of Global Warming, doi:10.1111/jfb.14599.
4. G. D. Sharma, M. I. Shah, U. Shahzad, M. Jain, R. Chopra, *Journal of Environmental Management*, **297** 113316 (2021), https://doi.org/10.1016/j.jenvman. 2021.113316.
5. W. F. Lamb, T. Wiedmann, J. Pongratz, R. Andrew, M. Crippa, J. G. J. Olivier, D. Wiedenhofer, G. Mattioli, A. A. Khourdajie, J. House, S. Pachauri, M. Figueroa, Y. Saheb, R. Slade, K. Hubacek, L. Sun, S. K. Ribeiro, S. Khennas, S. D. L. R. D. Can, L. Chapungu, S. J. Davis, I. Bashmakov, H. Dai, S. Dhakal, X. Tan, Y. Geng, B. Gu, J. Minx, *Environ. Res. Lett.*, **16** 073005 (2021), https://doi.org/10.1088/1748-9326/abee4e.
6. F. Russo, *Fuel Processing Technology*, 106643 (2020) https://doi.org/10.1016/j.fuproc.
7. Basile, E. P. Fawas, Current Trends and Future Developments on (Bio-) Membranes, Elsevier, 2018, 978-0-12-813645-4.
8. F. Macedonio, E. Drioli, *Engineering*, **3** 290 (2017), https://dx.doi.org/10.1016/J.ENG.2017.03.026.
9. Zh. Dai, V. Ottensen, J. Deng, R. M. L. Helberg, L. Deng, *Fibers*, **7**, 40 (2019), doi:10.3390/fib7050040
10. M. Wang, A Lawal, P Stephenson, J Sidders, C Ramshaw, *Chemical Engineering Research and Design* **89,** 1609 (2011), doi:10.1016/j.cherd. 2010.11.005.
11. M. Kanniche, R. Gros-Bonnivard, Ph. Jaud, J. Valle-Marcos, J.-M. Amann, Ch. Bouallou, *Applied Thermal Engineering*, **30,** 53 (2010), doi:10.1016/j.applthermaleng.2009.05.005.
12. M. B. Toftegaard, J. Brix, P. A. Jensen, P. Glarborg, A. D. Jensen, *Science*, **36,** 581 (2010), doi:10.1016/j.pecs.2010.02.001.
13. J. Kim, J. Choi, Y. S. Kang, J. Won, *J. Appl. Polym. Sci.*, **133**, 42853 (2016), DOI:10.1002/APP.42853.
14. M. Mon, R. Bruno, E. Tiburcio, A. G. Atienza, A. S. Escribano, E. V. R. Fernandez, A. Fuoco, E. Esposito,

M. Monteleone, J. C. Jansen, J. Cano, J. F. Soria**,** D. Armentano, E. Pardo**,** *Chem. Mater.*, **31**, 5856 (2019).
15. R. Castro-Munoz, J. Gonzalez-Valdez, *Molecules*, **24**, 3584 (2019), doi:10.3390/molecules24193584.
16. K.-J. Hwang, T.-T. Lin, *Journal of Membrane Science*, **199,** 41 (2002).
17. F. Galiano, K. Briceno, T. Marino, A. Moliono, K. V. Christensen, A. Figoli, *Journal of Membrane Science* **564,** 562 (2018), https://doi.org/10.1016/j.memsci.2018.07.059.
18. V. Zargar, M. Asghari, A. Dashti, *ChemBioEng Rev*, **2** (3), 204 (2015), DOI:10.1002/cben.201400025.
19. L. A. El-Azzami, E. A. Grulke, *Journal of Membrane Science*, **323,** 225 (2008), doi:10.1016/j.memsci.2008.05.019.
20. D. R. Lu, C. M. Xiao, S. J. Xu, *Express Polymer Letters*, **3** (6) 366 (2009), DOI:10.3144/expresspolymlett.2009.46.
21. Kh. M. Dang, R. Yoksan, *Carbohydrate Polymers* **115**, 575 (2015), https://dx.doi.org/10.1016/j.carbpol.2014.09.005.
22. J. Ren, H. Xuan, L. Ge, *Appl. Surface Sci.*, **469**, 213 (2018), https://doi.org/10.1016/ japsusc.2018.11.001.
23. M. Jamshidian, E. Arab Tehrany, M. Imran, M. Jacquot, S. Desobry, *Comprehensive Reviews in Food Science and Food Safety*, **9,** 552 (2010), doi:10.1111/j.1541-4337.2010.00126.x.
24. A. Ch. Chinyerena, H. Wang, Q. Zhang, Y. Zhuang, K. H. Munna, Ch, Ying, H. Yang, W. Xu, *Polymer*, **141**, 62 (2018), https://doi.org/10.1016/j.polymer.2018.03.011.
25. T. Tanaka, D. R. Lloyd, *Journal of Membrane Science* **238,** 65 (2004), doi:10.1016/j.memsci.2004.03.020.
26. A. Iulianeli, F. Russo, F. Galiano, G. Desiderio, A. Basile, A. Figoli, *Science and Technology*, **9** 360 (2019).
27. H. Xu, L. Zhu, Y. Nan, Y. Xie, D. Cheng, *Ind. Eng. Chem. Res*., 58, 21403 (2019), dx.doi.org/10.1021/ie502531w.
28. F. Liu, B. Qin, L. He, R. Song, *Carbohydrate Polymers*, **78,** 146 (2009), doi:10.1016/j.carbpol.2009. 03.021.
29. M. Saeed, L. Deng, *International Journal of Greenhouse Gas Control*, **53,** 254 (2016), https://dx.doi.org/10.1016/j.ijggc.2016.08.017.
30. L. Deng, T.-J. Kim, M.-B. Hagg, *Journal of Membrane Science*, **340,** 154 (2009).

Bulgarian Chemical Communications, Volume 54, Special Issue C (pp. 35-45) 2022 DOI: 10.34049/bcc.54.C.0035

Impact of extremozymes on the removal of pollutants for industrial wastewater treatment

P. Sharma, M. Debnath*

Department of Biosciences, Manipal University Jaipur, Rajasthan -303007, India

Accepted: July 06, 2022

The discharge of effluent-containing pollutants from various industries into soil and water requires wastewater treatment. These harmful by-products are difficult to degrade and are poisonous. They cause serious problems to aquatic habitats and organisms. Wastewater treatment methods like physical and chemical procedures have drawbacks such as high costs, toxic by-products, and low removal effectiveness. As a result, it is becoming increasingly important to create effective biological wastewater treatment technology using microbes. Extremophiles have recently been extensively investigated for their ability to degrade contaminants under extreme conditions of temperature, pH, and salinity. Extremophilic microbes are repositories for novel extremozymes offering several advantages over conventional chemical catalysts, including highly specific biocatalysis, reproducibility, and stability at severe industrial wastewater conditions. They aid to generate the least toxic, and biodegradable industrial waste. The choice for the use of these extremophiles containing specific extremozymes needs extensive study considering their adaptability for the removal of pollutants from industrial wastewater. The alteration of extremozyme protein structure for extremophilic bacteria survival in various environmental circumstances, their usage in wastewater treatment, and the mode of action for biodegradation of various contaminants during bioremediation are all discussed in this paper.

Keywords*:* Biodegradation, extremophiles, extremozymes, effluent, wastewater, treatment

INTRODUCTION

Despite the fact that water is one of the world's most abundant natural resources, just 1% of it is currently feasible for human consumption [1]**.** Waste water generation is increasing on a global scale as a result of increased urbanization and industrialization [2] . Global water consumption has increased in the twenty-first century, necessitating waste water management; a variety of biological treatments are required to recycle wastewater and make it appropriate for drinking, washing, and industrial [3]. The treatment of waste water is a significant concern for water treatment enterprises all over the world [4] . Water pollution is caused by the generation and discharge of industrial effluents all over the world, particularly in developing countries [1]. Pollutants and heavy metals cause ill effect on health and environment. They are found in industrial wastes such as metal, refinery, automobile, textile, printing, and pharmaceutical industries [2]. Wastewater treatment has become increasingly important in order to recover clean water from effluent treatment. The key problem for industries in this context is to implement the most efficient, cost-effective, and ecofriendly technologies to ensure reusability of this water in a sustainable manner [1]. Several bioremediation approaches based on enzyme-driven treatment systems are useful for polluted wastewater treatment [5].

Enzymes have recently used as a useful technique for improving pollution degradation. As a high-efficiency biocatalyst, enzymes offer remediation of these recalcitrant pollutants. It covers enzyme types and suppliers, enzymatic procedures in the remediation of resistant contaminants, enzymatic conversion product identification and ecotoxicological testing, and common enzymatic wastewater treatment systems [6]. Some of the potential advantages of extremozyme remediation over conventional therapy include: its industrial usability; manoeuvrability across a considerable pH, temperature, and salinity range; and a decrease in sludge volume. As a consequence, potential solutions to remove industrial contaminants from water are becoming more popular, and extremophilic extremozymes-based strategies are gaining popularity in this connection. The current state of the industrial waste water market for the various technologies that utilize extremozymes in the cleaning process. Extremozymes produced from extremophilic microbes can thrive at extreme environmental conditions [7] such as temperature stability, high stereo-selectivity, long half-life, solvent-tolerance, affinity to the substrate. They feature heat-stable and solvent-tolerant biocatalytic properties, as well as being environmentally acceptable [6]. Recently, extremozymes are proclaimed as a biological source of waste water treatment due to their high reproduction rate,

* To whom all correspondence should be sent:
E-mail: mousumi.debnath@jaipur.manipal.edu

resistance to catalyze reaction under extreme environmental conditions and significant potential [8].

With an annual increase of 4.9 percent, the worldwide economy for enzymes for various industrial applications was estimated to be worth 5.5 billion US dollars in 2018 [9]. The international enzyme industry is valued at $5.5 billion, with a forecasted value of $7.0 billion by 2023. With a combined market share of 35%, Europe and North America are the two most significant continents. between 30% and 40%, are the biggest customers [10]. Japan is also a leading enzyme manufacturer. Novozymes, Danisco, Genencor, DSM, and BASF occupy the top positions in the global market [11]. Among the enzymes, proteases, carbohydrase and lipases occupy the most sought forward category in the market [10, 12]. In this review, the significance of many enzymes from numerous extremophiles, as well as their activity in mitigating pollutants in effluent water, is reviewed.

Extremophiles and their extreme abilities

Extremophiles are microorganisms that can perish in extreme environments [13]. Extremophiles represent a diverse variety according to their area of occurrence and functioning such as hot spring, thermal vents with high temperature, Arctic and Antarctic regions with low temperature, acidic lakes, and high saline lakes. Thermophiles can thrive at high temperatures (> 80 °C up to > 110 °C), psychrophiles may sustain at low temperatures (-2 °C to 20 °C), acidophiles (pH 4), alkaliphiles (pH > 9) and halophiles can flourish at cold temperatures (-2 °C to 20 °C) (high salinity such as 2-5 M NaCl) [14]. Due to their cost-effectiveness, environmentally friendly character, and ability to create less sludge in extreme conditions, extremophiles were utilized as a plausible alternative source to remove contaminants (Fig. 1) in many industries [14, 15]. Microbially generated enzymes have been used to treat wastewater, with benefits such as cheaper costs, reduced environmental toxicity, simplicity of application, and flexibility.

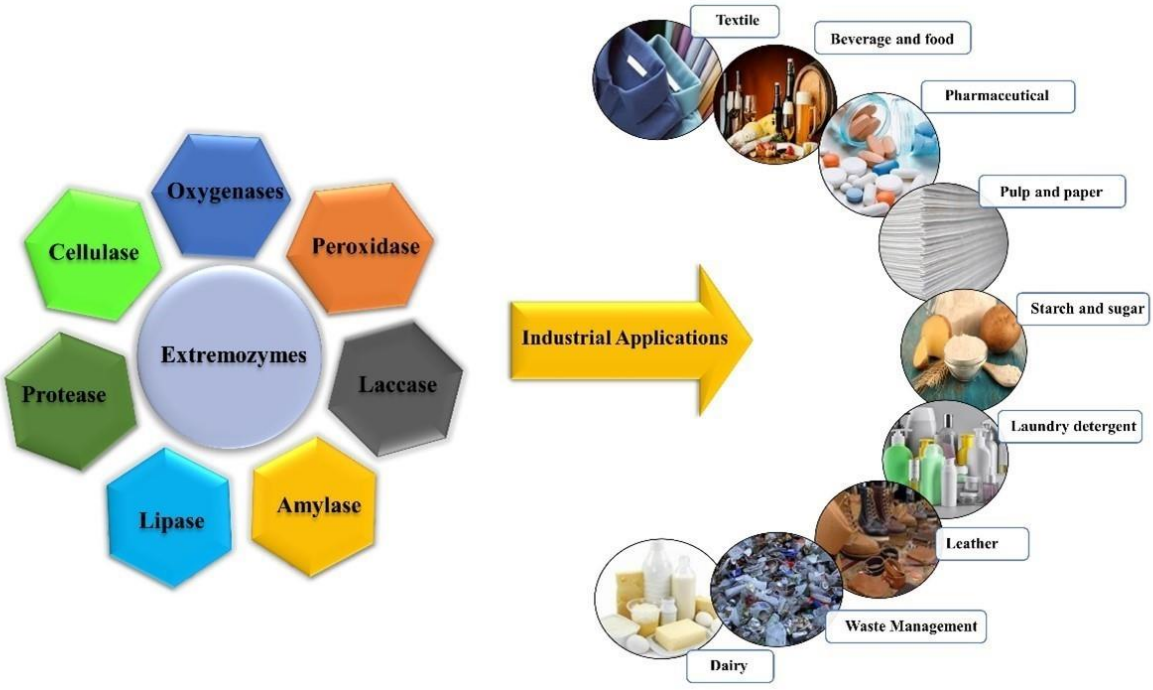

Fig. 1. Extremozymes and their application in different industries

Cold-adapted microorganisms produce psychrophilic enzymes with a high catalytic efficiency, which have important implications for the biotechnology sector [17]. Some cold active extremozyme producing strains, such as *Bacillus cereus* HSS [18] *Pseudomonas palleroniana* GBPI-508 [19], *Pseudomonas marinensis* gcc21 [20], are now gaining interest by industries such as textile and detergent due to their low temperature stability [21]. They can catalyze their respective processes in aqueous and nonaqueous environments, as well as in water/solvent combinations and at freezing temperatures. The features that are developed in synthetically designed enzymes through genetic manipulation, genome shuffling, genetic blending, truncation, or rational protein synthesis, are already existent in these enzymes [22].

Saltpans, salt mines and highly salted fermented

foods all provide a suitable environment for the halophilic enzymes that can live at high salt concentrations [23]. Halophilic bacteria *Hortaea* sp. was able to produce 1,2-dioxygenase and laccase and also degrade solvent green 3 into phthalic acid and 4-hydroxybenzoic acid [24]. FMN-dependent NADH azoreductase was produced by halophilic bacteria *Salinivibrio kushneri HTSP*, which is able to degrade and decolorize three pollutant dyes including safranin and congo red [25] The halophilic bacteria adapted to high salt concentrations have a large proportion of acidic amino acids and low percentage of lysine and aliphatic chains [26]. So, these halophilic extremozymes have industrial potential for textile, laundry detergent, leather, pharmaceutical and food industry because they able to degrade heavy metals, petroleum hydrocarbons, as well as decolorize industrial waste water [26, 27].

Thermophilic bacteria are found mostly in hot springs and can withstand temperatures of 45–80 degrees Celsius. Due to their unique qualities like high-temperature growth and different macromolecular characteristics, thermophiles can have a robust metabolism, chemically and physically stable enzymes, and lower growth but higher productivity than equivalent mesophilic species. Thermophilic enzymes are suitable for biotechnological procedures that need high temperatures, moreover, they are resistant to detergents, solvents, and acidic and alkaline pH [28]. *Brevibacillus borstelensis* strains UE10 and UE27, as well as *Aneurinibacillus thermoaerophilus* strain UE1, were found to be capable of producing cellulase, which was used in carbohydrate fermentation [29]. *Paenibacillus validus*, *Paenibacillus koreensis*, and *Bacillus nealsonii*, among other thermophilic lignocellulolytic bacteria isolates, produced ligninase, xylanase, protease, and urease, and were used to improve composting indices [30]. Protease was produced by the thermophilic bacterium *Thermomonas hydrothermalis*. This makes it a desirable source for thermostable enzymes with commercial applications in biotechnological and environmental applications [31].

Alkaliphile/acidophile enzymes from micro-organisms typically share other extremophilic habitat features like resistance to extreme pH levels. They are active chelators, thus can be very beneficial for application in detergent manufacture [23]. Acidophiles have a place in the bioprocessing of minerals because they share other extreme habitat features like thermophilicity, halophilicity, or heavy metal tolerance. Alkaline proteases are the significant enzymes of alkaliphiles with substantial impact as additives for biological detergents [17].

Extremophiles produce hydrolases, which are widely used in industry for a variety of reasons, including their resilience to organic solvents and severe temperatures [31]. As a result of their environmentally favorable characteristics, they can be used in bioremediation and waste treatment. as peroxidase [16]. In the treatment of industrial wastewater, these extremozymes play an essential function (Fig. 1) [32]. They can degrade dyes, heavy metal, plastics, polyhydroxyalkanoates, pesticides and many more pollutants (Fig. 2). These extremozymes are utilized in various industries such as biofuel, detergent, pharmaceutical, food, agricultural, bioenergy, textile and cosmetic industries [33].

Extremozymes in bioremediation of different pollutants

Several bioremediation approaches based on an enzyme-driven treatment system have been studied as an effective method for polluted wastewater treatment as they require low cost, less time and labor [5]. Extremophiles have hydrolase activity that is widely used in industries because they have resistance to organic solvents and extreme temperatures [31]. So, they can be applied in bioremediation and waste treatments due to their eco-friendly nature. Hydrolytic enzymes and oxidoreductases, are two types of extremozymes beneficial for waste water treatment [16]. These extremozymes are crucial in the treatment of industrial effluents. They can degrade dyes, heavy metals, plastics, polyhydroxyalkanoates, pesticides and many more pollutants (Fig. 2) [32]. These extremozymes are utilized in various industries such as biofuel, detergent, pharmaceutical, food, agricultural, bioenergy, textile and cosmetic industries [33].

The activity of these enzymes produced by extremophilic bacteria on various pollutants is shown in Table 1. Treatments with oxidoreductases and hydrolases of many types of synthetic and recalcitrant compounds, among other things, leads to simpler or covalently connected and less reactive components [34]. The principal extremozymes involved in contaminant bioremediation, including oxygenases, peroxidases, hydrolases, lipases, phosphodiesterase, and many others [35], will be discussed in this context for use in waste water treatment of hazardous substances.

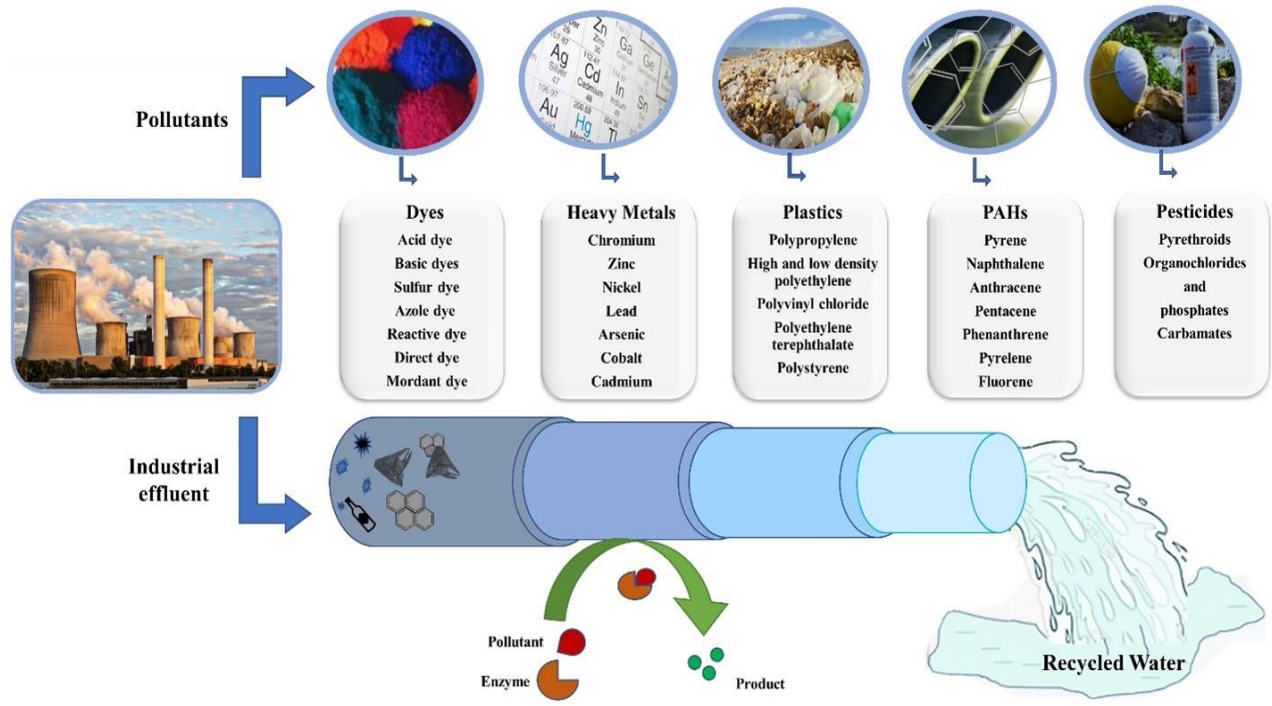

Fig. 2. Schematic diagram of waste water containing toxic industrial pollutants and their treatment using extremozymes produced from extremophiles

Oxidoreductase

Several microorganisms, fungi, and multicellular organisms produce and release oxidoreductases to eliminate compounds by chemical interactions, which entails the flow of energy from reducing agents to oxidizing agents, producing chloride, carbon dioxide, and methanol [36]. Resistant pollutants such as aromatic chemicals, textile dyes, petrochemical pollutants, and phenolics in waste water are biodegraded by the action of oxidoreductase [16]. At 100 degrees Celsius, the hyperthermophile archaeon *Pyrococcus furiosus* includes production *via* a new mechanism involving AdhA and the native enzyme aldehyde oxidoreductase [37].

Oxygenases. Oxygenases are enzymes that belong to the oxidoreductase family wherein the co-substrate FAD/NADH/NADPH contributes to the oxidation of reduced substrates [38]. Glyphosate oxidase (goxB), a FAD-dependent enzyme isolated from *Bacillus aryabhattai* FACU3, is engaged in glyphosate herbicide bioremediation. Glyphosate is converted to aminomethylphosphonate (AMPA) by goxB cleaving the C-N link and releasing the keto acid glyoxylate [39].

Peroxidases. Peroxidases catalyze the conversion of lignin and other phenolic compounds in the presence of hydrogen peroxide (H_2O_2). Lignin peroxidase and manganese-dependent peroxidase have been studied the most among peroxidases because of their remarkable potential to break down hazardous chemicals in nature [40]. Peroxidases are involved in the color removal and detoxification of diverse contaminants in wastewater, as well as the decomposition of polyphenols. *Bacillus albus* MW407057 is involved in the breakdown of methylene blue dye *via* lignin peroxidase [41]. *Bacillus velezensis* Al-Dhabi 140 produces manganese peroxidase, which is capable of degrading tetracycline [42].

Laccases. Laccases are multicopper oxidases, which are redox metalloenzymes. Copper ions in these glycoproteins have a high redox capacity, which enables them to facilitate the oxidation of a wide spectrum of aromatic substrates while also generating water as a by-product of molecular oxygen reduction [43]. The laccase producing thermophilic *Thermus* sp. 2.9 was shown to be resistant to a variety of pH levels, hazardous heavy metals, and has ability to decolorize and breakdown azo dyes such as xylidine and methyl orange found in wastewaters [44].

Hydrolases

Hydrolytic enzymes break down esters, peptide bonds, carbon-halide bonds, and other essential chemical molecules. When compared to physico-chemical remediation for the breakdown of toxic

organic compounds, bioremediation is both safe and cost effective [38].

Table 1. Extremophilic enzymes and their pollutant degradation efficiencies

S.No	Microorganisms	Enzymes	Pollutants	Ref.
1	*Anoxybacillus rupiensis 19S*	Oxidoreductases and hydrolytic enzymes	Phenol	[16]
2	*Novosphingobium* sp. ES2	Monooxygenase	*β*-Estradiol	[45]
3	*Pseudomonas synxantha* S2TR-26 *Pseudomonas mandelii* S2TR-08	Xylene monooxygenase; catechol 2, 3-dioxygenase	p-Xylene	[46]
4	*Pseudomonas stutzeri* OX1	Toluene/*o*-xylene monooxygenase	Toluene; benzene	[47]
5	*Pseudomonas* S2TR-1	Toluene/o-xylene monooxygenase	Benzene, toluene, ethylbenzene, and isomers of xylenes	[48]
6	*Pseudomonas aeruginosa* SJTD-1	AlkB monooxygenases	*n*-Alkanes	[49]
7	*Bacillus albus MW407057,*	Lignin peroxidase	Decolorize and detoxify MB dye for environmental safety.	[41]
8	*Bacillus velezensis* Al-Dhabi 140	Manganese peroxidase	Tetracycline	[42]
9	*Bacillus albus* MW407057	Lignin peroxidase	Methylene blue and removed COD	[41]
10	*Geobacillus stearothermophilus* ATCC 10149	Laccase	Remazol brilliant blue R dye	[50]
11	*Bacillus cohnni* (RKS9)	Laccase, azoreductase, lignin peroxidase and manganese peroxidase	Congo red dye and heavy metal removed cadmium, chromium, lead and nickel	[51]
12	*Bacillus sp. GZB*	Laccases	Bisphenol A, 2,2′-azino-bis (3-ethylbenzothiazoline-6-sulfonate) and syringaldazine	[52]
13	*Bacillus* sp. CF96	Laccases	Indigo dye	[53]
14	*Thermus* sp. 2.9	Laccases	Xylidine, Methyl orange	[44]
15	*Bacillus vietnamensis* sp. MSB17	Tyrosinase , laccase, and manganese peroxidase	Malachite green (MG)	[54]
16.	*Geobacillus* sp. G27	Dioxygenase	Naphthalene	[55]
17	*Planococcus maritimus* (MSB2 and MSB16), *Bacillus pumilus* (MSB6 and MSB8) and *Bacillus vietnamensis* (MSB10 and MSB17	Hydrolases (amylases, caseinases, cellulases, gelatinases, lipases, ligninases, and Malachite green dye degraders)	Malachite green dye degraders	[56]
18	*Bacillus cereus* KM201428	Proteases	Detoxification and degradation of Malachite green dye	[57]
19	*Geobacillus* sp. D4, *Geobacillus* sp. D7,	Lipase	Alkanes, toxic poly-aromatic hydrocarbons (PAHs), organosulfur, carboxylic acids,	[58]

	Anoxybacillus geothermalis D9		alkene, resins, organosilicon, alcohol, organochlorine, and ester	
20	*Pseudomonas nitroreducens* AR-3	Organophosphate hydrolase (OPH),	Chloropyrifos	[59]
21	*Bacillus licheniformis* HULUB1 and *Bacillus subtilis* SUNGB2	Amylase	Degradation of food waste	[60]
22	*Escherichia coli* IES-02	Carboxyesterases	Malathion	[61]
23	*Lysinibacillus sphaericus* YMM	Carboxyesterases	Malathion	[62]
24	*Pseudomonas aeruginosa* PA06 and *Achromobacter* sp. AC15	Catechol 1,2-dioxygenase (C12O) and 2,3-dioxygenase activities (C23O) enzyme	Pyrene	[63]
25	*Pseudomonas* sp. strain phDV1	PHA synthase	Degrades phenol and produces polyhydroxyalkanoates	[64]
26	*Comamonas testosterone*	PHB depolymerase (PhaZ)	Polyhydroxybutyrate (PHB)	[65]

Hydrolytic enzyme is highly successful in bioremediation of oil spills, organophosphate, and carbamate pesticides. The carbendazim hydrolysing enzyme obtained from *Klebsiella*, *Flavobacterium*, and *Stenotrophomonas* was recently found to be capable of breakdown of carbendazim into nontoxic forms [66]. Bacillus sp. strain TSCVKK produced extracellular detergent-stable alpha-amylase in the presence of halophilic alkali. As a result, these amylases could be feasible options for bioremediation of waste from paper and other sources [16, 67]. These well-known and fully characterized α-amylases elect this enzyme as a prime candidate for application on bioremediation. A halotolerant and thermostable lipase from *Oceanobacillus* sp. PUMB02 bacterium has a high degree of stability over a wide range of pH, salinity and temperature and is stable at 50-70°C and alkaline pH [68]. An halophilic strain *Halobacillus* sp. strain EG1HPQL degrades n-alkanes and has resistance to heavy metals including Cu, Pb, and Ni [69]. Furthermore, the thermophilic bacterium *Geobacillus sp. GS53* has high stability in the presence of organic solvents and detergent constituents [70]. Protease is used in waste management, food and feed, detergent industry, medicine, leather industry and protease engineering [71]. The bacterium *Bacillus amyloliquefaciens-ASK11* isolated from a tannery waste was found to produce cellulases [72]. Dicofol is an organic pollutant which is degraded by cellulase into 4,4'-dichloro-dibenzophenone by an oxidative process [73]. The mode of action of all these enzymes on different pollutants is explained in Table 2.

ADAPTATION OF EXTREMOZYMES

Extremozymes, or extremophilic microbe proteins, have been biochemically and molecularly modified to tolerate harsh industrial environments. Despite the fact that no single factor has been identified as creating extremozyme stability in the severe environments in which they must survive, a new study on extremophilic enzymes has aided in the understanding of the types of general patterns that influence extremophilic enzyme stability [74]. As the amino acid sequence changes, the structure, flexibility, charge, and/or hydrophobicity of extremozymes changes, resulting in changes in the enzymes. Extremophilic proteins adapt to similar harsh physical or chemical circumstances in a number of ways [75]. We'll look at the adaptations that extremophiles have made to survive in severe settings in the presence of enzymes farther down.

Changes in specific amino acid content on the protein surface

A protein's stability is largely determined by its amino acid composition. According to a study conducted by Enache *et al.,* 2010, labile amino acids are easily modified, especially when exposed to extremes such as extremely high or low temperatures, pH, or pressure. The denaturement of a protein can be caused by covalent alteration of these labile amino acids. The concentration of amino

acid residues such as glutamic acid, cysteine, and aspartic acid on the membrane of proteins is quite low, which contributes significantly to protein stability and flexibility in harsh environments [76].

Table 2. Mode of action of extremozymes on different pollutants

S.No.	Class of enzyme	Type of enzymes	Substrate/ pollutants	Mode of action	Ref.
1	Oxido-reductases	Oxygenases	Aromatic compounds such as PAHs, naphthalene, anthracene and phenanthrene, chlorinated biphenyls, aliphatic olefins, phenols, organic halogen compounds (herbicides, fungicides, and pesticides), aliphatic hydrocarbons	Coenzymes FAD, NADH, or NADPH are used to transport oxygen to organic or inorganic molecules.	[34], [77]
1.1		Monooxygenases (flavin and P450 monooxygenases)	Degrade chlorinated pesticides, hydrocarbons, xenobiotics and heme prosthetic group	Hydrolases are enzymes that transfer one oxygen atom to the substrate while the electrons of the coenzymes NADH or NADPH decrease the other oxygen to water.	[34], [77]
1.2		Dioxygenases	Naphthalene	Molecular oxygen transferred and incorporated into the substrate.	[55]
2		Peroxidases	Phenols, cresols, chlorinated phenolic compounds, polyphenols, amines, and heterocyclic amine polyamines, as well as nitroaromatic compounds such as TNT (2,4,6-trinitrotoluene), lignin, and dyes	Peroxides	[34]
2.1		Lip	Anthracene, pyrene, acenaphthene		[78]
2.2		MnP	Anthracene; fluorene; phenanthrene; dibenzothiophene		[78]
3		Laccases	PHAs, paints, plastics, dyes, estrogenic compounds, paper, and cellulose acenaphthene, anthracene, fluorene, and benzo[a]pyrene		[13], [34], [78]
3.1	Hydrolase	Amylases	Paper, food industries, textile industries, and fossil and fuel products; degradation of petroleum-derived compounds such as polyethylene; n-alkane; paraffin hydrocarbons	Starch and carbohydrate components, catalyse the hydrolysis of 1,4--D-glycosidic linkages.	[34], [60], [79]
3.2		Proteases	Phenols and proteins	Hydrolysis of peptides bonds in presence of water molecules	[16, [69], [80]
3.3		Lipases	Oil residues, petroleum contaminants, effluents, and soil recovery, kitchen waste	Hydrolysis, esterification, alcoholysis, and interesterification of fatty acids, esters, and glycerides	[81], [82]
3.4		Cellulases	Dicofol; cellulosic compounds	Hydrolysis of substrate to simple compounds.	[73]

Acidic residues are preferred in these conditions due to their great capacity for binding water molecules, but halophilic proteins also have repulsive electrostatic interactions at healthy pH levels. The carboxyl groups of glutamate and aspartate are used to maintain a hydrated protein surface. Polygalacturonase, a cold-active enzyme, was discovered to have low arginine concentrations, impairing thermo adaptation [83]. Psychrophilic enzymes have a reduced arginine/lysine proportion, more glycine residues for enhanced allosteric movement, fewer proline residues in loops but more in helices, and more non-polar residues on the protein surface, all of which make a contribution to a lower core hydrophobic nature but an increased surface chemistry [74]. The lack of surface lysine residues in halophilic proteins was a startling result. This observation corresponds to a decrease of hydrophobic surfaces, which results in an increase in hydration at the protein surface [84]. A small amount of bulky hydrophobic side chains has been identified on the surface of halophilic proteins [85]. *Thermovibrio ammonificans* makes an enzyme with a specific function. *Thermovibrio ammonificans* makes an enzyme with a distinctive core made up of two inter subunit disulfide connections and a single lysine residue from each monomer in the molecule's centre [85]. The stability and thermophilicity of extremozymes are greatly affected by modifying the N- and C-terminal residues. Thermophilic enzymes usually have high level of bisulfide bonds, shorter loops, which inhibit nonspecific interactions and improve structural rigidity and, as a result, resistance to unfolding at high temperatures [86].

Increased number of salt bridge formation/ increased ionic interaction

Ionic interactions have a big impact on protein stability. Extremophilic proteins interact to build salt bridges between oppositely charged neighboring residues, which aids protein folding, structure, and oligomerization while also improving enzyme stability at high salt concentrations [75]. Ion pairs have a vital role in the stabilization of hyperthermophilic proteins with a decreased hydrophobic impact, according to crystal structures of extremophilic proteins. Structure comparison, homology-based modelling, and site-directed mutagenesis are all aided by the availability of extremophilic protein crystal structures. The crystal structures of glutamate dehydrogenase, a hexameric protein isolated from hyperthermophilic organisms such as *Thermotoga maritima* (90°C), *Pyrococcus furiosus* (100°C), and *Thermococcus litoralis* (88°C), were studied [87, 88].

Modified protein structure

In nature, many proteins or protein families use the oligomerization mechanism in various ways, and they can form complexes with several polypeptide chains [89]. In oligomeric proteins, enzyme denaturation is frequently initiated by subunit dissociation, followed by irreversible monomeric denaturation in extreme cases. The oligomer structure of several extremozymes has been found to be more complex than that of mesophilic proteins, which are monomers or dimers [90]. In the other case, protein subunits undergo conformational changes that promote oligomer formation to compensate for the loss of individual component stability. The oligomerization method, on the other hand, can be utilized to promote protein flexibility and activity at low temperatures while decreasing protein stability [91]. Excellent lignocellulosic extremozyme production *in Pichia pastoris* has been demonstrated to have high enzyme properties and improved stability by a result of proper post-translational modifications [92]. A hyperthermophilic bacterium produced by iron hydrogenase, *Thermotoga maritime*, is a homotetramer, whereas dehydrogenases isolated from mesophilic species normally have one or two subunits [90].

Ionic charge changes at the surface

Extremozymes have unique properties in the solvent-exposed surface region, which contribute to their increased stability. Factors like extended nonpolar side chain exposure to solvent and an increase in total solvent accessible surface area aid in psychrophilic mannanase's thermal adaption at lower temperatures [93]. The very negative surface charge of halophilic enzymes like *Kocuria varians* and *Alicyclobacillus acidocaldarius* amylase improves their solubility and flexibility at high salt concentrations [94, 95]. The lack of surface lysine residues in halophilic proteins was an interesting finding. This finding is in line with the reduction in hydrophobic surfaces, which leads to an increase in hydration at the protein surface. Proteins that are halophilic have also been discovered and found to have a low content of bulky hydrophobic side chains on their surface [84].

Prominent catalytic mechanism

Extremozymes' catalytic processes are identical to those of their mesophilic counterparts, as evidenced by mechanistic research [96]. It's unclear

whether mesophiles and extremophiles share catalytic processes. Substrate specificities, pH dependences, kinetic isotope effects, and linear free energy connections were explored in recombinant glucosidase from *Pyrococcus furiosus*, a hyperthermophile, and *Agrobacterium faecalis*, for example [97]. As a result, enzymes with a diverse range of substrate specificities and pH sensitivity, similar Brønsted graphs, and a high correlation coefficient shared broad substrate specificities and pH sensitivity. Despite their somewhat differing optimal temperatures, both studies show that these enzymes have the same catalytic mechanism.

CONCLUSION

Due to urbanization and industrial expansion, the discharge of wastewater and the accumulation of contaminants in the environment has reached dangerous levels in recent years. These contaminants are poisonous and inflict significant harm to living beings. Extremophiles have consistently been investigated to be a great source of innovative extremozymes, which have a number of benefits over conventional chemical catalysts. Extremophile-derived enzymes, also known as extremozymes, have distinct molecular mechanisms for dealing with a variety of environmental extremes, including temperature extremes, acidic and increased metal concentrations, excessive salinity, and a basic pH. Extremozymes derived from microorganisms have been harnessed to biodegrade heavy metals, toxins, dyes, aromatic compounds, and plastics, among other contaminants. They disintegrate huge quantities of pollution quickly by using pollutants as feedstock. Extremozymes have biocatalytic activity in a specific substrate in challenging environments and have a long shelf life. Extremozymes are known for their consistency, repeatability, and higher yields under adverse conditions. Their ability to generate the least harmful and biodegradable industrial waste has pushed their use in a variety of products and processes. This review critically examines various aspects of extremozymes and their strategic protein structure adaptations for survival of extremophilic bacteria in various environmental conditions, as well as potential pollutant biodegradation during bioremediation for various industrial wastewater treatment.

Acknowledgement: *The corresponding author sincerely recognizes Manipal University Jaipur for their support of this work under the Enhanced seed grant dated 30.04.2019[EF/2019-20/QEO4-01].*

REFERENCES

1. M. Kamali, K. M. Persson, M. E. Costa, I. Capela, Environ Int., **125**, 261 (2019).
2. T. Shindhal, P. Rakholiya, S. Varjani, A. Pandey, H. H. Ngo, W. Guo, H. Y. Ng, M. J. Taherzadeh, *Bioengineered*., **12,** 70 (2021).
3. T. G. Ambaye, M. Vaccari, E. D. van Hullebusch, A. Amrane, S. Ritmi, *Int J Environ Sci Technol.,* **1** (2020).
4. T. O. Ajiboye, O. A. Oyewo, D. C. Onwudiwe, *Chemosphere*, **262**, 128379 (2021).
5. S. Mishra, A. Maiti, *Clean Technol Environ Policy*, **21**, 763 (2019).
6. S. Feng, H. Hao Ngo, W. Guo, S. W. Chang, D. D. Nguyen, D. Cheng, S. Varjani, Z. Lei, Y. Liu, *Bioresour. Technol.*, **335**,125278 (2021).
7. A. Mutlu-Ingok, D. Kahveci, F. Karbancioglu-Guler, B. Ozcelik, *Microb. Extrem.*, **197** (2022).
8. H. Nadaroglu, M. S. Polat, in: Microbial extremozymes, M. Kuddus (ed.), Elsevier, Saudi Arabia, 2022, p. 67**.**
9. R. R. Sousa, A. S. Silva, R. Fernandez-Lafuente, V. S. Ferreira-Leitão, *Catal. Sci. Technol.*, **11**, 5696 (2021).
10. A. Tarafdar, R. Sirohi, V. K. Gaur, S. Kumar, P. Sharma, S. Varjani, H. O. Pandey, *Bioresour. Technol*., 124771 (2021).
11. B. Sarrouh, T. M. Santos, A. Miyoshi, R. Dias, V. Azevedo, *J. Bioprocess. Biotech.*, **4**, 2 (2012).
12. S. Fatima, A. Faryad, A. Ataa, F. A. Joyia, A. Parviaz, *Biotechnol. Appl. Biochem.*, **68**, 445 (2021).
13. B. G. Aparna, .S. W. Meghmala, N. P. Neha, *Res. J. Biotechnol*., **16**, 240 (2021).
15. D. C. Roy, S. K. Biswas, A. K. Saha, B. Sikdar, M. Rahman, A. K. Roy, Z. H. Prodhan, S.-S.Tang, *Peer J.*, **6** (2018).
16. J L. Jardine, S. Stoychev, V. Mavumengwana, E. Ubomba-Jaswa, *J. Environ Manage*., **223,** 787 (2018).
17. D. C. Demirjian, F.Morís-Varas, C. S. Cassidy, *Curr. Opin. Chem. Biol*., **5**, 144 (2001).
18. S. W. M. Hassan, H. H. Abd El Latif, S. M. Ali, *Front Microbiol.*, **9**, 2377 (2018).
19. R. Jain, N. Pandey, A. Pandey, *Biocatal. Biotransformation*, **38,** 263 (2020).
20. C. Guo, R. Zheng, R. Cai, C. Sun, S. Wu, *Microorganisms*, **9**, 802 (2021).
21. N. Mhetras, V. Mapare, D. Gokhale, *Appl. Biochem. Biotechnol.*, **1** (2021).
22. S. Elleuche, C. Schroeder, K. Sahm, G. Antranikian, *Curr. Opin. Biotechnol.*, **29,** 116 (2014).
23. B. van den Burg, *Curr. Opin. Microbiol.*, **6**, 213 (2003).
24. D. A. Al Farraj, M. S. Elshikh, M. M. Al Khulaifi, T. Hadibarata, A. Yuniarto, A. Syafiuddin, *Int. Biodeterior./ Biodegradation*, **140,** 72 (2019).
25. J. John, R. Dineshram, K. R. Hemalatha, M. P. Dhassiah, D. Gopal, A. Kumar, *Front Microbiol.,* **11**, 3281 (2020).
26. A. C. Flores-Gallegos, M. Delgado-García, J. A. Ascacio-Valdés, S. Villareal-Morales, M. R. Michel-Michel, C.N Aguilar-González, R. Rodríguez-Herrera, in: Enzymes in Food Biotechnology, M.

Kuddus (ed.), Elsevier, United Kingdom, 2019, p. 197.
27. A. Sekar, K. Kim, *Encycl. Mar. Biotechnol*., **4**, 2061 (2020).
28. P. Abdollahi, M. Ghane, L. Babaeekhou, *Geomicrobiol. J*., **38**, 87 (2021).
29. U. Ejaz, S. Muhammad, I. A. Hashmi, F. I. Ali, M. Sohail, *J. Biotechnol.*, **317**, 34 (2020).
30. A. Hemati, N. Aliasgharzad, R. Khakvar, E. Khoshmanzar, B. A. Lajayer, E. D. van Hullebusch, *Waste Manag*., **119,** 122 (2021).
31. D. Pérez, S. Martín, G. Fernández-Lorente, M. Filice, J. M. Guisán, A. Ventosa, M. T. García, E. Mellado, *PLoS One*, **6** (2011).
32. R. L. Singh, R. P. Singh, R. Gupta, R. L. Singh, in: Advances in biological treatment of industrial waste water and their recycling for a sustainable future, R. L. Singh, R. P. Singh (eds.) Singapore, Springer, 2019, p. 1.
33. G. Z. L. Dalmaso, D. Ferreira, A. B. Vermelho, *Mar. Drugs*, **13**, 1925 (2015).
34. C. H. Okino-Delgado, M. R. Zanutto-Elgui, D. Z. do Prado, M. S. Pereira, L. F. Fleuri, in: Microbial metabolism of xenobiotic compounds, P. Arora (ed.) Singapore, Springer, 2019, p. 79.
35. S. Dave, J. Das, in: Bioremediation for Environmental Sustainability, G. Saxena, V. Kumar, M. P. Shah (eds.) Elsevier, 2021, p. 325.
36. J. D. C. Medina, A. L. Woiciechowski, L. R. C. Guimarães, S. G. Karp, C. R. Soccol, In: Current developments in biotechnology and bioengineering, A. Pandey, S. Negi, C. R. Soccol (eds.), Elsevier, 2017, p. 227.
37. M. W. Keller, G. L. Lipscomb, D. M. Nguyen, A. T. Crowley, G. J. Schut, I. Scott, R. M. Kelly, M. W. W. Adams, *Microb. Biotechnol.*, **10**, 1535 (2017).
38. C. S. Karigar, S. S. Rao, *Enzyme Research*, **3** (2011).
39. N. I. Elarabi, A. A. Abdelhadi, R. H. Ahmed, I. Saleh, I. A. Arif, G. Osman, D. S. Ahmed, *Saudi J. Biol. Sci*., **27**, 2207 (2020).
40. N. Bansal, S. S. Kanwar, *Sci. World J.*, (2013).
41. R. Kishor, G. D. Saratale, R. G. Saratale, R. G. Saratale, L. F. R. Ferreira, M. Bilal, H. M. N. Iqbal, R. N. Bharagava, *Colloid Surfaces B Biointerfaces*, **206**, 111947 (2021).
42. N. A. Al-Dhabi, G. A. Esmail, M. V. Arasu, *Chemosphere*, **268**, 128726 (2021).
43. S. Rodríguez-Couto, in: Current developments in biotechnology and bioengineering, A. Pandey, C. Larroche, C. R. Soccol (eds.), Netherland, Elsevier, 2018, p. 211.
44. L. E. Navas, R. Carballo, L. Levin, M. F. Berretta, *Extremophiles*, **24,** 705 (2020).
45. S. Li, K. Sun, X. Yan, C. Lu, M. G. Waigi, J. Liu, W. Ling, *Environ. Microbiol.*, **23**, 2550 (2021).
46. S. Miri, S. M. Davoodi, S. K. Brar, T. Rouissi, Y. Sheng, R. Martel, *Bioresour. Technol.*, **321**, 124464 (2021).
47. B. Wang, F. Gao, J. Xu, J. Gao, Z. Li, L. Wang, F. Zhang, Y. Wang, Y. Tian, R. Peng, Q. Yao, *Biotechnol. Biotechnol. Equip.*, **35**, 1632 (2021).
48. S. Miri, A. Rasooli, S. K. Brar, T. Rouissi, R. Martel, *Environ. Sci. Pollut. Res.*, **1** (2021).
49. N. Ji, X. Wang, C. Yin, W. Peng, R. Liang, *Front Microbiol*., **10**, 400 (2019).
50. J. E. Gianolini, C. N. Britos, C. B. Mulreedy, J. A. Trelles, *3 Biotech*., **10**, 1 (2020).
51. K. Roop, D. Purchase, G. D. Saratale, L. F. R. Ferreira, M. Bilal, H. M. N. Iqbal, R. N. Bharagava, *Environ. Technol. Innov*., **22**, 101425 (2021).
52. A. J. Das, R. Kumar, *Bioresour. Technol.*, **260**, 233. (2018).
53. S-G. Javadzadeh, A. Asoodeh, *Int. J. Biol, Macromol.*, **145,** 355 (2020).
54. F. A. Kabeer, N. John, M. H. Abdulla, *Bioremediat. J.*, **23**, 334 (2019).
55. S. Mallick, J. Chakraborty, T. K. Dutta, *Crit. Rev. Microbiol.*, **37**, 64 (2011).
56. A. K. Farha, T. R. Thasneem, A. Purushothaman, J. A. Salam, A. M. Hatha, *J. Genet. Eng. Biotechnol*., **16**, 253 (2018).
57. W. C. Wanyonyi, J. M. Onyari, P. M. Shiundu, F. J. Mulaa, *Energy Procedia* ,**119**, 38 (2017).
58. D. F. Yusoff, R. R. N. Z. Abd Rahman, M. Masomian, M. S. M. Ali, T. C. Leow, *Catalysts*, **10,** 851 (2020).
59. A. Aswathi, A. Pandey, R. K. Sukumaran, *Bioresour. Technol.*, **292**, 122025 (2019).
60. E. S. M. Pinto, M. Dorn, B. C. Feltes, *Chemosphere*, **250**, 126202 (2020).
61. S. Sirajuddin, M. A. Khan, S. A. U. Qader, S. Iqbal, H. Sattar, A. Ansar, *Int. J. Biol .Macromol*., **145,** 445 (2020).
62. G. ,I. K. Marei, Y. M. M. Mohammed, E. I. Rabea, M. E. I. Badawy, *Int. J. Environ. Stud.*, **76**, 616 (2019).
63. J. Li, W. Chen, W. Zhou, Y Wang, M, Deng, S. Zhou, *Ecotoxicology*, **1** (2020).
64. I. Kanavaki, A. Drakonaki, E. D. Geladas, A. Spyros, H. Xie, G. Tsiotis, *Microorganisms*, **9**,1636 (2021).
65. D. I. Martínez-Tobón, M. Gul, A. L. Elias, D. Sauvageau, *Appl. Microbiol. Biotechnol*., **102,** 8049 (2018).
66. M.L. Alvarado-Gutiérrez, N. Ruiz-Ordaz, J. Galíndez-Mayer, E. Curiel-Quesada, F. Santoyo-Tepole, *Environ. Sci. Pollut. Res*., **1** (2020).
67. S. Vaidya, P. Rathore, in: International conference on recent trends in agriculture, veterinary and life sciences (ICAVLS 2015), 2015, p.1.
68. G. S. Kiran, A. N. Lipton, J. Kennedy, A. DW. Dobson, J. Selvin, *Bioengineered*, **5,** 305 (2014).
69. I. M. Ibrahim, S. A. Konnova, E. N. Sigida, E. V. Lyuban, A. Y. Muratova, Y. P. Fedonenko, K. Elbanna, *Extremophiles*, **24**, 157 (2020).
70. S. G. Baykara, Y. Sürmeli, G. Şanlı-Mohamed, *Appl. Biochem. Biotechnol*., **193,** 1574 (2021).
71. P. Solanki, C. Putatunda, A. Kumar,R. Bhatia, A. Walia, *3 Biotech*., **11**, 1 (2021).
72. M. N. Khan, H. Lin, M. Li, J. Wang, Z. A. Mirani, S. I. Khan, M. A. Buzdar, I. Ali, K. Jamil, *Pak. J. Pharm. Sci.*, **30**, 839 (2017).
73. Z. Wang, T. Yang, Z. Zhai, B. Zhang, J. Zhang, *J.*

Environ. Sci., **36,** 22 (2015).
74. F. Sarmiento, R. Peralta, J. M. Blamey, *Front Bioeng. Biotechnol.*, **3** (2015).
75. M. Enache, M. Kamekura, *Rom. J. Biochem.*, **47,** 46 (2010).
76. F. T. Robb, D. S. Clark, *J. Mol. Microbiol. Biotechnol.*, **1,** 101 (1999).
77. O. Kweon, S-J Kim, J. P. Freeman, J. Song, S. Baek, C. E. Cerniglia, *MBio 1*, **1** (2010).
78. T. Kadri, T. Rouissi, S. K. Brar, M. Cledon, S. Sarma, M. Verma, *JES*, **52** (2017).
79. M. Karimi, D. Biria, *Sci. Rep*., **9**, 1 (2019).
80. N. Khoshnevis, S. Rezaei, A. Samaei-Nouroozi, M. Amin, M. Moshfegh, M. R. Khoshay, M. A. Faramarzi, *Iran. J. Pharm. Res.* IJPR, **17**, 1392 (2018).
81. J. Hu, W. Cai, C. Wang, X. Du, J. Lin, J. Cai, *Biotechnol. Biotechnol. Equip*., **32**, 583 (2018).
82. J. Zhao, S. Liu, Y. Gao Y, M. Ma, X. Yan, D. Cheng, D. Wan, Z. Zeng, P. Yu, D. Gong, *Int. J. Biol. Macromol.*, **176**, 126 (2021).
83. L. N. Ramya, *J. Food Sci .Technol*., **52,** 5484 (2015).
84. S. DasSarma, P. DasSarma, *Curr. Opin. Microbiol*., **25**, 120 (2015).
85. J. A. Littlechild, *Front Bioeng. Biotechnol*., **3**, 161 (2015).
86. M. Jin, Y. Gai, X. Guo, et al., *Mar. Drugs*, **17** (2019).
87. S. Knapp, W. M. de Vos, D. Rice, R. Ladenstein, *J. Mol. Biol.*, **267,** 916 (1997).
88. K. L. Britton, K. S. P. Yip, S. E. Sedelnikova, T. J. Stillman, M. W. W. Adams, K. Ma, D. L. Maeder, F. T. Robb, N. Tolliday, C. Vetriani, D. W. Rice, P. J. Baker, *J. Mol. Biol*., **293,** 1121 (1999).
89. C. M. Doyle, J. A. Rumfeldt, H. R. Broom, A. Broom, P. B. Stathopulos, K. A. Vassall, J. J. Almey, E. M. Meiering, *Archives of Biochemistry and Biophysics*, **531**, 44 (2013).
90. M. F. J. M. Verhagen, T. O'Rourke, M. W. W. Adams, *Biochim. Biophys. Acta (BBA)-Bioenergetics*, **1412**, 212 (1999).
91. F. Pucci, M. Rooman, *Curr. Opin. Struct. Biol.*, **42**, 117 (2017).
92. B. G. Ergün, P. Çalık, *Bioprocess Biosyst. Eng*., **39,** 1 (2016).
93. S. Parvizpour, N. Hussin, M. S. Shamsir, J. Razmara, *Appl. Microbiol. Biotechnol.*, **1** (2021).
94. R. Yamaguchi, H. Tokunaga, M. Ishibashi, T Arakawa, M. Tokunaga, *Appl. Microbiol. Biotechnol.*, **89,** 673 (2011).
95. J. Matzke, B. Schwermann, E. P. Bakker, *Comp. Biochem. Physiol. Part A Physiol*., **118,** 475 (1997).
96. J. Eichler, *Biotechnol. Adv.*, **19,** 261 (2001).
97. M. W. Bauer, R. M. Kelly. *Biochemistry***, 37**, 17170 (1998).

Bulgarian Chemical Communications, Volume 54, Special Issue C (pp. 46-49) 2022 DOI: 10.34049/bcc.54.C.0046

Electrochemical performance of LAGP based polymer electrolyte for solid-state battery application

A. Das[1,2], M. Goswami[1,2*]

[1]*Glass & Advanced Materials Division, Bhabha Atomic Research Centre, Trombay, Mumbai 400085, India*
[2]*Homi Bhabha National Institute, Anushaktinagar, Mumbai 400094, India*

Accepted: July 06, 2022

To address the safety issues of the commercial lithium ion batteries, composite solid electrolytes (CSEs) are promising alternatives. Fabrication of micron-size thin pure solid state electrolyte (SSE) is difficult. It can be solved by incorporating active filler (SSE) into the polymer. In this work we report synthesis of a CSE by incorporating LAGP (Li_2O-Al_2O_3-GeO_2-P_2O_5) (SSE), LiTFSI, EMIMTFSI into PVDF-HFP polymer. Cyclic voltammetry experiment of Li/CSE/LFP ($LiFePO_4$) showed only two broad peaks at 3.8 V and 3.1 V for oxidation and reduction of lithium, respectively. The value of transference number obtained from a symmetric cell study is 0.16. The galvanostatic charge/discharge profiles of the fabricated solid state cell were recorded at C/15. The value of discharge capacity was 150 $mAhg^{-1}$ (88% of theoretical capacity) which was almost constant up to the 40^{th} cycle.

Keywords: Glass ceramics; solid state battery; solid state electrolyte; NASICON; LAGP

INTRODUCTION

Lithium ion batteries (LIBs) are being widely used in recent years for their applications as energy storage device in various electronic gadgets. However, LIBs suffer with various shortcomings: (a) internal short circuit (b) fire or explosion at high temperature because of the uses of a flammable liquid electrolyte, etc. [1]. To avoid all these issues pertaining to conventional LIBs, ASSLBs (all solid state lithium batteries) are recognized as the safest alternative [2]. ASSLBs have mainly three components: cathode, anode and solid-state-electrolyte (SSE). The charging and discharging mechanism is the same as for LIBs. Lithium ion is transferred from cathode to anode through SSE while charging and during the discharge process the exactly reverse phenomenon takes place [3]. SSEs are mainly two types: organic and inorganic. Despite several advantages of organic SSE, it has few drawbacks like narrow temperature range and poor structural stability, whereas inorganic SSEs can have improved stability and safety over a wide temperature range. A promising SSE should have high ionic conductivity, thermal and electrochemical stability. Lithium ions hop from one stable position to another inside the SSE. Therefore, the ion diffusion is mainly related to the crystal lattice of the SSE. The ion migration channel can be widened by doping. Among other inorganic SSEs, oxide SSEs are more environment-friendly and can be easily processed. These kind of materials are mainly polycrystalline, where the lithium ion migrates through two regions: grain and grain boundary. The movement is slow inside the grain boundary as compared to the grain. Therefore, the oxide SSEs should have large and dense grains [4]. Among other oxides (i.e. perovskite, garnet, etc.) Li-based NASICON (Na super-ionic conductor) type materials ($LiM^{(IV)}_2(PO_4)_3$, $M^{(IV)}$: Ge^{4+}, Ti^{4+}, Zr^{4+}, etc.) with high ionic mobility show a potential application in ASSLBs as SSE [5]. Again, due to high interfacial resistance between rigid polycrystalline SSE and the electrode, modifications are required by mixing with polymer [6].

In this study glass ceramics-based NASICON type $Li_{1.5}Al_{0.5}Ge_{1.5}P_{2.9}Si_{0.1}O_{12}$ (LAGP) SSE was prepared. To enhance the electrochemical stability, the composite solid electrolyte (CSE) was synthesized by incorporating PVDF-HFP, lithium bis(tri-fluoromethanesulfonyl) imide (LiTFSI) and l-ethyl-3-methylimidazolium bis(trifluoromethyl sulfonyl) imide (EMITFSI). To ensure the lithium ion insertion/extraction reaction a cyclic voltammetry (CV) experiment was carried out. Lithium ion transference number was estimated using d.c. polarization experiment along with complex impedance spectroscopy (CIS). Automatic battery analyzer was used to study the cell performance.

EXPERIMENTAL

Preparation of LAGP glass & glass-ceramics

Glass with composition $Li_{1.5}Al_{0.5}Ge_{1.5}P_{2.9}Si_{0.1}O_{12}$ (LAGP) was prepared using conventional melt-

* To whom all correspondence should be sent:
E-mail:mgoswami@barc.gov.in

quenching technique. The purity of the constituent chemicals was 99.9% or higher. The batch was prepared in weight of 100 g. Calcination was performed after thorough mixing of the initial components. This process was repeated for complete decomposition of the initial constituents to the corresponding oxide forms. After that, the powder was taken in a Pt-Rh crucible and the latter was put inside a furnace at 1500°C for melting. Melt was kept at that temperature for sufficient time to ensure complete melting and finally cast into a pre-heated graphite mold. Prepared glass sample was annealed at 500°C for 4 h. LAGP glass-ceramics sample was prepared using optimized heat treatment based on DTA data.

Composite solid electrolyte (CSE) synthesis

PVDF-HFP + 20wt.% LAGP + 20wt.% LiTFSI + 35wt.% EMITFSI were mixed to prepare CSE by the solution casting method. In this technique, appropriate proportion of PVDF-HFP was dissolved in acetone under constant stirring at 100 rpm at 50°C for 3-4 hours to get crystal clear solution. Then, LiTFSI and EMITFSI were added to the solution and stirred magnetically for 2 hours. After that, LAGP powder was mixed with the solution and stirred for 20 hours for homogeneous mixing. Then the solution was cast on a glass plate and dried in ambient conditions for 3-4 days. Finally, the thin and flexible CSE film was peeled off from the glass surface and was dried in an oven at 50°C overnight. The thickness of the CSE obtained was 100-150 µm. The sample was transferred into a Ar-filled glove box for future studies.

Electrode preparation

$LiFePO_4$ (LFP) was used as active cathode material. For preparation of cathode, a slurry of 40wt.% LFP, 55 wt.% CSE and 5 wt.% carbon black was prepared using NMP as dispersant instead of acetone used for CSE preparation. Here, PVDF was used as a binder polymer. Film coater was used to coat the slurry onto an aluminium foil. After that, the coating was dried overnight at 60°C inside an oven. Then the cathode was cut into 1cm×1cm square pieces and kept inside the glove box. The amount of active material in the cathode was 2.86gcm^{-2}. The anode material was lithium metal. Before the cell fabrication the oxidised layer on the lithium foil was cleaned using hexane.

Cell fabrication

The cell was prepared by sandwiching CSE between prepared cathode and lithium metal anode inside the glove box. Automatic crimper and CR2032 coin cell were used for cell fabrication. The cell was kept overnight for stabilization.

Experimentation

Lithium ion transference number and cyclic voltammetry (CV) experiments were performed using Advanced Electrochemical System (PARSTAT 2273, Princeton Applied Research) at a scan rate of 0.1 Vsec^{-1} from 2.7 V to 4.2 V. NOVO Control Impedance analyzer was used for ac impedance measurements. The lithium ion transference number (t_{Li+}) of the CSE was evaluated using combined ac/dc technique. A dc volt of 5m V was applied on Li|CSE|Li symmetric cell for 2 hours for polarization and the corresponding current was measured. The cell resistance was also measured before and after polarization using complex impedance spectroscopy. The value of t_{Li+} was calculated using Bruce-Vincent's equation:

$$t_{Li+} = \cdots \quad (1)$$

where, ΔV is the applied small constant dc potential, I_0 and R_0 are the current and resistance before polarization, I_{ss} and R_{ss} are the current and resistance after polarization (or at steady sate) [7]. Galvanostatic charge/discharge experiments were carried out within the voltage range of 2.7-4.0 V at room temperature using Neware automatic battery analyzer.

RESULTS AND DISCUSSION

Fig. 1. shows the CV curves of Li|CSE|LFP solid state cell at room temperature. Two broad peaks were observed at 3.2 and 3.8 V *vs* Li/Li$^+$ due to lithium ion insertion and extraction, respectively [8]. There is no other peak found in the scans, which indicates the absence of any other side reaction within this voltage range.

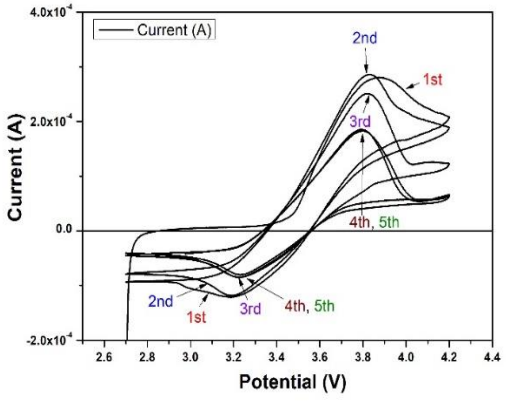

Fig. 1. CV scans of Li/CSE/LFP cell

After 4 cycles the peak current became steady. Amplitudes of the anodic and cathodic peaks are not

equal indicating that the diffusion behavior is not the same inside the cathode (LFP) and anode (lithium metal). Guo *et al.* also reported this kind of CV plot at room temperature [9].

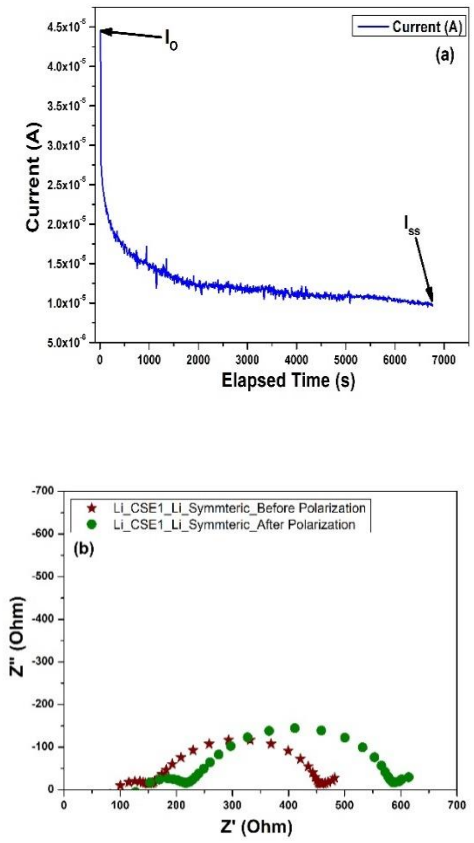

Fig. 2. (a) DC polarization curve of Li|CSE|Li symmetric cell at a fixed applied voltage. (b) AC impedance plot of the symmetric cell before and after polarization

Polarization current *versus* time plot of the symmetric cell (Li|CSE|Li) is shown in Fig. 2(a). After applying a constant voltage (ΔV) across the cell, ions move towards the electrode/electrolyte interface and start to accumulate there. This causes a current flow (I_0) initially as seen in Fig. 2(a). Ions are getting accumulated at the lithium metal surface and form a space charge region which reduces the polarization current with time [10]. Since the ions are getting absorbed at the lithium metal surface, the final current can be designated as a steady state current (I_{ss}) due to only lithium ions movement. Fig. 2(b) shows the complex impedance plot of the Li|CSE|Li cell before and after the d.c. polarization experiment. The small semicircular part in the high frequency region represents the bulk resistance of the CSE, while the mid frequency intercept indicates the combined effect of interfacial, charge-transfer and passive layer resistances. The lithium ion transference number (t_{Li+}) (Table 1) was estimated using equation 1, where total resistance, R_o and R_{ss}, was computed before and after d.c. polarization, respectively. Similar values of t_{Li+} are reported in the literature [11,12]. Hence, the value of 0.16 is sufficient to use as a solid electrolyte inside a lithium ion cell.

Table 1. Evaluation of t_{Li+}

ΔV(V)	R_0 (Ω)	I_0 (μA)	R_{ss} (Ω)	I_{ss} (μA)	t_{Li+}
0.05V	454	44	587	10	0.16

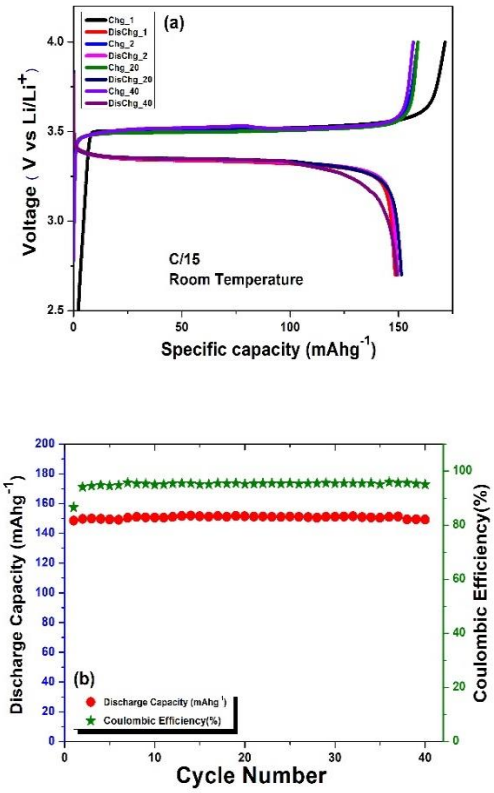

Fig. 3. (a) Galvanostatic charge/discharge profiles (b) Specific discharge capacity and coulombic efficiency, of Li|CSE|LFP solid state cell.

Fig. 3(a) shows the galnvanostatic charge/discharge profiles of the cell Li|CSE|LFP at C/15 current rate (1C=170 mAg^{-1}) within 2.7 to 4.0 V *vs.* Li/Li^+. The average voltage plateaux of charging and discharging curves are 3.50 and 3.34 V, respectively. The polarization obtained from Fig. 3(a) is around 0.16 V, which arises because of the interfacial, as well as the charge transfer resistance. Specific discharge capacity and coulombic efficiency are shown in Fig. 3(b) up to 40 cycles at C/15 rate. Specific discharge capacity of the solid state cell is ~150 $mAhg^{-1}$ and this value is higher than the previously reported values for the similar

composite solid electrolytes at room temperature [9, 13]. A stable coulombic efficiency of ~95% was observed up to 40 cycles except for the first cycle due to formation of a stable solid electrolyte interface (SEI) layer.

CONCLUSIONS

In this study LAGP based composite solid electrolyte (CSE) was prepared using PVDF-HFP, LiTFSI and EMITFSI. Cyclic voltammetry study revealed successful lithium intercalation/de-intercalation by indicating broad anodic and cathodic peaks. No other peak in the CV scans confirms that there was no side reaction. Lithium ion transference number (t_{Li+}) was obtained ~0.16 which is comparable to solid-state electrolytes. The fabricated solid-state cell (Li|CSE|LFP) exhibited good capacity retention and delivered 88% of the theoretical capacity (170 $mAhg^{-1}$). It also showed stable coulombic efficiency up to 40 cycles of charge/discharge.

REFERENCES

1. N. Kamaya, K. Homma, Y. Yamakawa, M. Hirayama, R. Kanno, M. Yonemura, T. Kamiyama, Y. Kato, S. Hama, K. Kawamoto, A. Mitsui, *Nat. Mater.*, **10**, 682 (2011).
2. M. Tatsumisago, M. Nagao, A. Hayashi, *J. Asian Ceram. Soc.*, **1**, 17 (2013).
3. B. Scrosati, G. Jürgen, *J. Power Sources*, **195**, 2419 (2010).
4. X. Yao, B. Huang, J. Yin, G. Peng, X. Xu, *Chin. Phys. B*, **25**, 018802 (2016).
5. L. Shi-Chun, L. Zu-Xiang, *Solid State Ion.*, **10**, 835 (1983).
6. A. Das, M. Goswami, P. Preetham, S. K. Deshpande, S. Mitra, M. Krishnan, Springer Conference Proceedings., doi:10.1007/978-981-15-5955-6_23.
7. Y. lin, J. Li, Y. Lai, C. Yuan, Y. Cheng, J. Liu, *RSC Adv.*, **3**, 10722 (2013).
8. H. Gupta, S. Kataria, L. Balo, V. K. Singh, S. K. Singh, A. K. Tripathi, Y. L. Verma, R. K. Singh, *Solid State Ion.*, **320**, 186 (2018).
9. Q. Guo, Y. Han, H. Wang. S. Xiong, W. Sun, C. Zheng, K. Xie, *Electrochim. Acta*, **296**, 693 (2019).
10. H. Cheng, C. B. Zhu, B. Huang, M. Lu, Y. Yang, *Electrochim. Acta*, **52**, 5789 (2007).
11. L. Balo, H. Gupta, S. K. Singh, V. K. Singh, S. Kataria, R. K. Singh, *J. Ind. Eng. Chem.*, **65**, 137 (2018).
12. S. K. Singh, D. Dutta, R. K. Singh, *Electrochim. Acta*, **343**, 136122 (2020).
13. Q. Guo, Y. Han, H. Wang. S. Xiong, W. Sun, C. Zheng, K. Xie, *J. Phys. Chem. C*, **122**, 10334 (2018).

Bulgarian Chemical Communications, Volume 54, Special Issue C (pp. 50-53) 2022 DOI: 10.34049/bcc.54.C.0050

Utility in organic synthesis and characterization of nanoparticle-based catalysts

Sh. S. Garge[1], P. Joglekar[2]*, S. Ray[1]*

[1]*Department of Chemistry, School of Basic Sciences, Faculty of Science, Manipal University Jaipur, Dehmi Kalan, Jaipur, Rajasthan 303007, India*
[2]*School of Physics, Dr. Vishwanath Karad MIT World Peace University, Pune, Maharashtra 411038, India*

Accepted: July 06, 2022

Various organic transformations are facilitated by catalysts. Even though different research groups are focusing on the homogeneous catalysts, their reusability is the prominent challenge. To overcome this challenge, researchers are exploring nano-sized catalysts, thereby trying to incorporate the useful characteristics of homogeneous catalysts into heterogeneous ones. Rational design of the nanoparticle-based catalysts is extremely important, as well as the interpretation of their structure-function relationship. In the various nanoparticles (NPs)/catalysts, the characterization is carried out using transmission electron microscopy (TEM), X-ray diffraction (XRD), X-ray absorption spectroscopy and X-ray photoelectron spectroscopy (XPS/ESCA). The size of the NPs using TEM and XRD analysis has been found to be in the range of 5 nm. The crystalline nature, analyzed using XRD, confirms the face-centred and body-centred structure for a variety of nanostructures at ambient conditions. In the study of nanocomposites, the morphology and facet design are investigated using scanning electron microscopy (SEM). Herein, we present a selective discussion of various organic syntheses involving heterogeneous nanoparticle-based catalysts and the techniques used for their characterization.

Keywords: Organic synthesis, heterogeneous catalysis, nanoparticle-based catalysts, TEM, XRD analysis.

INTRODUCTION

Chemical synthesis employed in different industries, be it for pharmaceuticals or utility chemicals, involve catalytic reactions. Right from the Haber's synthesis of converting the almost non-reactive dinitrogen molecule to extremely useful ammonia, the effectiveness of catalysts is a proven fact. The recyclable characteristics of catalysts enable them to be an essential part of Green Chemistry. Most of the established industrial processes involve different heterogeneous catalysts, which means that the catalysts are in a different phase from the reactants and hence, easily separable. But the main drawbacks of heterogeneous catalysts were that the reaction mechanism could not be defined properly and fine-tuning of those catalysts was almost impossible. So, the researchers tried to design specific homogeneous catalysts, which can be easily modified to suit the different chemical reactions involved. Another favorable fact was that having known the exact chemical structure of the homogeneous catalysts, predicting the reaction mechanisms was less complicated. Here the main obstacle was the separation of the catalyst from its homogeneous mixture with the reactants and products, thereby affecting the recyclability of the catalysts. In order to incorporate the favorable properties of both the heterogeneous and the homogeneous catalysts, different research groups started investigating catalysis facilitated by metal nanoparticles (NPs). These NPs, of dimensions between 1-10 nm, could catalyze chemical transformations at par or even better than the metal complexes [1]. One of the most beneficial aspects of NPs is the greater surface-to-volume ratio of the metal NPs than the ordinary metallic heterogeneous catalysts. In addition, the metal atoms are less coordinated to other species, thereby providing greater number of active sites for the catalytic reactions than homogeneous catalysts. Isolation of the catalytic metal NPs is also very convenient, thereby increasing their recyclability [2, 3].

The fundamental studies of the heterogeneous catalysts were carried out using *in situ* characterization techniques, as well as external techniques. In these techniques, the structures of catalytic nanocrystals were studied. These investigations included the study of crystal phases and morphology along with size, shape and orientation, surface and structural features [4-6].

Organic transformations catalyzed by metal NPs and their characterization

The carbon-carbon or the carbon-heteroatom bond formation reactions are ubiquitous reactions, utilized in the production of various essential chemicals. But these bond formations often need the boost from different catalysts. Initially, the emphasis was on the development of homogeneous catalysts which could effectively facilitate the organic trans-

* To whom all correspondence should be sent:
E-mail: sriparna.ray@gmail.com
pureprasad@gmail.com

formations, and be recycled a number of times.

Gradually, certain beneficial aspects of the heterogeneous catalysts shifted the investigations towards catalysis by metal nanoparticles. Many carbon-carbon cross-coupling reactions could be effectively carried out by nano-scale metal particles, embedded on a suitable support. Not only the metal NPs, but also the characteristics of the support, such as degree of hydroxylation, the size and nature of the crystals, etc., had profound effect on the C-C cross-coupling reactions.

One of the first reports of palladium NP-catalyzed Suzuki-Miyaura cross-coupling reactions involved the reaction between phenylboronic acid and aryl halides. Reetz and co-workers utilized not only aryl bromides, but also activated aryl chlorides to carry out the SM coupling reaction in presence of palladium nanoparticles [7, 8]. The same group had also successfully utilized these catalysts in Mizoroki-Heck cross-coupling reactions. In order to understand the mechanism of such reactions, detailed structural characterizations of the catalysts were carried in addition to those of the intermediates. This led El-Sayed and co-workers to report that the edge and the vertex atoms of palladium NPs act as active sites for this type of catalysis [9].

In 2011, Cai *et al.* reported palladium-based NPs supported on fluorous silica gel. The fluorine-substituted alkyl chains were able to adhere to the Pd-NPs through non-covalent bonding, thereby stabilizing the NPs and enabling these species to act as efficient catalysts for C-H functionalization reactions [10]. Arylation at the C2 positions of indoles could be successfully carried out in presence of 0.1 mol % of the heterogeneous catalyst. Specifically, it was observed that N-alkylated indoles exhibited better conversions than the non-alkylated substrates. In addition, a comparison between the aryl halides showed that aryl iodides were more efficient than the chlorides or bromides, as the arylating agent. In all these investigations, the Pd-NPs could be easily separated from the reaction mixture through centrifugation and decantation, thereby generating recyclable catalysts [11]. Another research group, Cao and co-workers reported the use of similar perfluorinated alkane-functionalized molecular organic frameworks (MOF), which could encapsulate Pd-NPs, and thereby act as efficient catalysts for C-H functionalization reactions. NU-1000 MOF [$Zr_6(\mu^3\text{-}OH)_8(OH)_8(TBAPy)_2$], where TBAPy = 1,3,6,8-tetrakis(p-benzoate)pyrene was reacted with perfluorinated alkanoic acids and this moiety was utilized to encapsulate the palladium nanoparticles. It is worth noting that the C2-H could be arylated in indoles and the reaction could be effectively carried out in the greenest solvent, which is water [12]. In many reports, the measurement of the yield, size and concentration of metal nanoparticle catalyst such as fluorous silica gel perfluoro-tagged palladium nanoparticles was carried out using th techniques like inductively coupled plasma atomic absorption spectroscopy (ICP AAS), XRF and TEM. Also, the degradation due to catalytic activity at the reaction temperature was also studied using XRD for metal nanoparticle catalysts [4].

Among the different transition metals, gold-catalyzed organic transformations are widely explored by various research groups [13-15], In particular, Au-NPs are found to be quite efficient catalysts and these are also observed to be structure-sensitive in nature. The structural sensitivity of the intrinsic Au nanocatalysts is studied through high resolution transmission electron microscopy (HRTEM), X-ray photoelectron spectroscopy (XPS) and X-ray absorption near edge spectroscopy (XANES) characterization. A correlated spectrum obtained of Au 4f XPS and Lm-edge XANES indicates the bulk Au like electronic structure for the Au nanoparticles supported on SiO_2 larger than 3 nm whereas the particles below 3nm showed structures deviating from the Au bulk structure. This characterization has shown how the controlled synthesis of the catalyst has affected the surface and interface design. *In-situ* diffuse reflectance infrared Fourier transform spectroscopy (DRIFTS) measurements were also conducted to analyze the CO adsorption on the low-coordinated Au atoms on Au nanoparticles supported on SiO_2. DRIFTS measurement showed that CO adsorption was proportional to the concentration of Au (3-4 nm) nanoparticles. This observation was logical, as the catalytic oxidation of CO occurs when it is adsorbed by the Au nanoparticles. Moreover, the low-coordinated Au atoms on Au/SiO_2 act like an active site at room temperature. For the larger-sized Au NPs (>4.5 nm) the CO adsorption was lower mainly due to size effects and smooth surfaces. Lower adsorption was also observed for the size below 3 nm reasoning the structure effects [5, 6]. In these investigations, Au NPs supported on TiO_2, Fe_2O_3 and Co_3O_4 have been extensively studied showing rapid catalytic activity for size below 5 nm.

One of the very important organic transformation reactions includes the Fischer–Tropsch synthesis (FTS) reaction. It is a prominent method to obtain synthetic petroleum through the conversion of syngas, which can be obtained from coal or shale gas, in presence of a suitable catalyst [16]. Among the different metal-based catalysts, ruthenium

nanocatalysts have been successfully utilized in these types of reactions [17]. In the characterization study of Ru nanocomposite catalysts, the annular dark-field image obtained from scanning tunneling electron microscope shows the FCC structures and (311, (211) active planes of the Ru nanocomposite catalysts. The images and the diffraction pattern can be seen in detail in ref [5]. Different structures and the facets of the Cu_2O nanocatalysts were also investigated using TEM. Cubic Cu, octahedral Cu, rhombic dodecahedra Cu NCs were observed.

An extensive analytical and structural characterization using nano X-ray computer tomography, electron tomography and TEM was reported by Spiecker and coworkers in 2021 [6]. Here the authors have explained the design and importance of Ga-Pd NP-based catalysts. For the samples above 100 nm the 3D structural characterization was carried out using FIB-SEM using slice and view method, for the samples below 100 nm the atomic probe tomography gave atomic resolution images. These Ga-Pd nanocatalysts had exhibited excellent activity in alkane dehydrogenation reactions.

In 2017, Kempasiddaiah *et al*. have reported an interesting green synthesis approach where biomass carbon-supported Pd heterogeneous catalyst is prepared for energy storage application [18]. In their report, they have used FESEM-EDX to study the surface morphology and its composition. The images revealed the porous nature of the synthesized materials. The TEM images showed a crystalline (111) plane and FCC nature of the Pd nanoparticles. Other tools of characterization, XRD, FTIR, ICP-OES, NMR, TGA, CHNS, were also employed to study the detailed structure and composition. Cyclic voltammetry, galvanostatic charge discharge (GCD) and electrochemical impedance spectroscopy (EIS) were used for electrochemical analysis.

Metal oxide nanoparticles in a biomass-based solvent like glycerol have been studied because of their wide applications. Chahdoura *et al*. have reported such synthesis of copper (I) oxide nanoparticles which were stabilized by poly vinylpyrrolidone in neat glycerol (under hydrogen atmosphere) [19]. TEM characterization showed particle size of NPs in the range of 3-6 nm along with formation of aggregates. XRD analysis, XPS and IR spectroscopy were also carried out to study the structure of the NPs.

In 2021, Pamidimukkala and Shaikh reported the catalytic utility of palladium-based nanocatalysts in a carbon-carbon cross-coupling reaction, like Suzuki-Miyaura reaction. The Pd-NPs were supported on magnetic chitosan. While the inherent magnetic property of these nanocatalysts allowed easy separation, the characterizations were carried out using a wide variety of spectroscopic methods, including infrared spectroscopy (IR), transmission electron microscope (TEM), and some methods based on X-ray, such as X-ray powder diffraction (XRD), X-ray absorption near edge structure (XANES) spectroscopy and X-ray photoelectron spectroscopy (XPS). The thermal behavior of the catalysts was analyzed using thermogravimetric analysis. The catalysts exhibited remarkable activity in Suzuki reaction, in which the catalyst loading was 0.0055 mol% and over 99 % yield was obtained.

Significance and future scope of NP-based catalysts

In order to efficiently follow the basic principles of Green Chemistry, catalysts are essential as opposed to stoichiometric reagents. In addition, the more recyclable a catalyst, the less wastage is produced and less resources are required. These factors ensure the importance of nanoparticle-based catalysts. Since researchers are now more aware of these facts, a wider group of nanoparticles are being investigated to find out specific catalytic applications. Hence, different characterization techniques are essential in both studying the NP-based catalysts and exploring their catalytic reactions.

Conclusion

Thus, we observed that owing to the excellent property of recyclability, the palladium-based nanocatalysts have been able to contribute effectively to the development of various organic reactions, which are industrially important. Different carbon-carbon cross-coupling reactions, like Suzuki-Miyaura, Sonogashira, Stille, etc., have been explored using Pd-NPs [20]. In addition, analysis of the newly designed catalysts is of prime importance, in order to fully understand the mechanism of the reactions involved and the catalytic process. Hence, heterogeneous nanoparticle-based catalysts have been extensively characterized using a wide range of spectroscopic methods.

Acknowledgements: *SR is grateful for the financial support of the Manipal University Jaipur Endowment Grant No. EF/2017-18/QE04-15.*

REFERENCES

1. M. Moreno-Manas, R. Pleixats, *Acc. Chem. Res.* **36**, 638 (2003).
2. D. Astruc, F. Lu, J.R. Aranzaes, *Angew. Chem., Int. Ed*., **44**, 7852 (2005).
3. R. Jin, *Nanotechnol. Rev.*, **1**, 31 (**2012)**.
4. S. Santoro, S.I. Kozhushkov, L. Ackermann, L. Vaccaro, *Green Chem.*, **18**, 3471 (2016).

5. W. Huang, W.-X. Li, *Phys. Chem. Chem. Phys.*, **21**, 523 (2019).
6. J. Wirth, S. Englisch, D. Drobek, B. A. Zubiri, M. Wu, N. Taccardi, N. Raman, P. Wasserscheid, E. Spiecker, E. *Catalysts*, **11**, 810 (2021).
7. M. T. Reetz, R. Breinbauer, K. Wanninger, *Tetrahedron Lett.* **37**, 4499 (1996).
8. M. T. Reetz, E. Westermann, *Angew. Chem., Int. Ed. Engl.* **39**, 165 (2000).
9. Y. Li, E. Boone, M. A. El-Sayed, *Langmuir*, **18**, 4921 (2002).
10. L. Wang, W.-B. Yi, C. Cai, *Chem. Commun.*, **47**, 806 (2001).
11. A. J. Reay, L. K. Neumann, I. J. S. Fairlamb, *Synlett*, **27**, 1211 (2016).
12. Y.-B. Huang, M. Shen, X. Wang, P. Huang, R. Chen, Z.-J. Lin, R. Cao, *J. Catal.*, **333**, 1 (2016).
13. I. Laoufi, M.-C. Saint-Lager, R. Lazzari, J. Jupille, O. Robach, S. Garaude´e, G. Cabailh, P. Dolle, H. Cruguel, A. Bailly, *J. Phys. Chem. C*, **115**, 4673 (2011).
14. K. Qian, L. Luo, H. Bao, Q. Hua, Z. Jiang, W. Huang, *Catal. Sci. Technol.*, **3**, 679 (2013).
15. S. Chang, M. Li, Q. Hua, L. Zhang, Y. Ma, B. Ye, W. Huang, *J. Catal.*, **293**, 195 (2012).
16. H. Schulz, *Appl. Catal., A*, **186**, 3 (1996).
17. W.-Z. Li, J.-X. Liu, J. Gu, W. Zhou, S.-Y. Yao, R. Si, Y. Guo, H.-Y. Su, C.-H. Yan, W.-X. Li, Y.-W. Zhang, D. Ma, *J. Am. Chem. Soc.*, **139**, 2267 (2017).
18. M. Kempasiddaiah, K. A. Sree Raja, V. Kandathil, R. B. Dateer, B. S. Sasidhar, C. V. Yelamaggad, C. S. Rout, S. A. Patil, *Appl. Surface Sci.*, **570**, 151156 (2021).
19. F. Chahdoura, C. Pradel, M. Gómez, *ChemCatChem*, **6**, 2929 (2014).
20. B. M. Choudary, S. Madhi, N. S. Chowdari, M. L. Kantam, B. Sreedhar, *J. Am. Chem. Soc.*, **124**, 14127 (2002).

Bulgarian Chemical Communications, Volume 54, Special Issue C (pp. 54-59) 2022 DOI: 0.34049/bcc.54.C.0054

Recent trends in manufacturing of silver nanoparticles and future applications

N. Mayekar*, A. Patil, R. Rajguru

Mechanical Engineering Department, D.J. Sanghvi College of Engineering, Mumbai, India

Accepted: July 06, 2022

Recently, there has been a sudden surge in anti-microbial or anti-bacterial materials, due to contagious viruses and bacteria. These bacteria spread exponentially by mutations and have developed immunity towards many antibiotics and other drugs over time. Hence, there is a need for an alternative mechanism to deactivate their severity and thus reduce their effects. In this regard, silver nanoparticles exhibit great potential in terms of anti-microbial properties. They deactivate the viruses and thus prevent their further mutation. This has led to a growing demand for silver nanoparticle-decorated materials, which ranges from clinical instruments to routine life materials. In this paper, we have focused on the manufacturing techniques involved in the manufacturing of AgNPs. These involve both top-down and bottom-up approaches such as physical methods, chemical methods, green synthesis, along with advanced techniques such as 3D printing and 4D printing. Considering the ample scope associated with silver nanoparticles, we have discussed the potential applications in consumer goods and industries which can be incorporated to prevent widespread infections.

Keywords: Silver nanoparticles; 3D printing; 4D printing; manufacturing.

INTRODUCTION

Nano-materials (1-100 nm materials) have gained great attention in the past few decades in many fields such as biomedicine, catalysis, energy storage, and sensors, due to their unique physicochemical properties as compared to their bulk states [1]. Silver nanoparticles (AgNPs) have received special attention, especially in the biomedical field due to their desirable properties such as high electrical conductivity, anti-microbial properties, optoelectric properties and so on.

Silver nanoparticles have unique optical, electrical, and thermal properties and are being incorporated into a wide range of products such as conductive inks due to their high electrical conductivity, stability, and low sintering temperatures [2]. Additional applications include anti-microbial fabrics, 3D printing filaments, optoelectronics. A few of the interesting applications include the use of silver nanoparticles for antimicrobial coatings, keyboards and wound dressings that continuously release a low level of silver ions to protect against bacteria. Due to rising concerns of hygiene and safety, due to the Covid-19 pandemic, AgNPs are looked upon as an important candidate to minimize the transmission of bacterial and viral infections.

Manufacturing of AgNPs

There are two broad categories of manufacturing processes of nano-materials:

1. Top-down approach
2. Bottom-up approach

In the top-down approach, bulk silver material is crushed down into fine particles by size reduction using numerous techniques such as grinding, milling, sputtering, and thermal/laser ablation. On the contrary, in the bottom-up approach, AgNPs are manufactured by using chemical, photochemical, and biological methods. The commonly used physical techniques involved are discharge, physical vapor deposition, high-energy ball milling, laser ablation, etc. The chemical techniques involve electrochemical, chemical vapor deposition, sonochemistry, sol-gel, co-precipitation, inverse micelles, or micro-emulsions, etc. Among the mentioned, wet chemical reduction techniques are extensively implemented for silver nanoparticles.

Recent inclination can be observed towards the green-synthesis of AgNPs using plant extracts as an alternative to the conventional synthetic methods. These greener syntheses of AgNPs offer a major upper hand over the conventional synthesis.

A) Physical vapor deposition

In this synthesis, AgNPs are produced by a vapor deposition technique, where a metallic silver precursor taken in a dish (also called boat) is vaporized, followed by the condensation of the vapor as carried by an inert gas. The vaporization is carried out in a tube furnace at 1 bar pressure and at a high temperature. In a study by McNally *et al.* [3], sputtered AgNPs were created alongside ethanol, a common solvent in laboratories. The procedure resulted in the creation of different-sized silver nanoparticles having varied morphology. The sputtering created a pink solution of AgNPs.

*To whom all correspondence should be sent:
E-mail: nimishsmayekar@gmail.com

Further, the relationship between methanol jet and AgNP size variation was studied.

Although the synthesis produces abrasion-resistant and impact-resistant AgNPs, it suffers from some drawbacks like high energy consumption, large space required for the furnace and slow rate of synthesis; hence it is expensive and not preferred for mass production.

B) Laser ablation

Another physical technique for the synthesis of AgNPs is laser ablation which produces colloidal AgNPs in a single step without any additional contamination, thereby eliminating the requirement of purification. It is cost-effective, safer and more environmentally friendly. Laser ablation system consists of a powerful laser source and feeding system. The laser beam is focused on the metal substrate which causes multiple metal particles to rise perpendicular to the substrate, commonly referred to as 'Plume'. These particles are then directed towards the collector using inert carrier gas. The concentration, size and distribution of AgNPs is influenced by the medium used in the ablation chamber, metal substrate used and laser operating parameters. Experimental estimations showed that the mass of generated nanoparticles in ambient air was up to 100 times higher than in water and that in argon gas was up to 100 times higher than in ambient air [4]. However, in terms of other preparation methods, laser ablation exhibits a few drawbacks as well. It incurs high investment costs because of the high price of the laser system. The process needs to be implemented on a large scale for being economical and sometimes there is a chance of particle agglomeration due to plume formation.

C) Electrochemical synthesis

In the electrochemical method, nanoparticles are produced by the dissolution of a metallic anode in a suitable solvent. For the synthesis of AgNPs, the silver anode is subjected to electric current. The particle size is controlled by administering the applied current density. As cited by Khaydarov *et al.* [5], inexpensive bulk silver electrodes were selected to produce AgNPs using electrochemical process. The electrodes were then placed in an electrochemical cell. The process was performed at 20–95 ºC at a constant voltage of 20 V. The morphology of AgNPs produced by the proposed method was studied. Spherically shaped AgNPs were produced exhibiting stability of up to 7 years under ambient conditions. The physical technique permits the production of mass-scale AgNPs in a single-step process. Electrosynthesis has some disadvantages too. It usually requires the use of a solvent to stabilize the reactants and products. Water is the ideal solvent but often organic solvents or co-solvents are required. Additionally, supporting electrolytes to carry the current are very often needed.

D) Chemical approach

Chemical synthesis is the most preferred approach for the synthesis of AgNPs due to its high yield and low cost. The general route for manufacturing silver ions is reduction using reducing agents followed by their stabilization using stabilizing and capping agents. Fine size and distribution of silver nanoparticles are achieved by producing the nuclei at the same time from the supersaturated conditions, with subsequent growth and stabilization. The parameters used for controlling the size and distribution of Ag ions include the concentration of silver ions, the concentration and efficacy of the reducing agent, the concentration and nature of the stabilizing agent, along with the reaction temperature, pH, pressure, etc. [6]. Different shapes and sizes of AgNPs can be obtained by utilizing suitable conditions and a shape directing agent. Although a great variety of chemical methods are available, most of the chemicals are toxic and cause environmental pollution and the synthesized AgNPs become cytotoxic. As these are technically and economically unfavorable, alternative greener methods are preferred.

E) Photochemical approach

The photochemical approach is a comparatively greener technique to produce AgNPs utilizing light energy. Reduction of Ag ions to silver occurs in the presence of photo-active chemicals such as acetone with isopropanol, carbon dots, modified clay suspension, etc. It can also act as a stabilizer for the nanoparticles, under exposure of UV or solar light irradiation, thus producing finely dispersed Ag nanoparticles. The most important parameters of the photochemical process are the capping and the stabilizing agent since they affect the size and distribution of AgNPs [7].

F) Green synthesis of AgNPs

As cited by Awwad *et al.* [8], numerous methods have been studied for the synthesis of silver sulfide nanoparticles (Ag_2SNPs) namely a template-based method at room temperature and ambient pressure, water-in-CO_2 micro-emulsions [9], modified homogeneous precipitation route [10], sonochemical synthesis, multi-solvent thermal decomposition method [11], modified chemical bath deposition technique, combretum molle black wattle extracts [12], metal-reducing bacterium *Shewanella oneidensis* MR-1, chemical method [13], multi-

solvent thermal decomposition method [14]. These methods have many disadvantages due to toxic chemicals used and waste products, which create a problem to the environment, also high energy consumption, difficulty of large-scale processes and wasteful purification. Recently, green synthesis has gained great attention due to its eco-friendly nature.

Herein, the objective of the present research work was to synthesize silver sulfide nanoparticles by a green route using rosemary (*Rosmarinus officinalis*) leaves aqueous extract at room temperature and studying antibacterial activity. Based on the paper, we cited that synthesized silver sulfide nanoparticles by the green synthesis method were studied for antimicrobial activity using the disc diffusion method; it was observed that silver sulfide nanoparticles have antibacterial activity at different concentrations. Chloramphenicol was used as a control antimicrobial agent. The Ag_2SNPs bio-synthesized by rosemary leaves aqueous extract displayed inhibition against gram-negative *Escherichia coli*, and gram-positive *Staphylococcus aureus*, *Shigella*, listeria bacteria. Thus green synthesis provides a cleaner route for the manufacturing of silver nanoparticles with considerable anti-microbial properties.

G) Methods and approaches for 3D printing with nanocomposites

Many processes have been explored for the manufacturing of AgNps. However, the possibility of manufacturing intricate and complex geometries with all materials (especially at nanoscale) is not an easy task. Newer approaches for the manufacturing of components with nano-composites will make it more accessible for printing a wide array of materials, as cited by Challagulla *et al.* [2].

H) 3D printed filaments

AgNPs in form of filaments can be effectively used for 3D printing (additive manufacturing) which provides extensive flexibility with regard to manufacturing. In a literature review of Podstawczyk *et al.* [15], we found that the filaments were produced by using dried PLA pellets dissolved in DCM with a concentration of 100 mg/mL under magnetic stirring with a rate of 300 rpm for 5 hours. The temperature was set at 35°C to fully dissolve the polymer (solution A). The next step involved the preparation of silver nitrate solutions with concentrations ensuring an appropriate silver content in the final solid nanocomposite (0.01%, 0.1%, 1%, 2.5%, and 5% w/w). Subsequently, solutions A and B were mixed under stirring until a homogeneous mixture was obtained (about 30 minutes), which was transferred onto petri dishes and placed in a laboratory drying oven with the temperature set at 50 °C for 48 hours to evaporate the solvents. Next, the dried material was mechanically ground using a blender and extruded by a screw extruder (Felfil Evo) with a nozzle of 1.75 mm at a temperature of 165 °C to 170 °C (temperature recommended by the extruder supplier). Filaments with diameters between 1.6 mm and 1.9 mm were chosen for 3D printing.

The antibacterial activity of 3D printed $AgNO_3$-PLA cuboids was evaluated against gram-positive *S aureus* sp *aureus* ATCC 6538, as well as gram-negative bacteria, *E. coli* ATCC 10536 and *Pseudomonas aeruginosa* ATCC 15442. Taking inspiration from this method, we can create filaments required for 3D printing which provides us with immense flexibility in terms of manufacturing low-volume complex materials. Thus, the antimicrobial activity of AgNPs coupled with advancements of 3D printing technology will enable new domains of manufacturing and applications.

I) Ink jetting of AgNPs

Material jetting is celebrated as one of the crucial enablers of MFAM (multifunctional additive manufacturing**)** because of its ability to print a wide range of materials including polymers, composites and inks containing metal nanoparticles. Inkjet printing (IJP) is a drop-on-demand, non-contact material jetting process capable of direct printing circuits of complex designs from a computer-aided design (CAD). It has advantages, namely, high material utilization rate and lower wastage compared to conventional methods. Ink-jet printing also has the potential to simplify the manufacturing process of circuits and reduce the associated costs.

In recent years, the use of inks containing MNPs such as silver, gold, copper and other conductive materials including graphene, carbon nanotubes, poly (3.4-ethylene dioxythiophene) polystyrene sulfonate and direct writing of liquid metals such as gallium, indium and tin have been extensively studied for printing circuitry. MNPs exhibit better resolution and thermal stability compared to conductive polymers and liquid metals and hence they are widely preferred for the manufacturing of circuitry.

In a study by Vaithilingam *et al.* [16], we cited that an ink containing AgNPs was printed using a bespoke 3D multi-material IJP system – JETx, followed by sintering using an in-built IR source. Essentially two sintering methods, swathe-by-swathe (SS) and layer-by-layer (LS) were employed to produce the AgNP ink. Briefly, during SS, each swathe of a layer was sintered using IR. It is envisioned that these sintering mechanisms can lead

to variation in the layer formation, surface profile, micro-structure and the associated electrical resistivity of the printed circuitry. Currently, findings the on inkjet printing and sintering of AgNPs are limited to only a countable layer (less than 20) and are implemented in multiple steps (i.e. printing and sintering on different equipment). In the studied literature, 50 layers of silver were inkjet-printed and sintered in a single step and the impact of SS and LS mechanisms on the printed structure is reported.

J) Polymerization method (coating method)

There are multiple ways studied for the polymer and nano-silver composite incorporation, where AgNPs are dispersed on the surface of a polymer. Initially, a polymer is fabricated with AgNPs, with a subsequent attachment to the surface, a polymer solidification process occurs on the surface of the targeted object and then, it is incorporated with nano-silver particles. The monomer gets attached to the nanoparticle (NP) surface, followed by polymerization. In every case, the most crucial step is the attachment of the polymer to the surface of the object. We have focused on the manufacturing pathways of coating polymer nano-silver composites *via* various attachment procedures.

There are numerous methods established for the insertion of nano-silver into the polymer matrix. Nano-silver incorporation is predominantly performed *via* direct adsorption or *in-situ* synthesis. The first approach, which is the direct adsorption of nanosilver, is very controllable and straightforward; however, AgNPs can easily aggregate during this method. The following method, which is the *in-situ* synthesis, is comparatively harder because of the silver ion loading. However, it is more beneficial when compared to direct attachment adsorption due to the formation of homogeneously distributed silver nanoparticles in the matrices. This matrix demonstrates the benefits of inorganic materials, namely chemical stability along with mechanical strength, porosity which results in an ion exchange with the surrounding medium.

K) 4-D manufacturing

4D printing is useful for an array of healthcare applications, ranging from nanoparticle designing to tissue engineering, to the manufacture of self-assembling human-scale biomaterials. From the works of Ryan *et al.* [17], we cited that Organovo Holdings Inc., U.S.A., has been involved in several bioprinting projects focused on the development of functional human tissues. This company is implementing 4D manufacturing to develop an artificial human liver. One of the core techniques for 4D printing is to design the materials for structural change thus enabling a completely new domain of research and development. Even though the smart material itself plays a crucial role in transforming a printed object into another shape or configuration under the influence of external stimuli, attention should be given to understanding the mechanisms, predicted behaviors, and required parameters to achieve controllable results. The critical advantage of 3D printing technology is the ability to fabricate complex 3D shapes with varied material distributions through the spatial arrangement. By integrating the orientation and position of smart materials such as shape memory polymer fibres within composite materials, we can facilitate morphological changes in response to external stimuli. Incorporating anti-microbial materials such as AgNPs can further expand their applications for biomedical applications thus facilitating adoptions in the bio-medical field.

Since 4D printing and 3D printing are disjoint from conventional manufacturing technology, these new technologies can help reduce the manufacturing time and labor required to assemble machines or goods.

Extensive applications of silver nanoparticles

The unique characteristics of AgNPs make them and their nano-composites very useful in the fields of medicine, catalysis, textile, biotechnology, electronics, optics, water treatment, etc. Significant inhibitory effects against different pathogens display them as effective antimicrobial agents in various consumer products such as cosmetics, air sanitizer sprays, respirators, socks, slippers, pillows, wet wipes, toothpaste, washing machines, wound dressings, bone cement, surgical dressings, cell phones, and food storage packaging, etc. The use of heterogeneous AgNPs based catalysts is proven to be an effective and important technique in terms of efficiency and selectivity for different organic transformations, in conduction to their antimicrobial activity. Again, the cost of such catalysts is much less compared to corresponding gold or platinum (1/50) or even to palladium (1/25) catalysts [6].

Antimicrobial devices. AgNPs are extensively used in numerous biomedical devices, namely, surgical instruments, bio-sensing devices, vascular prostheses, orthopaedics, ventricular drainage catheters, wound dressings, heart valves, etc. Additionally, AgNPs are used for dental hygiene and eye treatment, as well as for other infections. Ointments and creams containing AgNPs are widely in use to avoid infections to the burns and to close

the wounds. AgNPs are now also used as nanocarriers for a controlled drug delivery system.

Moving along the same lines, AgNPs can be extensively used in automobile interiors as an antimicrobial agent. The method commonly referred to as electro-spinning (or electrospraying, which yields nano- or microparticles due to lower solute concentration) is well-known and used in the production of nanomaterials, as well as for the theoretical study of electrohydrodynamic effects thus widening their applications. Electro-spinning's basic operation and nano-material production require a high-voltage power source (between approximately 50 and 500 kV/m) and two electrodes connected to opposite potentials. Thus, using the method of "electrospinning" we can produce AgNPs-impregnated fibres which can be used for automotive car interior (seat covers, dashboard, steering wheel cover and gear lever). A study by Mathavi *et al.* [18], indicates that an automotive steering wheel is the breeding ground for bacteria. A steering wheel is 11 times dirtier than a public toilet seat. A major source of bacteria comes from food spills, through air and heating vents and from the foot-wears of passengers. High concentrations of bacteria can be observed on dashboards, cup holders and children's car seats. The most common organisms include *Bacillus* species, *Staphylococcus*, *Escherichia coli*, *Salmonella* and *Campylobacter*. Thus, it is important to constantly clean and disinfect the car surfaces. Thus, using these anti-microbial materials helps to prevent the growth of micro-organisms and keeps the car safe and clean. This facilitates a significant reduction in viral infections thereby maintaining hygiene inside the vehicle.

As per the above study, the interior of cars was 8 times more infectious than a toilet seat. Incorporating AgNPs in seat covers, dashboards, gear level, handbrake lever can effectively mitigate the bacteria transmission to the passengers.

Opto-electronics. Silver nanomaterials have been extensively studied as an essential component of nanocomposites: thanks to their high dielectric constants in numerous systems. For example, silver nano-wires can be used as conductive coatings in flexible electronics and semiconductors due to their high electric conductivity. On the same lines, AgNPs have the potential to be utilized in silver paste for effective contact at electronic interfaces. Nanospheres consisting of Ag or Au have been utilized in optoelectronic light harvesting based on the plasmonic effect.

Silver-decorated composites. Black phosphorus (BP) has attractive nanoscale chemical and physical properties. In a study by Tang [19], black phosphorus decorated with silver nanoparticles (Ag/BP) was synthesized *via* an *in-situ* chemical reduction approach without utilizing a reductant.

The oil distributed with small amounts of Ag/BP nano additives exhibited excellent lubricating performance for the steel/steel contact surface. A significant reduction in coefficient was found. The friction reduction and wear reduction characteristics of Ag/BP are understood by studying the scar surfaces. During the operation, the Ag/BP nanomaterials served not only as a friction-reducing and anti-wear additive but also as a catalyst to decompose the base PAO oil for forming a carbon-based tribofilm further reducing the friction and wear.

The black phosphorus powder was prepared by high energy mechanical milling (HEMM). Briefly, red phosphorus and stainless-steel balls were put in a 50 ml stainless steel vial together with 10 mm, 6 mm and 4 mm milling balls After milling, the bulk black phosphorus was collected and finally stored in an argon glove box.

This technique can be essentially used for coating high-friction and wear surfaces such as piston rings. Piston rings are a highly dynamic and very important component from the point of view of I.C. engines. Incorporating low-friction coatings will not only improve the life of rings but also considerably improve the thermal performance. Further, the scope can be widened and effectively utilized to reduce frictional resistance in various machine components to improve the efficiency of the machinery and reduce wear.

Paint drying. We cited from the works of Lotfizadeh *et al.* [20] that the effects of nanoparticles on the paint-drying processes of automotive-based paints were experimentally investigated. In the study, rectangular aluminum plates covered by Alkyd Melamine (ES-665) car paint from Haviloox Company containing various amounts of 10 nm diameter silver nanoparticles from 0 to 25 ppm were prepared and tested. By varying the conditions such as air flow velocities, temperatures, and amounts of silver nanoparticles as important parameters during the drying process, an influence on the composition of the paint was indicated both during and at the end of the drying process, which has affected the quality of the final coating and improved the paint's chemical interactions. An increase of 22% at the surface temperature of the studied samples and the drying velocity was recorded for the 10 ppm nano silver amount, indicating an optimal nanoparticle amount, thus effectively reducing the time required for paint drying and corresponding lead times. This will help reduce the cost of manufacturing and

improve the paint quality. Further, it can result in creating extensive room for development in the paint industry.

Covid-19 equipment. There is a sudden surge in the demand for anti-viral surgical masks due to the ongoing pandemic. AgNPs have again proved to be an ideal selection for the same. Impregnating AgNPs in masks can improve their anti-viral performance thus ensuring better protection against SARS Cov 2. As per the studies of Rasmi *et al.* [21], nano-disinfectant coating on surgical masks was extensively studied which indicated sufficient anti-viral abilities. The further scope can be improved by impregnating AgNP fibres into surgical masks. We can also incorporate AgNPs in PPE kits, gloves and other accessories predominantly utilized during Covid-19. Since AgNPs have proved to be effective when incorporated in gloves, we can further extend it and use it in other equipment.

CONCLUSION

Considering the widespread benefits and importance of silver nanoparticles, they've numerous applications both from consumer and industry points of view. As it can be observed, the applications range from day-to-day commodities and medical devices. In this paper, we have discussed the methodologies for the synthesis of silver nanoparticles. We have covered all the manufacturing techniques ranging from physical methods, chemical methods, green synthesis and 3D and 4D printing as well. Further, growing health concerns due to ongoing pandemic have created essential awareness among the people regarding hygiene and safety measures. This will boost the acceptance of anti-microbial devices which utilize silver nanomaterials. This will require the efficient and cost-effective synthesis of AgNPs and the development of new techniques.

Acknowledgements*: Presented at the International Conference on "Cutting Edge Research in Materials and Sustainable Chemical Technologies" from January 27th to 29th, 2022, organized by the Department of Chemical Engineering & Department of Chemistry at Manipal University Jaipur, Jaipur, India (Organizing Chairmen: Dr. Anand G. Chakinala & Dr. Rahul Srivastava).*

REFERENCES

1. Y. Wang, Y. Yang, Y. Shi, H. Song, Ch. Yu, Advanced Materials, Wiley-VCH Verlag GmbH & Co. KGaA, Weinheim, 2019, p. 1.
2. N. V. Challagulla, V. Rohatgi, D. Sharma, R. Kumar, *Current Opinion in Chemical Engineering* Science *Direct*, **28**, 75 (2020).
3. M. J. McNally, G. Galinis, O. Youlea, M. Petrc, R. Prucekc, L. Machalac, K. von Haeften, *Nanoscale Adv.*, **1**, 4041 (2019).
4. C. A. Charitidis, P. Georgiou, M. A. Koklioti, A.-F. Trompeta, V. Markakis, *Manufacturing Rev.,* **1,** 11, (2014).
5. R. A. Khaydarov, R. R. Khaydarov, O. Gapurova, Yu. Estrin, Th. Scheper, *J. Nanopart. Res.*, **11**, 1193 (2009).
6. N. Karak, Nanomaterials and Polymer Nanocomposites, Elsevier, 2019, p. 47.
7. N. Jara, N. S. Milán, A. Rahman, L. Mouheb, D. C. Boffito, C. Jeffryes, S. A. Dahoumane, *MDPI Open Access Journals*, **26(15)**, 4585 (2021).
8. A. M. Awwad1, N. M. Salem, M. M. Aqarbeh, F. M. Abdulaziz, *Chemistry International*, **6 (1)**, 42 (2020).
9. J. Liu, P. Raveendran, Z. Shervani, Yu. Ikushima, *Chemical Communications*, **22**, 2582 (2004).
10. T. Xaba, M. J. Moloto, O. B. Nchoe, Z. Nate, N. Moloto, *Chalcogenide Letters*, **14 (**8), 337 (2017).
11. I. K. M. M. Sahib, D. Thangaraju, N. Prakash, Y. Masuda, *Chemistry International*, **6(1)** (2017).
12. P. N. Sibiya, M. I. Moloto, *Digest Journal of Nanomaterials and Bio-structures*, **13**, 411 (2018).
13. Y. Zhao, Z. Song, *Materials Letters*, **126**, 78 (2014).
14. M. M. S. I. Khaleelullah, T. Dheivasigamani, N. P, Masuda, Y, Inamib, W, Kawataa, Y, Hayakawa, *Journal of Crystal Growth*, **468**, 119 (2017).
15. D. Podstawczyk, D. Skrzypczak, X. Połomska, A. Stargała, A. Witek-Krowiak, A. G.Elie, Z. Galewski, *Polymer Composite*, **41** (11), 4692 (2020).
16. J. Vaithilingam, M. Simonelli, E. Saleh, N. Senin, R. D. Wildman, R. J.M. Hague, R. K Leach, Ch. J. Tuck, *ACS Appl. Mater. Interfaces*, **9**, 6560 (2017).
17. K. R. Ryan, M. P. Down, C. E. Banks*Chemical Engineering Journal*, **403**, 126162 (2020).
18. S. Mathavi, G. Sasikala, A. Kavitha, A. V. Raghavendra Rao, R. Indra Priyadharsini, *International Journal of Current Microbiology and Applied Sciences*, **5,** 528 (2016).
19. G. Tang, F. Su, X. Xu, P. K. Chu, *Chemical Engineering Journals*, **392** (2020).
20. H. Lotfizadeh, S. Rezazadeh, M. Reza Fathollahi, J. Jokar, A. A. Mehrizi, B. Soltannia, *International Journal of Advanced and Multidisciplinary Engineering Science*, **2(1)**, 7 (2018).
21. Y. Rasmi, K. S. Saloua, M. Nemati, J. R. Choi, *Nanomaterials (Basel)*, PMCID: PMC8308319, **11(7),** 1788, (2021).
22. R. A. Khaydarov, R. R. Khaydarov, O. Gapurova, Yu. Estrin, Th. Scheper, *Journal of Nanoparticle Research*, **11,** 1193 (2009).
23. N. Jara, N. S. Milán, A. Rahman, L. Mouheb, D. C. Boffito, C. Jeffryes, S. A. Dahoumane, *Molecules*, **26**, 4585 (2021), doi.org/10.3390/molecules 26154585.

Bulgarian Chemical Communications, Volume 54, Special Issue C (pp. 60-68) 2022 DOI: 10.34049/bcc.54.C.0060

Electrodialytic removal of arsenic from wastewater: a mini review of the present state of research

A. Shah, F. Q. Mir*

Department of Chemical Engineering, National Institute of Technology Srinagar, Hazratbal, Srinagar, Jammu and Kashmir 190006, India

Accepted: July 06, 2022

Arsenic is among the most damaging pollutants found in wastewater and as such requires special attention. It is highly toxic, carcinogenic and exposure to it has been linked to several respiratory, gastrointestinal, cardiovascular, renal and dermal conditions in humans. As such, strict environmental regulations are in place to maintain arsenic levels in groundwater to the lowest amount possible. There has been extensive research into strategies to remove arsenic from wastewater. Membrane separation processes have been an important part of research into the implementation of wastewater treatment at a scale large enough to meet the demand for human consumption. Among membrane separation processes, electrodialysis is a relatively new, yet especially appealing process due to significantly lower energy costs in comparison to the more commonly used reverse osmosis process, combined with high separation efficiencies for charged ions, making it more economically feasible for implementation. This paper gives an overview of arsenic, its sources, effects on human physiology, as well as an overview of the strategies in place for arsenic removal from wastewater. Further, the paper reviews the most recently published research into the area of arsenic removal from wastewater using electrodialysis, in order to provide a holistic view of the present state of research in the area.

Keywords*:* Electrodialysis; Arsenic; Membrane separation; Wastewater treatment.

INTRODUCTION

Arsenic is a highly toxic metal that can exist in water in two forms: arsenites, As(III), and arsenates, As(V). In either form, it is highly toxic and detrimental to both human and animal health. Out of those two forms, As(III) is more prevalent and also more toxic, but can easily be converted to As(V) *via* oxidation. The speciation of As(V) with pH is outlined in Fig 1 [1].

Under oxidizing conditions, such as surface water bodies, a commonly encountered compound is arsenic acid (H_3AsO_4) which can be further dissociated into $H_2AsO_4^-$, $HAsO_4^{2-}$, or AsO_4^{3-}. The trivalent form (H_3AsO_3), however, is mostly observed in reducing conditions, like deep sections of groundwater, where it is likely to dissociate into $H_2AsO_3^-$, $HAsO_3^{2-}$ or AsO_3^{3-} [2].

Arsenic has been reported to cause vomiting and diarrhea on short-term exposure, and in the long term has been reported to cause neuropathy, impairment of central nervous system functions, failure of kidneys and liver, as well as deficits in locomotion, learning ability, and other cognitive functions, and even cancer [2].

As such, its concentration has to be controlled and restricted to as low a value as possible, especially when it comes to water consumed by humans and animals. It has in fact been classed as a group 1 human carcinogen by the WHO [2]. Arsenic can affect humans either by ingestion or by inhalation, but given that it is oral ingestion that is the main source of arsenic toxicity in humans, it is the removal of arsenic from water that takes precedence when it comes to controlling arsenic-based toxicity [3].

The fact that arsenic is present in several industrial effluents, including dye industry, coal mining, thermal power plants, gold mining, and glass manufacture, makes it a difficult task to constrain arsenic and its effects downstream from such industries [4].

This paper outlines the sources of arsenic, their effects on human physiology, and strategies for their removal, as well as gives a review of the most recently published research on the use of electrodialysis as a viable method for arsenic removal from wastewater.

SOURCES OF ARSENIC

Arsenic can make its way into the water meant for human consumption *via* several sources, some being natural and some as a direct result of human activity. The concentration of arsenic can vary anywhere from 10 μg/L to 150 μg/L depending on a number of factors [1].

* To whom all correspondence should be sent:
E-mail: mirfasil@nitsri.ac.in

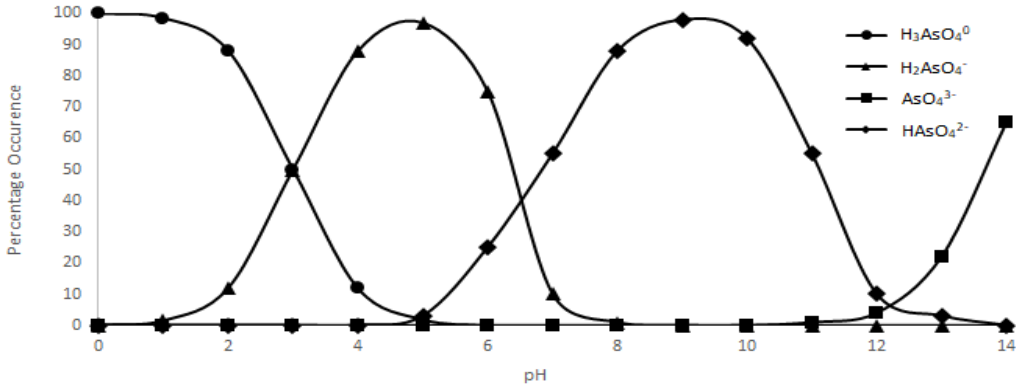

Fig. 1. As(V) speciation *vs* pH at 298 K [1]. Reproduced with permission from the copyright holder.

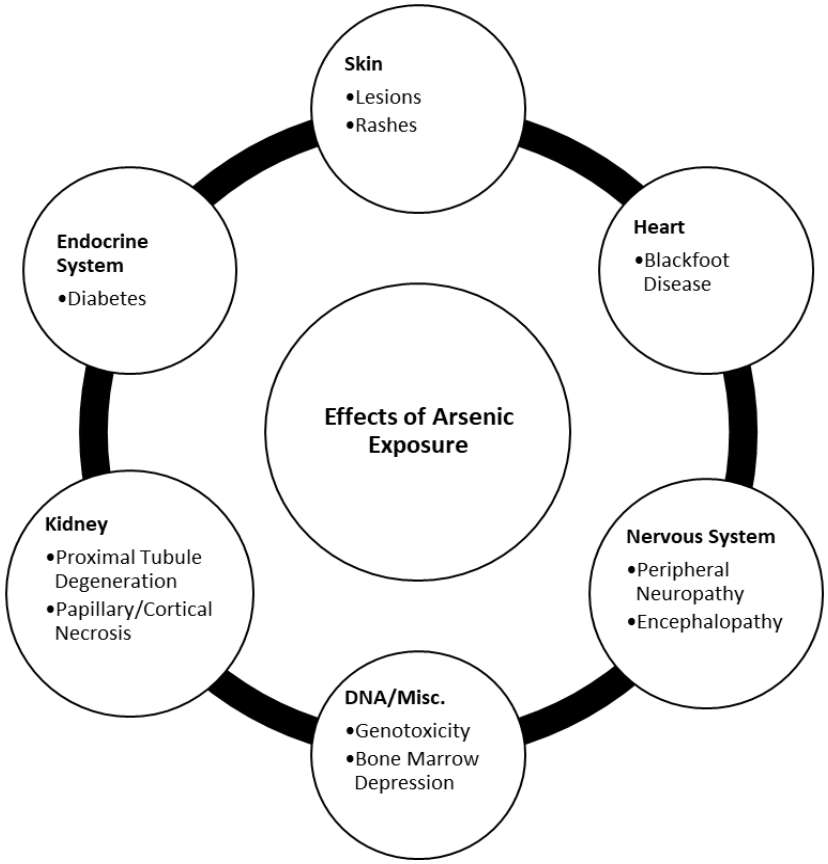

Fig. 2. Effect of arsenic exposure on human physiology.

Natural sources of arsenic

Arsenic is present in sedimentary rocks, especially in mountain ranges such as the Himalayas, as well as in igneous rocks and sulfidic ores [5, 6]. From these sources, by the mechanism of desorption from mineral rocks under alkaline conditions or release under anaerobic environments, the arsenic can reach water sources by a number of pathways [6]. The level of arsenic, as well as the concentration released varies significantly depending on the unique mineral makeup of the specific geographical location, for instance, rock deposits with high organic matter content are likely to contain a higher concentration of arsenic [7].

Other than this, geothermal water deposits, as well as locations close to frequent volcanic activities have also been observed to contain significantly high arsenic concentrations.

Anthropogenic sources of arsenic

Industrial activities. While it is clear from the previous section that arsenic does exist naturally, anthropogenic sources significantly multiply the severity of arsenic contamination and are the primary cause of arsenic levels increasing above recommended safe levels in water sources [8].

Industries responsible for the release of arsenic in effluents include mining industries, where arsenic mineral deposits are dissolved and leak into the

water table as a consequence of mining operations, and metallurgical industries, where smelting operations produce significant levels of arsenic which is released as effluent into water bodies [9–11] . Among these, mining operations are considered especially harmful not only due to arsenic release but also due to the release of several other heavy metals such as Zn, Cd and Ni [12].

Apart from these, tanning industry, as well as dye industries have also been observed to significantly contribute to arsenic toxicity. In both industries arsenic is used in various steps of the manufacturing processes and as a result the effluents from these industries usually contain high levels of arsenic unless the effluent is properly treated before release [13].

Agricultural activities. In the agricultural industry, arsenic toxicity has been historically caused by blatant overuse of pesticides, as well as insecticides containing arsenic as an ingredient. The arsenic from these sources can easily seep into the ground water, or can get absorbed by the crops and make its way up the food chain. These activities, however, have largely been phased out and replaced with less toxic alternatives [8]. Other agricultural activities such as farming of tobacco at scale are still widely associated with significant arsenic contamination to nearby soil and water bodies [14]. Further, the end product use, i.e. smoking of tobacco cigarettes, has been associated with increased arsenic levels in the user's lungs and an increase in the likelihood of tumour growth as a result of arsenic exposure [15].

Strategies for arsenic removal

Fig. 3. outlines the presently available methods of arsenic remediation and removal.

Pre-oxidation

Among the available methods, pre-oxidation is the simplest and easiest to implement method, wherein As(III) is converted to As(V). As(V) is significantly less toxic in comparison to As(III) and is also easily adsorbed onto solid surfaces, and thus is easily removed. Pre-oxidation is carried out in a number of ways, such as aeration, application of UV-rays, microbial activity, or use of chemicals such as chlorine and hydrogen peroxide.

Major parameters to control in this process are the oxidant used, its concentration, the presence of a catalyst, the temperature and the reaction time. [16]. This method is fairly easy to implement, however is held back due to difficulty in scaling the process as per requirement, slow reaction kinetics making the process take even weeks to achieve sufficient levels of purification, and production of toxic by-products such as bromate, iodate, products of organic matter oxidation, etc.

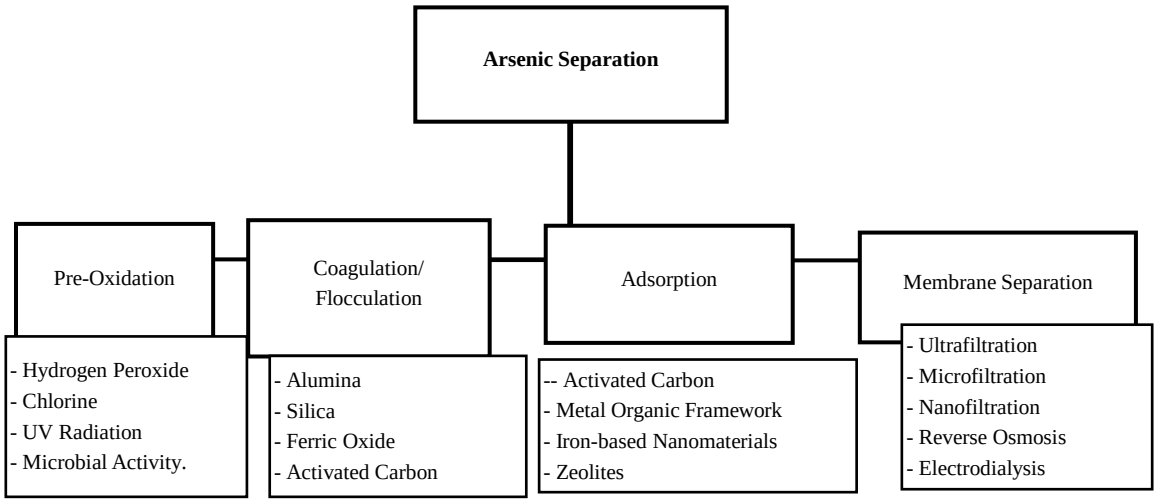

Fig. 3. Available methods for arsenic removal.

Coagulation-flocculation

Coagulation-flocculation is a much more industrially viable method; it involves addition of coagulant to the feed, causing agglomeration and subsequent precipitation into floc, resulting in removal of arsenic from the water [17, 18].

Coagulants such as alum and ferric chloride are the most commonly employed for this process. Apart from ferric salts, aluminium-based coagulants are among the ones most commonly used commercially [18, 19]. However, the separation efficiencies reported vary widely between plants (anywhere from 6% to 74%), depending on the coagulant used, dosage, and intensity of stirring and temperature [20]. This process is fairly efficient in arsenic removal from soil and wastewater, however, the method requires pre-oxidation, as well as pH control of the process in order to work as needed.

Adsorption

Adsorption and ion exchange are scalable and widely used methods for arsenic removal. Activated carbon is the most commonly employed adsorbent in arsenic separation applications, however the cost considerations of using activated carbon necessitate the need for research into cheaper or easily reusable adsorbent materials [21, 22]. These include metal organic frameworks, iron-based nanomaterials, graphene-oxide and iron oxide [23, 24]. This process is highly efficient, but is held back by cost considerations due to the need to constantly cycle adsorbents into the system [25]. Further, many materials such as commercial activated carbon are extremely cost restrictive, especially in the context of use in developing countries [18]. Due to this, extensive research efforts have been concentrated on low-cost sources of activated carbon with varying results [26, 27]. These include activated carbon derived from agricultural wastes such as rice husks, coconut husks, carbonized wood powder, sawdust, by-products of juice production, etc. [28-34]. Although a significant reduction in cost is achieved, due to the nature of the source materials, the availability of raw material is insufficient to sustain a scaled-up process.

Presently, metal oxides appear to be the most commercially viable options for this process due to easy access and lower costs. This has, in fact, been commercially applied to arsenic removal by Bayer AG, a German chemical company [18]. A simplified scheme of the SORB-33 treatment process is given in Fig. 4 [35]. The feed is introduced through the top of the tower, passes the proprietary absorbent media (G33 EFO), and purified product is obtained from the bottom of the setup. Adsorption processes report 95%+ efficiencies when the nature of adsorbent used, residence time, as well as temperature and pressure conditions are optimized.

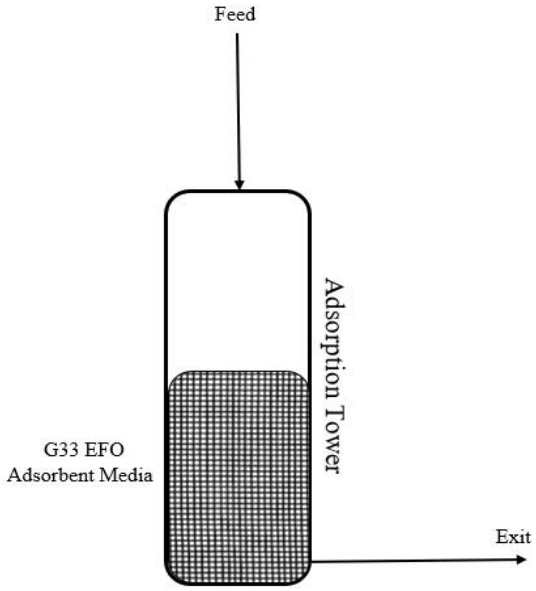

Fig. 4. Scheme of SORB-33 treatment process for separation of arsenic from wastewater.

Membrane separation

Membrane separation for arsenic removal has been gaining increased industrial adoption and research interest over time. It presents an environmentally benign, scalable and easy to implement alternative to the more conventionally employed methods, while maintaining high separation efficiencies. Several membrane separation processes are employed on a commercial scale, such as ultrafiltration, microfiltration, nanofiltration and reverse osmosis [16]. However, NF processes are considered the most competitive due to charge exclusion mechanisms that are unique to that process, resulting in high separation efficiencies. In case of arsenic removal, both NF and RO have been observed to achieve arsenic rejection of above 99%, with comparable separation efficiencies for both As(III) and As(V) [36, 37]. Further, NF has also widely substituted RO based on the significantly lower energy costs of NF processes compared to RO [38, 39]. An overview of the comparative effectiveness of all membrane separation processes towards As(III) and As(V) removal is outlined in Table 1.

Table 1. Comparison of different MSPs for arsenic removal from drinking water.

	Reverse osmosis	Nanofiltration	Ultrafiltration	Microfiltration
As(III)	Very effective	Possibly effective	Not effective	Not effective
As(V)	Very effective	Very effective	Possibly effective	Not effective

Further, more innovative membrane separation techniques such as electro-ultrafiltration, forward osmosis, as well as electrodialysis have been employed, with promising results [40-45].

PRESENT STATE OF RESEARCH INTO ELECTRODIALYSIS FOR SEPARATION OF ARSENIC INTO WASTEWATER

Research into membrane separation technology

The use of electrodialysis for arsenic removal is still a developing field, and hence the research into the area is scarce in comparison to other methods. Electrodialysis has either been used as a stand-alone process [46-52], or in conjunction with other processes [53-55].

The electrodialysis stacks used in research vary anywhere between 3 compartments to 20 compartments. Fig. 4 outlines the ED setup used by Rathi *et al*., consisting of three compartments, with the middle one being the feed compartment where the feed is introduced. As electric potential is applied to the system, arsenic moves across the AEM towards the adjacent compartment, and hence can be collected separately from the purified product [55].

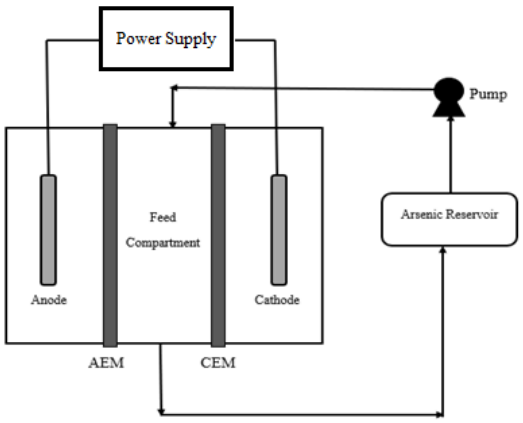

Fig. 5. Schematic setup used for electrodialytic separation of arsenic [4].

Among membranes used for separation, majority of the research has been carried out using commercially available membranes, most notably Neosepta (ASTOM Corp.) AMX and CMX membranes.

Aliaskari *et al.* in their publication used a 20-compartment stack of Neosepta AMX and CMX membranes for the electrodialytic removal of nitrate, fluoride and arsenic. Effects of a wide range of operational parameters such as flow rate, operational voltage, feed pH and salinity were also tested. Arsenic removal increased with increasing pH but decreased significantly with an increase in salinity. The system was able to reduce the arsenic levels to below the governmental guidelines [46]. Another paper, by Onorato *et al*. used an electrodialytic stack, consisting of 6 anion exchange membranes and 7 cation exchange membranes, for the removal of trace contaminants from brackish water, while studying the effect of applied voltage, as well as solution pH. The membranes were commercial, manufactured by ASTOM Corp. The separation performance was enhanced with increasing applied voltage. As for pH, the separation performance for monovalent ions was found to be pH dependent, while the separation performance of divalent ions was independent of pH. [47].

Studies have also been carried out for enhancement of electrodialysis performance using different substances, in case of Babilas *et al*., EDTA was used to enhance separation performance of a 5-compartment electrodialysis cell *via* metal complex formation [51]. Whereas the work by Xu *et al*. studied the removal of arsenic from a reverse-osmosis concentrate product, studying the impacts of coagulants, dosing, and pH on the separation performance, with highest separation achieved at 190 A/m^2. As a bonus, despite expected fouling, none was observed over the course of the research [48]. Another publication by Choi *et al.* used electrodialysis for removal of heavy metals including arsenic from groundwater using an 11-compartment electrodialysis cell, achieving up to 99.2% separation efficiency in the system [40].

Another publication by Pham *et al*. studied the effects of operational conditions on arsenic removal in an ED stack consisting of 10 cell pairs. The removal efficiency achieved was upwards of 96% when the initial concentration of As(V) was kept at 60 mg/L, while it reached 92% when the initial concentration of As(III) was kept 5 mg/L. The mass-transfer coefficient was observed to increase with increase in the discharged voltage, and the mass-transfer coefficients of As(V) were always higher in comparison to As(III) [56].

In terms of electrodialysis being used in conjunction with other processes, a publication by

Rathi *et al.* attempted a hybrid electrodialysis and ion exchange process, using a 3-compartment stack of one AEM and one CEM, with the middle (feed) compartment filled with anion exchange resin. The setup was able to achieve up to 100% removal of arsenic with the combination of the two processes [55]. Another research by Oehmen *et al*. studied a hybrid ED-coagulation process for arsenic removal. The system consisted of a two-compartment cell separated by an AEM. $FeCl_3$ was used as a coagulant to trigger precipitation of arsenic in the concentrate cell. The system was capable of achieving as low as 6.6 ppb arsenic levels [54]. Yet another attempt at a hybrid process was made in a publication by Ortega *et al.* wherein a hybrid ion exchange resin-electrodialysis system was used for arsenic removal from water. The system used was a five-compartment cell, with ion exchange resins in the middle compartment – similar to the work by Rathi *et al.* The system was applied to a feed containing up to 15 mg/L of arsenic, and was able to reduce the arsenic levels to below 10 µg/L, reaching current efficiencies of up to 47.7% and energy consumption as low as 7.5 kWh per kg of arsenic separated [53]. While studies on use of commercial membranes are available, ones with new membrane materials are rare. One such paper, by Bhadja *et al*. used polythene interpolymer membranes lab- fabricated for arsenic separation. The fabricated membrane showed superior fluoride removal capabilities compared to commercially available membranes and competitive arsenic separation performances as well [52]. Further, modelling has also been attempted on electrodialytic systems being used for arsenic removal. Honarparvar *et al*. developed a 2-D model based on Nernst-Planck equation and electroneutrality conditions. The results indicated an improvement in the selective removal of divalent ions with decreasing the cell length, potential, and ionic concentration of feed water. Enhanced mixing in spacer-filled cell was also observed to promote selective divalent ion removal. Further, higher concentrations of fixed charges on the membranes resulted in increased selectivity towards divalent ions [49]. A summary of papers with the membranes used is given in Table 2.

Research into membrane fabrication and novel membrane materials

As can be seen in Fig. 5, the research regarding new membrane materials for use in arsenic separation is scarce, while there are several publications using commercially available membranes. Research into original membrane materials tailor made for separation or arsenic ions is hence an area that can be looked into further. Membranes with better separation efficiency, lower costs of operation, higher temperature resistance, wider operational pH range, higher current efficiency, ion exchange capacity must be looked into.

Table 3 provides a summary of the properties of commonly used commercial membranes, and Table 4 provides a summary of the most recent research work undertaken regarding fabrication of novel anion exchange membranes. As can be seen from the table, several different materials can be chosen for such an operation, each offering different properties that can be useful for electrodialytic separation operations.

Table 2. Summary of recently published work on arsenic removal using electrodialysis.

Ref.	Operational parameters	Membrane
[46]	Membrane area: 210 cm^2 Voltage: 0 - 60 V pH: 2 – 12	Commercial Membranes
[47]	Membrane area: 58 cm^2 Voltage: 12 & 18 V pH: 3 – 11	Commercial Membranes
[51]	Membrane area: 64 cm^2 Current Density: 100 – 250 A/m^2 pH: 2 – 4	Commercial Membranes
[48]	Membrane area: 100 cm^2 Operating Pressure: 12 – 27 kPa pH: 6 – 8	Commercial Membranes`
[40]	Membrane area: 47 cm^2 Voltage: 12 & 18 V pH: 3 – 11	Commercial Membranes
[56]	Membrane area: 55 cm^2 Voltage: 10 - 30 V pH: 4 – 10	Commercial Membranes
[55]	Membrane area: 49 cm^2 Voltage: 5 - 25 V pH: 3 – 10	Commercial Membranes
[54]	Membrane area: 11.3 cm^2 pH: 7.8 – 8	Commercial Membranes
[53]	Membrane area: 10 cm^2 Voltage: 10 - 20 V pH: 6 – 10	Commercial Membranes
[52]	Membrane area: 200 cm^2 Voltage: 45 V Feed TDS: 200 ppm	Fabricated Membranes.
[49]	Membrane area: 47 cm^2 Voltage: 0 – 1.4 V pH: ~7	Commercial Membranes

Table 3. Properties of commonly used commercial membranes

Property	Range
pH tolerance	0 – 14
Temperature range	< 40° C
Ion exchange capacity	2.2 mmol/g
Water uptake	30%

Further, those materials once fabricated were only tested on common salts and hence their effectiveness for a more complex operation of heavy metal removal can be looked into.

.

Table 4. Summary of recent research on ion-exchange membrane fabrication

Ref.	Material	Properties of membranes
[52]	Polyethylene interpolymer-based ion-exchange membranes	Energy density (W) = 1.24 kWhr/Kg Current efficiency (CE) = 74.5% Ion exchange capacity (IEC) = 1.30 mmeq/g Temperature: 25° C
[57]	Pore-filling anion exchange membranes (PAEM). Trimethylammonium chloride mixed with piperazine diacrylamide as a crosslinking agent.	IEC: 1.645 mmeq/g, Water uptake (WU) = 34.47% Tensile strength: 148 Mpa, Resistance: 0.661 Ohm/cm^2 Temperature: 25° C
[58]	Photocured membrane made using N-dimethoxymethylsilylpropyl-N, N, N-trimethylammonium chloride, 50 wt% in MeOH) and 3-acrylamidopropyl trimethoxysilane	IEC: 2.2 mmol/g Temperature: 75 ° C WU: 128.18% Resistance: 0.224 Ohm/cm^2
[59]	Graphene oxide (rGO) crosslinked polysulfone-based AEM.	IEC: 33.5 mmol/g WU: 33.5% Tensile strength: 1730 MPa Temperature: 80° C
[60]	Brominated poly (2,6-dimethyl-1,4-phenylene oxide) as the polymer base and 4-methylpyridine as an ion exchanger.	Tensile strength: 33 MPa IEC: 2.2 mmol/g Temperature: 70° C
[61]	Imidazole-based anion exchange membranes created by photopolymerization.	Temperature: 100°C Tensile strength: 29.5 MPa IEC: 2.69 mmol/g, Resistance 1.78 Ohm/cm^2 Limiting current density: 13.23 mA/cm^2 W: 9.1 kWh/kg, CE: 81.9%
[62]	Membrane fabricated by single step crosslinking of porous brominated poly (phenylene oxide) membrane substrate with 1, 4-diazabicyclo [2.2.2] octane.	WU: 151% Temperature: 110° C IEC 1.7 mmol/g

One important factor for any fabricated membrane that decides whether it will achieve commercial viability is its stability. Maintenance is a major issue in electrodialysis processes. Hence, thermal and chemical stability of membranes are vital parameters for a membrane, which are assessed by studying the weight loss percentage of the membrane when subjected to thermal and chemical stress. However, not all publications have reported the stability of the membranes fabricated in their research. Bai *et al.* reported a 55% weight percentage over a course of 72-hour experimentation for oxidative stability tests and for thermal stability tests, a weight percentage of 80% at 200°C and 60% at 800°C [59]. Yang *et al*. in their thermal stability tests recorded a weight percentage ranging from 70–80% at 300°C and 10–20% at 700°C, depending on the membrane [58]. Thermal stability tests by Khan *et al*. showed a weight percentage ranging from 90–95% at 200°C and 10–45% at 600°C for the various membranes fabricated in the research [60]. Lin *et al.* recorded an impressive near 100% weight percentage at 300°C and nearly 50% at 500°C [62].

These are consistent with commercially used membranes and even surpass them in some cases.

Additionally, depending on the selectivity of the membrane being used, information regarding speciation of arsenic as described earlier in Fig 1 can be used to control the number of monovalent and divalent arsenic ions in the solution.

CONCLUSIONS

The paper briefly summarized the sources of arsenic, the effects – both short- and long-term of exposure on humans, the strategies in place for arsenic removal from water, as well as the place of electrodialysis among those processes. Further, the paper reviewed and summarised the research regarding separation of arsenic from wastewater using electrodialysis undertaken over the past decade.

The majority of work has been carried out on commercial membranes, hence a need for research into newer membrane materials is crucial for the commercial viability of the process for wastewater treatment. Membranes with better separation efficiency, lower costs of operation, higher temperature resistance, wider operational pH range, higher current efficiency, ion exchange capacity can be researched and developed.

Further, a summary of recent research on fabricated ion exchange membranes, as well as their properties was given. Based on the information, membranes can be tailor-made for the specific purposes of arsenic separation in particular or heavy metals in general, with properties superior to the ones found in commercially available membranes.

REFERENCES

1. B. S. Rathi, P. S. Kumar, J. Hazard. Mater., **418**, 126299 (2021), doi: 10.1016/j.jhazmat.2021. 126299.
2. V. R. Moreira, Y. A. R. Lebron, L. V. S. Santos, E. Coutinho de Paula, M. C. S. Amaral, *Process Saf. Environ. Prot.*, **148**, 604 (2021), doi: 10.1016/j.psep.2020.11.033.
3. V. M. Nurchi, A. B. Djordjevic, G. Crisponi, J. Alexander, G. Bjørklund, J. Aaseth, *Biomolecules*, **10** (2), 1 (2020), doi: 10.3390/biom10020235.
4. A. Parvaiz, J. A. Khattak, I. Hussain, N. Masood, T. Javed, A. Farooqi, *Environ. Pollut*., **268**, 115710 (2021), doi: 10.1016/j.envpol 2020.115710.
5. M. L. Polizzotto, B. D. Kocar, S. G. Benner, M. Sampson, S. Fendorf, *Nature*, **454** (7203), 505 (2008), doi: 10.1038/nature07093.
6. J. F. Ferguson, J. Gavis, *Water Res*., **6** (11), 1259 (1972), doi: 10.1016/0043-1354(72)90052-8.
7. W. Ali, A, Rasool, M. Junaid, H. Zhang, *Environmental Geochemistry and Health,* **41** (2), 737 (2019), doi: https://doi.org/10.1007/s10653-018-0169-x
8. V. R. Moreira, Y. A. R. Lebron, L. V. S. Santos, E. C. De Paula, M. C. S. Amaral, *Process Saf. Environ. Prot.*, **148**, 604 (2021), doi: 10.1016/j.psep. 2020.11.033.
9. I. D. Rae, *ChemTexts*, **6** (4), 1 (2020), doi: 10.1007/s40828-020-00118-7.
10. H. Zhou, G. Liu, L. Zhang, C. Zhou, M. M. Mian, A. I. Cheema, *Environ. Pollut*., **270**, 116203 (2021), doi: 10.1016/j.envpol.2020.116203.
11. R. J. Bowell, D. Craw, *Rev. Mineral. Geochemistry*, **79** (1), 507 (2014), doi: 10.2138/rmg.2014.79.11.
12. L. H. Andrade, W. L. Pires, L. B. Grossi, A. O. Aguiar, M. C. S. Amaral, *Environ. Technol. (United Kingdom)*, **40** (13), 1644 (2019), doi: 10.1080/09593330.2018.1432692.
13. V. M. Rodríguez, M. E. Jiménez-Capdeville, M. Giordano, *Toxicol. Lett.*, **145** (1|), (2003), doi: 10.1016/S0378-4274(03)00262-5.
14. L. Zanella, L. Fattprini, P. Brunetti, E. Roccotiello, L. Cornara, S. D'Angeli, F. D. Eovere, M. Cardarelli, M. Barbieri, L. Sanità di Toppi, F. Degola, S. Lindberg, M. M. Altamura, G. Falasca, *Planta*, **243** (3), 605 (2016), doi: 10.1007/s00425-015-2428-8.
15. R. C. J. Campbell, W. E. Stephens, A. A. Finch, K. Geraki, *Environ. Sci. Technol.*, **48** (6), 3449 (2014), doi: 10.1021/es4039243.
16. M. I. Litter, M. E. Morgada, J. Bundschuh, *Environ. Pollut*., **158** (5), 1105 (2010), doi: 10.1016/j.envpol.2010.01.028.
17. R. Singh, S. Singh, P. Parihar, V. P. Singh, S. M. Prasad, *Ecotoxicol. Environ. Saf*., **112**, 247 (2015), doi: 10.1016/j.ecoenv.2014.10.009.
18. T. S. Y. Choong, T. G. Chuah, Y. Robiah, F. L. Gregory Koay, I. Azni, *Desalination*, **217** (1–3), 139 (2007), doi: 10.1016/j.desal.2007.01.015.
19. J. Gregor, *Water Res.*, **35** (7), 1659 (2001), doi: 10.1016/S0043-1354(00)00424-3.
20. L. S. McNeill, M. Edwards, *J. Am. Water Works Assoc*., **87** (4), 105 (1995), doi: 10.1002/j.1551-8833.1995.tb06346.x.
21. F. O. Ochedi, Y. Liu, A. Hussain, *J. Clean. Prod*., 267, 122143 (2020), doi: 10.1016/j.jclepro. 2020.122143.
22. J. A. Rodríguez-Romero, D. I. Mendoza-Castillo, H. E. Reynel-Ávila, D. A. de Haro-Del Rio, L. M. González-Rodríguez, A. Bonilla-Petriciolet, C. J. Duran-Valle, K. I. Camacho-Aguilar, *J. Environ. Chem. Eng.*, **8** (4) 103928 (2020), doi: 10.1016/j.jece.2020.103928.
23. J. H. Gulledge, J. T. O'Connor, *J. Am. Water Work. Assoc.*, **65** (8) 548 (1973), doi: 10.1002/j.1551-8833.1973.tb01893.x.
24. M. Gallegos-Garcia, K. Ramírez-Muñiz, S. Song, *Miner. Process. Extr. Metall. Rev.*, **33** (5), 301 (2012), doi: 10.1080/08827508.2011.584219.
25. Q. Yang, C. W. Culbertson, M. G. Nielsen, C. W. Schalk, C. D. Johnson, R. G. Marvinney, M. Stute, Y. Zheng, *Sci. Total Environ.*, **505**, 1291 (2015), doi: 10.1016/j.scitotenv.2014.04.089.
26. S. J. T. Pollard, G. D. Fowler, C. J. Sollars, R. Perry, *Sci. Total Environ.*, **116** (1–2), 31 (1992), doi:

10.1016/0048-9697(92)90363-W.
27. S. E. Bailey, T. J. Olin, R. Mark Bricka, D. Dean Adrian, *Water Res.*, **33** (11), 2469 (1999).
28. G. N. Manju, C. Raji, T. S. Anirudhan, *Water Res*., **32** (10), 3062 (1998), doi: 10.1016/S0043-1354(98)00068-2.
29. A.U. Baes, T. Okuda, W. Nishijima, E. Shoto, M. Okada, *Water Sci. Technol*., **35** (7) 89 (1997)
30. N. Khalid, S. Ahmad, A. Toheed, J. Ahmed, *Adsorpt. Sci. Technol*., **16** (8), 655 (1998), doi: 10.1177/026361749801600806.
31. C. K. Lee, K. S. Low, S. C. Liew, C. S. Choo, *Environ. Technol. (United Kingdom)*, **20** (9), 971 (1999), doi: 10.1080/09593332008616892.
32. L. L. Pulido, T. Hata, *J. Wood Sci*., **44** (3), 237 (1998), doi: 10.1007/BF00521970.
33. B. Yasemin, T. Zeki, *J. Environ. Sci*., **19** (2), 160 (2007), [Online]. Available: www.jesc.ac.cn.
34. K. N. Ghimire, K. Inoue, K. Makino, T. Miyajima, *Sep. Sci. Technol*., **37** (12), 2785 (2002), doi: 10.1081/SS-120005466.
35. U. S. Environmental, Arsenic Treatment Technology Evaluation Handbook for Small Systems, 2012, p. 152, doi: EPA 816-R-03-014.
36. J. J. Waypa, M. Elimelech, J. G. Hering, *J. Am. Water Work. Assoc*., **89** (10), 102 (1997), doi: 10.1002/j.1551-8833.1997.tb08309.x.
37. E. O. Kartinen, C. J. Martin, *Desalination*, **103** (1–2), 79 (1995), doi: 10.1016/0011-9164(95)00089-5.
38. T. A. Siddique, N. K. Dutta, N. R. Choudhury, *Nanomaterials*, **10** (7), 1 (2020), doi: 10.3390/nano10071323.
39. M. Leist, R. J. Casey, D. Caridi, *J. Hazard. Mater*., **76** (1), 125 (2000), doi: 10.1016/S0304-3894(00)00188-6.
40. S. Y. Choi, K. Y. Park, Y. Yu, H. J. Kim, K. Y. Park, J. H. Kweon, J. W. Choe, *Desalin. Water Treat*., **57** (55), 26741 (2016), doi: 10.1080/19443994. 2016.1190112.
41. H. K. Hansen, A. Lazo, C. Gutierrez, M. Durán, P. Lazo, A. Rojo, *Miner. Eng*., **100**, 87 (2017), doi: 10.1016/j.mineng.2016.11.006.
42. P. Mondal, A. T. K. Tran, B. Van der Bruggen, *Desalination*, **348**, 33 (2014), doi: 10.1016/j.desal. 2014.06.001.
43. L. H. C. Hsieh, Y. H. Weng, C. P. Huang, K. C. Li, *Desalination*, **234** (1–3), 402 (2008), doi: 10.1016/j.desal.2007.09.110.
44. X. Jin, Q. She, X. Ang, C. Y. Tang, *J. Memb. Sci*., **389**, 182 (2012), doi:10.1016/j.memsci.2011. 10.028.
45. M. T. Pham, S. Nishihama, K. Yoshizuka, *J. Chem. Eng. Japan*, **53** (3), 95 (2020), doi: 10.1252/JCEJ.19WE207.
46. M. Aliaskari, A. I. Schäfer, *Water Res.*, **190**, 116683 (2021), doi: 10.1016/j.watres.2020. 116683.
47. C. Onorato, L. J. Banasiak, A. I. Schäfer, *Sep. Purif. Technol.*, **187**, 426 (2017), doi: 10.1016/j.seppur. 2017.06.016.
48. P. Xu, M. Capito, T. Y. Cath, *J. Hazard. Mater*., **260**, 885 (2013), doi: 10.1016/j.jhazmat.2013. 06.038.
49. S. Honarparvar, D. Reible, *Environ. Sci. Ecotechnology*, **1**, 100007 (2020), doi: 10.1016/j.ese.2019.100007.
50. B. Cohen, N. Lazarovitch, J. Gilron, *Desalination*, **431**, 126 (2018), doi: 10.1016/j.desal.2017.10.030.
51. D. Babilas, J. Muszyński, A. Milewski, K. Leśniak-Ziółkowska, P. Dydo, *Chemical Engineering Journal*, **408**, (2020, 2021), doi: 10.1016/j.cej.2020.127908.
52. V. Bhadja, J. S. Trivedia, U. Chatterjee, *RSC Adv*., **6** (71), 67118 (2016), doi: 10.1039/c6ra11450d.
53. A. Ortega, I. Oliva, K. E. Contreras, I. González, M. R. Cruz-díaz, E. P. Rivero, *Sep. Purif. Technol*., **184**, 319 (2017), doi: 10.1016/j.seppur.2017. 04.050.
54. A. Oehmen, R. Valerio, J. Llanos, J. Fradinho, S. Serra, M. A.M. Reis, J. G. Crespo, S. Velizarov, *Sep. Purif. Technol*., **83**, 137 (2011), doi: 10.1016/j.seppur.2011.09.027.
55. B. S. Rathi, P. S. Kumar, R. Ponprasath, K. Rohan, N. Jahnavi, *J. Hazard. Mater*., **412**, 125240 (2021), doi: 10.1016/j.jhazmat.2021.125240.
56. M. T. Pham, S. Nishihama, K. Yoshizuka, *Solvent Extr. Ion Exch*., **39** (5–6), 655 (2021), doi: 10.1080/07366299.2021.1876987.
57. S. C. Yang, Y. W. Choi, J. Choi, N. Jeong, H. Kim, H. Jeong, S. Y. Byeon, H. Yoon, Y. H. Kim, *J. Membr. Sci.*, **584**, 181 (2019), doi: 10.1016/j.memsci.2019.04.075.
58. S. C. Yang, W. Kim, J. Choi, Y. W. Choi, N. Jeong, H. Kim, J. Y. Nam, H. Jeong, Y. H. Kim, *J. Membr. Sci.*, **573** 544 (2019), doi: 10.1016/j.memsci. 2018.12.034.
59. Y. Bai, Y. Yuan, Y. Yang, C. Lu, Int. *J. Hydrogen Energy*, **44** (13), 6618 (2019), doi: 10.1016/j.ijhydene.2019.01.143.
60. M. Imran, M. Khraisheh, F. Almomani, *Sci. Total Environ.*, **686**, 90 (2019), doi: 10.1016/j.scitotenv. 2019.05.481.
61. J. Pan, Y. Tao, L. Zhao, X. Yu, X. Zhao, T. Wu, L. Liu, *Sep. Purif. Technol*., **276** 119220, (2021), doi: 10.1016/j.seppur.2021.119220.
62. J. Lin, J. Huang, J. Wang, J. Yu, X. You, X. Lin, B. V. Bruggen, S. Zhao, *J. Membr. Sci*., **624**, 119116 (2021), doi: 10.1016/j.memsci.2021. 119116.

Bulgarian Chemical Communications, Volume 54, Special Issue C (pp. 69-77) 2022 DOI: 10.34049/bcc.54.C.0069

Green approach for energy production by waste stabilization

F. Q. Mir*, A. Masoodi, A. Majeed, M. H. Beigh

Department of Chemical Engineering, National Institute of Technology Srinagar, Hazratbal, Srinagar, Jammu & Kashmir 190006, India

Accepted: July 06, 2022

In recent times, there has been a gap between the demand and supply of energy and there needs to be a reduction of the carbon footprint. Also, the depletion of non-renewable sources of energy has led to the intensification of research in the area of renewable sources of energy, since the reliance on fossil fuels is unsustainable. One of the most promising technologies in this area is the microbial fuel cell (MFC), which is not just a sustainable, eco-friendly and self-sustaining source of energy, but also an effective method for the treatment of wastewater. In MFCs, electrochemically active bacteria convert the organic substrate directly into energy. MFCs are the major types of bioelectrochemical systems, providing opportunities for the sustainable production of energy from eco-friendly reduced compounds. These cells can not only use carbohydrates as the substrate but also certain complex substrates present in wastewater. In this review paper, various designs of the MFC, its characterization and performance have been presented. The performance of an MFC depends on a number of different factors such as the material of the anode and cathode used, the choice of anode microbial catalyst and cathodic electron acceptor, and the amount and type of substrate available in the anaerobic anodic chamber. The recent updates in the research of MFCs are also presented in this paper and it addresses the different configurations of the cell, their effect on its performance, and ways to improve its performance in order to make it economical.

Keywords: Microbial fuel cells; Wastewater; Bioelectrochemical system

INTRODUCTION

The energy crisis has increased a great deal in the past few years and it is evident that we need an alternative source of energy to make up for it. Also, it is highly unlikely that a single source of energy will be in a position to replace the use of fossil fuels [1]. Therefore, we require several alternatives to be used under different situations. One of these is the MFC which has recently received a lot of attention since it can be used to generate electricity by converting the energy stored in organic compounds without causing any pollution to the environment, with no net carbon emission, and can also be used in wastewater treatment. Unlike most fuel cells, MFCs don't require metal catalysts at the anode [2]. Biocatalysts (microorganisms) are used, which biologically oxidize organic substrate and transfer electrons to the anode, which travel externally to the cathode, producing electricity. The organic matter used here is versatile, ranging from simple molecules, to complex mixtures of organic wastes [3], making it an ideal source of renewable bioenergy.

Taking glucose as a substrate, the reactions occurring in the anodic and cathodic chamber, respectively, are:

- Anodic reaction

$C_6H_{12}O_6 + 6H_2O \rightarrow 6CO_2 + 24e^- + 24H^+$

- Cathodic reaction

$O_2 + 4e^- + 4H^+ \rightarrow H_2O$

In order to make the use of MFCs economical, research is going on to increase its power output, which may depend on the available organic substrate and its particle size. Some MFCs are currently in use and certain applications of the MFCs are being worked upon. This review highlights the important parameters of the MFC, its design, mechanism and its applications.

The concept of MFCs is not new. The earliest hypothesis was demonstrated in 1910 [4], but it didn't gather much attention, due to low current density, low power output, and the use of electron mediators, to carry electrons from the cell to the anode. Research in the area of MFCs intensified after a major breakthrough in this field, which suggested that there exist certain microbes which can transfer electrons directly to the anode. *Shewanella putrefaciens* is one of the biochemically active bacteria which transfer electrons from the interior of the cell membrane to the anode. A bacterial strain, by the name of *Geobacter sulfurreducens* KN400, is said to be capable of higher current production, about eight times more efficient as compared to other strains [5].

The bacteria used to oxidize organic substrates in mediator MFCs include *Pseudomonas aeruginosa, Proteus mirabilis, Actinobacillus succinogenes, Streptococcus lactis, Erwinia dissolvens,* etc. [6]. These bacteria oxidise organic matter and do not pass on the electrons during metabolic activity

* To whom all correspondence should be sent:
E-mail: mirfasil@nitsri.ac.in

directly to the anode. Instead, they transfer these electrons to external mediators, such as thionine, methyl viologen, humic acid [7], which act as carriers for electrons from bacterial cells to the anode. The efficiency of these types of MFCs is very low and the mediators used are expensive and toxic, so the current research is focused on mediatorless MFCs only.

In mediatorless MFCs, the microbes used belong to the class of exoelectrogens like *Geobacter metallireducens, Geobacter sulfurreducens, Rhodoferax ferrireducens, Shewanella putrefaciens,* etc. [8]. The exoelectrogenic bacteria come in direct association with the anode and transfer electrons produced during oxidation to it either through protein carriers located in the cell membrane like porin-cytochrome complexes or through special cell membrane projections, like pilli, which act as microbial nanowires [4, 9].

One of the recent researches in MFC development involves the infusion of silver atoms in bacterial cells. This research is based on experiments which were carried out on the bacterial species, *Shewanella oneidensis.* These bacteria create a biofilm around the electrode in the anodic chamber and oxidise the substrate into smaller molecules, producing electrons as a by-product. The electrons are then carried outside the cell through the cell membrane, where they are received by the anode and transferred to the cathode through an outer circuit in order to generate an output current. But the rate at which the electrons diffuse outside the cell through the cell membrane, is very low, due to which only a small output current or power density is obtained. In one of the experiments, the nanoparticles of silver were added to the anode. These nanoparticles released silver ions, which were reduced by electrons released in the metabolic activity of microbes, into silver and were incorporated inside these bacterial cells, wherein these silver atoms worked as transmission wires for capturing and carrying the electrons, produced during metabolic activity, at very high rates, through the membrane to the anode. This infusion of silver atoms inside microbes increased the current density by many folds.

Design of the MFC

A prototypical MFC has two chambers: a cathodic chamber and an anodic chamber. These chambers are interconnected either by a salt bridge or a proton exchange membrane.

Oxidation of substrate occurs inside the anodic chamber, which results in the release of electrons and protons [10, 11]. In order to avoid the transfer of electrons directly to a final electron acceptor, i.e., oxygen, the anodic chamber is made anaerobic (deprived of oxygen). Also, the microbes used in the MFCs are mainly anaerobic in nature, therefore, the presence of oxygen will not affect their metabolism. Anaerobic conditions can be created by the purging technique. In this technique, a vacuum is created inside the anodic chamber and this vacuum pressure is released by nitrogen. The performance of an MFC depends on several factors, out of which the material of the electrode is an important one [4, 12]. The electrode, or anode, used in the anodic chamber, must possess certain qualities like high conductivity, resistance to corrosion, biocompatibility, high surface area and should be chemically stable [9, 13, 14]. In most MFCs, the electrodes used as anodes are made up of carbon like graphite rods.

The cathodic chamber involves the reduction of the final electron acceptor that may be oxygen or any other oxidizing agent. In case the final electron acceptor is oxygen, water is the by-product. The electrode used as the cathode is generally made of copper or graphite, due to its low-cost and high performance [9] The reduction of oxygen on electrodes made of carbon is very slow which generates low current density. Therefore, the use of carbon electrodes is a limiting factor in MFCs where oxygen acts the final oxidising agent. This limitation is overcome by replacing the final electron acceptor, i.e., oxygen with hexacyanoferrate, permanganate, nitrate, etc. Catalysts like platinum are also used to enhance its performance.

Two-chambered MFC can take up a number of different practical shapes, some of which are shown in Fig 1 (a) cylindrical shape, (b) rectangular shape, (c) miniature shape, (d) upflow oriented MFCs, and many others.

Currently, the cylindrical MFCs find practical use only in the laboratories, and although they can be operated in both batch and continuous mode, they are mostly run only in batch mode, with glucose or acetate solution [4] as a medium in order to generate electricity. Miniature ones find use in less accessible regions and for long operations. MFCs with upflow orientation are easier to scale up; and they are used extensively for wastewater treatment, rather than for electricity generation, because pumping fluid in these MFCs is costlier in terms of energy usage, as compared to the power output that they deliver.

MFCs do not necessarily have to be two-chambered. Single-compartment MFCs have also been developed since the cost is reduced in this case and also because they offer a much simpler design. These MFCs typically do not require a cathodic chamber. Cathode lies in the open air, the available oxygen in the air behaves as the final electron

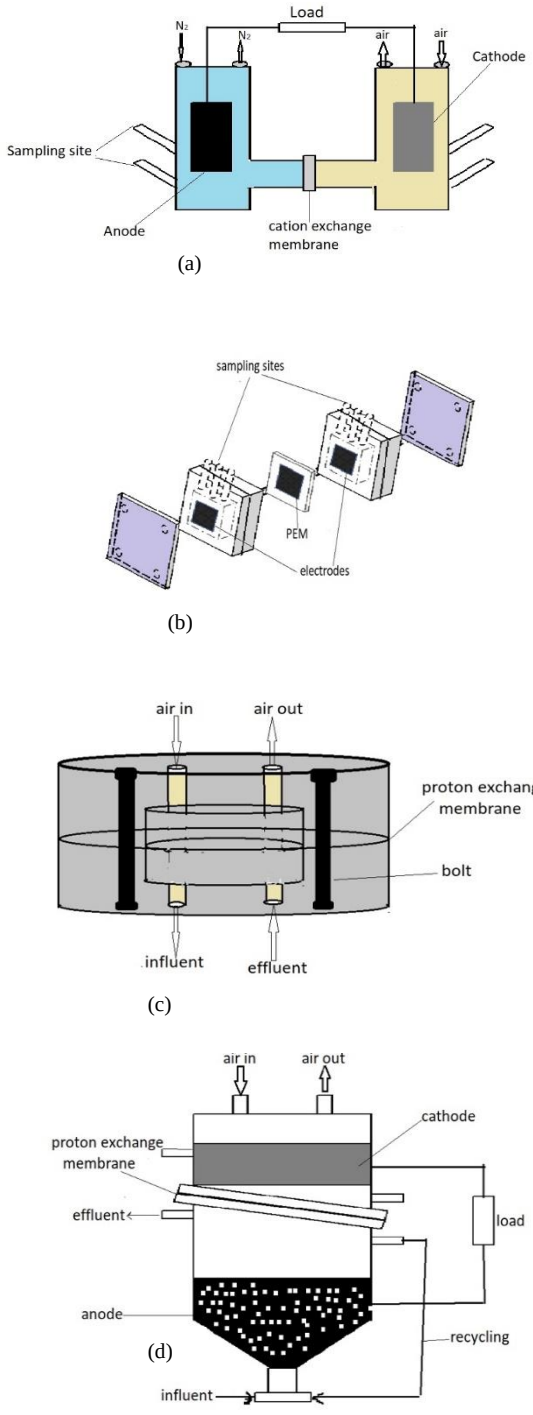

Fig. 1. Schematics of two-compartment MFCs in various shapes.

acceptor, while the anode lies in the anodic chamber. Fig 2 shows the schematics of different shapes of a single-compartment MFC, where (a) shows an MFC with the anode in the rectangular anodic chamber which contains the permeable air cathode lying outside the chamber; (b) shows MFC with the anode in the cylindrical anodic chamber and cathode lying outside; (c) shows a tubular one-compartment MFC with a granular anode, made of graphite, lying inside and cathode lying outside.

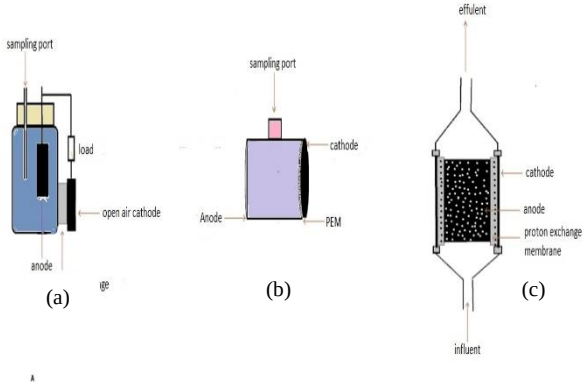

Fig. 2. Schematics of single-compartment MFCs in various shapes

In order to elevate the power output delivered by the MFC, several MFCs can be arranged together in parallel, or in series. This also helps to examine the performance of the microbial fuel cell. It has been observed that higher current output is achievable by stacking MFCs together. Fig. 3 shows five individual MFC units stacked together.

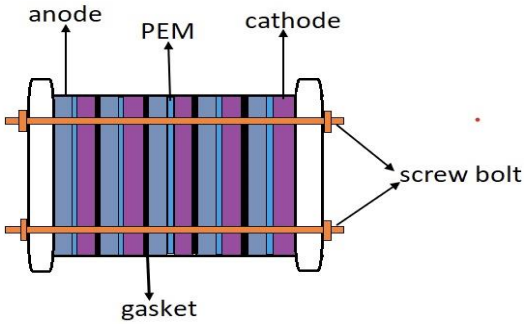

Fig. 3. Schematics of five MFC units

MECHANISM AND MICROORGANISMS USED

Since all living organisms require energy for their survival, this energy is obtained by performing certain metabolic activities like digestion, respiration, etc. Respiration is the main metabolic activity involved in releasing energy from different substrates like glucose, acetate, etc.

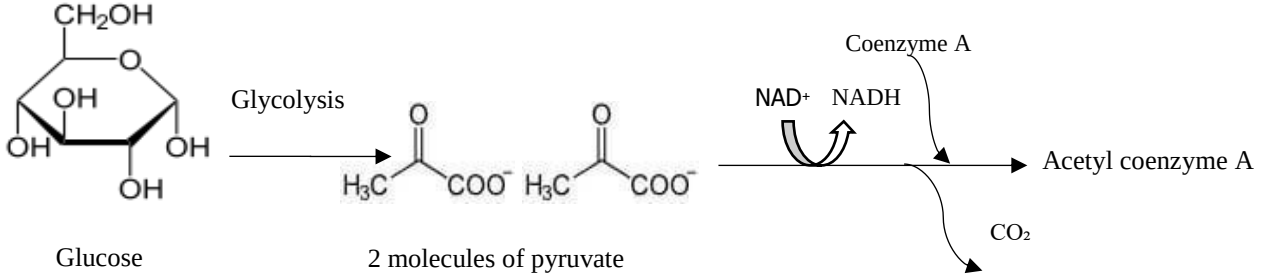

Scheme 1. Conversion of glucose to acetyl CoA by glycolysis

Microorganisms too use this metabolic process, i.e., respiration or more specifically, cellular respiration for the synthesis of ATP (energy-rich compounds). These microbes break down the organic molecules and produce electrons and protons through three respiratory pathways, namely glycolysis/EMP pathway, Krebs cycle and electron transport chain (ETC). In glycolysis, different organic compounds like carbohydrates, lipids, proteins, etc. are converted into acetyl coenzyme A (CoA).

This process can be explained by taking the example of glucose (a carbohydrate), the overall reaction of which is shown in Scheme 1:

✓ The glucose molecule is first phosphorylated to glucose-6-phosphate. In this reaction, ADP is converted to ATP (enzyme used: hexokinase).

✓ Glucose-6-phosphate (an aldose) is isomerised to fructose-6-phosphate (enzyme used: phosphohexose isomerase).

✓ Fructose-6-phosphate is then phosphorylated to fructose 1,6-bisphosphate by combining with another phosphoryl group (enzyme used: phosphofructokinase).

✓ Fructose 1,6-bisphosphate breaks down to form two different triose phosphates, dihydroxyacetone phosphate (DHAP) and glyceraldehyde-3-phosphate (GAP). Only one of the two isomers can directly continue the process of glycolysis.

✓ DHAP is rapidly converted to GAP (enzyme used: phosphotriose isomerase).

✓ GAP is oxidised to form 1,3-biphosphoglycerate (by combining with a phosphate group) (enzyme used: glyceraldehyde 3-phosphate dehydrogenase). NAD^+ is reduced to NADH and H^+ in the process.

✓ The phosphate group on 1,3-biphosphoglycerate is donated to ADP, converting it to ATP and turning 1,3-biphosphoglycerate into 3-phosphoglycerate.

✓ 3-Phosphoglycerate is isomerised to 2-phosphoglycerate (enzyme used: phosphoglycerate mutase).

✓ 2-Phosphoglycerate gets dehydrated, loses a molecule of water, and becomes phosphoenolpyruvate (PEP), an unstable molecule.

✓ A phosphate group from PEP is donated to ADP, making the second molecule of ATP. PEP itself gets converted to pyruvate. Pyruvate undergoes oxidative decarboxylation to form 2 molecules of acetyl coenzyme A.

This acetyl CoA is processed in Krebs cycle where it is first oxidised and the electrons released reduce NAD^+ to NADH. In order to maintain the continuity of metabolic processes, the NADH must get oxidised back to NAD^+ which is achieved by electron transport chain (ETC), wherein the reduced molecule, i.e., NADH is carried to the cell membrane where special membrane-embedded proteins oxidize it back to NAD^+ and shuttle the electrons and protons outside the cell membrane [15]. The shuttled electrons are then harvested by the anode and transmitted to the cathode *via* an outer circuit as shown in Fig. 4.

In MFCs, the microbes used are mostly anaerobic bacteria, as they do not directly transfer electrons to the final electron acceptor. These bacteria are capable of extracellularly transmitting the electrons produced while oxidizing the substrate to the anode, either indirectly (in mediated MFCs), or directly (mediatorless MFCs).

Complete oxidation of glucose by a bacterium, for example *R. ferrireducens* yields 900 Coulombs (amperes*seconds), the calculation of which goes as follows:

1 mol of electrons = 96,500 C;

1 mol of glucose = 96,500 × 24 C or 1 μmol of glucose = 2.316 C;

Therefore, 389 μmol of glucose = 2.316 × 389 = 900 C.

The recent MFC technology uses microbes that belong to the class of exoelectrogens like *Shewanella putrefaciens, Geobacter, Rhodoferax*, as they directly transfer electrons to the anode and generate relatively high power densities.

PROTON INHIBITION

While oxidizing the substrate, protons are also generated in the anodic chamber along with the

electrons. The electrons, as discussed earlier, are mediated by anode to the cathode through an outer circuit. It is essential to remove the protons from the anodic chamber in order to maintain electrical neutrality. Moreover, the increasing concentration of protons inside the anodic chamber will inhibit the metabolism of microbes. So, for this purpose, the anodic and the cathodic chambers are interconnected by a cation exchange membrane, like a polymeric electrolyte membrane, or salt bridge [8, 16] The polymeric electrolyte membrane or salt bridge facilitates the movement of protons from the anodic chamber to the cathodic chamber and therefore, inhibits the agglomeration of protons in the anodic chamber [17, 18]

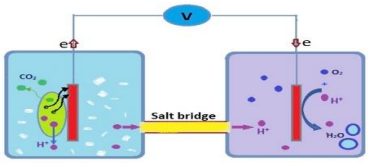

Fig. 4. Schematics of the mechanism of MFC

FACTORS AFFECTING THE PERFORMANCE OF MFCs

The performance of an MFC depends on a number of different parameters, which could be physical (material of the cathode and anode used [12], configuration of the MFC reactor), biological (inoculum type, which could be pure or mixed, substrate concentration) or operational (substrate type, external resistance, effect of temperature and pH) [19]. Table 1 shows the power output delivered by the MFC when different wastewater samples are used as substrate.

Experiments conducted on MFCs show that their performance depends on their configuration and materials used in their design, rather than just the microbes present in the wastewater, although they have a huge role to play.

For example, a membrane electrode assembly MFC, MFCs stacked in series and MFCs stacked in parallels delivered a maximum coulombic efficiency (% based on COD) of 0.9 [20], 12.4 [21] and 77.8 [21], respectively. Similarly, when brewery wastewater was used as the substrate, the coulombic efficiency (CE) delivered by a baffled MFC and serpentine type MFC has been found to be 19.1 [22] and 7.6 [23] respectively. The mixture of domestic wastewater and textile wastewater delivered a CE of 36 [24] in a membrane-less cross-linked MFC and thermo-chemically pretreated dairy wastewater activated sludge, when used as substrate in a two-chambered MFC delivered a CE of 9 [25].

The material used for electrodes has to be selected with the utmost care since there is a high chance of corrosion. Materials like copper, stainless steel, graphite, platinum and many others have been used, and each one seems to have its pros and cons. For example, it has been observed that MFC deliver higher power densities when copper was used as an electrode. This is due to galvanic corrosion [26]. But it was found out that copper shows antibacterial properties. Likewise, stainless steel has been used as electrode material, but it was found out that its use depends upon the amount of chromium present in the alloy [26]. Furthermore, the active surface of the electrode, its conductivity, the nature of its surface, its biocompatibility, are some other parameters that govern the performance of an MFC.

Several attempts have been made to upgrade the performance of an MFC, one of which was the usage of carbon cloth as anode material, treated with phosphate buffer and ammonia gas. This attempt gave an increase in power production by 98% as compared to the MFC without this treatment.

Materials used as electrodes could typically be the same for anode and cathode but properties such as high conductivity and mechanical strength along with effective catalytic nature can make up a potential cathode. In the past few decades, there has been substantial research in this area to develop and design MFCs such that the performance is enhanced. The problem still lies with commercialisation and scale-up which is being worked upon, to find permanent solutions. The temperature, at which bacteria grow and perform their metabolic activities, ranges from 0°C to 40°C. Below 0°C, the bacteria cease to grow and their metabolic activities also stop but they don't die. Above 40°C, proteins denature and protoplasm starts to coagulate, which ultimately leads to the death of the bacterial cell. In some species of bacteria, the temperature range is –5°C - 40°C. Thus, an MFC, in this case, can produce electricity in the temperature range of –5°C - 40°C, while the relatively higher amount of electricity produced at a particular temperature in this range depends upon the bacteria used and is determined experimentally. Table 2 shows the performance of MFC with different electrode materials; when different types of bacteria use the same substrate (glucose) for metabolism.

APPLICATIONS

Electricity generation

MFCs are different from other electricity-producing devices like heat engines in a way that

they directly produce electricity without the generation of heat, heat being a low-grade energy. Microbial fuel cells convert chemical energy into electrical energy with the help of microorganisms, hence, they are environmentally friendly. Therefore, microbial fuel cells serve a dual benefit by generating electricity and waste management. The rate of power generation is still low in MFCs. Hence, they can be used for power generation in small systems where low power input is required.

There are various factors responsible for the power output of the MFCs such as operating conditions (temperature, pH), the material of the electrode, and the proton exchange membrane. The rate of power production was high when the anode material used was biofilm-converted graphite.

Table 1. Power output delivered by MFCs using different substrates

Substrate	Anode material used	Cathode material used	Power output	Ref.
Domestic wastewater	Graphite rod	Carbon cloth	0.17 Wm^{-3}	[27]
Brewery wastewater	Carbon brush with titanium core	Activated carbon	0.097 $kWhm^{-2}$	[28]
Distillery wastewater	Graphite sheet	Platinized carbon powder	4.6 Wm^{-3}	[29]
Swine wastewater	Carbon felt	Activated carbon	0.750 W m^{-2}	[30]
Sewage sludge	Graphite with Neutral Red	Graphite coated with a 1mm thick porcelain septum	0.091 W m^{-2}	[31]
Anaerobic sludge	Carbon cloth	Carbon felt	0.468 W m^{-2}	[32]
Anaerobic sludge with glucose	Carbon paper	Carbon paper	0.182 W m^{-2}	[33]
Marine sediment in acetate	Graphite	Carbon paper coated with Pt/C or nitrogen	14 mWm^{-2}	[34]

Table 2. Performance of MFCs based on the same substrate consumed by different cultures of microorganisms

Substrate	Electrode type	Culture used	Power density (mW m^{-2})	Ref.
Glucose	Glazed carbon	*Proteus vulgaris*	4.5	[35]
Glucose	Woven graphite	*Erwina dissolvens*	0.27	[36]
Glucose	Graphite	*Rhodoferax ferrireducens*	8	[37]
	Woven graphite		17	[37]
	Graphite foam		33	[37]
Glucose	Graphite	*Pseudomonas aeruginosa*	88	[9]
Glucose	Graphite	Mixed consortium, batch	3600	[3]
Glucose	Graphite	Mixed consortium, continuous	18	[38]
Glucose	Graphite	*E. coli Geobacter*	760	[39]
Glucose	Carbon paper	*Geobacter*	40.3	[8]
Glucose	Graphite plate	*Saccharomyces cerevisiae*	16	[40]
Glucose	Carbon cloth	*P. aeruginosa*	52.5	[41]

The MFCs also work at a small scale, in which electrodes can be 6-8 μm thick and 2-4 cm long, hence, they can easily replace the batteries. As they provide an energy form that is renewable, batteries need not be recharged.

Wastewater treatment

MFCs can utilize wastewater as fuel and can treat this wastewater by using wastes such as sewage water, municipal solid waste, human wastes, etc., as

these wastes possess a large quantity of organic matter. Owing to the drawbacks of the conventional methods for wastewater treatment, such as high slug production, high treatment and high management cost, the microbial fuel cells provide a great alternative by minimizing the drawbacks of existing conventional methods. The stability of these MFCs is quite good for wastewater treatment. Some microbes used in the MFCs remove the sulfur content from wastewater and give the desired result.

MFCs are used to decrease the chemical oxygen demand (COD) of wastewater before it is liberated into the environment. Table 3 depicts the %COD removal in various types of wastewaters using MFCs. MFCs have proven to reduce the COD of wastewater by 98% [45]. The COD of the wastewaters can be further increased by optimizing the conditions such as maintaining moderate temperature, i.e., neither too hot, nor too cold. Usually, the optimum temperature is around 20-50°C.

Table 3. %COD removal using MFCs in various types of wastewater

Wastewater	%COD removal	Ref.
Domestic wastewater	88	[42]
Urban wastewater	70	[17]
Chemical wastewater	63	[43]
Cyanide wastewater	88	[44]

Hydrogen production

One of the other important roles that the MFC can serve us is in the production of hydrogen. For this to occur, the MFCs are modified to biochemically assisted reactors. In biochemically assisted reactors, the conditions applied are anaerobic in the cathodic chamber, hence the protons get reduced to hydrogen on the cathode and get the desired result. The electrical requirement needed for this reduction is greater than 0.3 volts [46]. Hydrogen can easily be stored in the MFCs, and hence, subsequently be used for electricity production. The type of substrate affects hydrogen production. For example, it has been found out that using 1 mole of glucose as substrate produced 10-12 moles of hydrogen [46].

Biosensors

MFCs can also be used as sensors for pollution analysis. Biosensors have a measuring system with a receptor in it. The MFCs-based biosensors can help us measure the biological oxygen demand (BOD) of the wastewater. The charge developed in typical MFCs is directly proportional to the wastewater strength, hence it can be used for BOD sensing. Biosensors can be operated for a period of five years, without maintenance [45]. Hence, they are stable and reliable.

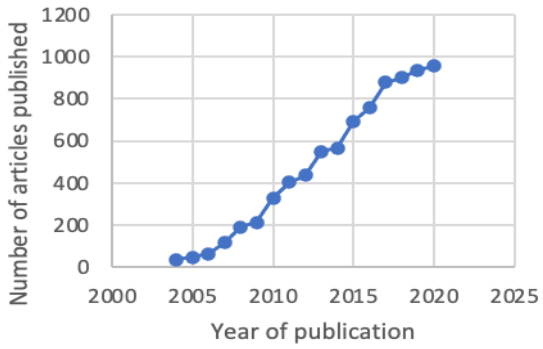

Fig. 5. Increase in the number of publications in MFC research over time.

CONCLUSION

Although the MFC is a low-power producing system when compared to other renewable sources of energy because of its thermodynamic limitations, we can see that MFCs can help a great deal in transitioning from conventional sources of energy to more renewable ones.

There are a number of challenges to be faced and overcome in order to commercialize the use of MFC, two of them being the higher power output and inexpensive electrode and PEM material. There are certainly other problems associated with MFCs like internal resistance, diffusion of the substrate and protons. In order to increase the power output, we need new microbes to be used as catalysts, which could increase the electron transport rate from the biofilm to the anode. It has been reported that if *Geobacter* transports electrons to the anode from the biofilm at the same rate at which it transports electrons to ferric iron, it could increase the current flow in an MFC by 4 orders. It is also possible to increase power output by metal catalysts like platinum but its scale-up would be impossible because of unendurable costs.

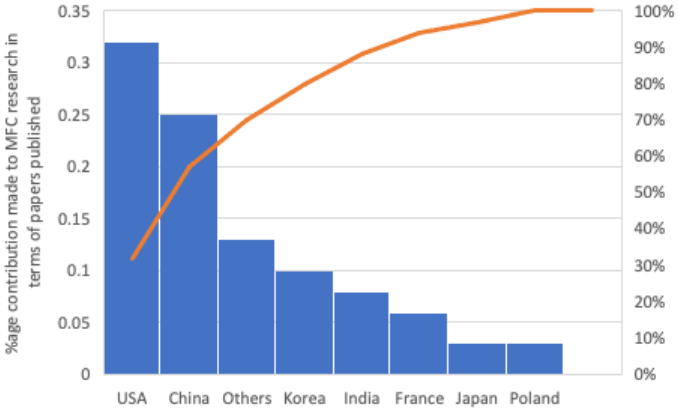

Fig. 6. Country-wise contribution made to MFC research field.

Carbon-based electrode materials can compete with expensive catalysts when it comes to power generation.

Research is being carried out in order to increase MFC performance by treating low-cost materials under different conditions, accompanied by minimum expenditure. Further exploring will widen its applications. We have mentioned the potential applications of MFCs in the previous section. MFCs, when used for wastewater treatment, need a larger surface area for the anode, since the biofilm builds on it. Therefore, we need to use a material for anode that doesn't deteriorate easily. Newer areas of application of MFCs are being developed. One of them is to power implanted medical devices for which blood would provide oxygen and glucose. Certain enzymatic catalysts are known which operate fuel cells, but their use is yet to be made feasible. The use of human white blood cells as a source of electrons has also been an area of interest lately.

In order to increase the efficiency of the MFCs, a number of various techniques are underway. The doping of catalysts on the electrode, the use of a more suitable oxidant in the cathode, increasing the area of the anode by replacing the use of the anode electrode with a mesh or foam, increasing the distance between the anode and the cathode are some of the efforts being put into increasing the efficiency and subsequently the power output generation of a microbial fuel cell.

This review presented a brief overview of MFC technology in general, its various designs, applications and limitations. To make further progress, we need to be able to understand the microbiology of the current-producing process. Although research has been increasing in this field over the past few years, and various countries from different parts of the world have been contributing to its research, in order to use MFC commercially in the industry and society, further progress in this field is expected in terms of scale-up for large-scale applications.

REFERENCES

1. A. E. Franks, K. P. Nevin, *Energies*, **3** (5), 899 (2010). doi: 10.3390/en3050899.
2. B. E. Logan, Exoelectrogenic bacteria that power microbial fuel cells, 2009, doi: 10.1038/nrmicro2113.
3. K. Rabaey W. Verstraete, *Trends Biotechnol.*, **23,** 291 (2005). doi: 10.1016/j.tibtech.2005.04.008.
4. Z. Du, H. Li, T. Gu, *Biotechnol. Adv.*, **25** (5) 464 (2007). doi: 10.1016/j.biotechadv. 2007.05.004.
5. The fifty best inventions of 2009 (5). http://content.time.com/time/specials/packages/article/0,28804,1934027_1934003_1933965,00.html (accessed Dec. 29, 2021).
6. G.-C. Gil , I.S. Chang, B.-H. Kim, M. Kim, J.-K. Jang, H.S. Park, H.-J. Kim, Operational parameters affecting the performance of a mediator-less microbial fuel cell. [Online]. Available: www.elsevier.com/locate/bios
7. G. Delaney, H. P. Bennetto, J. R. Mason, S. D. Roller, J. L. Stirling, C. F. Thurston, Electron-transfer Coupling in Microbial Fuel Cells. 2. Performance of Fuel Cells Containing Selected Microorganism-Mediator-Substrate Combinations, 1984.
8. S. Jung J. M. Regan, *Appl. Microbiol. Biotechnol.*, **77** (2), 393 (2007), doi: 10.1007/s00253-007-1162-y.
9. B. E. Logan, B. Hamelers, R. Rozendal, U. Schroder, J. Keller, S. Freguia, P. Aelterman, W. Verstraete, K. Rabaey, *Environ. Sci. Technol.*, **40** (17), 5181 (2006). doi: 10.1021/es0605016.

10. A. A. Yaqoob, M.N.M. Ibrahim, K. Umar, S. Bhawani, *Polymers*, **13** (1), 1 (2021), doi: 10.3390/polym13010135.
11. K. Rabaey, P. Clauwaert, P. Aelterman, W. Verstraete, *Environ. Sci. Technol.*, **39** (20), 8077 (2005), doi: 10.1021/es050986i.
12. U. Schröder, J. Nießen, F. Scholz, *Angew. Chemie – Int. Edn.*, **42**, 2880 (2003), doi: 10.1002/anie.200350918.
13. I. Gajda, J. Greenman, I. A. Ieropoulos, *Current Opinion Electrochem.*, **11**. 78 (2018), doi: 10.1016/j.coelec.2018.,9.006.
14. G. Pankratova L. Gorton, *Current Opinion Electrochem.*, **5**, 193 (2017). doi: 10.1016/j.coelec.2017.09.013.
15. O. Schaetzle, F. Barrière, K. Baronian, *Energy Environ. Sci*., **1**, 607 (2008). doi: 10.1039/b810642h.,
16. B. Min, S. Cheng, B. E. Logan, *Water Res.*, **39**, 1675 (2005), doi: 10.1016/j.watres.2005. 02.002.
17. B. E. Logan, C. Murano, K. Scott, N. D. Gray, I. M. Head, *Water Research*, **39** (5), 942 (2005), doi: 10.1016/j.watres.2004.11.019.
18. J. K. Jang, T.H. Pham, I.S. Chang, K.H. Kang, H. Moon, K.S. Cho, B.H. Kim, *Proc. Biochem.*, **39**, 1007 (2004), doi: 10.1016/S0032-9592(03)00203-6.
19. S. P. Jung, S. Pandit, in: Biomass, Biofuels, Biochemicals: Microbial Electrochemical Technology: Sustainable Platform for Fuels, Chemicals and Remediation, Elsevier, 2018, p. 377. doi: 10.1016/B978-0-444-64052-9.00015-7.
20. Y. J. Shen, O. Lefebvre, Z. Tan, H. Y. Ng, *Water Sci. Technol.* **65**, 1223 (2012), doi: 10.2166/wst.2012.957.
21. P. Aelterman, K. Rabaey, H. T. Pham, N. Boon, W. Verstraete, *Environ. Sci. Technol.*, **40** (10), 3388 (2006), doi: 10.1021/es0525511.
22. P. Liang, R. Duan, Y. Jiang, X. Zhang, Y. Qiu, X. Huang, *Water Research*, **141**, 1 (2018), doi: 10.1016/j.watres.2018.04.066.
23. L. Zhuang, Y. Yuan, Y. Wang, S. Zhou, *Bioresource Technol.*, **123**, 406 (2012), doi: 10.1016/j.biortech.2012.07.038.
24. P. Pushkar, A. K. Mungray, *Desalination and Water Treatment*, **57**, 6747 (2016), doi: 10.1080/19443994.2015.1013994.
25. J. Gajendiran, C. Jayashree, G. Janshi, I. T. Yeom, S. Adish Kumar, J. Rajesh Banu, 2014, [Online]. Available: www.electrochemsci.org.
26. G. Bhargavi, V. Venu, S. Renganathan, in *IOP Conference Series: Materials Science and Engineering*, **330** (1) (2018), doi: 10.1088/1757-899X/330/1/012034.
27. E. Martin, O. Savadogo, S. R. Guiot, B. Tartakovsky, *J. Appl. Electrochem.*, **43** (5), 533 (2013), doi: 10.1007/s10800-013-0537-2.
28. S. Choi, J. R. Kim, J. Cha, Y. Kim, G. C. Premier, C. Kim, *Bioresource Technol.*, **128**, 14 (2013), doi: 10.1016/j.biortech.2012.10.013.
29. A. K. Manohar, O. Bretschger, K. H. Nealson, F. Mansfeld, *Bioelectrochem.*, **72** (2), 149 (2008), doi: 10.1016/j.bioelechem.2008.01.004.
30. K. Y. Kim, W. Yang, P. J. Evans, B. E. Logan, *Bioresource Technol.*, **221**, 96 (2016), doi: 10.1016/j.biortech.2016.09.031.
31. A. J. Slate, K. A. Whitehead, D. A. C. Brownson, C. E. Banks, *Renew. Sustain. Energy Reviews*, **101**. 60 (2019). doi: 10.1016/j.rser.2018.09.044.
32. J. Hou, Z. Liu, P. Zhang, *J. Power Sources*, **224**, 139 (2013), doi: 10.1016/j.jpowsour.2012.09.091.
33. W. Guo, Y. Cui, H. Song, J. Sun, *Bioprocess Biosys. Eng.*, **37**, 1749 (2014), doi: 10.1007/s00449-014-1148-y.
34. D. R. Bond, D. E. Holmes, L. M. Tender, D. R. Lovley, *Science*, **295** (5554), 483 (2002), doi: 10.1126/science.1066771.
35. K. Rabaey, G. Lissens, S. D. Siciliano, W. Verstraete, A microbial fuel cell capable of converting glucose to electricity at high rate and efficiency, (2003), doi: 10.1023/A: 1025484009637
36. C. A. Vega, I. Fernandez, 951- Mediating Effect of Ferric Chelate Compounds in Microbial Fuel Cells with *Lactobacillus Plantar* L&I, *Streptococcus Lactis*, and *Erwinia Dissolvens*, Elsevier Sequoia S.A, 1987.
37. S. K. Dhuri, D. R. Lovley, *Nature Biotechnol.*, **21** (10), 1229 (2003), doi: 10.1038/nbt867.
38. K. Rabaey, W. Ossieur, M. Verhaege, W. Verstraete, *Water Sci. Technol.*, **52 (**1–2), 515 (2005), doi: 10.2166/wst.2005.0561.
39. T. Zhang, Y. Zeng, S. Chen, X. Ai, H. Yang, *Electrochem. Commun.*, **9** (3), 349 (2007), doi: 10.1016/j.elecom.2006.09.025.
40. G. D. Najafpour, M. Rahimnejad, N. Mokhtarian, W. Ramli, W. Daud, A. A. Ghoreyshi, *World Appl.Sci. J.*, **6**, 1585 (2009).
41. J. Liu, Y. Qiao, C. X. Guo, S. Lim, H. Song, C. M. Li, *Bioresource Technol.*, **114**, 275 (2012), doi: 10.1016/j.biortech.2012.02.116.
42. S. Cheng, H. Liu, B. E. Logan, *Electrochem. Commun.*, **8**, 489 (2006), doi: 10.1016/j.elecom.2006.01.010.
43. M. Zhou, H. Wang, D. J. Hassett, T. Gu, *J. Chem. Technol. Biotechnol.*, **88** (4), 508 (2013), doi: 10.1002/jctb.4004.
44. B. Min B. E. Logan, *Environ. Sci. Technol.*, **38** (21), 5809 (2004), doi: 10.1021/es0491026.
45. R. Kumar, L. Singh, A. W. Zularisam, in: Waste Biomass Management - A Holistic Approach, Springer International Publishing, 2017, p. 367. doi: 10.1007/978-3-319-49595-8_16.
46. B. E. Logan, J. M. Regan, Microbial fuel cells - Challenges and applications. *Environ. Sci. Technol.*, **40** (17), 5172 (2006), doi: 10.1021/es0627592.

Bulgarian Chemical Communications, Volume 54, Special Issue C (pp.78-83) 2022 DOI: 10.34049/bcc.54.C.0078

Wastewater treatment by emerging wastewater treatment technologies: A systematic review

Rukshar, N. Bhatnagar*

Department of Chemistry, Manipal University Jaipur, Jaipur-Ajmer Expressway, Jaipur, Rajasthan, 303007, India

Accepted: July 06, 2022

Environmental chemists, engineers, and water authorities face a significant difficulty in the treatment of industrial effluent. Non-biodegradable materials are commonly utilized in various industries such as textile dyeing and printing processes. Many pollutants and toxins are introduced into water bodies by agriculture and industry. This not only has an impact on water quality, but it also puts various aquatic species in jeopardy. Although considerable progress has been made in the treatment and management of such wastewater using chemical or biological processes, there is a developing shift in the approach, with the focus turning to resource recovery and sustainable wastewater management. By wastewater treatment process, solids in polluted water are partially extracted and converted by decomposition method into simple molecules or minerals. Primary and secondary treatment processes remove the bulk of BOD and total suspended solids found in polluted water. However, this treatment method is increasingly becoming unsuitable to safeguard receiving waterways or offer useable water for commercial and domestic recycling. Advanced treatment procedures rank quite high in terms of giving a true answer for destroying stuff that is resistant to traditional treatment. In this article, we have made a conscientious attempt to review advanced remediation techniques.

Keywords: Environment; Oxidation; Pollutants; Wastewater

INTRODUCTION

Waste effluents have always been recognized as a source of health and environmental hazards. Sometimes complicated compositions of waste fluids necessitate complex treatment techniques with correspondingly high prices, which are impracticable given the vast amounts of waste generated by both home and industrial use [1]. Therefore, it is required to develop low-cost and simple decontamination techniques for the treatment of waste water. Today various technologies like nanomembrane, advance oxidation process, nanopowder and biodegradation are used for isolation and elimination of biochemical substances which include various metals (e.g. Cd, Pb, Cu, Hg, Zn, Ni), nutrients (e.g. PO^{3-}, NH, NO^{-}, NO^{-}), CN^{-}, organic compounds, microorganisms (e.g. cyano-bacteria) viruses, antibiotics, bacteria and parasites [2]. The contamination of fresh water sources occurred by expanding population, urbanization, global climate warming, industrialization, and deficiency of efficient management practices of water resources [3]. Cholera, malaria, and diarrhea are caused by a lack of safe drinking water and sanitation in cities [4]. The first municipal water treatment plant was developed in Scotland in the 1800s, and since then, the method has been established for the treatment of municipal and other sewage all over the world [5]. The accumulation of dyes, insecticides, personal care products, phenols, and other organic pollutants in water has turned out to be a main cause of water pollution [6-9]. These pollutants have a negative impact on aquatic life, as well as human health. Conventional wastewater treatment systems have a hard time removing these organic contaminants [10]. Their decomposition is primarily accomplished through acidic putrefaction, heating of wastewater, or biological treatment techniques. The method is based on the biological breakdown of organic materials and contaminants, which is driven by bacterial consortia, in addition to any previous physical and mechanical treatment operations [11]. In recent years, there has been a surge in interest in using various emerging technologies for the treatment of wastewater.

ADVANCED WASTE WATER TREATMENT PROCESSES

Ceramic membrane filtration method:

Ceramic membranes have recently attracted a lot of attention due to their outstanding properties, such as a long operating cycle, easy cleaning, restoration, chemical dependability, and pollution-free treatment of wastewater [12]. Membrane technology is already being used for a range of purposes, and it is becoming more cost-effective as a result of advances in membrane research. Membranes are classified into four categories on the basis of pore size: microfiltration, ultrafiltration, nano-filtration, and reverse osmosis [13-15]. The other three membranes

To whom all correspondence should be sent:
E-mail: nitu.bhatnagar@jaipur.manipal.edu

with the exception of RO, are used in industrial wastewater treatment applications.

Ceramic membrane technology is increasingly being used in the treatment of industrial discarded water [16]. Ceramic membrane treatment is appealing due to inherent characteristics such as thermochemical stability, low fouling tendency, and durability, and the ceramic membrane technology market is expected to develop at a compound yearly with a growth rate of 12%. Advanced processes of oxidation, like *in-situ* ozonation, could be incorporated with ceramic membrane, which is not possible with polymeric membranes due to potential breakdown over long-term exposure [17]. Due to higher fluctuation, higher toxin removal, reduced fouling rate, and advanced spring-cleaning efficiency, hybrid-ceramic membrane systems like the ceramic membrane bioreactor outperform polymeric alternatives. Polymer-based membranes currently take over the polluted water treatment sector, and were actively explored for municipal and polluted water treatment since the 1990s. Diverse elements of polymer-based membranes have been studied, reported on, and reviewed, including fabrication methods, full-scale applications, fouling, and prevention [18].

Oxidation

Oxidation is one of the most effective treatment methods. This process produces hydroxyl free radical (OH), a highly reactive and unselective oxidant which has the capacity of abolishing even highly resistant pollutants [19]. Ozone (O_3), H_2O_2, TiO_2, heterogeneous catalyst-based photolysis, radiation, or strong electron ray radiation greatly speed up the generation of hydroxyl free radical [20].

Hydrogen peroxide/UV, hydrogen peroxide/Fe^{++}, H_2O_2/UV/Fe^{++}, O_3/UV are some of the oxidants which are used in this process [21-23]. A titanium peroxide semiconductor traps UV light and creates hydroxyl radicals in the TiO_2/UV light method [24]. Organic compounds can be degraded oxidatively by reacting with valence bond holes, hydroxyl and peroxide radicals, or reductively by reacting with electrons [25]. The ability to operate at divergent temperatures, the need of mass transfer limits when NPs are used for the treatment of polluted water as photo catalysts, and the use of solar irradiation are all advantages of this method [26]. Furthermore, TiO_2 is a low-cost, readily available substance with highly oxidizing photo generated pores. TiO_2 can oxidize a broad range of organic pollutants to produce nontoxic components like CO_2 and H_2O [27]. Injection of hydrogen peroxide and subsequent mixing occur in a reactor equipped with ultra-violet light in the hydrogen peroxide/UV light process (200 to 280 nm) [28]. Ultraviolet light is utilized to break the O-O link in H_2O_2 and form the hydroxyl free radical during this process. Phenolic compounds, malachite green and reactive blue 19 have all been decolorized and degraded by using the UV/H_2O_2 technique. The Fenton process produces $OH^{\cdot}$ by combining ferrous iron (Fe (II)) and H_2O_2 under acidic conditions [29, 30]. The Fenton process has several advantages, including minimal operating costs and the ability to easily magnetically separate residual iron. In this method, a large number of OH free radicals with a powerful oxidizing potential (2.8 V) are formed, which have a short life but are very reactive and target dyes and other pollutants by either extracting a H atom or attaching themselves to multiple bonds. Enhanced ferrous sulfate concentration improves dye removal capacity [31].

Bioremediation

Bioremediation is the most convenient way for emerging organic micro pollutants in wastewater to be removed, and it's a promising way to totally remove these compounds during the treatment of wastewater [32]. Organic contaminants such as aromatic hydrocarbon compounds, phenols, nitro-aromatics compounds, and azo dyes are abundant in salty wastewater generated by the agro-food, petrochemical, textile, and leather manufacturing sectors. Because of the capacity to breakdown hazardous compounds efficiently under high salt conditions, microorganisms such as algae, bacteria are gaining popularity in industrial waste treatment. In co-metabolism techniques, degrading microorganisms use one molecule as a carbon source and another as an energy source, and may be used to biodegrade emerging organic pollutants [33-35].

Nowadays, dye treatment focuses on microorganisms that may break and absorb dyes in wastewater. A variety of microorganisms, including yeast, actinomycetes, fungi, bacteria and algae, have been identified which have dye decolorizing abilities [37]. Microorganism-based detection and removal of heavy metals has a number of distinct benefits, comprising ease of application, low cost, high capacity of adsorption, and widespread availability [38]. Plant-based treatment makes use of a plant's natural biological functions to benefit humans. Water plants are important in biological treatment of wastewater because they may be utilized for phytoremediation technologies such as rhizo-filtration method, phyto-extraction method, phyto-stabilization method, phyto-degradation method, and phyto-transformation method [39].

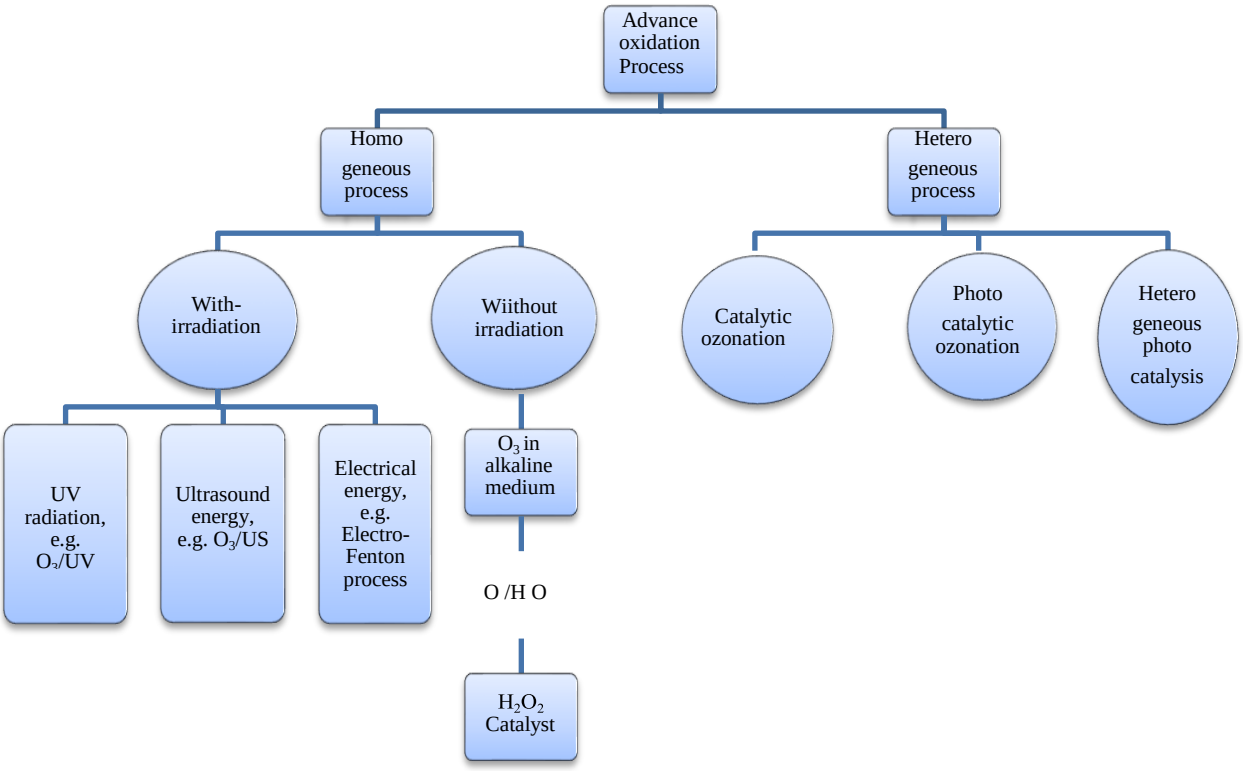

Fig. 1. Classification of advance oxidation processes.

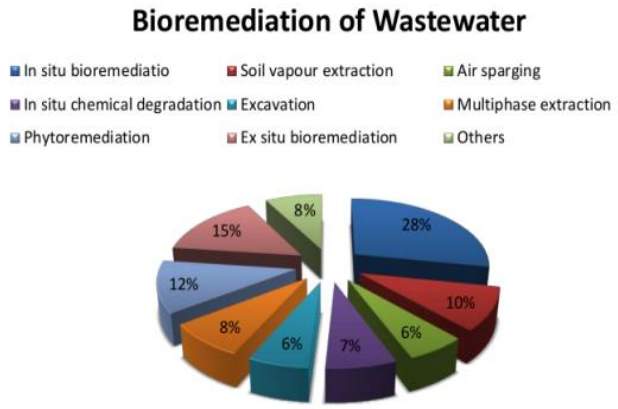

Fig. 2. Various bioremediation methods for the treatment of waste water [36].

Nano particle based treatment

In the twenty-first century, the world's most pressing concern is managing water demand, which is a result of global progress and weather variability. This necessitates current understanding and ways to maintain the safety of clean water and its supply for drinking [40]. The application of fresh and unique nanotechnology opens up possibilities for ensuring the purification of water. The basic demand of industries is to provide cost-effective and steady resources to deliver drinking water at a reasonable level [41]. Because the expanding demand is linked to severe varied health recommendations and pollutants, polluted water treatment techniques are ineffective in giving enough clean water [42]. The extremely resourceful way includes the use of developed nano sized particles as active adsorbents for the removal of contamination from wastewater. Fe-MNPs which are very stable and have high efficiency for the removal of organic pollutants are synthesized by a unique oxidative precipitation-pooled iono-thermal synthesis method and degrade the organic pollutants with H_2O_2 [54].

Table 1. Various NPs and their pollutant removal application.

NPs	Nature of contaminants removed	Ref.
Ag NPs on the surface of PDA-functionalized Al- MOF/Fe_3O_4 nanocatalyst	Organic pollutants such as ciprofloxacin (CIP), norfloxacin (NOR) methyl orange (MO)	[43]
Pd NPs@UN nanocatalyst	4-Nitrophenol (4-NP), hexavalent chromium [Cr(VI)], rhodamine B (RhB), congo red (CR), potassium- hexacyanoferrate(III) ($K_3[Fe(CN)_6]$)	[44]
Nano-ZnO	Phenol	[45]
Metal−organic framework-engineered FeS_2/C nanocatalyst	Fluoxetine	[46]
Iron(II) molybdate nanocatalyst coated anode	sugarcane wastewater industry	[47]
Ag-NP	Rhodamine B and Methylene blue, heavy metal removal	[48,49]
γ-Fe_2O_3-NPs	Textile dyes and heavy metals	[50]
TiO_2 NPs	Photocatalytic treatment of tannery wastewater (COD removal, 82.26%; Cr removal, 76.48%)	[51]
	Photo catalytic degradation of organic dyes (malachite green (MG), 94.15%, and eriochrome black T (EBT), 76.13%)	[52]
Potassium zinc hexacyanoferrate nanocubes	Reduction of hexavalent Cr	[53]
Fe NPs		

Pathogenic magnetic NPs have demonstrated greater nontoxic manufacturing potential and higher pollutant removal performance [55, 56]. However, regeneration and reusability are required in nano-technological applications, particularly for nanoparticles, and have a direct impact on treatment costs and sustainable development [57]. Water filtration technique for the removal or reduction of pollutants, such as suspended particles, microorganisms, and other harmful biological and chemical contaminants in water, in order to produce safe and clean water for drinking, pharmaceutical, and biomedical purposes [58, 59]. The nano-filtration (NF) membrane is the most significant innovation in membrane-based technology. Nano-filtration membranes feature a molecular mass cut-off for nonpolar objects in the nano-metric scales [60, 61].

Adsorption

Adsorption is a rapid, economical, and ubiquitous technique of water filtration and recycling among numerous technologies. The rapid increase of research interests in this subject has been fueled by the introduction of low-cost adsorbents [62]. Adsorption experimental techniques are quickly evolving for the discovery and evaluation of cost-effective adsorbents for water purification and recycling. Carbon-based adsorbents have attracted a lot of interest in the field of wastewater treatment chemistry because of the advantages they provide, such as thermal properties, extracting behavior, adsorptive nature, and specificity [63]. Carbon nanotubes (CNTs), graphene, chitosan biopolymer and bio-char are all examples of adsorbents. Chemisorption, electrolysis, solvent evaporation, nano membrane filtration process, adsorption process, and reverse osmosis are some of the most well studied and widely utilized wastewater treatment methods [64]. Adsorption process is the most important of these techniques because of its qualities such as high efficiency, cost effectiveness, ease of handling, and abundance of adsorbents [65]. New findings have emphasized on the utilization of

chitosan biopolymer as a bio-sorbent for heavy metal ion removal, with adsorption being found to be a reliable approach [66]. Electrolysis, micro-precipitation, chelation, and electrostatic attraction are some of the interactions that lead to the creation of bonds between chitosan biopolymer and metal ion during bio-sorption [67].

CONCLUSION

One of the most serious environmental issues is the poisoning of water bodies with chemical toxins. Pollution in water bodies causes a great deal of devastation. As a result, wastewater must be treated before being discarded into the water bodies. A significant increase in the literature on polluted water and advanced treatment processes from 2000 to 2021 has been observed, indicating an emerging research interest in this field. From 2005 onwards, the rise in the number of publications has been particularly notable. The primary goal of treating wastewater is to enable urban and industrial effluents to be disposed of without endangering human health or causing unacceptable environmental harm. Raw municipal wastewater, on the other hand, usually requires some treatment before it can be used for various purposes. Any level of treatment can be achieved using advanced treatment process. In some treatment systems, further processing is required to remove pollutants from contaminated water. Advanced techniques and equipment are used in advanced wastewater treatment plants. They are highly costly to operate, and both operational costs and water quality are affected by the efficiency of operation. To preserve the water bodies that collect effluents, wastewater management operations must be carefully managed. Operators at treatment plants are trained and qualified to monitor and measure the discharged sewage, the treatment process, and the finally discarded effluent. The true objective of treating wastewater should be to manage waste in water in an efficient, cost-effective, and environmentally friendly manner. The main future challenges in using AOPs in treating wastewater may include the development of efficient and low-cost materials to enhance adequate treatment, the use of alternative energy sources, the implementation of process integration methods trying to target various pollutants, and the monetization of laboratory-developed processes.

Acknowledgements: *Presented at the International Conference on "Cutting Edge Research in Materials and Sustainable Chemical Technologies" from January 27 to 29, 2022, organized by Department of Chemical Engineering & Department of Chemistry at Manipal University Jaipur, Jaipur, India (Organizing Chairman: Dr. Anand G. Chakinala & Dr. Rahul Srivastava).*

REFERENCES

1. G. Crini, E. Lichtfouse, *Environmental Chemistry Letters*, **17** (1), 145 (2019).
2. M. Salgot, M. Folch, *Current Opinion in Environmental Science & Health*, **2**, 64 (2018).
3. M. Salgot, G. Oron, G. L. Cirelli, N. R. Dalezios, A. Díaz, A. N. Angelakis, CRC Press, Boca Raton FL, USA, 2016.
4. A. S. Laura, G. A. W. L. I. K. Bernd, Minimum quality requirements for water reuse in agricultural irrigation and aquifer recharge-Towards a water reuse regulatory instrument at EU level, Réédition, (2017).
5. S. Wacławek, H. V. Lutze, K. Grübel, V. V. T. Padil, M. Černík, D. D. Dionysiou, *Chemical Engineering Journal*, **330**, 44 (2017).
6. I. A. Saleh, N. Zouari, & M. A. Al-Ghouti, *Environmental Technology & Innovation*, **19**, 101026 (2020).
7. S. Karimifard, M. R. A. Moghaddam, *Science of the Total Environment*, **640**, 772 (2018).
8. M. M. Emamjomeh, M. Mousazadeh, N. Mokhtari, H. A. Jamali, M. Makkiabadi, Z. Naghdali,... R. Ghanbari, *Separation Science and Technology*, **55**(17), 3184 (2020).
9. R. Qadri, M. A. Faiq, Freshwater pollution: effects on aquatic life and human health, in: Fresh water pollution dynamics and remediation, Springer, Singapore. 2020, p. 15.
10. C. P. Ahada, S. Suthar, *Environmental Science and Pollution Research*, **25**(25), 25336 (2018).
11. S.S. Kumar, S. Shantkriti, T. Muruganandham, E. Murugesh, N. Rane, S. P. Govindwar, *Ecological Informatics*, **31,** 112 (2016).
12. A. Alengebawy, K. Jin, Y. Ran, J. Peng, X. Zhang, P. Ai, *Chemosphere*, **267**, 129197 (2021).
13. T. R. Al-Husseini, A. H. Ghawi, A. H. Ali, *Journal of Water Process Engineering*, **30**, 100590 (2020).
14. M. R. Bilad, N. I. M. Nawi, D. D. Subramaniam, N. Shamsuddin, A. L. Khan, J. Jaafar, A. B. D. Nandiyanto, *Journal of Water Process Engineering*, **36**, 101264 (2020).
15. X. Chen, X. Chen, Y. Zhao, H. Zhou, X. Xiong, C. Wu, *Science of the Total Environment*, **719**, 137276. (2020).
16. B. I. Harman, H. Koseoglu, N. O. Yigit, E. Sayilgan, M. Beyhan, M. Kitis, *Water Sci. Technol.*, **62**, 547 (2010).
17. N. U. Barambu, M. R. Bilad, M. A. Bustam, K. A. Kurnia, M. H. D. Othman, N. A. H. M. Nordin, *Ain Shams Eng. J*. (2020).
18. W. Zhang, X. Liu, D. Wang, Y. Jin, *Biores. Technol.*, **243**, 1020 (2017).
19. S. O. Ganiyu, C. A. Martínez-Huitle, M. A. Oturan, *Current Opinion in Electrochemistry*, **27**, 100678. (2021).
20. D. Y. An, J. Y. Park, *Desalin. Water Treat.*, **57**,

26595 2016.
21. K. Barbari, R. Delimi, Z. Benredjem, S. Saaidia, A. Djemel, T. Chouchane, N. Oturan, M. A. Oturan, *Chemosphere*, **203**, 1 2018.
22. B. Bethi, S. H. Sonawane, B. A. Bhanvase, S. P. Gumfekar, *Chem. Eng. Process. Process Intensif.* **109**, 178 *2016)
23. E. B. Cavalcanti, S. Garcia-Segura, F. Centellas, E. Brillas, *Water Res*., (2013).
24. M. R. Espino-Estévez, C. Fernández-Rodríguez, O. M. González-Díaz, J. Arana, J. P. Espinós, J. A. Ortega- Méndez, J. M. Dona-Rodríguez, *Chem. Eng. J.*, (2016).
25. F. A. Gagol, M. Makos, P. Khan, J. A. Boczkaj, *Sep. Purif. Technol*. **224**, 1 (2019).
26. W. De Schepper, J. Dries, L. Geuens, J. Robbens, R. Blust, *Water Res.*, **43**, 4037 (2009).
27. O. Gimeno, J.nF. García-Araya, F. J. Beltrán, F. J. Rivas, A. Espejo, *Chem. Eng. J.* **290**, 12 (2016).
28. S. D. Jojoa-Sierra, J. Silva-Agredo, E. Herrera-Calderon, R. A. Torres-Palma, *Sci. Total Environ*., **575**, 1228 (2017).
29. G. M. Gyeong, J. Y. Park, *Desalin. Water Treat*. **54**, 1029 (2015).
30. M. Kermani, F. Mohammadi, B. Kakavandi, A. Esrafili, Z. Rostamifasih, *J. Phys. Chem. Solids*, (2018).
31. P. Thanekar, S. Garg, P. R. Gogate, *Ind. Eng. Chem. Res.*, **59**, 4058 (2020).
32. E. A. Cezare-Gomes, L. del Carmen Mejia-da-Silva, L. S. Perez-Mora, M. C. Matsudo, L. S. Ferreira-Camargo, A. K. Singh, J. C. M. de Carvalho, *Appl. Biochem. Biotechnol*. **188 (3)**, 602. (2019).
33. D. P. Singh, J. S. Khattar, A. Rajput, R. Chaudhary, R. Singh. *PloS one* ,**14** (9), e0221930. (2019).
34. D. Cheng, H. Ngo, W. Guo, S. Chang, D. Nguyen, S. Kumar, *Bioresour. Technol*. **275**, 109 (2019).
35. G. P. Arone Soul Raj, S. Elumalai, T. Sangeetha, D. Roop Singh, *J. Bioremed. Biodeg.* **6(**294), 2 (2015).
36. J. Pandey, A. Chauhan, R. K. Jain, *FEMS Microbiology Reviews*, **33 (2)** , 324 (2009).
37. S. A. Khan, G. K. Sharma, F. A. Malla, A. Kumar, N. Gupta, *J. Clean. Prod*. **211**, 1412 (2019).
38. M. Aray-Andrade, C. Moreira, V. Santander, L. Mendoza, R. Bermúdez, in: European Biomass Conference and Exhibition Proceedings, Lisbon, Portugal, 2019, p. 241.
39. M. M. Mirzaee, M. Zakeri Nia, M. Farasati, *Cleaner Engineering and Technology*, **4**, 100210 (2021).
40. A. B. Abou Hammad, A. M. El Nahwary, B. A. Hemdan, A. L. K. Abia, *Environmental Science and Pollution Research*, **27**(21), 26668 (2020).
41. F. Almomani, R. Bhosale, M. Khraisheh, T. Almomani, *Applied Surface Science***, 506,** 144924 (2020).
42. M. Govarthanan, C. H. Jeon, Y. H. Jeon, J. H. Kwon, H. Bae, W. Kim, *International Journal of Biological Macromolecules***, 162,** 1241 (2020).
43. Y. Wang, L. He, Y. Li, L. Jing, J. Wang, X. Li, *Journal of Alloys and Compounds*, **828**, 154340. (2020).
44. M. Sajjadi, N. Y. Baran, T. Baran, M. Nasrollahzadeh, M. Reza Tahsili, M. Shokouhimehr, *Separation and Purification Technology*, 116383 (2019).
45. Y. Tao, Z. L. Cheng, K. E. Ting, X. J. Yin, *Journal of Catalysts*, **(1–6)** *(*2013).
46. Z. Ye, J. A. Padilla, E. Xuriguera, J. L. L. Beltran, F. Alcaide, E. Brillas, I. Sirés, *Environmental Science & Technology*, (2020).
47. S. Naina Mohamed, N. Thomas, J. Tamilmani, T. Boobalan, M. Matheswaran, P. Kalaichelvi, A. Pugazhendhi, *Fuel*, **277**, 118119 (2020).
48. X. Meng, C. Duan, Y. Zhang, W. Lu, W. Wang, Y. Ni, *Composites Science and Technology*, 108384. (2020).
49. K. O. Shittu, O. Ihebunna, *Adv. Nat. Sci. Nanosci. Nanotechnol*.. **8,** 1 (2017).
50. A. Fouda, S. E.-D. Hassan, E. Saied, M. S. Azab, *Journal of Environmental Chemical Engineering*, **9(1)**, 104693 (2021).
51. S. P. Goutam, G. Saxena, V. Singh, A. K. Yadav, R. N. Bharagava, K. B. Thapa, *Chem. Eng. J.*, **336,** 386 (2018).
52. V. Jassal, U. Shanker, B. S. Kaitha, S. Shankarb, *RSC Adv.*, **5(33).** 26141 (2015).
53. C. Mystrioti, T. D. Xanthopoulou, N. Papassiopi, A. Xenidis, *Sci. Total. Environ.*, **539,** 105 (2016).
54. M. Malakootian, M. R. Heidari, *Zeitschrift für Physikalische Chemie*, **235(6)**, 683 (2020).
55. A. H. Sadek, M. S. Asker, S. A. Abdelhamid, *Biologia*, **76(9)**, *2785* (2021).
56. J. You, L. Wang, Y. Zhao, W. Bao, *Journal of Cleaner Production*, **281**, 124668 (2021).
57. P. Punia, M. K. Bharti, S. Chalia, R. Dhar, B. Ravelo, P. Thakur, A. Thakur, *Ceramics International*, (2020).
58. M. Anjum, R. Miandad, M. Waqas, F. Gehany, M. A. Barakat, *Arab. J. Chem*., **12**, 4897 (2019)
59. S. Sharma, A. Bhattacharya, Drinking water contamination and treatment techniques, *Appl. Water Sci.*, **7,** 1043 (2017).
60. A. Boretti, L. Rosa, *Npj Clean Water*, **2,** 1 (2019).
61. D.K. Tiwari, J. Behari, P. Sen, *World Appl. Sci. J.*, **3,** 417 (2008).
62. A. E. Burakov, E. V. Galunin, I. V. Burakova, A. E. Kucherova, S. Agarwal, A. G. Tkachev, V. K. Gupta, *Ecotoxicol. Environ. Saf*., **148**, 702e712 (2018).
63. S. Y. Cheng, P. L. Show, B. F. Lau, J. S. Chang, T. C. Ling, *Trends Biotechnol*., **37**, 1255e1268 (2019).
64. W. S. Chai, J. Y. Cheun, P. S. Kumar, M. Mubashir, Z. Majeed, F. Banat, P. L. Show, *Journal of Cleaner Production*, **296**, 126589 (2021).
65. C. A. Guerrero-Fajardo, L. Giraldo, J. C. Moreno-Pirajan, *Nanomaterials*, **10** (2020).
66. M. Ahmad, M. Yousaf, A. Nasir, I.A. Bhatti, A. Mahmood, X. Fang, X. Jian, K. Kalantar-Zadeh, N. Mahmood, *Environ. Sci. Technol.*, **53,** 2161 (2019).
67. R. Chakraborty, R. Verma, A. Asthana, S. S. Vidya, A. K. Singh, *Int. J. Environ. Anal. Chem.*, **1,** 1, (2019).

Bulgarian Chemical Communications, Volume 54, Special Issue C (pp. 84-94) 2022 DOI: 10.34049/bcc.54.C.084

Physicochemical analysis on molecular interactions in 2-methoxyaniline with aliphatic alcohols (propan-1-ol, 2-propen-1-ol, 2-propyn-1-ol) at various temperatures and 0.1 MPa

Ch. R. Kiran[1], Sk. Fakruddin[2]*, Ch. V. Lakshmi[1], M. Gowrisankar[3], G. S. Sastry[4]

[1]*Department of Chemistry, Acharya Nagarjuna University, Guntur (A.P), India*
[*2]*Department of Physics, V.R. Siddhartha Engineering College, Vijayawada (A.P), India*
[3]*Department of Chemistry, J.K.C. College, Guntur (A.P), India*
[4]*Department of Chemistry, Andhra Loyola College, Vijayawada (A.P), India*

Received: October 27, 2021; Revised: July 06, 2022

The density (ρ), viscosity (η), and sound speed (u) are presented for binary combinations of 2-methoxyaniline with aliphatic primary alcohols (propan-1-ol, 2-propen-1-ol, 2-propyn-1-ol) at temperatures ranging from 303.15 K to 313.15 K at a pressure of 0.1 MPa. Some other parameters (V^E, κ_s^E) and viscosity deviation were calculated from the density, sound speed and viscosity with experiment temperature values. The difference among these properties with the mixture composition proposes hydrogen bond and charge-transfer compound formation between 2-methoxyaniline and primary alcohols. A theory named Prigogine Flory Patterson theory was utilized for the analysis of results V^E. All mixtures generate negative values for free volume effect.

Keywords: 2-Methoxyaniline, Density, Sound speeds, PFP theory, Primary alcohol.

INTRODUCTION

In industry point of view binary liquid mixtures play a key role as they generate huge varieties of mixtures with desired functionalities which can be utilized as a solvent in various chemical industries and biological process. Additionally, viscosity is utilized in hydraulic calculation, fluid transportation, energy and mass within industry [1]. Density, viscosity and sound speed values of binary liquid mixture help in understanding thermo physical properties. These values are a successfull source helpful in assumption of inter molecular interaction and characterization of structure alignment among liquid molecule components and also for enhancement of molecular models [2, 3].

In this research work, the molecular interactions are understood about the liquid components 2-methoxyaniline and primary alcohols (propan-1-ol, 2-propen-1-ol, 2-propyn-1-ol). Various fields of chemistry widely make use of these solvents as they are conventional organic liquids widely applied and used in chemical industries. The current examination is a continuation of previous studies conducted on binary liquid mixtures and their thermodynamic properties [4]. The current analysis is made for discovering the consequences of multiple bonds between carbon- carbon atoms in aliphatic primary alcohol molecules that can show impact on both magnitude and sign of different functionalities of thermodynamic when they are combined with 2-methoxyaniline. Data are not accessible representing enumerated material properties such as density, viscosity and sound speed for the binary mixture of 2-methoxyaniline with primary alcohols. Therefore, a study is conducted on the binary mixtures. In this study, densities (ρ), viscosities (η), sound speed (u) of pure 2-methoxyaniline, primary alcohols and the binary mixtures at temperatures ranging from T = 303.15 K to 313.15 K were determined. From the observations of experiment, the surplus values of these experimental data, the values of isentropic flexibility variations in viscosity and surplus Gibbs free energy in actuation of viscous flow are calculated in view of hydrogen bond formation and complex charge transfers.

EXPERIMENTAL

Materials

The sources required for experiment including resultant purity and analysis procedure are presented in Table 1. Table 2 presents density, viscosity and sound speed values. The available data in the literature [5-19] are compatible with the tabular values.

* To whom all correspondence should be sent:
E-mail: sfdnspnl@gmail.com

Table 1. Source details of chemicals, CAS number, water content and purity.

Name of the chemical	CAS Number	Source	**Water content (%)	Mass fraction purity
2-methoxyaniline	90-04-0	Sigma Aldrich, India	0.045	0.995
Propan-1-ol	71-23-8	S.D. Fine chemicals	0.042	0.995
2-propen-1-ol	107-18-6	Sigma Aldrich, India	0.042	0.995
2-propyn-1-ol	107-19-7	Sigma Aldrich, India	0.042	0.997

** Karl Fischer method.

Table 2. Density, viscosity and sound speed data of pure elements at various temperatures and pressures.

Component	Density (ρ /g·cm^{-3})		Sound speed (u / m·s^{-1})		C_P (J· K^{-1} · mol^{-1})	Viscosity (η / mPa·s)	
(in K)	Exp.	Lit.	Exp.	Lit.	Lit.	Exp.	Lit.
2-methoxy aniline							
303.15	1.09157	1.0917[5]	1597.4		190.52[6]	4.923	4.924[5]
308.15	1.08799		1583.2		192.05[6]	4.571	
313.15	1.08432		1569.9		193.62[6]	4.217	-
2-propen-1-ol							
303.15	0.84460	0.8446[8]	1307		141.5[6]	1.122	1.122[9]
308.15	0.84041	0.8404[8]	1287		143.2[6]	1.019	1.016[9]
313.15	0.83591	0.8359[8]	1266		145.6[6]	0.921	0.921[9]
2-propyn-1-ol							
303.15	0.94201	0.9420[8]	1404		146.5[6]	1.345	1.3447[9]
308.15	0.93701	0.9370[8]	1384		148.1[6]	1.221	1.2143[9]
313.15	0.93270	0.9327[8]	1364		151.1[6]	1.104	1.103[9]
1-propanol							
303.15	0.79577[7]	0.7958[8]	1194.8[4]	1189.26[19]	147.36[6]	1.735[4]	1.735[9]
		0.79597[19]		1192[17]			1.7309[14]
		0.7961[15]		1189[11]			1.705[16]
		0.79540[16]		1189[12]			1.720[10]
		0.79559[17]					
		0.7953[14]					
		0.7956[10]					
		0.7955[11]					
308.15	0.79181	0.7918[8]	1174.6	1172.37[19]	150.62[6]	1.547	1.548[9]
		0.79189[19]		1175.2[18]			1.546[15]
		0.7911[15]		1171.41[13]			1.526[16]
		0.79130[16]					1.5440[14]
		0.7912[14]					
313.15	0.78771	0.7877[08]	1155.3	1155.53[19]	153.20[6]	1.385	1.386[9]
		0.78777[19]		1158[17]			1.372[16]
		0.78720[17]					1.390[10]
		0.7873[10]					1.376[15]
		0.7871[14]					1.380[14]
		0.78710[16]					

The standard unpredictability is u(x_1) = 1×10^{-4}, u (ρ) ±2×10^{-5}g.cm^{-3}, u (u) = ±0.4%., u (η) = ±0.08mPa·s, u (T) = 0.01 K for density, sound speed and viscosity, and u (P) = 1 kPa.

Apparatus and procedure

Electric balance is used to weigh the amount of pure liquids which is used in preparation of binary liquid mixtures (ER-120A, Afoset, India) with an accuracy of ± 0.1 mg by syringing each element in to an air-tight container to avoid loss occurred due to evaporation. The molar fraction uncertainty is ± 1×10^{-4}. The particulars of procedure and

measurement techniques have been described elsewhere [20]. The unpredictability of liquid mixtures density value is $\pm 2\times10^{-5}$g.cm^{-3}. The sound speed unpredictability is ±0.4%. The viscosity unpredictability value is ±0.08 mPa.s. The stable temperature is maintained in the range of ±0.01 K. Circular pump is to circulate thermostatic water bath within the cell.

RESULTS

The following equations are useful to calculate surplus parameters and deviating functions are as follows:

$$V^E = V - (x_1 V_1 + x_2 V_2) \quad (1)$$

$$\Delta\eta = \eta - (x_1\eta_1 + x_1\eta_1) \quad (2)$$

$$\Delta G^{*E} = RT\,[\ln\eta V - (x_1 \ln\eta_1 V_1 + x_2 \ln\eta_2 V_2 \quad (3)$$

where η, η_1, η_2, *and* V, V_1, V_2 are viscosity and molecular values of mixture and pure components correspondingly.

From the relation [21] the isentropic flexibilities are calculated:

$$\kappa_s = (u^2\rho)^{-1} \quad (4)$$

In a mixture ρ is used to present density and u is used to present sound speed. Later, surplus isentropic flexibilities (k_s^E) are assessed with the help of relations below as suggested by Benson and Kiyohara [22]:

$$k_s^E = k_s - k_s^{id} \quad (5)$$

$$k_s^{id} = \sum_{i=1}^{2}\varphi_i\left[\kappa_{s,i} + \frac{TV_i\left(\alpha_i^2\right)}{C_{p,i}}\right] - \left\{\frac{T\left(\sum_{i=1}^{2}x_iV_i\right)\left(\sum_{i=1}^{2}\varphi_i\alpha_i\right)^2}{\sum_{i=1}^{2}x_iC_{p,i}}\right\} \quad (6)$$

where φ_i, $C_{p,i}$, V_i, $\kappa_{s,i}$ and α_i are volume fractions, heat capacity of molar, volume of molars, isentropic flexibility and isobaric thermal expansion coefficient of pure elements correspondingly.

The density, viscosity and sound speed for binary mixture of different molar fractions of 2-methoxyaniline are represented in Table.3 including surplus or deviation in parameters such as (V^E, κ_s^E, $\Delta\eta$ and ΔG^{*E}) at different temperatures. The values of V^E, κ_s^E $\Delta\eta$ and ΔG^{*E} are represented as a function in the form of molar fraction of 2-methoxyaniline in Figures 1, 2, 3 and 4, respectively.

Surplus / deviation in parameters such as V^E, κ_s^E, $\Delta\eta$ and ΔG^{*E} depends on different factors as follows:

(a) Degree of unsaturation in hydrocarbon chains of alcohols;

(b) Hybridization of carbon;

(c) Boiling point of aliphatic primary alcohols.

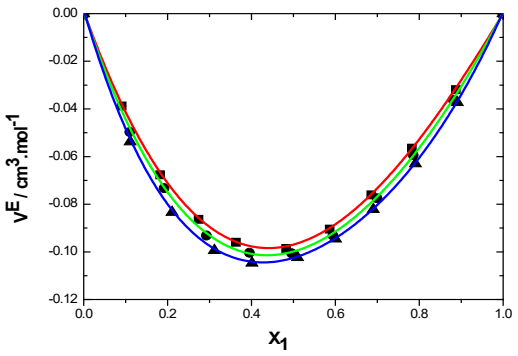

Fig 1. Surplus molar volume (V^E) curves with molar fraction for the binary mixtures of 2-methoxyaniline with 2-propyn-1-ol (**!**); 2-propen-1-ol (,) and propan-1-ol (▲) at 303.15 K

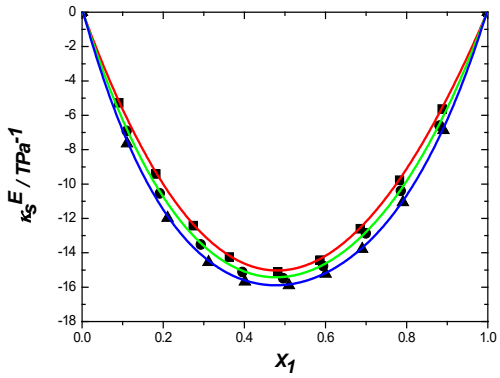

Fig. 2. Surplus isentropic flexibility curves with mole fraction for the binary mixtures of 2-methoxyaniline with 2-propyn-1-ol (**!**); 2-propen-1-ol (,) and propan-1-ol (▲) at 303.15 K

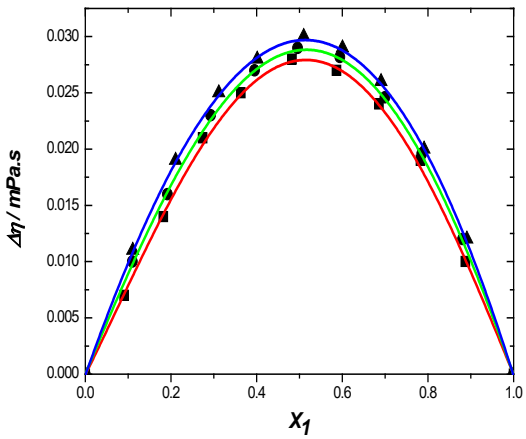

Fig. 3. Deviation in viscosity (Δη) curves with mole fraction for the binary mixtures of 2-methoxyaniline with 2-propyn-1-ol (**!**); 2-propen-1-ol (,) and propanol-1 (▲) at 303.15 K

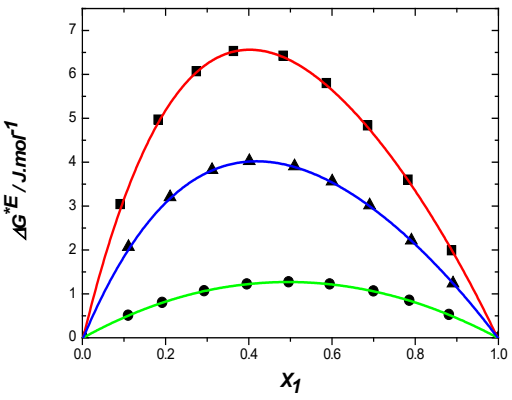

Fig. 4. Surplus Gibbs energy curves for actuation of viscous flow (ΔG^{*E}) with mole fraction for the binary mixtures of 2-methoxyaniline with 2-propyn-1-ol **(!);** 2-prpen-1-ol (,) and propan-1-ol (▲) at 303.15 K.

Negative deviations in V^E and κ_s^E and positive deviation in 8η and $8G^{*E}$ are recorded. The observations are from the entire system with complete range of composition at each temperature value of the experiment.

Negative deviations arise due to:

(a) Attractive forces between unlike polar molecules

(b) Dipole-dipole forces between unlike molecules.

(c) Hydrogen bonding interaction among opposite molecules.

From Table 3, the negative V^E and κ_s^E values suggest that attractive forces among unlike molecules are more powerful than the repulsive forces when compared with like molecules of binary liquid mixtures.

In the investigation, due to compression of free volume negative values arise which convert the ideal mixture to a more compressible one which in turn leads to negative values that are represented as V^E and κ_s^E in binary liquid mixtures. The identical pattern is followed by Jayalakshmi and Reddy [23] for the surplus amounts of ketone and nitrobenzene mixture Yang *et al*. [24], Kiyohara and Benson [22] explained the reasons for occurrence of such deviation.

V^E and κ_s^E values of 2-methoxyaniline with three primary alcohols decrease in the order:

propan-1-ol >2-propen-1-ol >2-propyn-1-ol

This order suggests that attractive forces decrease from propan-1-ol to 2-propyn-1-ol with 2-methoxyaniline as increases number of pi bonds between carbon-carbon atoms in primary alcohols. This may be because of the fact that the increase in temperature ultimately leads to increase in thermal energy which disrupts the self-associated primary alcohols molecules releasing more and more primary alcohols molecules for the formation of hetero-association molecules with 2-methoxyaniline molecules. Syal *et al.* [25] explain about dimethylsulfoxide/acetone in a binary mixture which is identical and supported by ultrasonic studies. Palani *et al.* [26] also explain ultrasonic studies dealing with monohydric alcohols and dimethylsulfoxide system.

Table. 3 represents the attributes to the association of 2-methoxyaniline and primary alcohols which gives out the positive value for viscosity deviation due to intermolecular hydrogen bonds among –OH groups within primary alcohols and the 2-methoxyaniline.

Table 3. Surplus molar volume (V^E), density (ρ), sound speed (u), viscosity (η), surplus isentropic flexibility (κ_s^E), viscosity deviation ($\Delta\eta$) and surplus Gibbs energy for operation of viscous flow (G^{*E}) as a function of mole fraction, x_1 of 2-methoxyaniline of binary liquid mixture at T= (303.15 to 313.15) K and 0.1MPa pressure.

x_1	Density (ρ) g·cm^{-3}	V^E cm^3·mol^{-1}	u m.s^{-1}	κ_s^E /TPa^{-1}	Viscosity (η / mPa·s)	$\Delta\eta$ / mPa·s	ΔG^{*E} / J·mol^{-1}
2-Methoxyaniline (1)+ 2-propyn-1-ol (2)							
303.15 K							
0.0000	0.94201	0.0000	1404.0	0.000	1.345	0.000	0.000
0.0908	0.96640	-0.0388	1431.9	-5.280	1.677	0.007	3.046
0.1822	0.98739	-0.0677	1458.9	-9.418	2.011	0.014	4.970
0.2742	1.00560	-0.0864	1484.6	-12.42	2.347	0.021	6.073
0.3631	1.02094	-0.0960	1507.4	-14.25	2.669	0.025	6.530
0.4825	1.03873	-0.0986	1534.6	-15.11	3.099	0.028	6.426
0.5865	1.05208	-0.0905	1554.7	-14.43	3.471	0.027	5.802

0.6856	1.06328	-0.0761	1570.4	-12.61	3.822	0.024	4.837
0.7825	1.07304	-0.0565	1582.4	-9.783	4.163	0.019	3.602
0.8873	1.08250	-0.0319	1591.6	-5.634	4.530	0.010	1.992
1.0000	1.09157	0.0000	1597.4	0.000	4.923	0.000	0.000
308.15 K							
0.0000	0.93701	0.0000	1384.0	0.000	1.221	0.000	0.000
0.0908	0.96164	-0.0425	1412.7	-5.855	1.533	0.008	3.216
0.1822	0.98279	-0.0714	1440.2	-10.12	1.847	0.016	5.232
0.2742	1.00114	-0.0892	1466.0	-13.02	2.161	0.022	6.373
0.3631	1.01664	-0.1002	1489.0	-14.69	2.463	0.026	6.838
0.4825	1.03460	-0.1023	1516.7	-15.43	2.866	0.029	6.715
0.5865	1.04807	-0.0933	1537.5	-14.80	3.214	0.028	6.058
0.6856	1.05940	-0.0789	1554.3	-13.13	3.543	0.025	5.045
0.7825	1.06928	-0.0602	1567.5	-10.46	3.862	0.020	3.756
0.8873	1.07885	-0.0351	1577.6	-6.267	4.205	0.011	2.079
1.0000	1.08799	0.0000	1583.2	0.000	4.571	0.000	0.000
313.15 K							
0.0000	0.93270	0.0000	1364.0	0.000	1.104	0.000	0.000
0.0908	0.95745	-0.0462	1393.6	-6.430	1.395	0.009	3.387
0.1822	0.97867	-0.0751	1421.6	-10.82	1.688	0.017	5.495
0.2742	0.99708	-0.0919	1447.8	-13.61	1.980	0.023	6.671
0.3631	1.01266	-0.1043	1471.0	-15.13	2.261	0.027	7.142
0.4825	1.03069	-0.1060	1499.3	-15.74	2.635	0.029	7.002
0.5865	1.04422	-0.0960	1521.0	-15.16	2.959	0.029	6.311
0.6856	1.05560	-0.0816	1538.9	-13.65	3.264	0.026	5.252
0.7825	1.06554	-0.0639	1553.3	-11.13	3.561	0.021	3.909
0.8873	1.07515	-0.0384	1564.4	-6.901	3.879	0.013	2.167
1.0000	1.08432	0.0000	1569.9	0.000	4.217	0.000	0.000
2-Methoxyaniline (1) + 2-propen-1-ol (2)							
303.15 K							
0.0000	0.84460	0.0000	1307.0	0.000	7.146	0.000	0.000
0.1099	0.88680	-0.0497	1338.0	-6.918	6.912	0.010	0.512
0.1918	0.91468	-0.0733	1362.5	-10.55	6.736	0.016	0.804
0.2927	0.94555	-0.0932	1393.7	-13.52	6.518	0.023	1.069
0.3952	0.97351	-0.1004	1426.0	-15.12	6.294	0.027	1.226
0.4957	0.99815	-0.1006	1457.8	-15.48	6.073	0.029	1.276
0.5942	1.01998	-0.0932	1488.6	-14.77	5.853	0.028	1.226
0.6995	1.04113	-0.0775	1520.5	-12.87	5.616	0.025	1.066
0.7856	1.05695	-0.0594	1545.2	-10.40	5.419	0.020	0.853
0.8808	1.07311	-0.0362	1570.4	-6.604	5.200	0.012	0.531

1.0000	1.09157	0.0000	1597.4	0.000	4.923	0.000	0.000
308.15K							
0.0000	0.84041	0.0000	1287.0	0.000	6.012	0.000	0.000
0.1099	0.88270	-0.0539	1318.4	-7.500	5.864	0.011	0.457
0.1918	0.91062	-0.0774	1343.1	-11.20	5.753	0.017	0.716
0.2927	0.94153	-0.0960	1374.4	-14.04	5.614	0.024	0.945
0.3952	0.96956	-0.1036	1407.1	-15.63	5.471	0.028	1.076
0.4957	0.99426	-0.1038	1439.4	-15.99	5.328	0.030	1.114
0.5942	1.01616	-0.0964	1470.8	-15.27	5.185	0.029	1.063
0.6995	1.03739	-0.0812	1503.6	-13.38	5.030	0.026	0.918
0.7856	1.05329	-0.0649	1529.3	-10.99	4.901	0.021	0.730
0.8808	1.06949	-0.0399	1555.8	-7.259	4.756	0.013	0.452
1.0000	1.08799	0.0000	1583.2	0.000	4.571	0.000	0.000
313.15K							
0.0000	0.83591	0.0000	1266.0	0.000	4.774	0.000	0.000
0.1099	0.87831	-0.0580	1298.0	-8.082	4.724	0.012	0.407
0.1918	0.90629	-0.0815	1322.9	-11.85	4.686	0.019	0.635
0.2927	0.93727	-0.0987	1354.3	-14.55	4.636	0.025	0.831
0.3952	0.96539	-0.1069	1387.5	-16.14	4.583	0.029	0.939
0.4957	0.99018	-0.1070	1420.5	-16.49	4.529	0.031	0.965
0.5942	1.01217	-0.0997	1452.8	-15.78	4.473	0.030	0.914
0.6995	1.03350	-0.0848	1486.7	-13.89	4.411	0.027	0.784
0.7856	1.04949	-0.0705	1513.7	-11.57	4.358	0.022	0.620
0.8808	1.06575	-0.0435	1541.8	-7.914	4.297	0.014	0.383
1.0000	1.08432	0.0000	1569.9	0.000	4.217	0.000	0.000
2-Methoxyaniline (1) + propan-1-ol (2)							
303.15K							
0.0000	0.79577	0.0000	1194.8	0.000	1.735	0.000	0.000
0.1109	0.84280	-0.0538	1224.9	-7.648	2.100	0.011	2.072
0.2108	0.88102	-0.0834	1255.9	-11.98	2.426	0.019	3.205
0.3116	0.91615	-0.0994	1290.5	-14.55	2.753	0.025	3.824
0.4015	0.94493	-0.1047	1324.0	-15.68	3.043	0.028	4.028
0.5099	0.97682	-0.1024	1367.8	-15.90	3.391	0.030	3.909
0.6004	1.00137	-0.0946	1407.0	-15.23	3.678	0.029	3.560
0.6906	1.02416	-0.0822	1448.3	-13.78	3.963	0.026	3.018
0.7908	1.04770	-0.0630	1496.2	-11.07	4.276	0.020	2.217
0.8908	1.06951	-0.0373	1545.1	-6.874	4.587	0.012	1.240
1.0000	1.09157	0.0000	1597.4	0.000	4.923	0.000	0.000
308.15K							
0.0000	0.79181	0.0000	1174.6	0.000	1.547	0.000	0.000

0.1109	0.83887	-0.0579	1204.9	-8.227	1.895	0.012	2.292
0.2108	0.87710	-0.0871	1235.9	-12.70	2.205	0.020	3.519
0.3116	0.91225	-0.1029	1270.6	-15.23	2.515	0.026	4.176
0.4015	0.94105	-0.1077	1304.3	-16.29	2.790	0.029	4.383
0.5099	0.97301	-0.1069	1348.4	-16.46	3.120	0.031	4.244
0.6004	0.99761	-0.0991	1388.2	-15.81	3.393	0.030	3.855
0.6906	1.02044	-0.0870	1430.3	-14.40	3.663	0.027	3.262
0.7908	1.04403	-0.0672	1479.4	-11.72	3.960	0.022	2.396
0.8908	1.06590	-0.0413	1529.6	-7.397	4.254	0.013	1.341
1.0000	1.08799	0.0000	1583.2	0.000	4.571	0.000	0.000
313.15K							
0.0000	0.78771	0.0000	1155.3	0.000	1.385	0.000	0.000
0.1109	0.83481	-0.0620	1185.7	-8.805	1.712	0.013	2.479
0.2108	0.87304	-0.0909	1216.8	-13.41	2.003	0.021	3.788
0.3116	0.90822	-0.1064	1251.5	-15.91	2.294	0.027	4.484
0.4015	0.93705	-0.1107	1285.3	-16.90	2.552	0.030	4.688
0.5099	0.96908	-0.1113	1329.8	-17.02	2.861	0.032	4.530
0.6004	0.99373	-0.1036	1370.1	-16.39	3.116	0.031	4.108
0.6906	1.01662	-0.0917	1413.1	-15.03	3.369	0.028	3.472
0.7908	1.04027	-0.0714	1463.4	-12.37	3.648	0.023	2.552
0.8908	1.06219	-0.0452	1515.0	-7.920	3.922	0.014	1.428
1.0000	1.08432	0.0000	1569.9	0.000	4.217	0.000	0.000

Table 4. Redlich – Kister equation coefficients and standard deviation (σ) values for liquid mixtures of 2-methoxyaniline with 2-propyn-1-ol, 2-propen-1-ol and propan-1-ol at T= (303.15 - 313.15) K

T/K	A_0	A_1	A_2	σ
2-Methoxyaniline + 2-propyn-1-ol				
V^E/ cm^3·mol^{-1}				
303.15	-0.389	0.097	-0.004	0.001
308.15	-0.400	0.104	-0.044	0.001
313.15	-0.410	0.104	-0.086	0.002
κ_s^E/ TPa^{-1}				
303.15	-60.35	4.80	0.485	0.001
308.15	-61.60	4.83	-8.014	0.001
313.15	-62.85	4.85	-16.53	0.002
$\Delta\eta$/ mPa· s				
303.15	0.113	0.009	-0.031	0.001
308.15	0.117	0.007	-0.018	0.001
313.15	0.118	0.011	0.003	0.001
2-Methoxyaniline + 2-propen-1-ol				
V^E/ cm^3·mol^{-1}				
303.15	-0.401	0.102	-0.039	0.001
308.15	-0.412	0.101	-0.086	0.001
313.15	-0.423	0.099	-0.132	0.002
κ_s^E/ TPa^{-1}				
303.15	-61.87	4.919	-8.229	0.003
308.15	-63.52	4.832	-15.30	0.075

313.15	-65.15	4.745	-22.37	0.153
$\Delta\eta$/ mPa· s				
303.15	0.117	0.009	-0.015	0.001
308.15	0.119	0.013	0.003	0.001
313.15	0.123	0.008	0.009	0.001
2-Methoxyaniline + propan-1-ol				
V^E/ $cm^3 \cdot mol^{-1}$				
303.15	-0.412	0.104	-0.087	0.001
308.15	-0.426	0.102	-0.129	0.001
313.15	-0.439	0.101	-0.169	0.001
κ_s^E/ TPa^{-1}				
303.15	-63.70	4.473	-17.13	0.002
308.15	-65.95	4.827	-22.68	0.002
313.15	-68.21	5.144	-28.21	0.003
$\Delta\eta$/ mPa· s				
303.15	0.119	0.007	-0.033	0.001
308.15	0.123	0.009	0.008	0.001
313.15	0.127	0.009	0.018	0.001

Table 5. The values of $\overline{V}^{\circ}_{m,1}$, $V^{*}_{m,1}$, $\overline{V}^{\circ E}_{m,1}$, $\overline{V}^{\circ}_{m,2}$, $V^{*}_{m,2}$ and $\overline{V}^{\circ E}_{m,2}$ of elements for 2-methoxyaniline with 2-propyn-1-ol, 2-propen-1-ol and propan-1-ol of binary mixtures at T= (303.15 - 313.15) K

T/K	$\overline{V}^{\circ}_{m,1}$	$V^{*}_{m,1}$	$\cdot\overline{V}^{\circ E}_{m,1}$	$\overline{V}^{\circ}_{m,2}$	$V^{*}_{m,2}$	$\overline{V}^{\circ E}_{m,2}$
($cm^3 \cdot mol^{-1}$)						
2-Methoxyaniline (1) + 2-propyn-1-ol (2)						
303.15	112.52	112.82	-0.296	59.02	59.51	-0.490
308.15	112.85	113.19	-0.340	59.28	59.83	-0.548
313.15	113.18	113.57	-0.392	59.51	60.11	-0.600
2-Methoxyaniline (1) + 2-propen-1-ol (2)						
303.15	112.48	112.82	-0.338	68.22	68.77	-0.542
308.15	112.79	113.19	-0.397	68.51	69.11	-0.599
313.15	113.12	113.57	-0.456	68.83	69.48	-0.654
2-Methoxyaniline (1) + propan-1-ol (2)						
303.15	112.42	112.82	-0.395	74.92	75.52	-0.603
308.15	112.74	113.19	-0.453	75.24	75.90	-0.657
313.15	113.07	113.57	-0.507	75.58	76.29	-0.709

Table 6. The values of $\overline{K}^{\circ}_{s,m,1}$, $K^{*}_{s,m,1}$, $\overline{K}^{\circ E}_{s,m,1}$, $\overline{K}^{\circ}_{s,m,2}$, $K^{*}_{s,m,2}$ and $\overline{K}^{\circ E}_{s,m,2}$ of elements for 2-methoxyaniline with propan-1-ol, 2-propen-1-ol and 2-propyn-1-ol of binary mixtures at T= (303.15 - 313.15) K

T/K	$\overline{K}^{\circ}_{s,m,1}$	$K^{*}_{s,m,1}$	$\overline{K}^{\circ E}_{s,m,1}$	$\cdot\overline{K}^{\circ}_{s,m,2}$	$K^{*}_{s,m,2}$	$\overline{K}^{\circ E}_{s,m,2}$
TPa^{-1}						
2-Methoxyaniline (1) + 2-propyn-1-ol (2)						
303.15	-59.32	4.050	-63.38	-37.83	3.205	-41.04
308.15	-69.26	4.151	-73.42	-45.20	3.333	-48.54
313.15	-79.36	4.250	-83.61	-52.63	3.464	-56.09
2-Methoxyaniline (1) +2-propen-1-ol(2)						
303.15	-69.75	4.050	-73.80	-51.47	4.766	-56.23
308.15	-79.26	4.151	-83.41	-58.86	4.965	-63.83
313.15	-88.90	4.250	-93.15	-66.38	5.186	-71.57
2-Methoxyaniline (1) + propan-1-ol (2)						
303.15	-82.02	4.050	-86.07	-64.70	6.648	-71.35
308.15	-90.31	4.151	-94.46	-72.11	6.947	-79.06
313.15	-98.86	4.250	-103.1	-79.64	7.256	-86.89

Positive deviation in viscosity of 2-methoxyaniline with primary alcohols is in the following order:

propan-1-ol > 2-propen-1-ol >2-propyn-1-ol

The experimental temperature of all binary mixture results in positive deviation is $8G^{*E}$ in overall composition of mixtures. Such functionality is promoted by the negative value of surplus molar volume and explains that association strength emerging due to the interaction of unlike molecules is higher when compared with the association strength of like molecules.

Surplus/ deviated functions (V^E, $\kappa_s{}^E$ and $\Delta\eta$) data are used in an equation called Redlich Kister polynomial equation [27]:

$$Y^E = x_1 x_2 \sum_{i=0}^{j=n-1} A_i (1-2x_1)^i \quad (7)$$

where Y^E is V^E, $\Delta\eta$ and κ_s^E. By using least squares method the coefficient values of A_i is determined and σ (Y^E) is the standard deviation, calculated by using the formula as given below:

$$\sigma(Y^E) = [\,\Sigma(Y^E_{exp} - Y^E_{cal})^2/(m\text{-}n)]^{1/2} \quad (8)$$

where m represents the total number of experiment points and the number of parameters is represented with n. The standard deviation value (σ) and coefficients A_i are shown in Table 4.

Partial molar properties

Surplus partial molar properties $\overline{V}^{E}_{m,1}$, $\overline{V}^{E}_{m,2}$, $\overline{K}^{E}_{s,m,1}$ and $\overline{K}^{E}_{s,m,2}$ and surplus partial molar property at infinite dilution $\overline{V}^{\circ E}_{m,1}$, $\overline{V}^{\circ E}_{m,2}$ $\overline{K}^{\circ E}_{s,m,1}$ and $\overline{K}^{\circ E}_{s,m,2}$ are determined for two components which is already explained [20].

Experimental temperature range of complete composition represents that $\overline{V}^{\circ E}_{m,1}$ and $\overline{V}^{\circ E}_{m,2}$ are negative values that are presented in Table 5. Negative values of the experimental observations explain that specific interactions predominated over non-specific interaction in binary mixtures [28].

Experimental temperature range of complete composition represents that $\overline{K}^{\circ E}_{s,m,1}$ and $\overline{K}^{\circ E}_{s,m,2}$ values are negative values that are presented in Table 6. Improved hydrogen bonding interaction is attributed to negative values among unlike molecular values [29].

Prigogine Flory Patterson Theory

A conventional theory named Prigogine Flory Patterson theory (PFP) can be used for quantitative prediction of various contributions to V^E. This PFP theory is explained clearly by Patterson and other researchers [30-34] and has been largely utilized for analysis of surplus properties with various types of mixtures which includes polar compounds explained by a number of authors. The three contributions used for estimated expression for V^E are given below as follows:

$$\frac{V^E}{x_1V_1^* + x_2V_2^*} = \frac{(\tilde{V}^{1/3}-1)\tilde{V}^{2/3}\Psi_1\theta_2\chi_{12}}{[\left(\frac{4}{3}\right)\tilde{V}^{\frac{1}{3}}-1]P_1^*}(\text{int.contribution})$$

$$+ \frac{-(\tilde{V}_1-\tilde{V}_2)[(14/9)\tilde{V}^{-1/3}-1]\Psi_1\Psi_2}{[\left(\frac{4}{3}\right)\tilde{V}^{\frac{1}{3}}-1]\tilde{V}}(\text{fv.contribution})$$

$$+ \frac{(\tilde{V}_1-\tilde{V}_2)(P_1^*-P_2^*)\Psi_1\Psi_2}{P_2^*\Psi_1+P_1^*\Psi_2}(P^*\text{contribution}) \quad (9)$$

The pure component volume $\tilde{V}_i$ is reduced and calculated from isobaric thermal expression α_i by using the equation:

$$\tilde{V}_i = \left(\frac{1+\left(\frac{4}{3}\right)\alpha_i T}{1+\alpha_i T}\right) \quad (10)$$

The volume $\tilde{V}$ of the mixture is estimated by using an equation (18)

Divided by $\tilde{V} = \Psi_1\tilde{V}_1 + \Psi_2\tilde{V}_2$ (11)

The energy fraction of contact molecular elements Ψ_1 is calculated by:

$$\Psi_1 = 1 - \Psi_2 = \frac{\phi_1 P_1^*}{\phi_1 P_1^* + \phi_2 P_2^*} \quad (12)$$

The typical volume is $V_i^* = V_i^*/\tilde{V}_i$ and the typical pressure is represented by:

$$P_i^* = \frac{T\tilde{V}_i^2\alpha_i}{\kappa_{Ti}} \quad (13)$$

where κ_{Ti} is the isothermal flexibility of pure component 'i'.

The hard core volume components of the elements 1 and 2($\phi_1$andϕ_2) are represented by

$$\phi_1\text{=}1\text{-}\phi_2 = \frac{x_1V_1^*}{x_1V_1^* + x_2V_2^*} \quad (14)$$

The κ_T value is calculated by using the expression below,

$$\kappa_T = \kappa_S + \frac{TV\alpha^2}{C_P} \quad (15)$$

By using Prigogine Flory Patterson theory the χ_{12} parameters needed for V^E expression calculation to the experiment, equimolar value of V^E for a system were examined. The three contributions for calculation of equimolar values having χ_{12} parameters for this system are shown in Table 7 and Fig. 5. The latter gives the graphical representation of comparative experimental values and calculated values of V^E from Prigogine Flory Patterson theory.

Table 7. Interaction parameter of PFP theory, χ_{12} and calculated value of the three contributions from the PFP theory with experiment surplus molar volumes at x_1= 0.5 at 303.15K

Binary mixtures	χ_{12} (10^{7})	Calculated contributions			V^E (x=0.5) $m^3.mol^{-1}$		
		Interactional (10^{-9})	Free volume	P* effect	EXP	PFP	δ / $m^3.mol^{-1}$
2-Methoxyaniline + 2-propyn-1-ol	-2.555	8.024	-0.2428	0.3505	-0.0973	-0.0974	0.0001
2-Methoxyaniline + 2-propen-1-ol	2.032	9.201	-0.0968	-0.1904	-0.1003	-0.1001	-0.0002
2-Methoxyaniline + propan-1-ol	4.261	10.40	-0.1123	-0.4338	-0.1030	-0.1032	0.0002

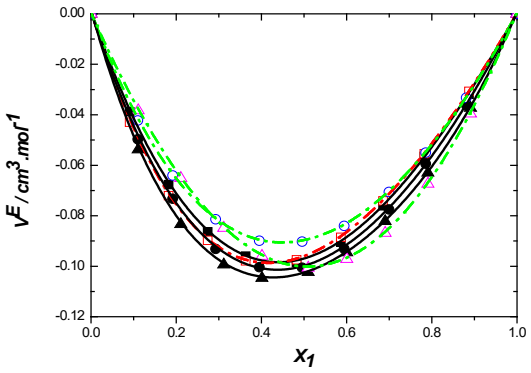

Figure 5. Surplus molar volumes with mole fraction (x_1) of 2-methoxyaniline binary liquid mixtures of 2-methoxyaniline with 2-propyn-1-ol (■); 2-propen-1-ol (●) and propan-1-ol (▲) at 303.15 K and (---) calculated with PFP theory using parameters

CONCLUSIONS

Current research presents experiment results of density, viscosities and sound speeds of 2-methoxyaniline with propan-1-ol, 2-propen-1-ol and 2-propyn-1-ol binary mixture above the entire configuration range of temperature is 303.15 K, 308.15 K and 313.15 K with a five-degree difference among the values. These experiment values are used for computation of surplus molar volume, surplus isentropic flexibility and viscosity deviation involving surplus Gibbs energy actuation of viscous flow at various temperatures 303.15 K, 308.15 K and 313.15 K. The surplus deviation parameters may be attribution to the attractive forces through the hetero-association interaction among the elements of mixtures that leads to associated complex formation through interactions of hydrogen bond. The analysis of result is performed in view of the molecular interaction through the hydrogen bond formed in the binary liquid mixtures by the unlike molecules.

Three contributions were examined to calculate V^E represents that interaction contribution is positive for entire system. All binary system values consisting of free volume contribution values are observed as negative. From Table 7, it is clearly seen that free volume effect is concerned element for magnitude and sign of surplus volumes for every binary mixture.

REFERENCES

Author, please reformat the list of references as shown with the first five numbers. Consult the Instructions for authors at the Journal's site.

1. G. P. Dubey, K. Kumar, *Thermochim. Acta*, **524**, 7 (2011).
2. C. S. Priya, S. Nithya, G Velraj, A. N. Kanappan, *Int. J. Adv. Sci. Technol*., **18**, 59 (2010).
3. G. P. Dubey, P. Kaur, *J. Chem. Thermodynamics*, **64,** 239 (2013).
4. B. Srikanth, M. Gowrisankar, M. Raveendra, D. Ramachandran, *Phys. Chem. Liq*., **59,** 249 (2021), *DOI:* 10.1080/00319104.2019.1706175
5. S. Kumar, P. Jeevanandham, *J. Mol. Liq*., **174,** 34 (2012).
6. Zábranský, M. and Vlastimil Růžička Jr (2004). "Estimation of the Heat Capacities of Organic Liquids as a Function of Temperature Using Group Additivity: An Amendment." J. Phys. Chem. 33: 1071-1081.
7. Gowrisankar, M., Venkateswarlu, P., Sivakumar, K. and S. Sivarambabu (2013). "Density, ultrasonic velocity, viscosity and their excess parameters of the binary mixtures of N,N-dimethylaniline+1-alkanols (C_3-C_5), +2-alkanols (C3-C4),+2-methyl-1-propanol, +2-methyl-2-propanol at 303.15 K. " Korean J. Chem. Eng. 5: 1131-1141.
8. Muhammad A. Saleh , Shamim Akhtar, Meherun Nessa, Muhammad S. Uddin and Mohammad M. H. Bhuiyan (1998). "Excess Molar Volumes of Aqueous Solutions of 1Propanol,2-Propanol, Allyl Alcohol and Propargyl Alcohol." Phys. Chem. Lid. 36: 53-65.
9. Shamim Akhtar, Mohammad M. H. Bhuiyan, Muhammad S. Uddin, Bilkis Sultana. Meherun Nessa and Muhammad A. Saleh (1999). "Viscosity of aqueous solutions of some alcohols." Phys. Chem. Lid. 37: 215- 227.
10. Ming-Jer Lee, Ting-Kuei Lin, Yung-Hsiang Pai, and Kuo-Sheng Lin (1997). "Density and Viscosity for Monoethanolamine + 1-Propanol,+ 1-Hexanol, and + 1-Octanol." J. Chem. Eng. Data 42: 854-857.
11. Rodriguez, A., J. Canosa and J. Tojo (2001). "Density, refractive index, and speed of sound of binary mixtures (diethyl carbonate+ alcohols) at several temperatures." J. Chem. Eng. Data 46: 1506–1515.
12. Benson, G.C., Darcy, P. J. and O. Kiyohara (1980). "Thermodynamics of aqueous mixtures of nonelectrolytes II. Isobaric heat capacities of water-n-alcohol mixtures at 25°C." J. Soln. Chem. 9: 931–938.
13. Venkatesu, P., Chandrashekar, G. and M. V. Prabharakara Rao (2006) "Ultrasonic studies of N,N-dimethylformamide +cyclohexanone + 1-alkanols at 303.15 K." Phys. Chem. Liq. 44: 287–291.
14. Saleh, M.A., Habibullah, M., Shamsuddin Ahmed, M., Ashraf Uddin, Uddin, S. M. H., Afsar Uddin, M. and F. M. Khan (2005). "Viscosity of the systems m-xylene, 1-propanol,2-propanol, 1-butanol, t-butanol." Phy. Chem. Liq. 43: 485–494.
15. Tejraj M. Aminabhavi and Kamalika Banerjee (1998) "Density, Viscosity, Refractive Index and Speed of Sound in Binary Mixtures of 2-Chloroethanol with Alkanols (C1-C6) at 298.15, 303.15, and 308.15 K" J. Chem. Eng. Data 43: 509-513
16. Nikam, P.S., Bapu S. Jagdale, Arun B. Sawant and Mehdi Hasan (2000) "Densities and Viscosities for Binary Mixtures of Benzonitrile with Methanol, Ethanol, Propan-1-ol, Butan-1-ol, Pentan-1-ol, and 2-Methylpropan-2-ol at (303.15, 308.15, and 313.15) K." J. Chem. Eng. Data 45: 214-218.
17. Venkatramana, L., Sreenivasulu, K., Sivakumar, K and K. Dayananda Reddy (2014) "Thermodynamic properties of binary mixtures containing 1-alkanols." J Therm Anal Calorim 115: 1829–1834.
18. N. Anil Kumar (2008) "Ultrasonic and viscometric studies of molecular interactions in binary mixtures of formamide with ethanol, 1-propanol, 1,2-ethanediol and 1,2-propanediol at different temperatures." J. Mol. Liq. 140: 108-116.
19. Sangeeta Singh, Martín Aznar and Nirmala Deenadayalu (2013) "Densities, speeds of sound, and refractive indices for binary mixtures of 1-butyl-3-methylimidazolium methyl sulphate ionic liquid with alcohols at T = (298.15, 303.15, 308.15, and 313.15) K. " J. Chem. Thermodyn. 57: 238–247.
20. P. Venkateswara Rao, P., Gowrisankar, M., Venkatramana, L., Srinivasa Krishna, T and K. Ravindhranath (2016) "Studies on the importance of nature of substituent on the thermodynamic and transport properties of liquid mixtures at various temperatures." J. Chem. Thermodyn. 101: 92-102.
21. Theodor F H RHB. Sonics. sydney: John Wiley; 1955.Benson GC and O. Kiyohara (1979) "Evaluation of excess isentropic compressibilities and isochoric heat capacities." J. Chem. Thermodyn.11: 1061–1064.
22. Jayalakshmi, T and K. Subramanyam Reddy 1985) “Excess volumes of binary liquid mixtures. Methyl Ethyl Ketone + Benzene, + Toluene, +Chlorobenzene, + Bromobenzene, and + Nitrobenzene at 303.15 and313.15 K.” J. Chem. Eng. Data 30: 51–53.
23. Yang, C.S., Lai, H., Liu, Z.G and P. S. Ma (2006) “Density and viscosity of binary mixtures of Diethyl Carbonate with Alcohols at (293.15 to 363.15)K and Predictive Results by UNIFAC-VISCO Group Contribution Method,” J. Chem. Eng. Data 51: 1345-1351.Syal, V. K., Chauhan, S and Uma Kumari (2005) "Ultrasonic velocity of binary mixtures of acetone and dioxane with dimethylsulphoxide as one component." Indian J Pure Appl Phys, 43: 844-848.

24. Palani, R., Saravanan, S and R. Kumar (2009) "Ultrasonic studies on some ternary organic liquid mixtures at 303, 308 and 313K." Rasayan J Chem, 2: 622-629.
25. Redlich, O and A.T. Kister (1948) "Algebraic Representation of Thermodynamic Properties and the Classification of Solutions." J. Ind. Eng. Chem. 40: 345-348.
26. Bindhani, S.K., Roy, G.K., Mohanty, Y.K. and T. R. Kubendran (2015) "Thermo-Physical Properties for the Binary System of Propiophenone–Methyl Acetate at 303.15–313.15 K." Russian J. Physical Chemistry A 89: 1828–1837.
27. Ramana Reddy, K. V., Rambabu, V., Devarajulu, T and A. Krishnaiah (1994) "volumetric behaviour of mixtures of butoxy ethanol with aliphatic alcohols." Phys. Chem. Liq., 28: 161-164.
28. P.J. Flory (1965) "Statistical thermodynamics of liquid mixtures" J. Am. Chem. Soc.,87: 1833-1838.
29. Flory, P.J., Orwoll, R.A and A. Vrij (1964) "Statistical thermodynamics of chain molecule liquids. II. Liquid mixtures of normal paraffin hydrocarbons" J. Am. Chem. Soc, 86: 3515-3520
30. I. Prigogine, the molecular Theory of Solutions. North Holland. Amsterdam. 1957.
31. Van, H.T. and D. Patterson (1982) "Volumes of mixing and the P* effect, Hexane isomers with normal and branched hexadecane." *J. Sol. Chem.* 11:793-805.
32. Patterson, D and G. Delmas (1970) "corresponding states theories and liquid models, Discuss." Faraday Soc., 49: 98-105.

Bulgarian Chemical Communications, Volume 54, Special Issue C (pp. 95-99) 2022 DOI: 10.34049/bcc.54.C.0095

Thermo-acoustic Redlich-Kister coefficients analysis in functional materials by excess parameters at temperatures 303.15K - 318.15K

Sk. Fakruddin Babavali[1*], T. Sarma Nori[2], Ch. Srinivasu[3]

[1]*Department of Physics, V. R. Siddhartha Engineering College, Vijayawada, Krishna Dist (A.P), India*
[2]*Department of Physics, Lakireddy Balireddy College of Engineering, Mylavaram, Krishna Dist (A.P), India*
[3]*Department of Physics, Andhra Loyola College, Vijayawada, Krishna Dist (A.P), India.*

Received: October 27, 2021; Revised: July 06, 2022

Acoustic thermodynamic analysis in the present work is an investigation of excess parameters and respective Redlich Kister coefficients at temperatures of 303.15K to 318.15K in liquid mixtures containing three different functional material groups of combinations such as benzene with toluene, benzene with o-xylene and benzene with mesitylene. The obtained corresponding excess acoustic parameters such as Gibbs free energy excess value (G^{*E}), enthalpy excess value (H^E) and internal pressure excess value (π^E) were computed from experimentally measured data. The results were helpful to obtain Redlich-Kister coefficients from a polynomial equation. Thermo acoustic excess parameters are discussed along with Redlich-Kister coefficients generally for investigating interactions among the molecules of liquid species.

Keywords*:* Redlich Kister coefficients; Benzene; Toluene; Mesitylene; Internal pressure.

INTRODUCTION

Clearly, the study of thermos-acoustic excess parameters is a highly important instrument in understanding interactions between molecules in a liquid mixture [1-9]. Molecular interactions frequently impact the study of shape and size. Research on the speed of sound and the corresponding thermo acoustic properties of liquids and liquid mixtures may help to understand molecular activity and their normal behavior [10-14]. The authors' purpose in this research is to study alterations in functional materials in three liquid compounds with binary combinations of thermo acoustic excess variables, Gibbs free energy (G^{*E}), enthalpy (H^E), and internal pressure (π^E) at four known temperatures ranging from 303.15K to 318.15K in liquid mixtures, namely, benzene with toluene, benzene with o-xylene, and benzene with mesitylene. Benzene may be used in glues, adhesives, cleaning products, paint strippers. xylene is also widely used as a cleaning agent, a thinner for paint, and in varnishes. Mesitylene is used in the laboratory as a specialty solvent. In the electronics industry, mesitylene is used as a developer for photopatternable silicones due to its solvent properties. Toluene is useful in paints, chemical reactants, rubber, adhesives (glues) and as a disinfectant. The irregularities of investigation indicate the presence of molecular interactions between the combination of distinct liquid molecules. Finally, the Redlich-Keister equation is allowed to apply. These findings were discussed in terms of molecular interactions along with the coefficients of thermo-acoustic parameters of their respective liquid mixture [15-17].

EXPERIMENTAL

To measure ultrasonic speeds, the ultrasonic pulse echo interferometer (Mittal Enterprises, India) was utilized; The measurements were made at a frequency of 3 MHz. The temperature was controlled using a thermal bath. For the research of liquid combination densities, a 10 mL specific gravity container was employed. To measure loads of liquid mixes, a computerized Shimadzu AUY220 (Japan) weight balance with an accuracy of $\pm$ 0.1 mg was used. An Ostwald's viscometer was utilized for evaluating the viscosities of liquid mixtures.

THEORY

Internal pressure excess value (π^E), Gibbs free energy excess value (G^{*E}), and excess enthalpy H^E were determined for the following individual combinations:

$$\pi^E = \pi_{exp} - (x_1\pi_1 + x_2\pi_2) \qquad \text{Joule/mole}$$

Internal pressure excess value is represented by π^E in this equation, π_1 and π_2 indicate the internal pressures of each pure liquid, respectively, whereas x_1 and x_2 represent the mole fractions of the first liquid and second liquid, respectively.

$$G^{*E} = G_{exp} - (x_1G_1 + x_2G_2) \qquad \text{Joule/mole}$$

* To whom all correspondence should be sent:
E-mail: drfakruddin786@gmail.com

G^{*E} represents excess Gibbs free energy where G_1, G_2 are the free energies of the molecule of each pure liquid, and x_1 and x_2 are the mole fractions of the first liquid and second liquid, respectively.

$$H^E = H_{exp} - (x_1H_1 + x_2H_2)\ J/mole$$

where H^E stands for excess enthalpy. H_1, H_2 are the enthalpies of each pure liquid and the x_1 and x_2 are mole fractions of the first liquid and second liquid, respectively.

All of the following thermo-acoustic properties are allowed to fit the Redlich-Kister equation [18].

$$Y^E = X_1.X_2\sum_{i=0}^{n} A_i\left(X_1 - X_2\right)^i$$

The Redlich-Kister equation's coefficient is A_i. The least squares approach was used to compute the coefficients. These coefficients are essential for improving excess parameter fit.

In addition, the standard deviation for each excess parameter Y^E was computed.

$$\sigma(Y^E) = \left[\frac{\sum_{i=1}^{n}(Y^E_{expt} - Y^E_{cal})^2}{m-n}\right]^{1/2}$$

The sign of an excess thermo-acoustic parameter was utilized to analyze molecular interactions between the component molecules of liquid mixtures.

RESULTS AND DISCUSSION

The excess parameters π^E, G^{*E}, and H^E computed from the basic measurements and their Redlich-Kister coefficients, in benzene with toluene, benzene with o-xylene and benzene with mesitylene) are presented in Tables 1-3. The variations of these excess parameters with the mole fraction of benzene are presented in Fig, 1(a,b,c) to Fig. 3(a,b,c).

Figure 1 shows the variations in excess internal pressure (π^E) with mole fraction of benzene at four different temperatures. Excess internal pressure variations show a positive trend up to 0.8 mole fraction of benzene and negative trend above 0.8 mole fraction. It's worth noting that only the binary liquid mixture combination benzene and toluene has both positive and negative variations. That means both positive and negative trends for benzene and toluene liquid mixtures, whereas the other two binary liquid mixture combinations only have positive trends. The mixed trend of positive and negative variations in benzene-toluene combinations is caused by dispersive forces and dipole-induced dipole type interactions.

Table 1. Redlich-Kister coefficient values for a binary liquid mixture of benzene and toluene at four known temperatures: 303.15 K, 308.15 K, 313.15 K, and 318.15 K.

Benzene mixed with Toluene				
Co-efficient	**303.15K**	**308.15K**	**313.15K**	**318.15K**
Excess Internal Pressure (π^E)				
A_0	0.1499	0.1090	0.0948	0.1522
A_1	0.1572	0.1141	0.0992	0.1596
A_2	0.1644	0.1193	0.1037	0.1670
A_3	0.1717	0.1245	0.1081	0.1744
A_4	0.1790	0.1296	0.1125	0.1818
Σ	0.1862	0.1348	0.1170	0.1892
Excess free Gibb's Energy (G^{*E})				
A_0	0.1768	0.0911	0.1374	0.1227
A_1	0.1821	0.0938	0.1415	0.1263
A_2	0.1875	0.0964	0.1455	0.1299
A_3	0.1928	0.099	0.1496	0.1336
A_4	0.1981	0.1016	0.1537	0.1372
Σ	0.2035	0.1042	0.1578	0.1408
Excess Enthalpy (H^E)				
A_0	0.1270	0.1230	0.1857	0.0886
A_1	0.1316	0.1275	0.1926	0.0918
A_2	0.1363	0.132	0.1996	0.0949
A_3	0.1409	0.1365	0.2066	0.098
A_4	0.1456	0.141	0.2135	0.1012
Σ	0.1502	0.1455	0.2205	0.1043

Table 2. Redlich-Kister coefficient values for a binary liquid mixture, benzene mixed with o-xylene, at four different temperatures: 303.15 K, 308.15 K, 313.15 K, and 318.15 K.

Benzene mixed o-Xylene				
Co-efficient	**303.15K**	**308.15K**	**313.15K**	**318.15K**
Excess Internal Pressure (π^E)				
A_0	0.3545	0.3075	0.2407	0.1848
A_1	1.0823	0.856	0.8188	0.7831
A_2	0.4998	0.8181	0.9247	1.0891
A_3	0.2877	0.0798	0.0223	0.1165
A_4	0.2463	0.7814	1.0258	1.4343
σ	0.0235	0.024	0.025	0.0256
Excess free Gibb's Energy (G^{*E})				
A_0	0.9334	0.9302	0.9230	0.9193
A_1	0.1299	0.2323	0.2357	0.2750
A_2	-0.0060	0.1750	0.1972	0.3164
A_3	-0.5611	-0.7528	-0.6384	-0.7011
A_4	0.8779	0.4171	0.2708	0.2484
σ	0.0126	0.0126	0.0123	0.0126
Excess Enthalpy (H^E)				
A_0	0.4788	0.4447	0.4008	0.3786
A_1	0.5294	0.6819	0.7	0.7182
A_2	0.2327	0.0914	0.2138	0.313
A_3	0.9441	1.1863	1.1428	0.9815
A_4	1.0675	0.2979	0.0609	0.1381
σ	0.0208	0.021	0.0212	0.0214

Table 3. Redlich-Kister coefficient values for a binary liquid mixture of benzene and mesitylene at four known temperatures: 303.15 K, 308.15 K, 313.15 K, and 318.15 K.

Benzene mixed Mesitylene				
Co-efficient	**303.15K**	**308.15K**	**313.15K**	**318.15K**
Excess Internal Pressure (π^E)				
A_0	1.6357	1.5887	1.5219	1.466
A_1	0.1173	0.6436	0.4608	1.2165
A_2	1.781	2.0993	2.2059	2.3703
A_3	1.7689	1.2198	1.2773	1.3977
A_4	3.5275	1.5182	2.2138	2.8653
σ	1.3047	1.3052	1.3062	1.3068
Excess free Gibb's Energy (G^{*E})				
A_0	2.2146	2.2114	2.2042	4.1314
A_1	1.4111	1.5135	1.5169	3.1482
A_2	2.2173	1.4562	2.1204	1.5976
A_3	0.7201	2.2304	0.6428	0.5801
A_4	3.1679	1.6983	1.552	1.5296
σ	1.2938	1.2938	1.2935	1.2938
Excess Enthalpy (H^E)				
A_0	1.7600	1.7259	1.6820	1.6598
A_1	1.8106	1.9631	1.9812	1.7182
A_2	2.0669	1.3726	1.4950	1.5330
A_3	0.3455	0.1133	0.1568	0.3181
A_4	2.3487	1.5791	5.3421	1.1615
σ	3.3020	4.3022	1.3024	1.3026

Positive excess internal pressure values indicate the presence of a strong type of interactions between component molecules of the liquid mixture, whereas negative values indicate the presence of weak type interactions [19, 20]. Figure 2 depicts the changes in excess Gibbs free energy with mole fraction of benzene for all three functional materials combinations of liquid mixtures. For all three combinations, Fig. 2, variations are positive. Gibbs free energy function, which is confirmed by positive Redlich-Kister coefficients [21, 22], indicates the presence of strong molecular interactions among liquid mixture molecules. Excess enthalpy (H^E) changes in all three functional materials liquid mixtures of binary combinations with benzene mole fraction are presented in Fig. 3, according to which H^E values in the benzene-toluene combination are positive up to 0.8 mole fraction and negative for the remaining mole fraction ranges of benzene. The H^E values for the other binary combinations, on the other hand, are all positive. When compared to other pure fluids, the results show that the molecules in binary compounds interacted. It is also suggested that the most desirable types of interactions, such as hydrogen bonding, dipole-dipole type interchanges in excess actions, and others, take place between component molecules [23-25]. Redlich-Kiester coefficients and standard deviations follow the same pattern for benzene functional binary material combinations with toluene. Redlich-Kiester coefficients and standard deviations study at four known temperatures supports the latter two binary functional material combinations, with benzene-o-xylene and benzene-mesitylene liquid mixtures [26].

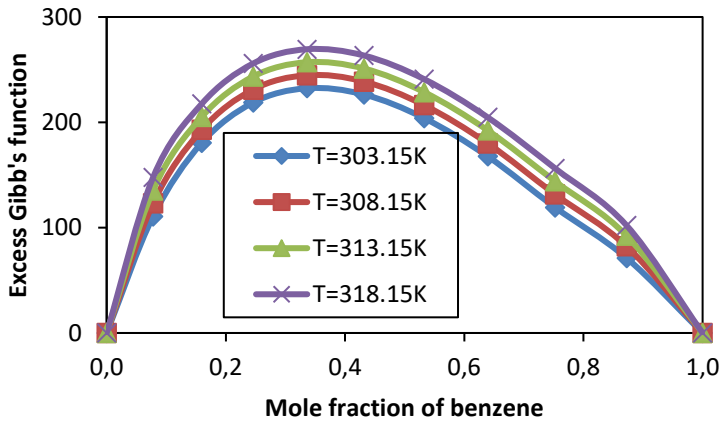

Fig. 2(a). Excess Gibbs free energy of activation (G^{*E}) varying with benzene mole fraction in the binary combination benzene mixed with toluene)

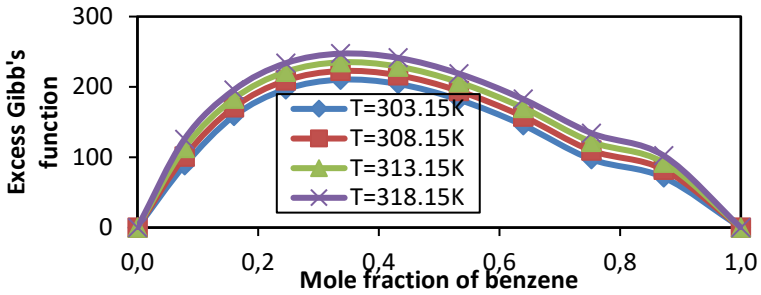

Fig. 2(b). Excess Gibbs free energy of activation (G^{*E}) varying with benzene mole fraction in the binary combination benzene mixed with o-xylene

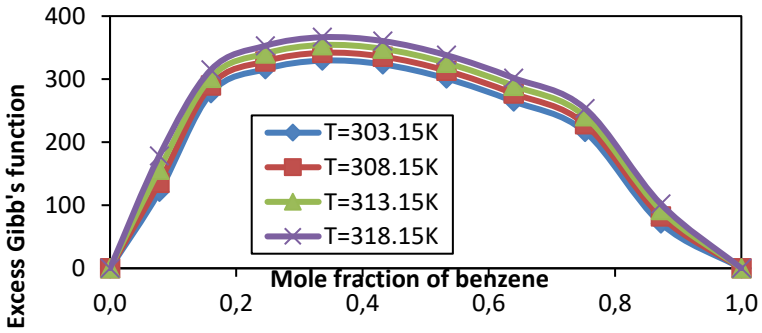

Fig. 2(c). Excess Gibbs free energy of activation (G^{*E}) varying with benzene mole fraction in the binary combination benzene mixed with mesitylene

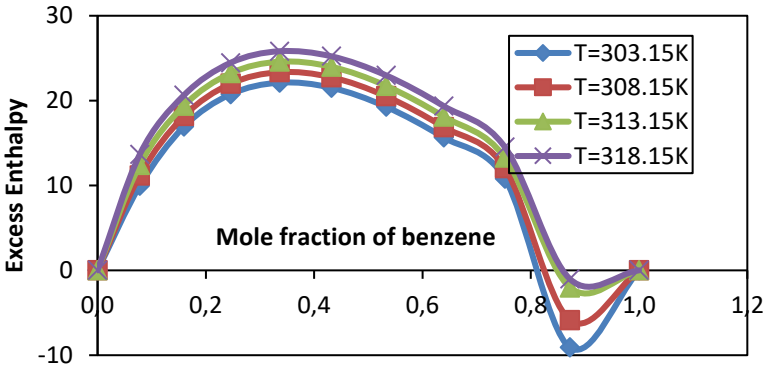

Fig. 3(a). Excess enthalpy (H^E) variations with benzene mole fraction in a binary combination of benzene mixed with toluene

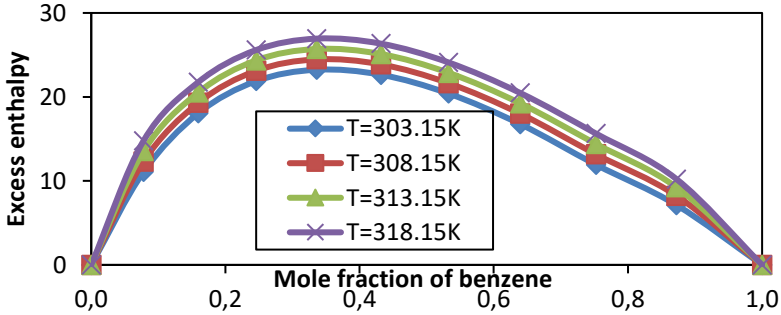

Fig. 3(b). Excess enthalpy (H^E) variations with benzene mole fraction in a binary combination of benzene mixed with o-xylene

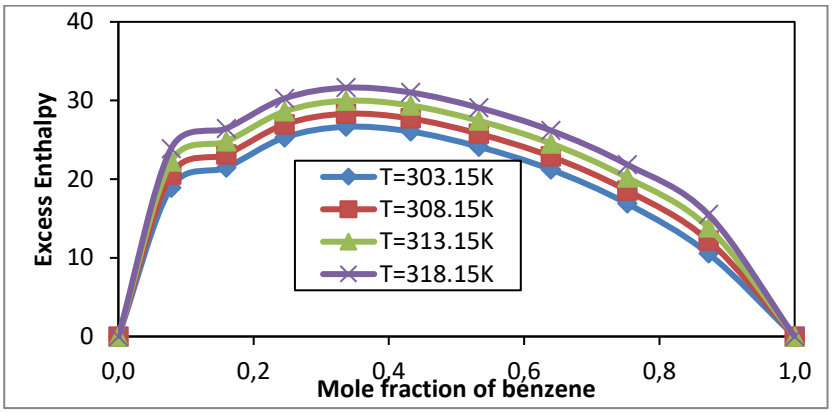

Fig. 3(c). Excess enthalpy (H^E) variations with benzene mole fraction in a binary combination of benzene mixed with mesitylene

CONCLUSION

Thermo-acoustic excess factors, namely excess free Gibbs energy (G^{*E}), excess internal pressure (π^E) and excess enthalpy (H^E), were determined across the total mole fraction of benzene at four known temperatures ranging from 303.15K to 318.15K. These findings show that interactions are strong in all three binary combinations of functional materials and become weak as temperature rises. The Redlich-Kister coefficient fluctuations and standard deviations back up these conclusions.

REFERENCES

1. G. V. Rama Rao, A Viswanatha Sarma, C. Rambabu, *Indian J. Pure & Appl. Phys*., **42,** 820 (2004).
2. T. Sumathi, S. Govindarajan, *Int. J. Bio. Pharm. Allied Sci***. 1(8),** 1153 (2012).
3. M. Eswari Bai, M. C. S. Subha, G. Narayana Swami, K. Chowdoji Rao, *J. Pure Appl. Ultrason*., **26,** 79 (2004).
4. M. Alculea Palofax, *Indian J. Pure Appl. Phys*. **31,** 90 (1993).
5. S. C. Bhatia, R. Rani, R. Bhatia, H. Anand, *J. Chem. Thermodyn.*, **43,** 479 (2011).
6. R. J. Fort, W. R. Moore, *Trans. Faraday Soc*., **61,** 2102 (1965).
7. V. D. Bhandakkar, Sh. Rode, S. Jajodia, *Archives of Applied Science Research*, **5 (4),** 12 (2013).
8. C. Yang, Z, Liu, H. Lai, P. Ma, *J. Chem. Eng. Data*, **51,** 457 (2006).
9. T. Yang, Sh. Xia, Sh. Song, X. Fu, P. Ma, *J. Chem. Eng. Data*, **52,** 2062 (2007).
10. G. V. Rama Rao, A. Viswanatha Sarma, D. Ramachandran, C. Rambabu, *Indian J. Chem*. **46A,** 1972 (2007).
11. L. Palanippan, R. Thiyagarajan, *Ind. J. Chem*. **47 B,** 1906 (2008).
12. S. Oswal, M. V. Tathnam, *Can. J. Chem*., **62,** 2851 (1984).
13. A. Misra, I. Vibhu, R. K. Singh, M. Gupta J. Shukla, *Phys, Chem. Liq.*, **45,** 93 (2007).
14. E. Dixon Dikio, *Orient. J. Chem*. **30(3),** 953 (2014).
15. T. M. Reed, T. E. Taylor, *J. Phys. Chem*., **63,** 58 (1959).
16. Ch. Saxena, A. Saxena, N. Kumar Shukla, *Chem. Sci. Trans*., **4,** 955 (2015).
17. S. Kumar, P. Jeevanandham, *J. Mol. Liq*., **174,** 34 (2012).
18. O. Redlich, A. T. Kister, *Indian Eng. Chem*., **40,** 345 **(**1948).
19. M. V. Rathnam, S. Mohite, M. S. S. Kumar, *Indian J. Chem. Tech*., **15,** 409 (2008).
20. M. Chorazewski, *J. Chem. Eng. Data*, **52,** 154 (2007).
21. P. Narayani, R, P. K. Ray, K. Mano, *J. Pure Appl. Ultrason.*, **36,** 97 (2014).
22. A N. Prajapati, *Indian J. Pure Appl. Phys.*, **55,** 297 (2017).
23. R. Mehra, M. Pancholi, *Indian J. Phys.*, **80 (3),** 253 (2007).
24. S. Chauhan, V K. Syal, *Indian J. Pure Appl. Phys.*, **32,** 187 (1994).
25. V. K. Syal, S. Chauhan, U. Kumari, *Indian J. Pure Appl. Phys*., **43,** 844 (2005).
26. N. Y. Reddy, P. S. Naidu K. R. Prasad, *Indian J. Pure Appl. Phys*., **32,** 958 (1994).

BULGARIAN CHEMICAL COMMUNICATIONS

Instructions about Preparation of Manuscripts

General remarks: Manuscripts are submitted in English by e-mail or by mail (in duplicate). The text must be typed double-spaced, on A4 format paper using Times New Roman font size 12, normal character spacing. The manuscript should not exceed 15 pages (about 3500 words), including photographs, tables, drawings, formulae, etc. Authors are requested to use margins of 3 cm on all sides. For mail submission hard copies, made by a clearly legible duplication process, are requested. Manuscripts should be subdivided into labelled sections, e.g. **Introduction, Experimental, Results and Discussion**, *etc*.

The title page comprises headline, author's names and affiliations, abstract and key words.

Attention is drawn to the following:

a) **The title** of the manuscript should reflect concisely the purpose and findings of the work. Abbreviations, symbols, chemical formulas, references and footnotes should be avoided. If indispensable, abbreviations and formulas should be given in parentheses immediately after the respective full form.

b) **The author**'s first and middle name initials, and family name in full should be given, followed by the address (or addresses) of the contributing laboratory (laboratories). **The affiliation** of the author(s) should be listed in detail (no abbreviations!). The author to whom correspondence and/or inquiries should be sent should be indicated by asterisk (*).

The abstract should be self-explanatory and intelligible without any references to the text and containing not more than 250 words. It should be followed by key words (not more than six).

References should be numbered sequentially in the order, in which they are cited in the text. The numbers in the text should be enclosed in brackets [2], [5, 6], [9−12], etc., set on the text line. References, typed with double spacing, are to be listed in numerical order on a separate sheet. All references are to be given in Latin letters. The names of the authors are given without inversion. Titles of journals must be abbreviated according to Chemical Abstracts and given in italics, the volume is typed in bold, the initial page is given and the year in parentheses. Attention is drawn to the following conventions:

a) The names of all authors of a certain publications should be given. The use of "*et al*." in the list of references is not acceptable.

b) Only the initials of the first and middle names should be given.

In the manuscripts, the reference to author(s) of cited works should be made without giving initials, e.g. "Bush and Smith [7] pioneered...". If the reference carries the names of three or more authors it should be quoted as "Bush *et al*. [7]", if Bush is the first author, or as "Bush and co-workers [7]", if Bush is the senior author.

Footnotes should be reduced to a minimum. Each footnote should be typed double-spaced at the bottom of the page, on which its subject is first mentioned.

Tables are numbered with Arabic numerals on the left-hand top. Each table should be referred to in the text. Column headings should be as short as possible but they must define units unambiguously. The units are to be separated from the preceding symbols by a comma or brackets.

Note: The following format should be used when figures, equations, *etc*. are referred to the text (followed by the respective numbers): Fig., Eqns., Table, Scheme.

Schemes and figures. Each manuscript (hard copy) should contain or be accompanied by the respective illustrative material as well as by the respective figure captions in a separate file (sheet). As far as presentation of units is concerned, SI units are to be used. However, some non-SI units are also acceptable, such as °C, ml, l, etc.

The author(s) name(s), the title of the manuscript, the number of drawings, photographs, diagrams, etc., should be written in black pencil on the back of the illustrative material (hard copies) in accordance with the list enclosed. Avoid using more than 6 (12 for reviews, respectively) figures in the manuscript. Since most of the illustrative materials are to be presented as 8-cm wide pictures, attention should be paid that all axis titles, numerals, legend(s) and texts are legible.

The authors are asked to submit **the final text** (after the manuscript has been accepted for publication) in electronic form either by e-mail or mail on a 3.5'' diskette (CD) using a PC Word-processor. The main text, list of references, tables and figure captions should be saved in separate files (as *.rtf or *.doc) with clearly identifiable file names. It is essential that the name and version of

the word-processing program and the format of the text files is clearly indicated. It is recommended that the pictures are presented in *.tif, *.jpg, *.cdr or *.bmp format, the equations are written using "Equation Editor" and chemical reaction schemes are written using ISIS Draw or ChemDraw programme.

The authors are required to submit the final text with a list of three individuals and their e-mail addresses that can be considered by the Editors as potential reviewers. Please, note that the reviewers should be outside the authors' own institution or organization. The Editorial Board of the journal is not obliged to accept these proposals.

EXAMPLES FOR PRESENTATION OF REFERENCES

REFERENCES

1. D. S. Newsome, *Catal. Rev.–Sci. Eng*., **21**, 275 (1980).
2. C.-H. Lin, C.-Y. Hsu, *J. Chem. Soc. Chem. Commun*., 1479 (1992).
3. R. G. Parr, W. Yang, Density Functional Theory of Atoms and Molecules, Oxford Univ. Press, New York, 1989.
4. V. Ponec, G. C. Bond, Catalysis by Metals and Alloys (Stud. Surf. Sci. Catal., vol. 95), Elsevier, Amsterdam, 1995.
5. G. Kadinov, S. Todorova, A. Palazov, in: New Frontiers in Catalysis (Proc. 10th Int. Congr. Catal., Budapest, 1992), L. Guczi, F. Solymosi, P. Tetenyi (eds.), Akademiai Kiado, Budapest, 1993, Part C, p. 2817.
6. G. L. C. Maire, F. Garin, in: Catalysis. Science and Technology, J. R. Anderson, M. Boudart (eds), vol. 6, Springer-Verlag, Berlin, 1984, p. 161.
7. D. Pocknell, *GB Patent* 2 207 355 (1949).
8. G. Angelov, PhD Thesis, UCTM, Sofia, 2001.
9. JCPDS International Center for Diffraction Data, Power Diffraction File, Swarthmore, PA, 1991.
10. CA **127**, 184 762q (1998).
11. P. Hou, H. Wise, *J. Catal.*, in press.
12. M. Sinev, private communication.
13. http://www.chemweb.com/alchem/articles/1051611477211.html.

CONTENTS

Conference on Cutting Edge Research in Materials and Sustainable Chemical Technologies (CRMSCT-2022) – Department of Chemical Engineering and Department of Chemistry, Decennial year celebrations, Manipal University Jaipur, Jaipur, India